

**Stable isotope composition of benthic foraminifera:
Species-specific differences and their application**

Dissertation zur Erlangung des Doktorgrades
an der

Fakultät für Mathematik, Informatik und Naturwissenschaften
Fachbereich Geowissenschaften
der Universität Hamburg

vorgelegt von
Marc Theodor
aus Neubukow

Hamburg
2016

Tag der Disputation: 21.10.2016

Folgende Gutachter empfehlen die Annahme der Dissertation

Prof. Dr. Gerhard Schmiedl

Prof. Dr. Andreas Mackensen

Eidesstattliche Versicherung

Declaration on oath

Hiermit erkläre ich an Eides statt, dass die vorliegende Dissertationsschrift von mir selbst verfasst wurde und ich keine anderen als die angegebenen Quellen und Hilfsmittel benutzt habe.

I hereby declare, on oath, that I have written the present dissertation by my own and have not used other than the acknowledged resources and aids.

Hamburg, den

In stetem Gedenken ist diese Arbeit André Theodor und Siegfried Kaiser gewidmet.

Zusammenfassung

Die Zusammensetzung stabiler Isotope in den Schalen von Foraminiferen liefert eine große Bandbreite an Informationen sowohl über die Biologie dieser Protisten als auch über die sie umgebende Umwelt. Daher sind die Verhältnisse von ^{13}C zu ^{12}C Isotopen ($\delta^{13}\text{C}$) als auch ^{18}O zu ^{16}O Isotopen ($\delta^{18}\text{O}$) in Schalen benthischer Foraminiferen weitverbreitete und oft genutzte Proxys in der Paläozeanographie. Überraschenderweise ist bislang noch relativ wenig bekannt über artspezifische Unterschiede und deren auslösende Faktoren. Aus diesem Grund wurden in der vorliegenden Arbeit die stabilen Sauerstoff- und Kohlenstoffisotopenverhältnisse in gefärbten (lebend bei der Beprobung) und ungefärbten (bereits tot bei der Beprobung) Gehäusen diverser Arten von benthischen Foraminiferen aus verschiedenen Regionen des Mittelmeeres untersucht. Bei der Feststellung der Einflussfaktoren zeigte sich beim $\delta^{13}\text{C}$ -Verhältnis ein deutlicher Zusammenhang mit der Lebendtiefe im Sediment, dem sogenannten Mikrohabitat. Die Verhältnisse verringerten sich mit zunehmender Tiefe um bis zu $-2,3\text{‰}$ und spiegeln damit vor allem den isotopischen Porenwassergradienten an gelöstem anorganischem Kohlenstoff (DIC) wider. Ein wiederkehrender Unterschied von ungefähr $0,2\text{‰}$ zwischen gefärbten und ungefärbten Gehäusen lässt sich auf den neuzeitlichen anthropogenen Ausstoß isotopisch leichten Kohlenstoffs aus fossilen Energiequellen zurückführen (Suess-Effekt). Dies resultiert aus der Beprobung in unterschiedlichen Sedimenttiefen und damit auch Altern der Foraminiferen. Sowohl für Kohlenstoff als auch für Sauerstoff konnte eine Zunahme der Verhältnisse von bis zu $1,2$ bzw. $1,3\text{‰}$ mit zunehmender Gehäusegröße bei buliminiden Arten (*Globobulimina* spp., *Uvigerina* spp.) beobachtet werden. Rotaliide Arten hingegen (*Lobatula lobatula*, *Cibicidoides pachydermus*, *Planulina ariminensis*, *Melonis barleeanum*) zeigten keinen Zusammenhang zwischen der Gehäusegröße und den stabilen Isotopenverhältnissen. Bei *Uvigerina peregrina* war diese metabolische Fraktionierung in kleinen Gehäusen besonders ausgeprägt und überprägte den Porenwassergradienten zu noch niedrigeren Werten. Im Gegensatz dazu zeigt die ebenfalls flach-infaunal lebende *Uvigerina mediterranea* eine geringere biologische Beeinflussung, so dass unterschiedliche Trophie-Bedingungen der Umwelt besser aufgezeichnet werden, mit insgesamt niedrigeren Werten bei eutrophischeren Bedingungen. Daher scheint diese Art geeigneter zu sein, um sie als Proxy für die Rekonstruktion des Eintrags von organischem Material zu nutzen.

Aufgrund dieser Grundlagen wurden explizit die $\delta^{13}\text{C}$ Verhältnisse von epifaunalen Arten und *U. mediterranea* von weiteren Stationen aus dem gesamten Mittelmeer verglichen. Für diese Erweiterung des Datensatzes wurden 13 gut belüftete Stationen vom Kontinentalhang beprobt, welche hauptsächlich im Einfluss des Levantinischen Zwischenwassers (LIW) liegen. Um die lokalen Porenwassergradienten rekonstruieren zu können, wurden die $\delta^{13}\text{C}$ Verhältnisse epifaunaler Arten gemessen, als Vergleichswert für das Bodenwasser herangezogen und vom Isotopenverhältnis von

U. mediterranea subtrahiert ($\Delta\delta^{13}\text{C}_{Umed-Epi}$). Die erhaltenen Werte schwankten zwischen -0,5 und -2,1 ‰, mit generell stärkeren Abweichungen an eutrophen Stationen. Die Flussraten an organischem Kohlenstoff (C_{org}) konnten mit Hilfe von Satellitenmessungen gewonnen werden und zeigten vor allem für offene marine Bedingungen (Alborán-Meer, Meeresstraße zwischen Mallorca und Ibiza, Straße von Sizilien, südliche Ägäis) eine Korrelation mit den $\Delta\delta^{13}\text{C}_{Umed-Epi}$ Werten. In Regionen hingegen, die stärker von lateralen Umlagerungen beeinflusst sind (untermeerische Canyons im Golf von Lyon, isolierte Becken der nördlichen und zentralen Ägäis), waren die errechneten vertikalen Flussraten zu gering. Diese möglichen Fehlerquellen beachtend, war es aber möglich eine erste Transferfunktion zwischen C_{org} -Flüssen und den $\delta^{13}\text{C}$ -Abweichungen zwischen den verschiedenen benthischen Foraminiferen aufzustellen.

Um diese Funktion zu testen, wurden die stabilen Isotopenwerte dieser sowie vergleichbarer Foraminiferen aus zwei Bohrkernen (Straße von Sizilien, Ligurisches Meer) untersucht. Die deutlichen Veränderungen der Temperaturen und der Salzgehalte während des letzten Glazial-Interglazial-Übergangs wurden in den $\delta^{18}\text{O}$ -Verhältnissen aller Arten aufgezeichnet. Trotz dieser allgemeinen Konkordanz sind artspezifische Unterschiede von bis zu 1,2 ‰ vor allem während des letzten Glazialen Maximums (LGM) zu beobachten. Die noch deutlich stärkeren Unterschiede im $\delta^{13}\text{C}$ -Verhältnis von bis zu 2,5 ‰ lassen sich hauptsächlich auf biologische Effekte und unterschiedliche Tiefen des Mikrohabitats zurückführen. Die vergleichbaren Kohlenstoff-Werte von *P. ariminensis* und *Cibicoides wuellerstorfi* unterstützen die Ansicht, dass diese beiden Arten geeignete Anzeiger für das $\delta^{13}\text{C}$ -Verhältnis im DIC des Bodenwassers sind. Trotz des unterbrochenen Vorkommens der tief-infaunalen Art *Globobulimina affinis* in der Straße von Sizilien, konnte deren isotopische Abweichung zur Epifauna ($\Delta\delta^{13}\text{C}_{Gaff-Epi}$) genutzt werden um die Sauerstoffkonzentration des Bodenwassers, insbesondere während des Ablagerungszeitraums des Sapropels S1, quantitativ abzuschätzen. Die mit Hilfe des $\Delta\delta^{13}\text{C}_{Umed-Epi}$ -Verhältnisses rekonstruierten C_{org} -Flüsse zeigen für beide Regionen erhöhte Flussraten von bis zu $5 \text{ gC m}^{-2} \text{ a}^{-1}$ während des letzten Glaziales und dem Jüngeren Dryas-Stadial im Vergleich zum Bølling/Allerød-Interstadial und dem Holozän. Durch die offene-marine Lage der Station vor Sizilien war es darüber hinaus möglich eine belastbare Rückberechnung der marinen Primärproduktion durchzuführen. Die erhaltenen Werte schwankten dabei zwischen $200 \text{ gC m}^{-2} \text{ a}^{-1}$ in den Kaltphasen und $140 \text{ gC m}^{-2} \text{ a}^{-1}$ im Holozän.

Abstract

The stable isotope composition of foraminiferal tests contains a wide range of environmental and biological information. Although the $\delta^{13}\text{C}$ and $\delta^{18}\text{O}$ records of benthic foraminifera are a commonly used proxy in paleoceanographic studies, still little is known on the species-specific differences of the stable isotope signal and the factors controlling them. In this thesis live (stained) and dead (unstained) tests of different benthic foraminiferal species from the Mediterranean Sea were investigated with regard to their stable oxygen and carbon isotope ratios. The identification of environmental and biological influences revealed a strong dependency of the $\delta^{13}\text{C}$ values on the microhabitat, showing lower ratios down to -2.3 ‰ with increasing living depth within the sediment, mirroring the pore water gradient in dissolved inorganic carbon (DIC). A recurring offset of 0.2 ‰ between stained and unstained tests at western Mediterranean sites can be addressed to the increased anthropogenic emission of ^{12}C from fossil fuels (Suess-effect). This was a result of different sampling depths and therefore different ages. Ontogenetic shifts towards higher $\delta^{13}\text{C}$ and $\delta^{18}\text{O}$ ratios with increasing test sizes of 1.2 and 1.3 ‰, respectively, were observed in buliminid (*Globobulimina* spp., *Uvigerina* spp.), but not in rotaliid taxa (*Lobatula lobatula*, *Cibicidoides pachydermus*, *Melonis barleanum*). *Uvigerina peregrina* revealed a strong metabolic fractionation for small tests, suppressing the pore water signal towards more negative ratios. In contrast the likewise shallow infaunal *Uvigerina mediterranea* appears to be less biological influenced and reflects the more eutrophic conditions at the Alboran Sea by a complete shift towards lower $\delta^{13}\text{C}$ values. Therefore the $\delta^{13}\text{C}$ ratio of this species seem to be a preferable proxy for trophic gradient reconstructions.

Expanding the data set, the stable carbon isotope ratios of epifaunal species and *U. mediterranea* were measured from 13 well-oxygenated continental slope sites of the whole Mediterranean Sea, general bathed in the Levantine Intermediate Water (LIW). To calculate the local pore water gradients the differences between the $\delta^{13}\text{C}$ ratios of the shallow infaunal *U. mediterranea* and three epifaunal species, representing bottom water conditions, were measured ($\Delta\delta^{13}\text{C}_{U\text{med-Epi}}$). These values range between -0.5 to -2.1 ‰ with generally stronger differences at more eutrophic sites. Satellite-borne quantifications of Primary Production (PP) were utilized to estimate the C_{org} fluxes at each site for the year previously of sampling. The $\Delta\delta^{13}\text{C}_{U\text{med-Epi}}$ and the C_{org} flux data showed a good correlation for open marine sites (Alboran Sea, Mallorca Channel, Strait of Sicily, Southern Aegean Sea), while the C_{org} supply is underestimated for regions influenced by lateral fluxes, due to intense resuspension (Canyons at the Gulf of Lions, isolated basins in the Northern and Central Aegean Sea). Considering these local biases, a first transfer function for C_{org} fluxes based on the stable carbon isotope differences of benthic foraminifera could be established.

To determine the reliability of the developed transfer function, down-core stable isotope values of various benthic foraminifera from two sediment cores of the Mediterranean Sea (Strait of Sicily;

Ligurian Sea) were investigated. The dramatic shifts in salinity and temperature during the last Glacial-Interglacial transition were generally recorded by the $\delta^{18}\text{O}$ ratios, though specific offsets of more than 1.2 ‰ were measured during the Last Glacial Maximum. The stronger species-specific $\delta^{13}\text{C}$ differences of up to 2.5 ‰ result from vital effects and different living depths. The comparable values of *Planulina ariminensis* and *Cibicides wuellerstorfi* corroborating the preferable application of these species to reconstruct bottom water $\delta^{13}\text{C}_{\text{DIC}}$ conditions. Despite a discontinuous record, the difference of these species and the deep infaunal *Globobulimina affinis* ($\Delta\delta^{13}\text{C}_{\text{Gaff-Epi}}$) revealed reliable oxygen concentrations of the bottom water, especially during the sapropel S1 formation. The reconstructed C_{org} fluxes, applying the $\Delta\delta^{13}\text{C}_{\text{Umed-Epi}}$ signal, showed higher C_{org} supply of more than $5 \text{ gC m}^{-2} \text{ a}^{-1}$ during the Late Glacial and the Younger Dryas Stadial compared to the Bølling/Allerød Interstadial and the Holocene. The open-ocean setting at the Strait of Sicily site made a reliable recalculation of past primary production possible, ranging between 140 to $200 \text{ gC m}^{-2} \text{ a}^{-1}$.

Table of contents

| | |
|--|----|
| 1. Introduction..... | 1 |
| 1.1 Research questions | 1 |
| 1.2 Outline | 5 |
| 2. Study area..... | 7 |
| 2.1 Geography of the Mediterranean region..... | 7 |
| 2.2 Oceanographic conditions | 9 |
| 2.3 Development of the Mediterranean Sea | 11 |
| 3. Stable isotope composition of deep-sea benthic foraminifera under contrasting trophic conditions in the western Mediterranean Sea | 13 |
| Abstract..... | 13 |
| 3.1 Introduction..... | 14 |
| 3.2 Study area..... | 16 |
| 3.3 Material and Methods | 18 |
| 3.4 Results..... | 21 |
| 3.4.1 Biogeochemistry and distribution of calcareous benthic foraminifera..... | 21 |
| 3.4.2 Stable isotope composition in relation to equilibrium calcite and bottom water DIC..... | 22 |
| 3.4.3 Test size distribution and ontogenic trends in stable isotope composition | 23 |
| 3.5 Discussion..... | 24 |
| 3.5.1 Influence of trophic conditions on distribution, microhabitats, and test sizes of benthic foraminifera..... | 24 |
| 3.5.2 Influence of microhabitat on the stable isotope signal..... | 26 |

| | |
|--|----|
| 3.5.3 Ontogenetic fractionation of the stable isotope signal | 30 |
| 3.5.4 Influence of organic matter fluxes on the stable carbon isotope signal of <i>Uvigerina</i> species..... | 31 |
| 3.5.5 Taphonomic alteration and anthropogenic influence on the stable isotope signal..... | 33 |
| 3.6 Conclusions..... | 34 |
| | |
| 4. Stable carbon isotope deviations in benthic foraminifera as proxy for organic carbon fluxes in the Mediterranean Sea | 37 |
| Abstract..... | 37 |
| 4.1 Introduction..... | 38 |
| 4.2 Material and methods | 41 |
| 4.3 Results..... | 44 |
| 4.4 Discussion..... | 47 |
| 4.4.1 Stable carbon isotope signal of epifaunal foraminifera in relation to surrounding water masses | 47 |
| 4.4.2 Biological and environmental effects on the stable carbon isotope signal of <i>Uvigerina mediterranea</i> | 49 |
| 4.4.3 Development of a stable carbon isotope based transfer function for organic carbon fluxes..... | 52 |
| 4.5 Conclusions..... | 56 |
| | |
| 5. Quantitative reconstruction of past Mediterranean organic matter fluxes and oxygen concentrations using multi-species benthic foraminiferal isotopes..... | 57 |
| Abstract..... | 57 |
| 5.1 Introduction..... | 58 |
| 5.2 Regional setting | 60 |
| 5.3 Material and methods | 63 |

| | |
|---|-----|
| 5.4 Results..... | 67 |
| 5.5 Discussion..... | 68 |
| 5.5.1 Stable isotope signal of different epibenthic foraminifera as bottom water proxy..... | 68 |
| 5.5.2 The applicability of species-specific stable carbon isotope differences as proxy for organic carbon flux and oxygen concentration | 70 |
| 5.5.3 Changes of intermediate water circulation and oxygenation | 73 |
| 5.5.4 Changes of organic matter fluxes and surface productivity | 75 |
| 5.6 Conclusions..... | 79 |
| | |
| 6. Conclusions and Outlook | 81 |
| 6.1 Conclusions..... | 81 |
| 6.2 Outlook..... | 83 |
| | |
| Bibliography..... | 85 |
| | |
| Appendix..... | 113 |
| Appendix I Taxonomy | 113 |
| Appendix II Counted benthic foraminifera | 115 |
| Appendix III Test size distribution | 115 |
| Appendix IV Stable isotope data | 115 |
| | |
| Plates | |

1. Introduction

1.1 Research questions

To investigate the global development of climatic changes in the past the oceans are an essential source of information. Due to the ideally steady sedimentation at the sea floor, past environmental conditions are recorded via proxies in marine sediments. As one component of a various number of different biogeochemical and paleontological proxies, shelled microfossils, e.g. foraminifera, are a widely used tool, because they are diverse, often highly abundant and have a wide distribution in marine environments. Foraminifera are single-celled heterotrophic protists that often build up shells, so called tests. These tests can be made of organic material, agglutinated components or calcium carbonate (calcite, aragonite). Planktonic foraminifera, which have always calcitic tests, can provide information about temperature or salinity of the sea surface. The more diverse benthic foraminifera reflect bottom water conditions from coastal areas down to the abyssal sea floor (Sen Gupta, 1999). They can occupy different microhabitats, which can be attached on surfaces or directly at the sediment-water interface, so called epifaunal microhabitats, or at different depths up to several cm within the sediment, referred as infaunal microhabitats (Corliss, 1985). Besides the utilization of benthic faunal assemblages for the reconstruction of past oceanic and climatic conditions, the geochemical composition of their carbonate tests offer additional information. Especially the stable oxygen and carbon isotope ratios are common and well used proxies to reconstruct past climate conditions (reviews in Rohling & Cooke, 1999; Pearson, 2012). The conventional agreement to work with the different ratios of ^{16}O to ^{18}O as well as ^{12}C to ^{13}C the δ -notation ($\delta^{18}\text{O}$ & $\delta^{13}\text{C}$) is used, referring to the Vienna Pee Dee Belemnite (VPDB) (Gonfiantini et al., 1995). The marine $\delta^{18}\text{O}$ signal is mainly influenced by the amounts of ice at the high latitudes and the sea water salinity, while the marine $\delta^{13}\text{C}$ is mostly triggered by the surrounding carbonate ion concentration and the preferred utilization of ^{12}C during photosynthesis. To apply foraminiferal tests, it has to be assumed, that the isotopic composition of the tests is in equilibrium with the surrounding water conditions. Unfortunately, differences of the isotope ratios between different genera and species of the same site were recognized for planktonic and benthic foraminifera since the first investigations (Duplessy et al., 1970; Shackleton et al., 1973). These differences were explained by numerous environmental factors, i.e. slightly different habitat conditions (e.g. McCorkle et al., 1997), and by biological fractionation altering the isotopic composition of the test in a distinct manner (e.g. McConnaughey, 1989a, b). However, due to the investigation of just a few species, mostly epifaunal ones such as *Cibicides wuellerstorfi*, or the lumping of different species, still little is known about the factors

1.1 Research questions

causing species-specific different signals under identical conditions. These basic insecurities led to the first research question:

To which extent are the $\delta^{13}\text{C}$ and $\delta^{18}\text{O}$ differences of benthic foraminifera species-specific?
And which factors control the isotopic composition of individual species?

Stable isotope differences can be the result of external (environmental) as well as internal (biological) factors. The environmental effects are mainly caused by minor local shifts, e.g. differences in the carbonate ion concentration (Spero et al., 1997; Mackensen & Licari, 2004) or the pore water gradient (Grossman, 1984a; b; McCorkle et al., 1985). The biological factors are isotopic fractionations of the $\delta^{18}\text{O}$ and $\delta^{13}\text{C}$ signals caused by metabolic and kinetic effects, and are known as 'vital effects' (McConnaughey et al. 1989a, b). Preferring lighter ^{12}C and ^{16}O , these fractionations led towards lower isotope ratios and can be caused by a changing calcification rate, due to the metabolic speed, or by divergent sources of the utilized oxygen or carbon. The influence of ontogeny, resulting in higher isotope ratios with increasing test size, is common and well-known in planktonic foraminifera (Ravelo & Fairbanks, 1995; Spero & Lea, 1996), while benthic foraminifera show variable results (Wefer & Berger, 1991; Corliss et al., 2002; Schumacher et al., 2010). There is also evidence for an influence of varying calcification strategies on the isotopic composition of the test, e.g. within cysts, that cause distinct biochemical conditions, differing from the environment (Diz et al., 2012). 'Vital effects' can strongly alter the isotopic composition of foraminiferal tests and biases the results for environmental reconstructions. Though some species seem to be less influenced by internal effects, e.g. *C. wuellerstorfi*, while other are clearly affected, e.g. the aragonitic *Hoeglundina elegans* (Wefer & Berger, 1991; McCorkle et al., 1997; Fontanier et al., 2006), the next research question emerges:

Which benthic foraminiferal species are less influenced by biological effects and, hence, are preferable indicator species for past environmental conditions?

The pore water gradient in $\delta^{13}\text{C}$ of dissolved inorganic carbon (DIC) tends towards lower values with increasing sediment depth as a result of microbial remineralization of isotopically light organic matter (OM) (Grossman, 1984a, b; McCorkle et al., 1985, 1990). The reduction of microbial activity, linked to no assessable electron acceptors (O_2 , NO_3^-), also marks the sediment depth where the steady decrease in $\delta^{13}\text{C}_{\text{DIC}}$ ceases (e.g. Koho & Piña-Ochoa, 2012). This depth extant of microbial activity is mainly controlled by the oxygen concentrations of the bottom water as well as the OM decomposition and the sedimentation rates (Rutgers van der Loeff, 1990; McCorkle et al., 1997; Schmiedl & Mackensen, 2006). Although the oxygen concentration and the OM supply interact, the amount of OM is influencing the shape of the gradient towards a more curved trend with higher

1. Introduction

input, due to a faster remineralization close to the sediment-water interface (McCorkle & Emerson, 1988; Stott et al., 2000) (Fig. 1). As mentioned before benthic foraminifera live in different sediment depths, calcifying their tests under the influence of different pore water conditions (McCorkle et al., 1990, 1997). Despite the fact, that individuals of the same species can occur over a wide depth range within the sediment, their stable isotope signal remains relatively constant, representing the pore water signal close to their favored living depth (McCorkle et al., 1990; Rathburn et al., 1996; Mackensen & Licari, 2004). Although the reasons for this are not completely understood (review in Mackensen, 2008), this is an important precondition for the species-specific recording of the pore water gradient. For example, infaunal foraminifera can actively change their living depth and react quickly to shifts of the oxygen concentrations and food supply (Ohga & Kitazato, 1997). For the well oxygenated bottom water conditions at intermediate depths in the Mediterranean Sea (e.g. Tanhua et al., 2013), the C_{org} flux is the main trigger controlling the pore water $\delta^{13}C$ gradient. Assuming this, the third research question is:

Is it possible to correlate organic matter fluxes with epi- and infaunal benthic foraminiferal $\delta^{13}C$ ratio differences ($\Delta\delta^{13}C_{inf-epi}$), which mirror the pore water gradient?

Indeed, the stable carbon isotope ratios of benthic foraminifera or their $\Delta\delta^{13}C_{inf-epi}$ where previously applied for the reconstruction of OM fluxes (Zahn et al., 1986; Schilman et al., 2003; Schmiedl & Mackensen, 2006; Kuhnt et al., 2008). However, no comparison with recent data sets was made to check the reliability and quantify the results. To test the previous results of the possible organic carbon flux and $\Delta\delta^{13}C_{inf-epi}$ correlation, an application on down-core measurements seems worthwhile. Due to major shifts in the bottom water oxygenation as well as in trophic conditions during the last Glacial-Interglacial transition (e.g. Vergnaud-Grazzini & Pierre, 1991; Cacho et al., 2000; Jimenez-Espejo et al., 2007) the Mediterranean Sea appears as a preferable research region. This motivates the last research question:

Are the stable carbon isotope ratio differences between benthic foraminiferal species applicable to reconstruct past trophic conditions of the Mediterranean Sea?

1.1 Research questions

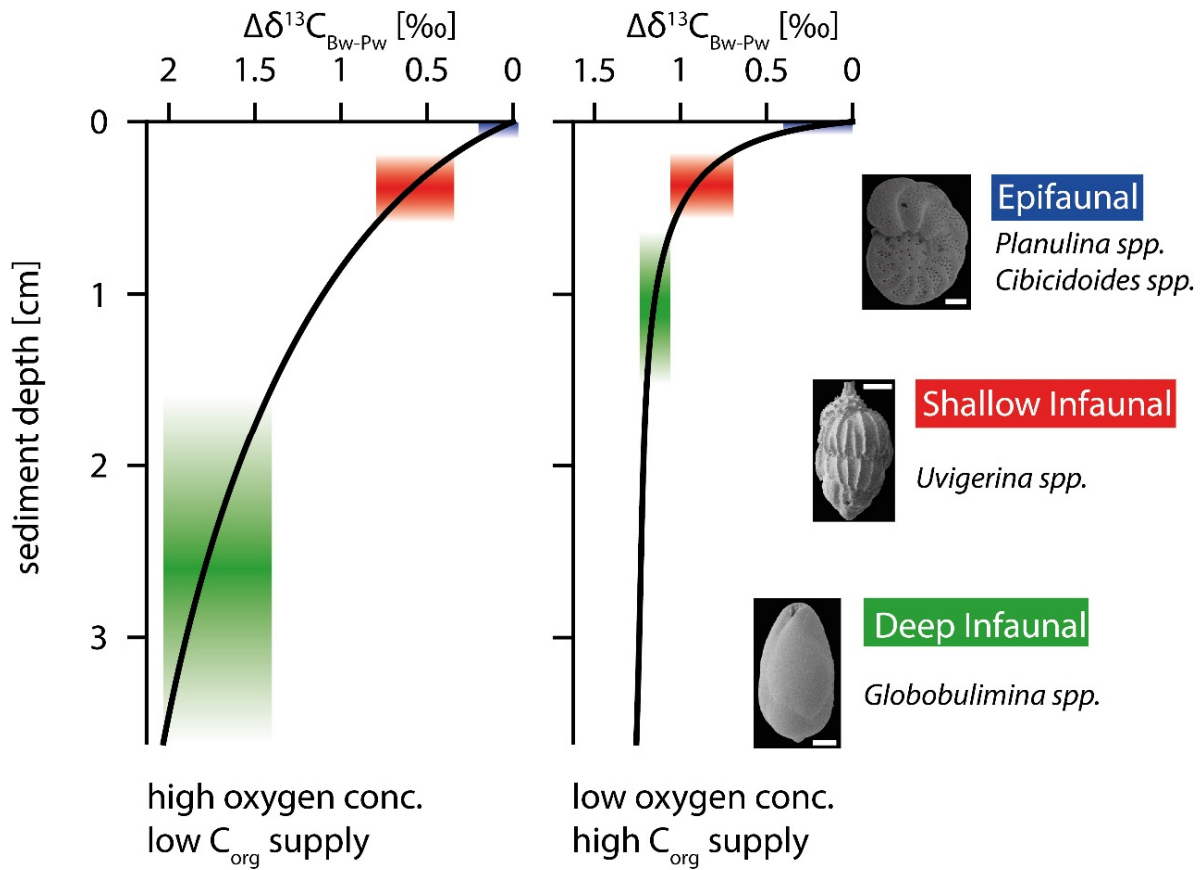


Figure 1. Schematic correspondence of the $\delta^{13}\text{C}_{\text{DIC}}$ pore water gradient against bottom water DIC ($\Delta\delta^{13}\text{C}_{\text{BW-Pw}}$, black line) to differing oxygenation and trophic conditions. Benthic foraminifera record these different carbon isotope values, due to their favored living depths (colored intervals). The different colors represent three general microhabitats with examples of common genera (right side). The $\Delta\delta^{13}\text{C}_{\text{BW-For}}$ values of deep infaunal species decrease with reduced oxygen concentrations of the bottom water or higher organic carbon supply. In contrast shallow infaunal species show gaining $\Delta\delta^{13}\text{C}_{\text{BW-For}}$ values with increasing C_{org} input. Modified after Schmiedl & Mackensen, 2006.

1.2 Outline

To answer the aforementioned research questions the present thesis is divided into six chapters. This first chapter gives an introducing overview with the motivation and aims of this study. Chapter 2 contains a brief introduction into the recent geographic and oceanographic setting of the Mediterranean Sea and its development towards recent conditions. The focus of the third chapter is on the distribution of different benthic foraminifera and the influencing factors on their stable isotope composition under contrasting trophic conditions. In chapter 4 additional $\delta^{13}\text{C}$ measurements on specific species at different sites of the Mediterranean Sea are compared with satellite derived primary productivity values to deduce a transfer function. The results of chapter 4 were applied to stable isotope records of two sediment cores from the central Mediterranean covering the Holocene and the Late Glacial, which is presented in chapter 5. Chapter 6 finishes with the conclusions of this thesis and gives an outlook on further research perspectives.

2. Study area

2.1 Geography of the Mediterranean region

The Mediterranean Sea is surrounded by Africa in the south, Asia in the east and Europe in the north (Fig. 2). It has a semi-enclosed character with the 14.5 km wide Strait of Gibraltar at the western end as single connection with the Atlantic Ocean (Tsimplis & Bryden, 2000). In the east it is connected to the likewise enclosed Black Sea via the Bosphorus, the Marmara Sea, and the Dardanelles. The small connection to the Red Sea via the artificial Suez Canal can be neglected from an oceanographic point of view. The Italian Peninsula, Sicily and the north-eastern tip of Tunisia separate the Mediterranean Sea into an eastern and a western sub-basin, connected through the at least 150 km wide Strait of Sicily and the 3-5 km wide Strait of Messina. The discrete thermohaline circulation in connection with the few connections to other Seas, makes the Mediterranean Sea to a 'miniature ocean' (Bethoux et al., 1999; Malanotte-Rizzoli et al., 2014).

With an east-west-extension of about 3700 km and 1600 km from north to south, resulting in an approximately surface area of $2.5 \cdot 10^6 \text{ km}^2$, this large marginal sea is an important factor for the climatic pattern of the even larger Mediterranean realm (Lionello et al., 2012). Situated between the temperate climatic zone in the North and the subtropical zone in the South, strong spatial contrasts appear in the regional and local climates. The basin is mainly influenced by mid-latitude teleconnection patterns, such as the North Atlantic Oscillation (NAO), but also less prominent patterns, e.g. East Atlantic pattern, West Russian pattern, Scandinavian pattern (Lionello & Galati, 2008; Josey et al., 2011). During summer subtropical conditions prevail over the Mediterranean Sea, with only exceptional depressions entering from the Atlantic, leading to dry and warm to hot conditions (Trigo et al., 2006). During winter and spring European air masses entering the Mediterranean and are channeled due to mountains (e.g. Pyrenees, Alps) inducing increased evaporation and heat loss of the sea surface in the Gulf of Lions, the Adriatic Sea and the Aegean Sea (Josey et al., 2011). Likewise, cyclogenesis is caused in these areas, especially the Ligurian Sea and the Aegean Sea, triggering the enhanced precipitation during winter (Trigo et al., 1999). Therefore, the Mediterranean Sea itself is the main water source for precipitation (e.g. Matthews et al., 2000).

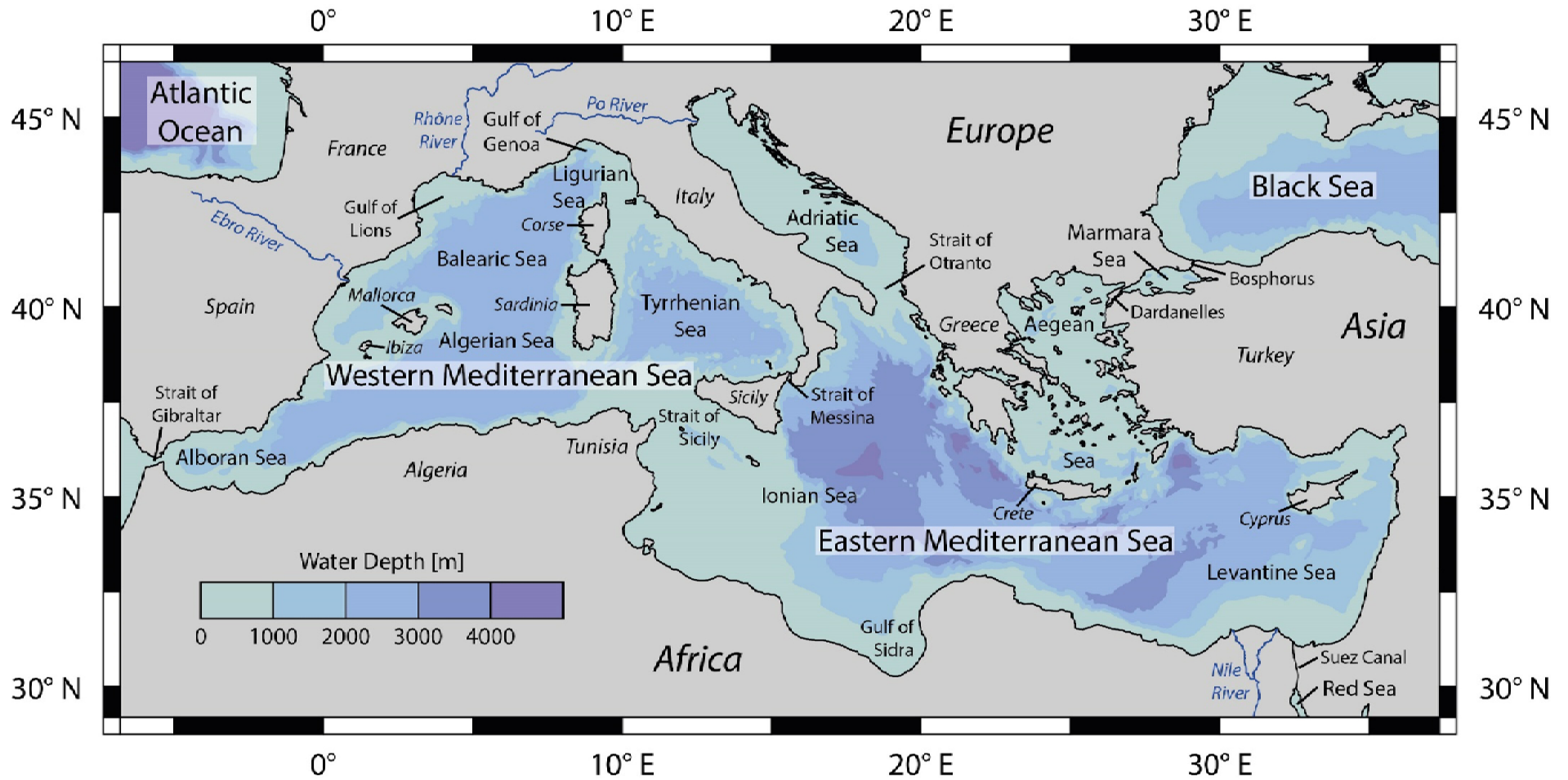


Figure 2. Geographic and bathymetric map of the Mediterranean Sea. The main seas, basins, gulfs, straits, islands, adjacent countries, and rivers mentioned in this thesis are given. Depth differences of 1000m are shown by a different blue colors.

2. Study area

2.2 Oceanographic conditions

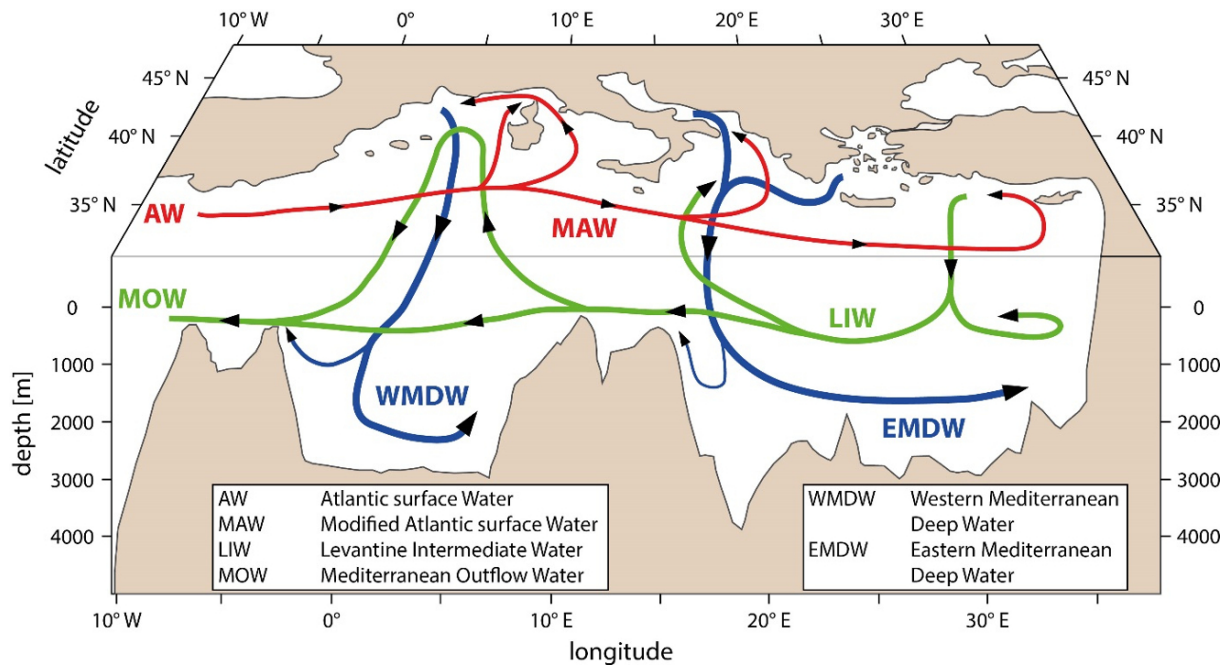


Figure 3. A simplified general circulation scheme of the Mediterranean Sea (modified after Millot & Taupier-Letage, 2005; Tsimplis et al., 2006; Pinardi et al., 2015). Surface water is marked in red, intermediate water in green and deep water in blue. The names and abbreviations of the most important currents are mentioned.

The anti-estuarine circulation of the Mediterranean Sea, with a negative water budget, fast water exchange and discrete intermediate and deep water formation lead to a highly complex current system (Fig. 3), susceptible even to small climatic shifts (Adloff et al., 2011; Lionello et al., 2012; Tanhua et al., 2013; Malanotte-Rizzoli et al., 2014). Due to the high number of islands and peninsulas, the Mediterranean Sea is separated into different sub-basins, which lead to numerous and variable surface current branches (Millot & Taupier-Letage, 2005; Poulain et al., 2013; Pinardi et al., 2015). The surface water originates from the Atlantic Ocean with salinity values below 37 psu at the Strait of Gibraltar (Wüst, 1961; Tanhua et al., 2013). After an eastward direction, the surface water is divided at the Strait of Sicily in a northern branch, flowing through the Tyrrhenian Sea or West of Sardinia to the north and a southern branch towards the Eastern Mediterranean Sea. In both basins a counterclockwise current pattern prevail. Due to stronger evaporation than precipitation and river run-off, the surface water salinity increases from west to east up to 39 psu in the central Levantine Basin (Wüst, 1961; Tanhua et al., 2013). This water property in combination with the high sea surface temperature is crucial for the formation of the warm and saline Levantine Intermediate Water (LIW) in the northern part of the Levantine Basin (Ovchinnikov, 1984; Pinardi & Massetti, 2000) (Fig. 3). Cold winds from Turkey cool down the surface water during winter, initiating the down welling towards a depth of about 200 to 600 m. The LIW fills the intermediate depths of the Eastern Mediterranean

2.2 Oceanographic conditions

Sea, flows westward into the Western Mediterranean Sea and finally into the Atlantic Ocean as main component of the Mediterranean Outflow (Millot, 2009). Within the Mediterranean Sea, the LIW is the most important source for the deep water formation in both sub-basins. The deep water masses are in general separated between the eastern and the western Mediterranean Sea due to the 360-430 m deep sill at the Strait of Sicily (Astraldi et al., 1999) (Fig. 3). The Western Mediterranean Deep Water (WMDW) is mainly formed in the Gulf of Lions during cold winters, due to the surface cooling by strong northern winds (Mistral, Tramontana) (MEDOC Group, 1970; Send et al., 1999; Smith et al., 2008). Due to variable winter temperatures, the deep water formation fluctuates and can be inhibited during warmer conditions (Millot, 1999). With a comparable mechanism, the Eastern Mediterranean Deep water (EMDW) is formed in the Adriatic and the Aegean Sea. For long time the Adriatic Sea was seen as the more important source of the EMDW (Wüst, 1961; POEM Group, 1992). However, a remarkable shift towards the Aegean Sea as main source in the early 1990s, the so called Eastern Mediterranean Transient (EMT), appeared (Roether et al., 1996; Lascaratos et al., 1999) and is still in the focus of investigation (Roether et al., 2014; Cardin et al., 2015). Due to Bernoulli aspiration, upper parts of the EMDW can be uplifted above the Sicily sill (Beranger et al., 2004) and are mixed with the LIW, thus forming a deep intermediate water mass between LIW and WMDW, the Tyrrhenian Deep Water (TDW) (Send et al., 1999).

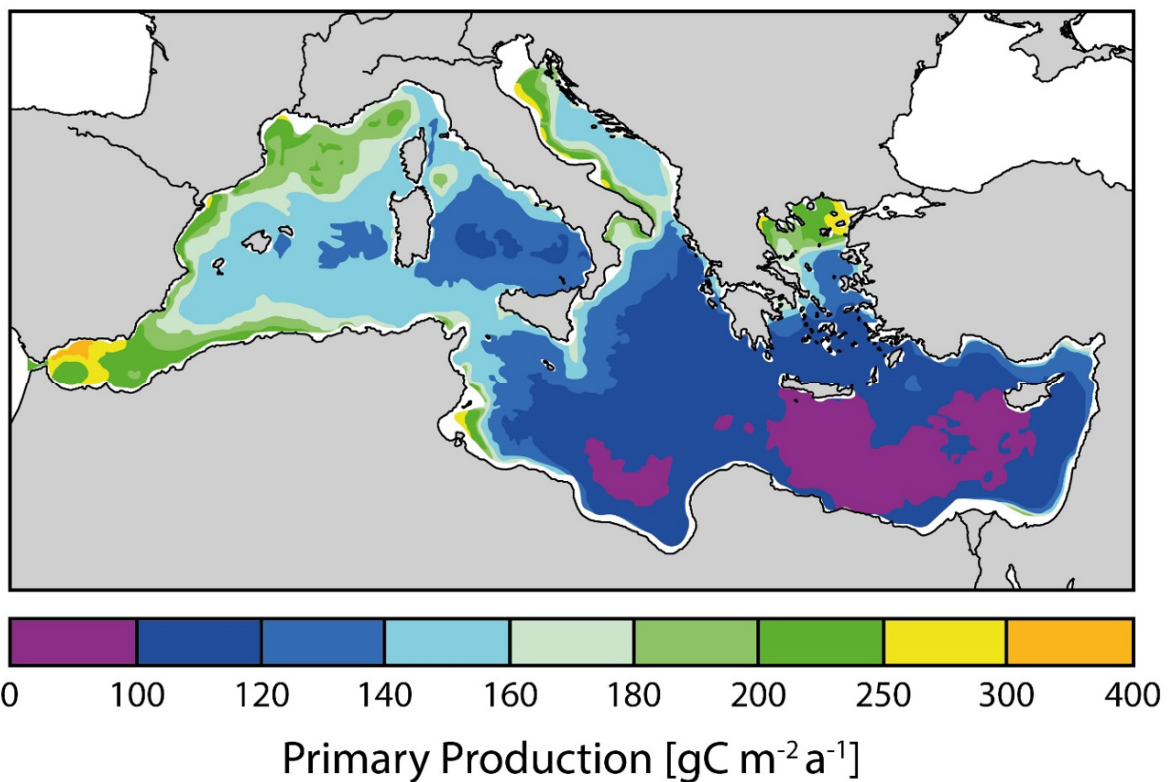


Figure 4. Map of the Mediterranean Sea with calculated annual values of primary production from satellite-borne measurements between 1997 and 2001. Modified after Bosc et al. (2004).

2. Study area

As a result of the anti-estuarine circulation and the net nutrient export, oligotrophic conditions prevail in the Mediterranean Sea (Tanhua et al., 2013). Especially the open Levantine Sea south of Crete shows ultra-oligotrophic conditions with an annual primary productivity below $100 \text{ gC m}^{-2} \text{ a}^{-1}$ (Psarra et al., 2000; Bosc et al., 2004) (Fig. 4). In contrast, the strong water column mixing of the two anti-cyclonic gyres in the Alboran Sea together with the direct supply of relatively nutrient enriched Atlantic water, makes this region to one of the most productive of the Mediterranean Sea. The stronger oligotrophic conditions of the eastern Mediterranean are a result of the higher water column stratification, leading to nearly nutrient depleted surface waters (e.g. Pujo-Pay et al., 2011). If these are supplied by external sources, e.g. Nile River, Po River, Black Sea, the productivity increases remarkably (Fig. 4).

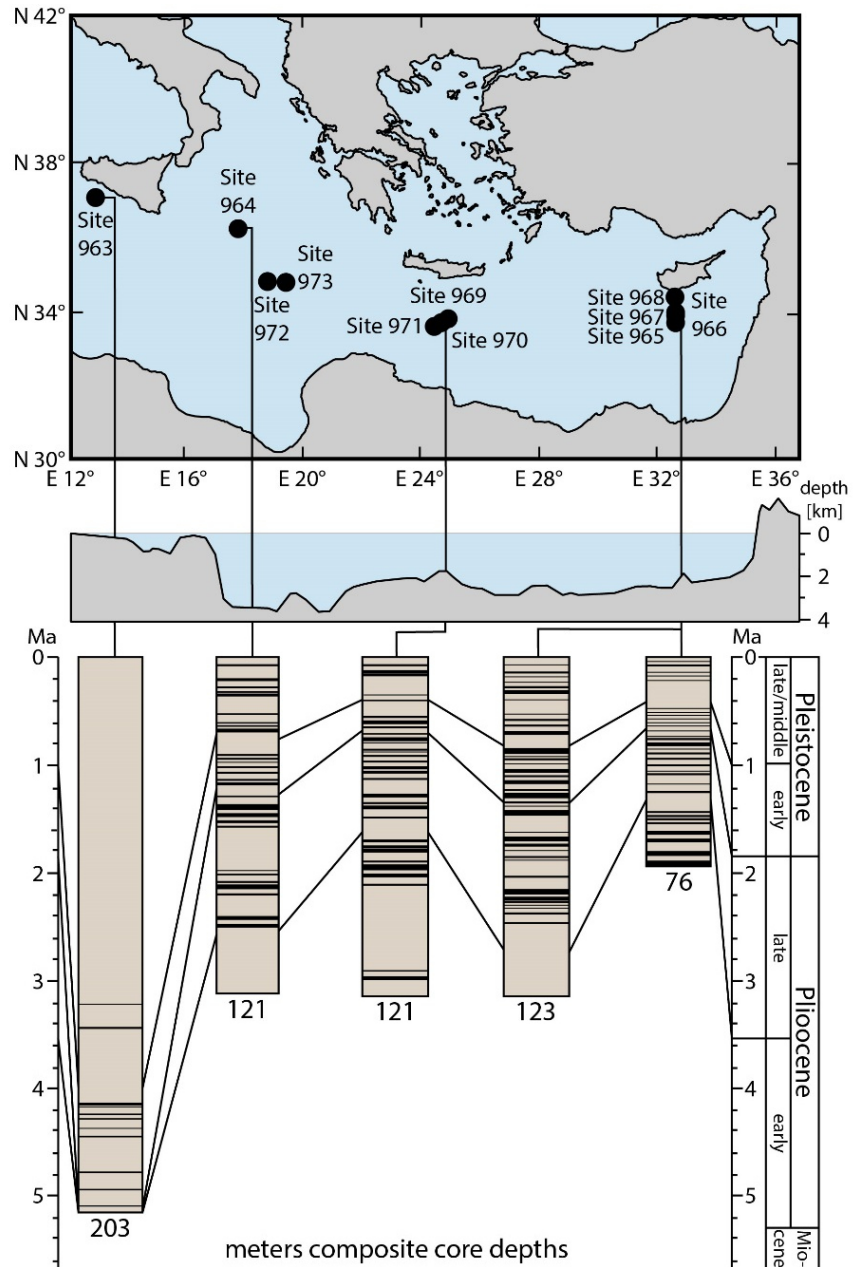
2.3 Development of the Mediterranean Sea

The present Mediterranean Sea is a remnant of the Tethys Ocean, which was a large Gulf east of Gondwana during the Mesozoic. With the breakup of Gondwana this Gulf became connected to the early Atlantic in the west and was compressed by the northward movement of the African plate. This led to the closure of the Tethys during the Cenozoic (Rögl, 1999). With the collision of the African, the Arabian and the Eurasian plates the separation and differentiation of the Mediterranean Sea and the Paratethys took place (Abrantes et al., 2012). The Paratethys was a large epicontinental sea in the north and east of the Mediterranean Basin, which existed since the early Oligocene and was the precursor of the recent Black and Caspian Seas (Rögl, 1999; Schulz et al., 2005). During the Miocene, approx. 11 Ma ago, the eastern seaway closed ultimately (Hüsing et al., 2009) and the connection towards the Atlantic Ocean existed via a northern (through the Betic Strait) and a southern seaway (Riffian Gateway) (Abrantes et al., 2012). The continuing compression closed these connections during the Late Miocene, which resulted in the Mediterranean Salinity Crisis during the Messinian, with a partially to complete desiccation of the Mediterranean Sea between 5.96 to 5.33 Ma BP (Hsü et al., 1973; 1977; Cita et al., 1978; Hilgen et al., 2007). The rapid flooding of the basin at the Miocene/Pliocene boundary was caused either by tectonic movements or by fluvial incisions due to the extreme sea level differences between the Atlantic and Mediterranean Sea of at least 1500 m (Loget & van den Driessche, 2006; Sierro et al., 2008; Garcia-Castellanos et al., 2009). Afterwards a stepwise global cooling led to the onset of glacial-interglacial cycles at the transition to the Pleistocene (Combourieu-Nebout et al., 2000; Popescu et al., 2010). However, during the early Pliocene comparable conditions to the present Mediterranean Sea set on, i.e. the anti-estuarine current system at the Strait of Gibraltar and the recurring appearance of organic rich layers, so called sapropels (Rossignol-Strick, 1984; Cramp & O'Sullivan, 1999; Rohling et al., 2015) (Fig. 5). The short-term sapropel events, which are linked to maxima in summer insolation of the northern hemisphere,

2.3 Development of the Mediterranean Sea

reveal dramatic changes in the Mediterranean oceanography (Rohling et al., 2015). Although they are more abundant in deeper parts of the Eastern Mediterranean Sea, sapropels with lower C_{org} contents also occurred in the deeper western basin, especially in the Tyrrhenian Sea (Emeis et al., 1991; Murat, 1999; Rogerson et al., 2008). It is still under debate, if sapropel depositions are caused by stagnating deep water with resulting bottom water anoxia (Rossignol-Strick, 1983; Rohling & Hilgen, 1991; Grimm et al., 2015), increased productivity (Calvert, 1983; Calvert et al., 1992) or a combination of both factors (Rohling, 1994; Emeis et al., 1998; Rohling et al., 2015).

Figure 5. Sites of ODP Leg 160 (1995) in the Eastern Mediterranean Sea with schematic occurrences of sapropels during the Pleistocene and Pliocene. Modified after Emeis et al. (1996).



3. Stable isotope composition of deep-sea benthic foraminifera under contrasting trophic conditions in the western Mediterranean Sea

Abstract

We have evaluated the environmental and biological processes affecting the stable oxygen and carbon isotope composition of live (Rose Bengal stained) and dead (unstained) tests of different benthic foraminiferal species from the western Mediterranean Sea. Samples were retrieved from comparable water depths but contrasting trophic regimes, comprising the meso- to eutrophic Alboran Sea and the oligo- to mesotrophic Mallorca Channel. The recorded isotope signatures mirror the average microhabitat depth of each species and reflect the specific gradients in pore water $\delta^{13}\text{C}$ of dissolved inorganic carbon ($\delta^{13}\text{C}_{\text{DIC}}$) and oxygen. Maximum $\delta^{13}\text{C}_{\text{DIC}}$ pore water gradients of up to -2.3‰ were estimated under the influence of meso- to eutrophic conditions in the Alboran Sea. The $\delta^{13}\text{C}$ signal of *Uvigerina mediterranea* reflects the opportunistic behavior of this species as its $\delta^{13}\text{C}$ is shifted to more negative values at higher organic matter fluxes. Accordingly, the $\delta^{13}\text{C}$ signal of *U. mediterranea* appears particularly suitable as a proxy for quantitative reconstructions of past trophic conditions. Previously reported ontogenetic increase of stable isotope values is confirmed for buliminid taxa (genera *Uvigerina* and *Globobulimina*), while it is largely absent in rotaliid taxa (genera *Cicidides*, *Cibicidoides*, and *Melonis*). Particularly strong metabolic fractionation is observed in small specimens of *Uvigerina peregrina* overprinting the pore-water $\delta^{13}\text{C}_{\text{DIC}}$ signal and resulting in steep ontogenetic $\delta^{13}\text{C}$ gradients. The $\delta^{18}\text{O}$ values of epifaunal taxa, which thrive under high dissolved oxygen concentrations, and the shallow to intermediate infaunal *Melonis barleeanum*, are up to 1.2‰ lower relative to equilibrium calcite. In epifaunal taxa, this depletion can be attributed to enhanced fractionation at high concentrations of metabolically utilizable oxygen.

This chapter is based on:

Theodor, M., Schmiedl, G., Mackensen, A., 2016. Stable isotope composition of deep-sea benthic foraminifera under contrasting trophic conditions in the western Mediterranean Sea. *Marine Micropaleontology* 124, 16-28, doi:10.1016/j.marmicro.2016.02.001

3. Stable isotope composition of benthic foraminifera under contrasting trophic conditions

3.1 Introduction

The stable oxygen and carbon isotope compositions of foraminifera are widely used as proxies for the reconstruction of past climate and ocean circulation changes. The $\delta^{18}\text{O}$ signal of deep-sea benthic foraminifera ($\delta^{18}\text{O}_{\text{For}}$) mainly contains the signal of global ice volume and is commonly applied to the reconstruction of global glaciation states, sea-level changes and for stratigraphic purposes (e.g. Shackleton & Opdyke, 1973; Zachos et al., 2001; Waelbroeck et al., 2002; Lisiecki & Raymo, 2005). The benthic foraminiferal $\delta^{13}\text{C}$ ($\delta^{13}\text{C}_{\text{For}}$) signal provides information on past ocean circulation changes and the marine carbon cycle (e.g. Curry & Lohmann, 1982; Zahn et al., 1986; Duplessy et al., 1988; Bickert & Mackensen, 2004; Mackensen, 2008). In a simplified view, the foraminiferal stable isotope signal mirrors the physical conditions and composition of ambient bottom and pore waters at the time of calcification, i.e. for oxygen the equilibrium calcite $\delta^{18}\text{O}$ ($\delta^{18}\text{O}_{\text{EQ}}$) and for carbon the $\delta^{13}\text{C}$ of dissolved inorganic carbon ($\delta^{13}\text{C}_{\text{DIC}}$). However, the isotope signal is additionally influenced by various ecological and biological effects, which result in significant offsets relative to the ambient bottom water and equilibrium conditions (Rohling & Cook, 1999; Ravelo & Hillaire-Marcel, 2007; Mackensen, 2008).

One important process is related to microbial remineralization of organic matter at the sea floor resulting in a decrease of pore water $\delta^{13}\text{C}_{\text{DIC}}$ with increasing sediment depth of up to -1.0‰ cm^{-1} (McCorkle et al., 1985; Stott et al., 2000; Holsten et al., 2004). Since different benthic foraminifera inhabit different microhabitats on or within the sediment (Corliss, 1985; Jorissen et al., 1995), the pore water effect accounts for significantly lower $\delta^{13}\text{C}_{\text{For}}$ values of infaunal species, with lowest values observed in deep infaunal taxa such as *Chilostomella* spp., *Globobulimina* spp. and *Pleurostomella* spp. (Grossman 1984a; McCorkle et al., 1990, 1997; Schmiedl et al., 2004). At sites of rapid phytodetritus deposition, negative offsets of $\delta^{13}\text{C}_{\text{For}}$ from ambient bottom water DIC can even occur in the strictly epifaunal species *Cibicoides wuellerstorfi* (Mackensen et al., 1993). On the other hand, most taxa seem to reflect the isotopic composition of the porewater $\delta^{13}\text{C}_{\text{DIC}}$ close to the upper part of their average living depth (McCorkle et al., 1990; Loubere et al. 1995; Rathburn et al., 1996; Schmiedl et al., 2004; Mackensen & Licari, 2004) although specimens are able to shift their microhabitat responding to changes in oxygen and food availability and are often found alive over a relatively wide depth range (Linke & Lutze, 1993; Ohga & Kitazato, 1993). Accordingly, the $\delta^{13}\text{C}_{\text{For}}$ difference between epifaunal and preferentially shallow infaunal taxa reflects the intensity of organic matter remineralization and can thus be used for the estimation of organic matter flux rates (Zahn et al., 1986; McCorkle and Emerson, 1988; Vergnaud-Grazzini & Pierre, 1991; Schilman et al., 2003). In addition, at depth in the sediment where oxygen approaches zero the $\delta^{13}\text{C}_{\text{DIC}}$ is directly proportional to the oxygen concentration of the bottom water mass (McCorkle and Emerson, 1988). Based on this observation, the difference between $\delta^{13}\text{C}_{\text{For}}$ of epifaunal and deep infaunal species was

3.1 Introduction

successfully applied to the quantification of changes in bottom water oxygenation during the late Quaternary (Schmiedl & Mackensen, 2006; Hoogakker et al., 2014).

There is increasing evidence that the stable isotope signal of foraminifera is also influenced by the carbonate ion concentration of the ambient water, which is closely related to alkalinity and pH (Spero et al., 1997; Bemis et al., 1998; Zeebe et al., 1999; Mackensen, 2008). The magnitude of this effect in benthic foraminifera is not yet well constrained but both carbonate ion gradients in the pore water (Jahnke et al., 1994; Martin & Sayles 1996) and within cysts during calcification (Diz et al., 2012) may play a relevant role.

Additional isotope fractionation in the form of species-specific 'vital effects' are caused by incorporation of metabolic CO₂ during precipitation of test calcite and during the processes of hydration and hydroxylation at variable metabolic rates (Erez, 1978; Grossman, 1984a, b; McConnaughey, 1989a, b; Mackensen, 2008). It is generally assumed that the metabolic rate decreases during ontogeny of planktonic foraminifera, explaining increasingly heavier stable isotope values with increasing test size (Spero & Lea, 1996; Spero et al., 1997). Comparable ontogenetic trends in benthic foraminifera reveal a more inconsistent picture, with species-dependent constant, increasing or decreasing $\delta^{13}\text{C}_{\text{For}}$ and $\delta^{18}\text{O}_{\text{For}}$ values with increasing test sizes (Dunbar & Wefer, 1984; Grossman, 1984a, b, 1987; Wefer & Berger, 1991; Corliss et al., 2002; Schmiedl et al., 2004, McCorkle et al., 2008, Schumacher et al., 2010; Diz et al., 2012). To date, only one study (Dunbar & Wefer, 1984) included a comprehensive multi-species approach.

Here, we evaluate the biological and environmental effects on the stable isotope signatures of live (Rose Bengal stained) and dead (unstained) benthic foraminifera from several middle bathyal sites of the western Mediterranean Sea. The major target of our study is to improve the applicability of deep-sea benthic foraminifera in quantitative paleoenvironmental reconstructions. The present western Mediterranean Sea is ideally suited for this study, because it is well ventilated and its intermediate and deep-water $\delta^{18}\text{O}_{\text{Water}}$ and $\delta^{13}\text{C}_{\text{DIC}}$ compositions are relatively homogenous (Pierre, 1999). The measured benthic foraminiferal tests have grown under contrasting trophic regimes, including the meso- to eutrophic Alboran Sea and the oligo- to mesotrophic Mallorca Channel, SW of Mallorca Island (Fig. 6). A total of nine different species, representing the full range of epifaunal to deep infaunal microhabitats and associated pore water signals, have been included in the analysis. For further characterization of metabolic processes and ontogenetic effects, the stable isotope signals of three common shallow to intermediate infaunal species (*Uvigerina peregrina*, *Uvigerina mediterranea* and *Melonis barleeanum*) were determined for various test size classes.

3.2 Study Area

The semi-enclosed Mediterranean Sea exhibits strong gradients in temperature, salinity and surface water productivity, which are caused by the overall anti-estuarine circulation, high evaporation rates, inflow of nutrients through rivers and with Atlantic surface waters and loss of salt and nutrients through the Mediterranean outflow (Pinardi & Masetti, 2000; Tanhua et al., 2013; Rohling et al., 2015). Due to the anticlockwise surface circulation of the western Mediterranean Sea, the Alboran Sea is influenced by relatively fresh Atlantic surface waters, while the areas around

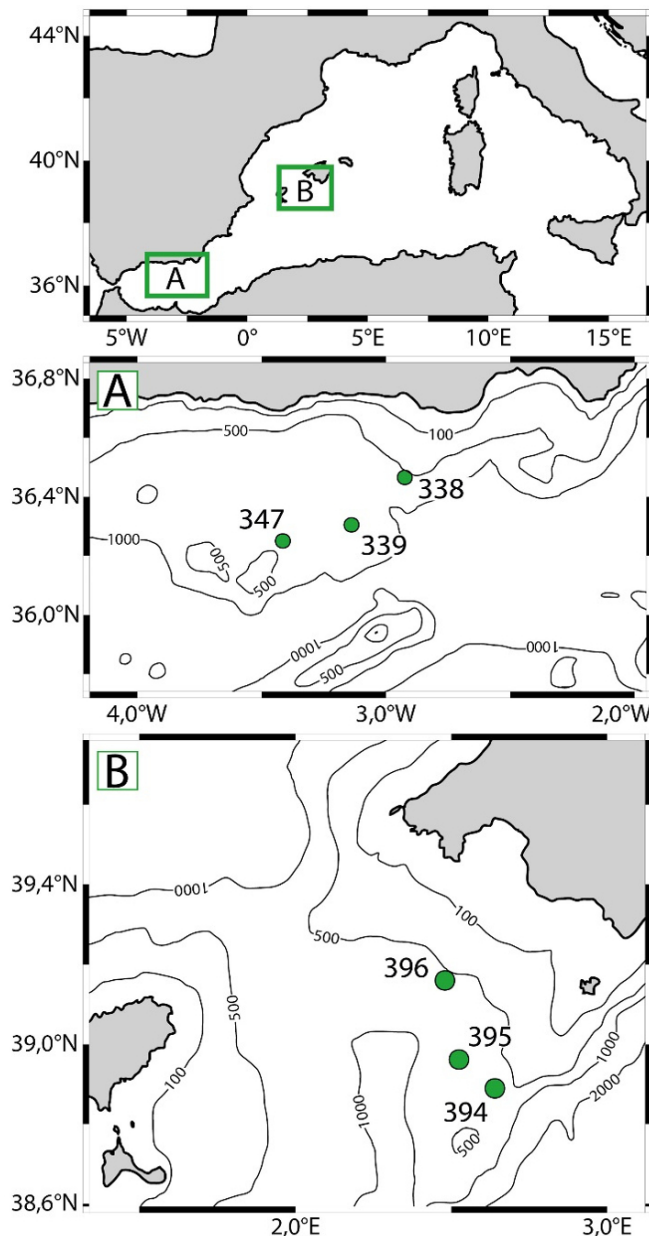


Figure 6. Location of the study areas in the western Mediterranean Sea and regional bathymetric maps with location of sample sites in the (a) Alboran Sea and the (b) Mallorca Channel southwest of Mallorca Island.

Mallorca exhibit significantly higher salinities because surface waters are derived from Algerian Basin eddies in the south and the Liguro-Provençal-Catalan Current (LPCC) in the north (Millot, 1999; Millot & Taupier-Letage, 2005). The investigated sites are all located within a depth range of 500 to 1000 m, implying a bathing by the lower part of the Levantine Intermediate Water (LIW) and the upper part of the Tyrrhenian Deep Water (TDW) (Fig. 6, Table 1). The LIW originates in the eastern Mediterranean Sea and its salinity maximum is observed between 200 and 500 m water depth (e.g. Tanhua et al., 2013). The LIW is an important factor for western Mediterranean deep-water formation (Millot, 1999; 2013). The TDW emerges in the Tyrrhenian Sea probably as a mixture of LIW and Western Mediterranean Deep Water (WMDW) (Rhein et al., 1999; Send et al., 1999) or as a result of deep-water formation east of the Bonifacio Strait (Fuda et al., 2002). The TDW is distributed at 600-1600/1900 m (Rhein et al., 1999) respectively 900-1300 m depth (Send et al., 1999) within the Algero-Provençal Basin.

3.2 Study Area

The Alboran Sea contains two anti-cyclonic gyres, the stable Western Alboran Gyre (WAG) and the more variable Eastern Alboran Gyre (EAG) (Millot, 1999; Millot & Taupier-Letage, 2005). The LIW and parts of the underlying deep water flow westward and leave the Alboran Sea through the Strait of Gibraltar (Millot, 1999; 2009). At 500-1000 m water depth, salinities range between 38.44 to 38.47 psu, temperatures are around 13 °C, $\delta^{18}\text{O}_{\text{Water}}$ values are 1.44-1.45 ‰ SMOW, and $\delta^{13}\text{C}_{\text{DIC}}$ values are 1.04-1.06 ‰ PDB (Pierre, 1999; Rhein et al., 1999; Tanhua et al., 2013) (Table 1). In contrast to most other parts of the Mediterranean Sea, surface productivity is high in the Alboran Sea, with values of 200-300 gC m⁻² a⁻¹ (Bosc et al., 2004). Highest productivity occurs in upwelling zones at the northern part of the WAG and at the Almeria-Oran-Front (AOF) (Garcia-Gorriz & Carr, 2001; Bárcena et al., 2004; Hernández-Almeida et al., 2011). The spatial distribution and intensity of phytoplankton blooms depend on the variable size and position of the EAG (Heburn & La Violette, 1990; Moran & Estrada, 2001; Fabres et al., 2002; Sanchez-Vidal et al., 2004). The main phytoplankton blooms occur between November and March, while blooms are absent in stratified surface waters from May to September (Garcia-Gorriz & Carr, 1999). The amount of organic matter (OM) arriving at the sea floor is decreasing from west to east and with increasing distance to the coast (Masqué et al., 2003). Comparisons between sediment trap and surface sediment data indicate lateral particle transport in nepheloid layers at the sediment-water interface leading to a homogenization of the spatial OM distribution (Fabres et al., 2002; Masqué et al., 2003; Sanchez-Vidal et al., 2005).

The Balearic Sea is characterized by an open marine setting with transitional conditions between the Algerian Basin in the south, mainly influenced by anticyclonic coastal eddies originating at the Algerian Coast, and the strong LPCC north of the Balearic promontory (Millot & Taupier-Letage, 2005). While the LPCC is mostly passing the sill of the Ibiza Channel to the south, the water of the Algerian Basin is passing northwards through the 500 m deep Mallorca Channel, also bathing the study sites (Pinot et al., 2002) (Fig. 6). The water masses between 500 and 1000 m are dominated by LIW, with salinities around 38.5 psu, temperatures between 12.5 and 12.7 °C, $\delta^{18}\text{O}_{\text{Water}}$ values of 1.48-1.53 ‰ SMOW, and $\delta^{13}\text{C}_{\text{DIC}}$ values between 0.96 and 0.98 ‰ PDB (Pierre, 1999; Rhein et al., 1999; Tanhua et al., 2013) (Table 1). The open Algerian Basin south of Mallorca is characterized by oligo- to mesotrophic conditions, with an annual primary production of 140-160 gC m⁻² a⁻¹ (Bosc et al., 2004). Highest chlorophyll a values occur during winter and early spring, while nutrient input is low during summer related to weak physical mixing and enhanced thermal stratification (Zúñiga et al., 2007; 2008).

3. Stable isotope composition of benthic foraminifera under contrasting trophic conditions

Table 1. Position, water depth, sampling date, oceanographic, geochemical, and selected calcareous benthic foraminiferal faunal data of the studied multicorer sites from the Alboran Sea and the Mallorca Channel. Temperature, salinity and stable isotope data interpolated from Pierre (1999), equilibrium calcite $\delta^{18}\text{O}$ calculated after O'Neil et al. (1969) as well as Kim & O'Neil (1997).

| Region | Alboran Sea | | | Mallorca Channel | | |
|---|-------------|-------------|-------------|------------------|-------------|-------------|
| | Site | 338 | 339 | 347 | 394 | 395 |
| Latitude | 36°15.03' N | 36°18.30' N | 36°27.90' N | 38°53.39' N | 38°57.70' N | 39°09.60' N |
| Longitude | 3°24.98' W | 3°08.39' W | 2°55.50' W | 2°38.40' E | 2°31.51' E | 2°28.78' E |
| Water depth [m] | 732 | 849 | 629 | 646 | 834 | 562 |
| Sampling date (d/m/y) | 17/08/2006 | 17/08/2006 | 18/08/2006 | 25/08/2006 | 25/08/2006 | 25/08/2006 |
| Bottom water temp. [°C] | 12.8-13.0 | 12.8-13.0 | 12.8-13.0 | 12.6 | 12.6 | 12.6-12.7 |
| Bottom water salinity [psu] | 38.44-38.47 | 38.44-38.46 | 38.45-38.47 | 38.48 | 38.48 | 38.48-38.49 |
| TOC (0-1 cm) [wt.-%] | 0.83 | 0.77 | 0.83 | --- | 0.46 | 0.40 |
| C/N (0-1 cm) | 4.12 | 3.96 | 3.61 | --- | 6.96 | 7.94 |
| Redox boundary depth [cm] | 1.5 | 2.5 | 1.5 | 8.0 | 7.0 | 12.0 |
| Bottom water $\delta^{18}\text{O}$ [‰ VSMOW] | 1.44-1.45 | 1.44-1.45 | 1.44-1.45 | 1.51-1.53 | 1.48-1.51 | 1.48-1.53 |
| $\delta^{18}\text{O}$ equilibrium calcite [‰ VPDB]; Kim & O'Neil, 1997 | 1.85-1.91 | 1.85-1.91 | 1.85-1.91 | 2.01-2.03 | 1.98-2.01 | 1.96-2.03 |
| $\delta^{18}\text{O}$ equilibrium calcite [‰ VPDB]; O'Neil et al., 1969 | 2.11-2.16 | 2.11-2.16 | 2.11-2.16 | 2.27-2.30 | 2.25-2.28 | 2.23-2.29 |
| Bottom water $\delta^{13}\text{C}$ [‰ VPDB] | 1.04 | 1.05 | 1.06 | 0.97 | 0.98 | 0.96 |
| Median/ Average Living depth (calc. fauna) [cm] | 0.90/1.54 | 0.92/1.66 | 0.86/1.32 | 1.00/2.04 | 0.77/1.41 | 0.74/1.19 |
| Standing stock live (calc. fauna) [Ind. cm ⁻²] | 14.14 | 10.05 | 12.70 | 2.79 | 4.06 | 2.34 |
| Standing stock dead (total fauna) [Ind. cm ⁻³] | 251.24 | 154.85 | 376.98 | 775.17 | 298.87 | 594.13 |
| Diversity live (calc. fauna) [H(S)] | 2.19 | 2.13 | 2.53 | 1.59 | 1.20 | 1.73 |
| Diversity dead (total fauna) [H(S)] | 2.98 | 2.97 | 3.05 | 3.83 | 3.04 | 3.50 |

The study areas in the Western Mediterranean Sea are characterized by hemipelagic sedimentation, typically comprising pteropod-bearing foraminiferal and nannofossil mud or ooze with minor contribution of terrigenous components (Vazquez & Zamarreño, 1993; Weldeab et al., 2003). Dust input from northern Africa forms an important source for terrigenous components. In addition to the siliciclastic components, eolian input of degraded terrestrial organic matter to the open Algerian-Balearic Basin sporadically occurs during summer (Migon et al., 2002; Zúñiga et al., 2008).

3.3 Material and Methods

Undisturbed surface sediment samples were recovered with a multicorer in August 2006 during R.V. *Meteor* cruise M69/1 along middle bathyal transects (560-850 m water depth) on the open slope of the Alboran Sea and the southern Mallorca Channel (western Mediterranean Sea) (Hübscher et al., 2010) (Fig. 6, Table 1). For the study of benthic foraminifera, the uppermost 10 cm of surface sediment were cut into slices of 0.5 cm (for the uppermost cm) and 1 cm (below 1 cm depth). All samples were preserved with Rose Bengal stained ethanol (1.5 g l⁻¹) immediately after core retrieval as a common method to stain cytoplasm of (recently) living foraminifera (Walton, 1952; Bernhard, 2000). In summer 2009, the sediment samples were wet-sieved over a 63 µm mesh and after drying at 40 °C, dry-sieved over a 125 µm mesh sieve in the laboratory. With respect to the oxygen and carbon isotope measurements only calcareous foraminifera from the size fraction >125 µm were selected from the cores. Tests that showed at least three subsequent clearly red stained chambers were considered as living.

Total standing stocks of calcareous taxa were integrated over the 0-10 cm interval and referred to 1 cm². The Shannon-Wiener diversity index was calculated according to Buzas and Gibson (1969). In addition to the Average Living Depth ALD_x (Jorissen et al., 1995) we determined the Median Living Depth (MLD). For MLD calculation, the depth interval of the median has to be identified, which is (n/2) of all encountered tests from top downward. Subsequently, the MLD can be calculated as

$$MLD = ((l_m - u_m) / n_m) * (n / 2 - c_{n-1}) + u_m \quad [cm] \quad [1]$$

with n = total number of tests, n_m = number of tests in the median depth interval, c_{n-1} = number of tests shallower than the median depth interval; u_m = upper limit of the median depth interval; l_m = lower limit of the median depth interval. In contrast to the ALD_x, a reference of the MLD to a specific depth range is not necessary. However, it is important to count the sediment until the complete distribution is determined, which in general should be within the uppermost 10 cm. Differences between ALD₁₀ and MLD are commonly negligible, but can be relevant if a considerable number of stained tests of preferentially shallow infaunal taxa appears at greater depths or in case of other than unimodal down-core distributions. Specifically, such ALD₁₀/MLD differences are observed for *Uvigerina mediterranea* and deep infaunal species, which often show a wide range of down-core occurrences.

For general reference, the complete foraminiferal thanatocoenosis (including agglutinated tests) was determined from representative splits of the >125 µm fraction of the 4-5 cm interval. This depth was chosen, to minimize a microhabitat bias, but still obtaining an almost recent assemblage. The foraminiferal counts were normalized to a wet volume of 1 cm³. The test sizes of three abundant species (*U. peregrina*, *U. mediterranea*, *M. barleeanum*) were measured with an objective micrometer and divided into size classes at 50 µm (*Uvigerina* spp.) or 25 µm (*M. barleeanum*) spacing. Test sizes

3. Stable isotope composition of benthic foraminifera under contrasting trophic conditions

of the epifaunal and deep infaunal taxa were also determined, but due to their lower abundances no size classes were distinguished.

Between 1 and 7 individuals of nine different species were selected for size-dependent stable isotope measurements. For *U. peregrina*, *U. mediterranea* and *M. barleeanum* stained and unstained tests were measured from all stations. In addition, stained as well as unstained tests of various epifaunal (*Cibicidoides pachydermus*, *Planulina ariminensis*, *Lobatula lobatula*) and deep infaunal (*Globobulimina affinis*, *Globobulimina pseudospinescens* and *Globobulimina ovata*) species were measured based on their occurrences (Table A.3).

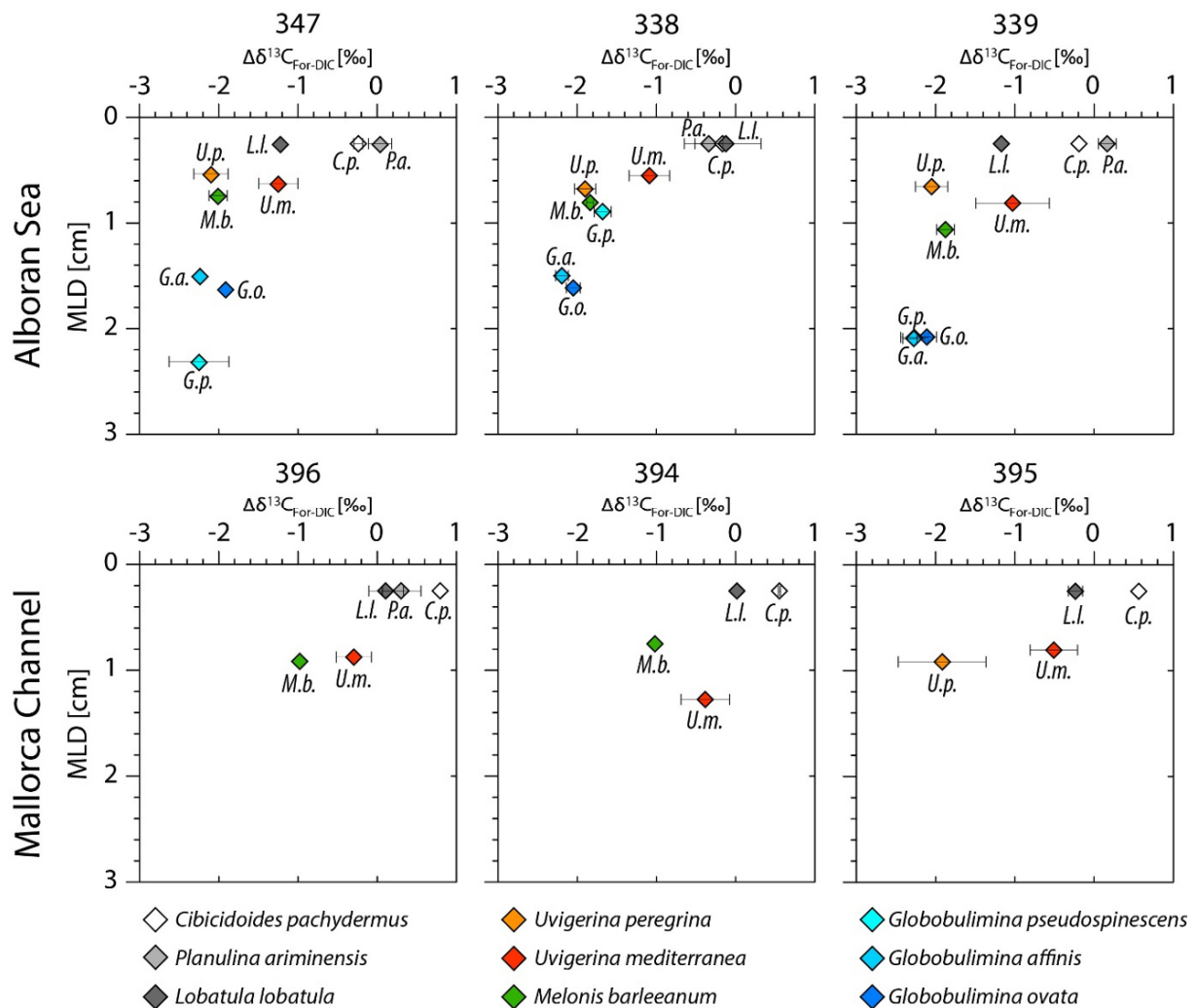


Figure 7. Difference between stable carbon isotope composition of stained foraminiferal test calcite $\delta^{13}C_{\text{For}}$ and ambient bottom water $\delta^{13}C_{\text{DIC}}$ ($\Delta\delta^{13}C_{\text{For-DIC}}$) versus median living depth from the Alboran Sea (upper panels) and the Mallorca Channel (lower panels). Due to a lack of stained epifaunal species (*C. pachydermus*, *P. ariminensis*, *L. lobatula*), the $\delta^{13}C_{\text{For}}$ values of unstained tests were used with a living depth of 0.25 cm.

Stable carbon and oxygen isotope measurements were carried out at the Alfred Wegener Institute Helmholtz Centre for Polar and Marine Research (Bremerhaven) with a Finnigan MAT 253 isotope ratio gas mass spectrometer coupled to an automatic carbonate preparation device (Kiel IV). The mass spectrometer was calibrated via the international standard NBS19 to the PDB scale and

3.4 Results

results are given in δ -notation versus VPDB. The precision of $\delta^{18}\text{O}$ and $\delta^{13}\text{C}$ measurements, based on an internal laboratory standard (Solnhofen limestone) measured over a one-year period, was better than ± 0.08 ‰ and ± 0.06 ‰ for Oxygen and Carbon, respectively. Total carbon, organic carbon and total nitrogen were analyzed using a Carlo Erba 1500 CNS Analyser. The precision of measurements was 0.01 % for total carbon and 0.002 % for nitrogen. Total organic carbon was measured after removal of CaCO_3 by adding 1N HCl, with a precision of 0.02 %. The recurring color change in surface sediments from yellowish brown to greenish grey was used as an indicator for the change in redox potential from positive to negative values (Lyle, 1983). Although this color/redox change is not necessarily identical to the depth of utilizable or free oxygen in the sediment, it can be used as an approximation of aerobic organic matter remineralization and thus oxygen consumption in the surface sediment (Schmiedl et al., 2000). Temperature, salinity, as well as bottom water carbon and oxygen isotope values were interpolated from the literature (Pierre, 1999) (Table 1). To calculate $\delta^{18}\text{O}_{\text{EQ}}$ we used the linear equation of Bemis et al. (1998), based on Kim and O'Neil (1997) on equilibrium oxygen isotopic fractionation of inorganically precipitated calcite. To facilitate comparison with Schmiedl et al. (2004) we calculated $\delta^{18}\text{O}_{\text{EQ}}$ after Shackleton's (1974) quadratic approximation of the data of O'Neil et al. (1969). Although the offsets varied clearly, the deviation between calculated mean $\delta^{18}\text{O}_{\text{EQ}}$ values was constantly at 0.26-0.27 ‰.

3.4 Results

3.4.1 Biogeochemistry and distribution of calcareous benthic foraminifera

The depth of the principal redox boundary, marked by a color change, as well as TOC and C/N values of the uppermost 0.5 cm of the surface sediment reveal significant contrasts between the two study areas. At middle bathyal depth of the Alboran Sea, the main redox boundary occurred at 1.5-2.5 cm depth, TOC values ranged between 0.77 and 0.85 wgt.-% and C/N ratios were 3.6-4.1 (Table 1). At middle bathyal depth of the Mallorca Channel, the principal redox boundary was considerably deeper (7-12 cm), TOC values were lower and ranged between 0.4 and 0.46 wgt.-% and C/N ratios were higher (7.0-7.9) (Table 1).

The total standing stocks of calcareous benthic foraminifera, integrated over the interval of the upper 10 cm of the surface sediment, are 10-14 Ind. cm^{-2} in the Alboran Sea and 2-4 Ind. cm^{-2} in the Mallorca Channel. Shannon-Wiener diversity values of the biocoenosis range from $H(S) = 2.13-2.53$ in the Alboran Sea to $H(S) = 1.20-1.73$ in the Mallorca Channel (Table 1). In contrast, density and diversity of the dead assemblage in the 4-5 cm depth interval are 155-377 Ind. cm^{-3} and $H(S) = 2.97-3.05$ in the Alboran Sea, and 299-775 Ind. cm^{-3} and $H(S) = 3.04-3.83$ in the Mallorca Channel (Table 1). The benthic foraminiferal fauna is dominated by epifaunal and shallow infaunal taxa at all sites. Deep infaunal globobuliminids are completely absent in the Mallorca Channel, while they

3. Stable isotope composition of benthic foraminifera under contrasting trophic conditions

represent 17-31 % of the total calcareous live assemblages in the Alboran Sea (Table A.1). At Sites 338 and 339 of the Alboran Sea, *U. peregrina* dominates the live and dead assemblages with 39-43 % and 25-26 %, respectively. Site 347 reveals significant differences between the biocoenosis and thanatocoenosis. In the Mallorca Channel, all sites are dominated by *U. mediterranea*, with values of 44-65 %, associated with *Bulimina marginata* (8.8-13.9 %) and *U. peregrina* (2.6-18.7 %) (Table A.2).

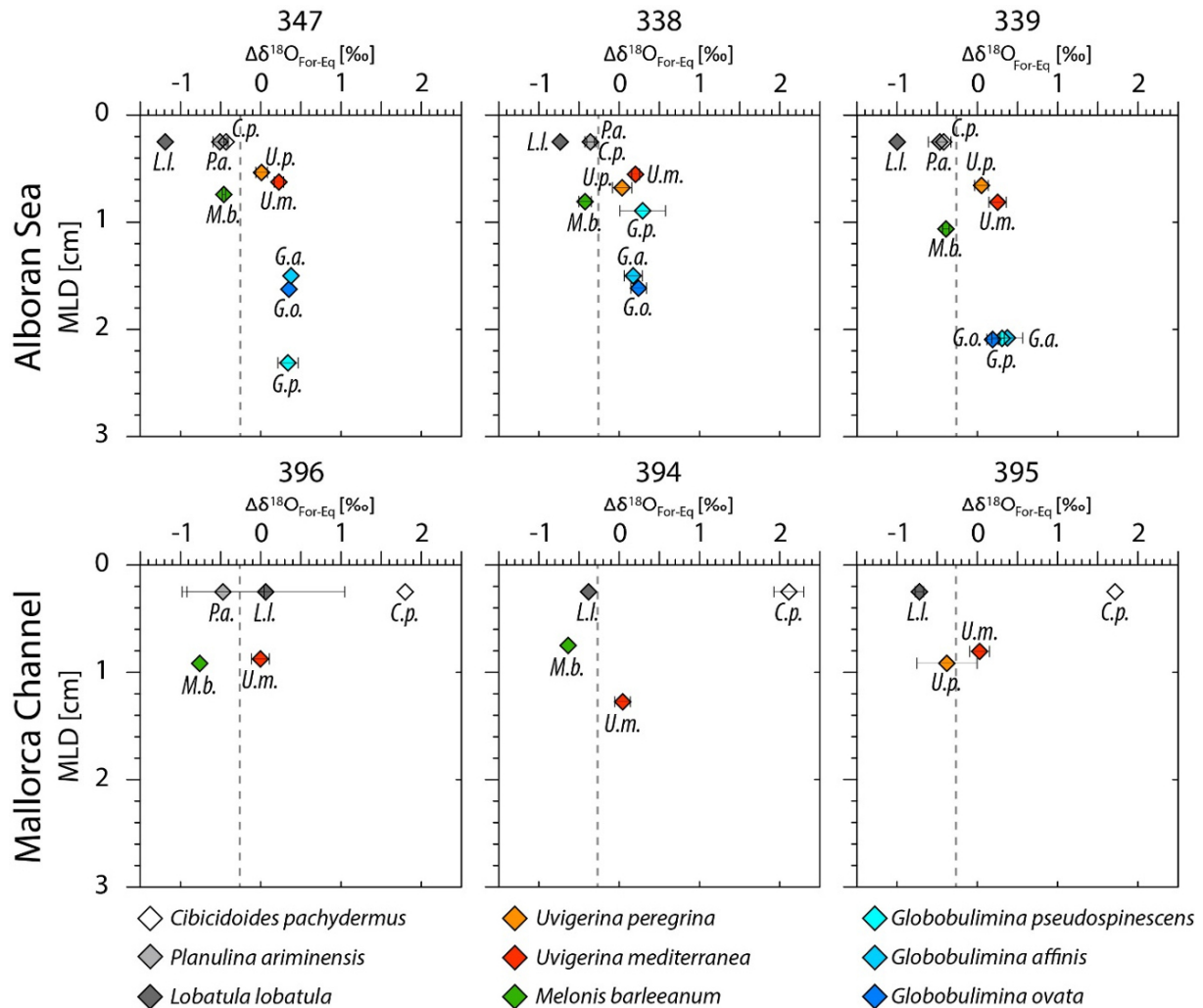


Figure 8. Difference between stable oxygen isotope composition of stained foraminiferal test calcite $\delta^{18}\text{O}_{\text{For}}$ and equilibrium calcite $\delta^{18}\text{O}_{\text{Eq}}$ after O'Neil et al. (1969) ($\Delta\delta^{18}\text{O}_{\text{For-Eq}}$) versus median living depth from the Alboran Sea (upper panels) and the Mallorca Channel (lower panels). Due to a lack of stained epifaunal species (*C. pachydermus*, *P. ariminensis*, *L. lobatula*), the $\delta^{18}\text{O}_{\text{For}}$ values of unstained tests were used at an estimated living depth of 0.25 cm. For a better comparison the equilibrium calcite $\delta^{18}\text{O}_{\text{Eq}}$ calculated after Kim & O'Neil (1997) is marked by the stippled line.

3.4.2 Stable isotope composition in relation to equilibrium calcite and bottom water DIC

The stable isotope compositions of live specimens display a wide range of values and characteristic deviations from $\delta^{13}\text{C}_{\text{DIC}}$ of bottom water dissolved inorganic carbon and from equilibrium $\delta^{18}\text{O}_{\text{Eq}}$ of calcite (Figs. 7, 8, Table A.4). The total ranges of the stable isotope values are -1.93 to 1.05 ‰ for $\delta^{13}\text{C}_{\text{For}}$ and 0.83 to 2.88 ‰ for $\delta^{18}\text{O}_{\text{For}}$ in live individuals and are -1.43 to 1.76 ‰

3.4 Results

for $\delta^{13}\text{C}_{\text{For}}$ and 0.95 to 4.53 ‰ for $\delta^{18}\text{O}_{\text{For}}$ in dead individuals. The different taxa exhibit species-specific deviations from $\delta^{13}\text{C}_{\text{DIC}}$ and $\delta^{18}\text{O}_{\text{EQ}}$. Generally, the $\Delta\delta^{13}\text{C}_{\text{For-DIC}}$ values become more negative with increasing microhabitat depth, but values of the shallow infaunal *U. peregrina* (MLD <1 cm) are similarly depleted as those of the deep infauna (MLD 1.5-2.5 cm) (Fig. 7). The $\Delta\delta^{18}\text{O}_{\text{For-EQ}}$ values are negative in epifaunal taxa and *M. barleeanum*, but positive or close to zero in *Uvigerina* and *Globobulimina* spp. (Fig. 8).

In each study area, similar isotope offsets and downcore patterns are observed. Mean $\Delta\delta^{13}\text{C}_{\text{For-DIC}}$ values of live *U. peregrina*, *U. mediterranea* and *M. barleeanum* are on average 0.10 ± 0.10 ‰, 0.73 ± 0.14 ‰, and 0.91 ± 0.09 ‰ lower in the Alboran Sea relative to the Mallorca Channel, respectively (Fig. 7). Excluding Site 396, $\delta^{13}\text{C}_{\text{For}}$ values of dead individuals are on average 0.30 ± 0.18 ‰ heavier in *U. peregrina* and 0.13 ± 0.11 ‰ heavier in *U. mediterranea* when compared to live individuals (Figs. 7, 9). Similar live-dead offsets are observed in *M. barleeanum*, where $\delta^{13}\text{C}_{\text{For}}$ values of dead individuals are on average 0.33 ± 0.28 ‰ heavier relative to live individuals (Figs. 7, 10).

3.4.3 Test size distribution and ontogenetic trends in stable isotope composition

The test size distributions of benthic foraminifera in the size fraction >125 μm display distinct intraspecific differences between locations as well as deviations between stained and unstained tests (Table A.3). The 584 tests of *U. mediterranea* show the widest size range of 140 to 1260 μm , with negligible differences between the study areas. A difference is observed between stained and unstained tests, with peaks around 700-800 μm in the live assemblage and around 200 μm in the dead assemblage (Fig. 9).

For *U. peregrina* marked differences of the test size distributions can be observed between the Alboran Sea and the Mallorca Channel as well as between stained and unstained tests. Within the live population, average sizes vary between 327 μm (Site 347) and 410 μm (Site 396), where the lower number of measured tests at the Mallorca Channel (n=31) compared to the Alboran Sea (n=288) should be kept in mind. For the dead assemblage regional differences are more pronounced, with 332-392 μm in the Alboran Sea (n=424) and 272-293 μm in the Mallorca Channel (n=130). A bimodal test size distribution is observed at all sites for *U. peregrina* with peaks around 200-225 μm and 400 μm , the latter peak is more emphasized in the dead assemblage (Fig. 9).

Average test sizes of 265 stained tests of *M. barleeanum* vary between 258 μm (Site 338) and 317 μm (Site 394) (Fig. 10). In epifaunal species the ranges in average test size are 460-606 μm for *C. pachydermus* (n=63), 480-568 μm for *P. ariminensis* (n=120) and 343-618 μm for *L. lobatula* (n=58). Test sizes of live *G. pseudospinescens* range from 220 to 775 μm (n=86) exhibiting a bimodal distribution with variable peak positions between approximately 225-350 μm and 425-625 μm . A similar range is observed for *G. ovata* tests (n=104), with 200-650 μm . The test sizes of *G. affinis* (n=26)

3. Stable isotope composition of benthic foraminifera under contrasting trophic conditions

range from 275 to 660 μm but due to the low number of measured tests a bimodal distribution cannot be confirmed (Fig. 10).

In the stable isotope signal, ontogenetic trends to heavier values with increasing test size are documented similarly in live and dead populations of *Uvigerina* and *Globobulimina* but are not evident in epifaunal taxa and *M. barleeanum* (Figs. 9, 10). With the exception of the stained tests of Site 338, the $\delta^{13}\text{C}_{\text{For}}$ values of *U. peregrina* exhibit an average $0.19 \pm 0.02 \text{‰} (100 \mu\text{m})^{-1}$ increase in the Alboran Sea ($R^2 = 0.77$, $p = 0.001$), while steeper slopes of $0.38 \pm 0.05 \text{‰} (100 \mu\text{m})^{-1}$ are observed in the Mallorca Channel ($R^2 = 0.81$, $p = 0.101$). The ontogenetic $\delta^{18}\text{O}_{\text{For}}$ increase of this species is $0.07 \pm 0.01 \text{‰} (100 \mu\text{m})^{-1}$ in the Alboran Sea ($R^2 = 0.67$, $p = 0.007$) and $0.37 \pm 0.16 \text{‰} (100 \mu\text{m})^{-1}$ in the Mallorca Channel ($R^2 = 0.69$, $p = 0.130$). The stable isotope composition of *U. mediterranea* exhibits similar ontogenetic trends in both study areas, with generally $0.10 \pm 0.04 \text{‰} (100 \mu\text{m})^{-1}$ in $\delta^{13}\text{C}_{\text{For}}$ ($R^2 = 0.50$, $p = 0.020$) and $0.05 \pm 0.02 \text{‰} (100 \mu\text{m})^{-1}$ in $\delta^{18}\text{O}_{\text{For}}$ ($R^2 = 0.54$, $p = 0.023$). The stable isotope data of the unstained *U. mediterranea* tests at Site 396 have been disregarded, due to strongly deviating values (Fig. 9). The low number of data available for *Globobulimina* does not allow for a species-specific evaluation of ontogenetic trends. However, by combination of the stable isotope signals of *G. affinis*, *G. ovata*, and *G. pseudospinescens*, an ontogenetic trend of $0.08 \pm 0.02 \text{‰} (100 \mu\text{m})^{-1}$ in $\delta^{13}\text{C}_{\text{For}}$ ($R^2 = 0.33$, $p = 0.160$) and $0.07 \pm 0.03 \text{‰} (100 \mu\text{m})^{-1}$ in $\delta^{18}\text{O}_{\text{For}}$ ($R^2 = 0.32$, $p = 0.054$) is observed (Fig. 10).

3.5 Discussion

3.5.1 Influence of trophic conditions on distribution, microhabitats and test sizes of benthic foraminifera

The observed faunal distributions and microhabitats mirror the trophic contrasts between the Alboran Sea ($200\text{-}300 \text{ gC m}^{-2} \text{ a}^{-1}$) and the Mallorca Channel ($140\text{-}160 \text{ gC m}^{-2} \text{ a}^{-1}$) (Bosc et al., 2004) and are in accordance with the observed differences in TOC values and the depths of the redox potential shifts (Table 1). The remarkably low C/N values (3.6 to 4.1) of sedimentary organic matter in the Alboran Sea suggest a predominantly bacterial origin linked to high organic matter fluxes, which are caused by regional upwelling (Sanchez-Vidal et al., 2005; Fabres et al., 2002). In contrast, in the Mallorca Channel, the production of phytodetritus is limited and mainly restricted to the winter season with additional terrestrial sources of organic matter (Zúñiga et al., 2007), explaining its higher C/N values (7.0-7.9) and thus relatively lower nutritional value. Accordingly, benthic foraminiferal standing stocks and diversities are higher in the Alboran Sea when compared to the Mallorca Channel. Likewise, the enhanced food availability is also reflected by development of deep infaunal niches (according to Jorissen et al., 1995) in the Alboran Sea, which are virtually absent at the Mallorca sites. The tolerance of globobuliminids to dysoxic or even temporarily anoxic conditions

3.5 Discussion

(Koho & Piña-Ochoa, 2012) suggests that the faunal distribution and niche separation in the Alboran Sea is both food- and oxygen limited, while in the Mallorca Channel food limitation plays a more critical role. This interpretation can be further refined by contrasts between the regional differences in the dominant shallow infaunal taxa of the biocoenoses and thanatocoenoses. In the Alboran Sea, the most abundant calcareous species is the shallow infaunal *U. peregrina*. This species is commonly associated with fine-grained organic-rich substrates (Schmiedl et al., 2000, Schönfeld, 2006). Further studies consider *U. peregrina* or the related *U. peregrina* var. *celtica* as a highly opportunistic species favored by pulses of labile organic matter (Fontanier et al., 2003; Koho et al., 2008). In the Mallorca Channel, the shallow infauna is dominated by *U. mediterranea*, while *U. peregrina*, *M. barleeanum* and *B. marginata* play a subordinate role. This faunal contrast is accompanied by a redox change relatively deep within the sediment (7-12 cm) and reflects the relatively lower organic matter fluxes and probably lower nutritional value of the available food at the sea floor. Therefore, a greater tolerance to limited organic matter supply and more degraded food can be assumed for *U. mediterranea* compared to *U. peregrina*. This is in accordance to observations from the Gulf of Lions (Schmiedl et al., 2000) but at least partly in contrast to findings of relatively high demands of food amount and quality for *U. mediterranea* (Altenbach et al., 1999; Koho et al., 2008).

The test size distributions exhibit species-specific and regional contrasts including narrow ranges around 250 µm in *M. barleeanum* and extreme test sizes of more than 1000 µm in *U. mediterranea* (Figs. 9, 10). Most of the measured populations lack simple Gaussian distributions but reveal a more complex, often bi- or multimodal pattern. This suggests the presence of more than one generation in the live population (Gooday, 1988). In our data, multiple peaks are mainly obvious in the populations of shallow and deep infaunal species, supporting reported individual life spans of more than two years (Ohga & Kitazato, 1997), if the reproduction events are annual. Even though shorter life spans are possible, if numerous reproduction events occur within one year, possibly coupled to phases of increased phytodetritus supply. *Uvigerina mediterranea* exhibits up to three distinguished peaks (e.g. Site 395) (Fig. 9) likely representing three reproduction events. The rate at which test sizes of different deep-sea benthic foraminifera increase during the specific life cycle is not yet well constrained but ontogenetic trends in stable isotope signals suggest a non-linear growth (see below, Schmiedl et al., 2004). Under the more eutrophic conditions of the Alboran Sea, average test sizes of *U. peregrina* are distinctively larger when compared to values from the Mallorca Channel suggesting a positive impact of more eutrophic conditions on test size, at least for this species.

The strong size differences between stained and unstained tests of *Uvigerina mediterranea* tests in the Mallorca Channel can be attributed to the generally low food supply and pronounced seasonality of this region. The samples represent the summer situations when only a low amount of more degraded food is available (Zúñiga et al., 2007). This coincides with a dominance of relatively older and larger *U. mediterranea* tests in the life fauna. The much higher number of small tests in the

3. Stable isotope composition of benthic foraminifera under contrasting trophic conditions

dead fauna likely echoes preceding reproduction events during the winter/spring bloom and subsequent high mortality rates. Comparable life/dead contrasts are less expressed for *U. peregrina*, corroborating weaker seasonal fluctuations in food fluxes in the Alboran Sea.

The observed test size distributions may also reflect the presence of relatively smaller megalospheric and larger microspheric tests within the same population (e.g. Goldstein, 1999, and references therein). Different life styles of the generation types were postulated for *Bolivina argentea* and *B. subadvena* from the Gulf of California (Douglas & Staines-Urías, 2007; Staines-Urías & Douglas, 2009). While the differentiation between megalospheric and microspheric tests in biserial bolivinids appears relatively easy based on significant contrasts in proloculus size (Grossman, 1984a, Schumacher et al., 2010), it turned out more problematic in *Uvigerina* species (Schweizer, 2006).

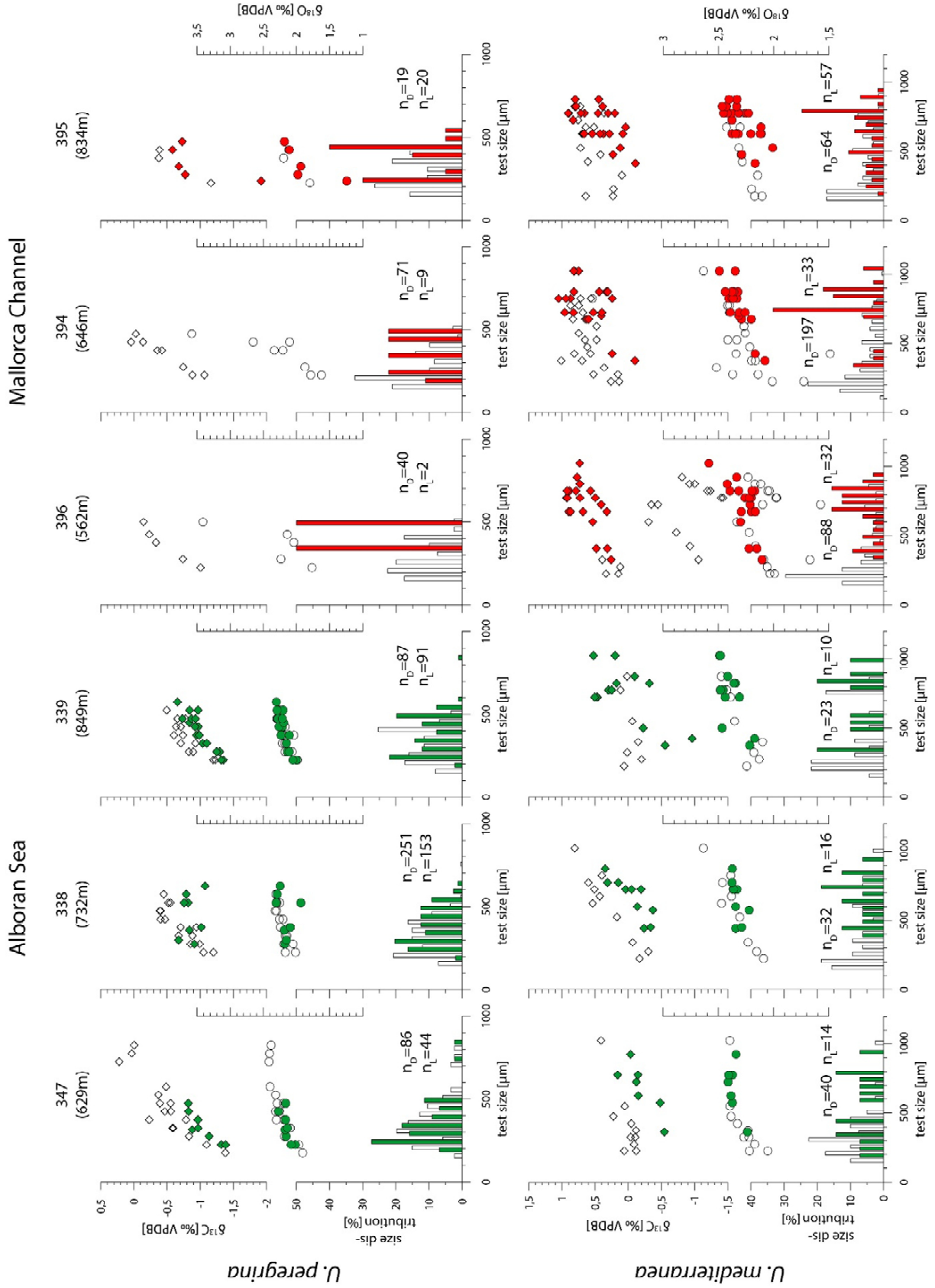
3.5.2 Influence of microhabitat on the stable isotope signal

In the Alboran Sea, where shallow to deep infaunal niches are developed, the observed species-specific deviations of $\delta^{13}\text{C}_{\text{For}}$ from the ambient $\delta^{13}\text{C}_{\text{DIC}}$ basically reflect the delivery of ^{12}C during microbial remineralization of organic matter to the sediment (e.g. McCorkle et al., 1985, 1997; Mackensen, 2008). It has to be noted that only unstained epifaunal tests were measured due to the lack of stained ones, which probably biases the observed gradients. A maximum $\Delta\delta^{13}\text{C}$ value of -2.44‰ between epifaunal and deep infaunal taxa is observed at Site 339. The inferred $\delta^{13}\text{C}_{\text{DIC}}$ pore water gradient of -1 to -1.4‰ cm^{-1} is higher when compared to reported values from oligotrophic to mesotrophic sites in the Gulf of Lions and Bay of Biscay (-0.3 to -0.5‰ cm^{-1}) (Schmiedl et al., 2004; Fontanier et al., 2006) but of similar magnitude when compared to bottom and pore water measurements from eutrophic environments in the Pacific and Atlantic Ocean (McCorkle et al., 1985; Stott et al., 2000; Holsten et al., 2004). Pore water gradients could not be reconstructed for sites of the Mallorca Channel due to the lack of deep infaunal species.

The analyzed shallow to intermediate infaunal taxa *U. mediterranea*, *U. peregrina*, and *M. barleeanum* exhibit similar MLDs, ranging from 0.5 and 1 cm in the Alboran Sea and from 0.7 and 1.3 cm in the Mallorca Channel (Fig. 7). The ALD₁₀ are deeper but in a comparable range of 0.6 to 2.2 cm in the Alboran Sea and 0.8 to 2.4 cm in the Mallorca Channel. Because of this, similar $\delta^{13}\text{C}_{\text{For}}$ values could be expected for these species. However, $\delta^{13}\text{C}_{\text{For}}$ values of *M. barleeanum* are 0.6-0.8 ‰ and those of *U. peregrina* 0.8-1.4 ‰ lower than corresponding $\delta^{13}\text{C}_{\text{For}}$ values of *U. mediterranea*. Deviations of similar magnitude have been previously reported and assigned to strong species-specific vital effects (Wefer & Berger 1991; Rathburn et al. 1996, 2000; McCorkle et al. 1997; Schmiedl et al., 2004).

Figure 9. Stable carbon and oxygen isotope signals of *Uvigerina peregrina* (upper panels) and *U. mediterranea* (lower panels) against test size distribution of the population. Live individuals (Rose Bengal stained tests) from the Alboran Sea and Mallorca Channel are marked in green and red, respectively.

3.5 Discussion



3. Stable isotope composition of benthic foraminifera under contrasting trophic conditions

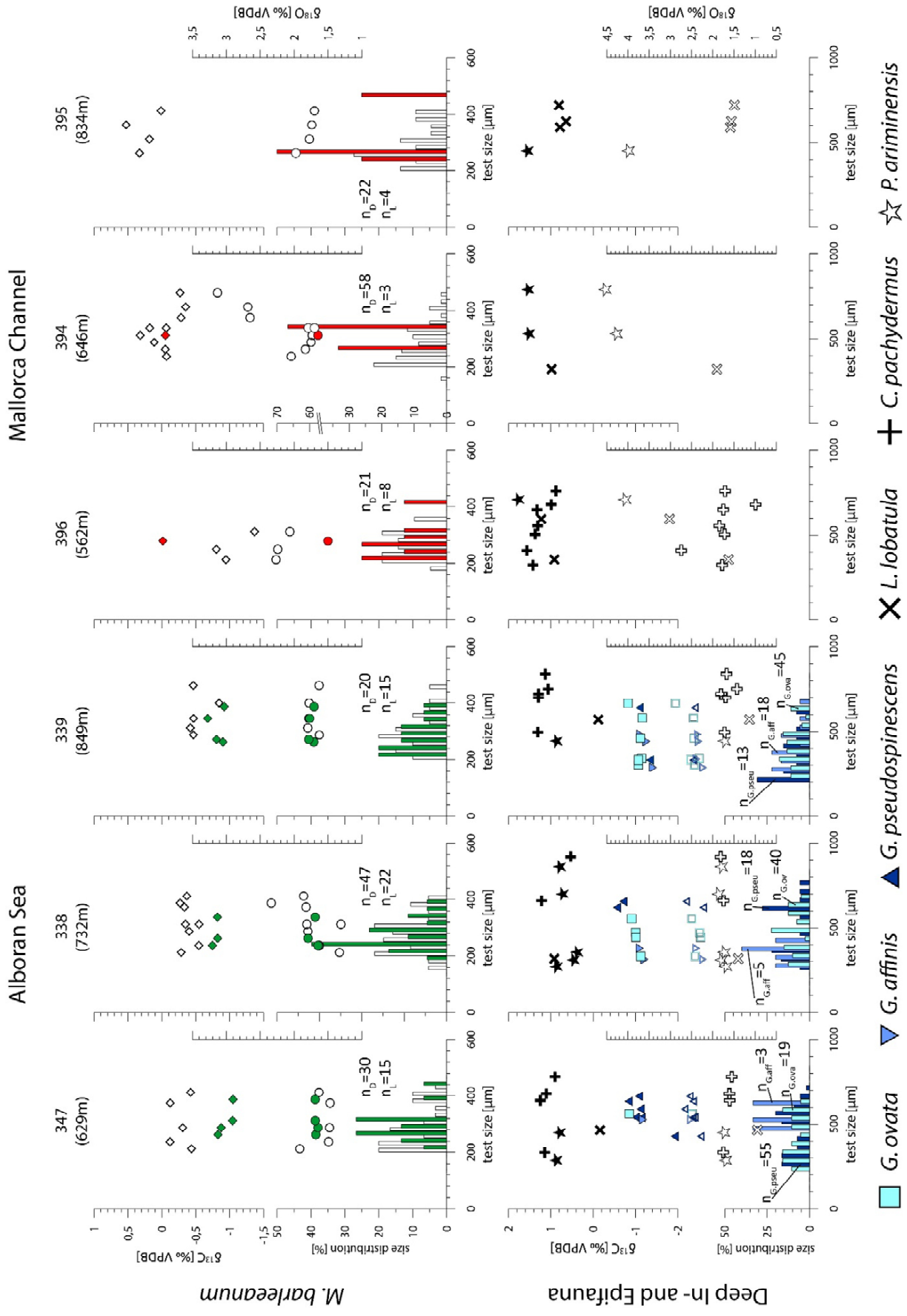
Our data show in general an increase in ^{18}O in foraminiferal tests with increasing microhabitat depths (Fig. 8), which was also observed in previous studies (Schmiedl et al., 2004; Fontanier et al., 2006). As an exception, the $\delta^{18}\text{O}_{\text{For}}$ of unstained *C. pachydermus* at the Mallorca sites are consistently 1.7 to 2.1 ‰ heavier than equilibrium calcite (after O'Neil et al., 1969), which can be expected for glacial values (e.g. Schmiedl & Mackensen, 2006). It appears possible that robust tests of *C. pachydermus* and its high abundances in the Mediterranean Sea during the last glacial (e.g. Kuhnt et al., 2007; Abu-Zied et al., 2008; Melki et al., 2009) fostered reworking and subsequent redeposition (Fig. 8). The $\delta^{18}\text{O}_{\text{For}}$ values of deep infaunal *Globobulimina* and shallow infaunal *Uvigerina* species are close to $\delta^{18}\text{O}_{\text{EQ}}$ (after O'Neil et al., 1969). The positive deviations in the Alboran Sea can be likely attributed to inaccuracies in $\delta^{18}\text{O}_{\text{Water}}$, which in our study was based on interpolated bottom water values from literature (Pierre, 1999) and the chosen $\delta^{18}\text{O}_{\text{EQ}}$ calculation (Barras et al., 2010; Filipsson et al., 2010).

The effect of different calcite-water fractionation factors has to be considered (e.g. Bemis et al., 1998; Mackensen & Nam, 2014). If the fractionation factor of Kim & O'Neil (1997) was chosen, the resulting $\delta^{18}\text{O}_{\text{EQ}}$ would be 0.26 to 0.27‰ lower and thus closer to but not in accordance with epifaunal $\delta^{18}\text{O}_{\text{For}}$ values (Hoogakker et al., 2010; Mackensen & Nam, 2014). Although this calculation appears more reasonable in the application of epifaunal species as bottom water proxy, both results could also be a coincidence due to the lack of direct measurements of bottom water during sampling. However, concerning the discussion if epifaunal foraminifera calcify in equilibrium (Kim & O'Neil, 1997; Hoogakker et al., 2010), we do not support this hypothesis, for biological reasons. If epifaunal species would represent $\delta^{18}\text{O}_{\text{EQ}}$, *U. mediterranea* and *Globobulimina* spp. would calcify with a positive offset, which is unusual and hard to explain with biological factors. Therefore, we decided to use the fractionation factor of O'Neil et al. (1969) (Figs. 8, 11), but are aware of possible mismatches with isotopic results from other studies.

The $\delta^{18}\text{O}_{\text{For}}$ values of epifaunal species (*L. lobatula*, *C. pachydermus*, *P. ariminensis*) and the shallow to intermediate infaunal *M. barleeaanum* are depleted by -0.5 to -1 ‰ or even more relative to $\delta^{18}\text{O}_{\text{For}}$ of deep infaunal *Globobulimina* spp. and *U. mediterranea* (Fig. 8). Down-core changes in temperature and salinity as a possible explanation for these deviations can be excluded (McCorkle et al., 1990, 1997). Negative $\Delta\delta^{18}\text{O}_{\text{For-EQ}}$ values could also be attributed to enhanced respiration rates in opportunistic epifaunal taxa (Schmiedl et al., 2004). However, such an effect should be even more pronounced in the corresponding $\Delta\delta^{13}\text{C}_{\text{For-DIC}}$ values, which is not the case in our data where epibenthic species are in equilibrium with bottom water $\delta^{13}\text{C}_{\text{DIC}}$ (Fig. 7).

Figure 10. Stable carbon and oxygen isotope signals of *Melonis barleeaanum* (upper panels) and three epifaunal and three deep infaunal species (lower panels) against test size. Live individuals of *M. barleeaanum* (Rose Bengal stained tests) from the Alboran Sea and Mallorca Channel are marked in green and red, respectively. In the lower panels, stable carbon and oxygen isotope values of stained and unstained tests are indicated by filled and open symbols, respectively.

3.5 Discussion



3. Stable isotope composition of benthic foraminifera under contrasting trophic conditions

Here we propose an alternative, yet speculative, explanation for the observed offsets that we attribute to the concentrations of utilizable oxygen for metabolism in the bottom and pore waters. Although previous studies did not report a significant oxygen fractionation during metabolism (McConnaughey, 1989a, b), it is obvious, that epifaunal species show the lightest $\delta^{18}\text{O}_{\text{For}}$ values at a site, suggesting the strongest fractionation. Compared to species from infaunal habitats, epifaunal taxa have the best access to dissolved oxygen at a site. Conversely, the possible metabolic oxygen fractionation could decrease when approaching anoxic conditions, leading to equilibrium values in infaunal species, with *Globobulimina* spp. probably representing $\delta^{18}\text{O}_{\text{EQ}}$ (Fontanier et al. 2006; Schmiedl & Mackensen, 2006). The $\delta^{18}\text{O}$ of the shallow infaunal *Uvigerina* spp. resemble those of the deep infauna, but minor deviations towards lighter values have been observed in fossil data (e.g. Schmiedl & Mackensen, 2006). Our hypothesis cannot explain the observed $\delta^{18}\text{O}_{\text{For}}$ difference between species of the same microhabitat like the shallow to intermediate infaunal *M. barleeaanum* and *Uvigerina* spp. or the epifaunal *L. lobatula* compared to *P. ariminensis* and *C. pachydermus* (Fig. 8). It remains unclear, which factors account for these inconsistencies. Probably, different sources of the oxygen atoms were used during calcification, including metabolic CO_2 from internal reservoirs or $[\text{CO}_3^{2-}]$ from interstitial waters (de Nooijer et al., 2014).

3.5.3 Ontogenetic fractionation of the stable isotope signal

Our data reveal species-specific differences in the relation between test size and the stable carbon and oxygen isotope signals (Figs. 9-11). The $\delta^{13}\text{C}_{\text{For}}$ and $\delta^{18}\text{O}_{\text{For}}$ values of the genera *Uvigerina* and *Globobulimina* increase more or less linearly during ontogenesis. Our data confirm previous information of ontogenetic stable isotope trends in shallow to intermediate infaunal bi- or triserial taxa, such as *Bulimina aculeata/marginata* (McCorkle et al., 2008; Filipson et al., 2010; Barras et al., 2010), *Bolivina* aff. *B. dilatata*, *Uvigerina* ex gr. *U. semiornata* (Schumacher et al., 2010) and *Uvigerina mediterranea* (Schmiedl et al., 2004). The common explanation for increasing stable isotope values with increasing test size is a slow-down of the individual metabolism during ontogenesis associated with reduced fractionation in adult specimens (Berger et al., 1978; Spero & Lea, 1996; Schmiedl et al., 2004; Mackensen, 2008; Schumacher, 2010). In addition, the ontogenetic $\delta^{18}\text{O}_{\text{For}}$ increase is commonly smaller than for $\delta^{13}\text{C}_{\text{For}}$ (Fig. 9), which can be attributed to the larger reservoir of available oxygen atoms (McConnaughey, 1989a, b; Grossman, 1987).

In contrast, *M. barleeaanum*, *C. pachydermus*, *L. lobatula*, and *P. ariminensis* lack clear ontogenetic trends in their $\delta^{18}\text{O}_{\text{For}}$ and $\delta^{13}\text{C}_{\text{For}}$ values, but limited amount of available data hampers a proper statistical evaluation (Fig. 10). Existing literature data confirm the absence of ontogenetic isotope trends in trochospiral taxa such as *Cibicidoides wuellerstorfi* (Franco-Fraguas et al., 2011; Corliss et al., 2002), *Planulina ornata* (Dunbar & Wefer, 1984), and the aragonite-walled *Hoeglundina elegans* (Corliss et al., 2002). Accordingly, these species should record reliable information of the surrounding

water composition even when different size classes are integrated in a single measurement. This observation is relevant since epifaunal species (e.g. *Lobatula* spp., *Cibicidoides* spp., *Planulina* spp.) are commonly used for bottom water reconstructions and often occur only in low abundances. As an exception, increasing $\delta^{13}\text{C}_{\text{For}}$ but constant $\delta^{18}\text{O}_{\text{For}}$ values during ontogenesis have been reported for *Ammonia tepida* (Diz et al., 2012). This demonstrates that further studies of potential ontogenetic isotope effects in epifaunal trochospiral taxa should be carried out, based on a statistically significant number of measurements.

3.5.4 Influence of organic matter fluxes on the stable carbon isotope signal of *Uvigerina* species

The intra-generic comparison of *U. peregrina* and *U. mediterranea* reveals a species-specific response of the $\delta^{13}\text{C}_{\text{For}}$ signal to varying OM fluxes. The $\Delta\delta^{13}\text{C}_{\text{For-DIC}}$ values of *U. mediterranea* range from -1.45 to -0.65 ‰ under mesotrophic conditions in the Alboran Sea, and from -0.96 to 0 ‰ under oligotrophic conditions in the Mallorca Channel and exhibit a more or less constant ontogenetic slope of 0.1-0.2 ‰ (100 μm)⁻¹ in both study areas (Fig. 11). The observed ~0.5 ‰ lower values in the Alboran Sea can be attributed to a stronger pore water gradient under enhanced OM fluxes, resulting in higher availability of ¹²C at a comparable living depth (McCorkle & Emerson, 1988; Schmiedl et al., 2004; Schmiedl & Mackensen, 2006). The more or less constant ontogenetic slope under the influence of different OM fluxes reflects the opportunistic life strategy of *U. mediterranea*.

Although this species prefers to feed from fresh and non-degraded organic matter (Koho et al., 2008), it can exist under a wide range of organic matter fluxes and is able to survive seasonal periods of food shortage (Fontanier et al., 2003; Schmiedl et al., 2010). The observed trophic control of the shifts in ontogenetic $\delta^{13}\text{C}_{\text{For}}$ trends of *U. mediterranea* allows for test-size corrected estimation of pore water $\delta^{13}\text{C}_{\text{DIC}}$ gradients in the uppermost sediment centimeter (compare McCorkle et al., 1990) and thus, provides a proxy for quantification of organic matter flux rates (Fig. 11).

The $\Delta\delta^{13}\text{C}_{\text{For-DIC}}$ values of the smallest *U. peregrina* are as low as -2.3 ‰ at all sites, independent from OM fluxes. The ontogenetic increase is steeper (0.36-0.42 ‰ (100 μm)⁻¹) in the Mallorca Channel than in the Alboran Sea (0.17-0.21 ‰ (100 μm)⁻¹), resulting in ~0.5 ‰ lower $\delta^{13}\text{C}_{\text{For}}$ values in the largest tests under high OM fluxes in the Alboran Sea (Fig. 11). The low $\delta^{13}\text{C}_{\text{For}}$ values of *U. peregrina* are in accordance with observations from the Gulf of Lions (Schmiedl et al., 2004) and can be attributed to its opportunistic feeding strategy and strong metabolic effects, particularly expressed in young and small individuals. Recent ecological studies propose a close link between *U. peregrina* and strong pulses of fresh phytodetritus (Koho et al., 2008; Schmiedl et al., 2010), which in the western Mediterranean occur during the spring season.

3. Stable isotope composition of benthic foraminifera under contrasting trophic conditions

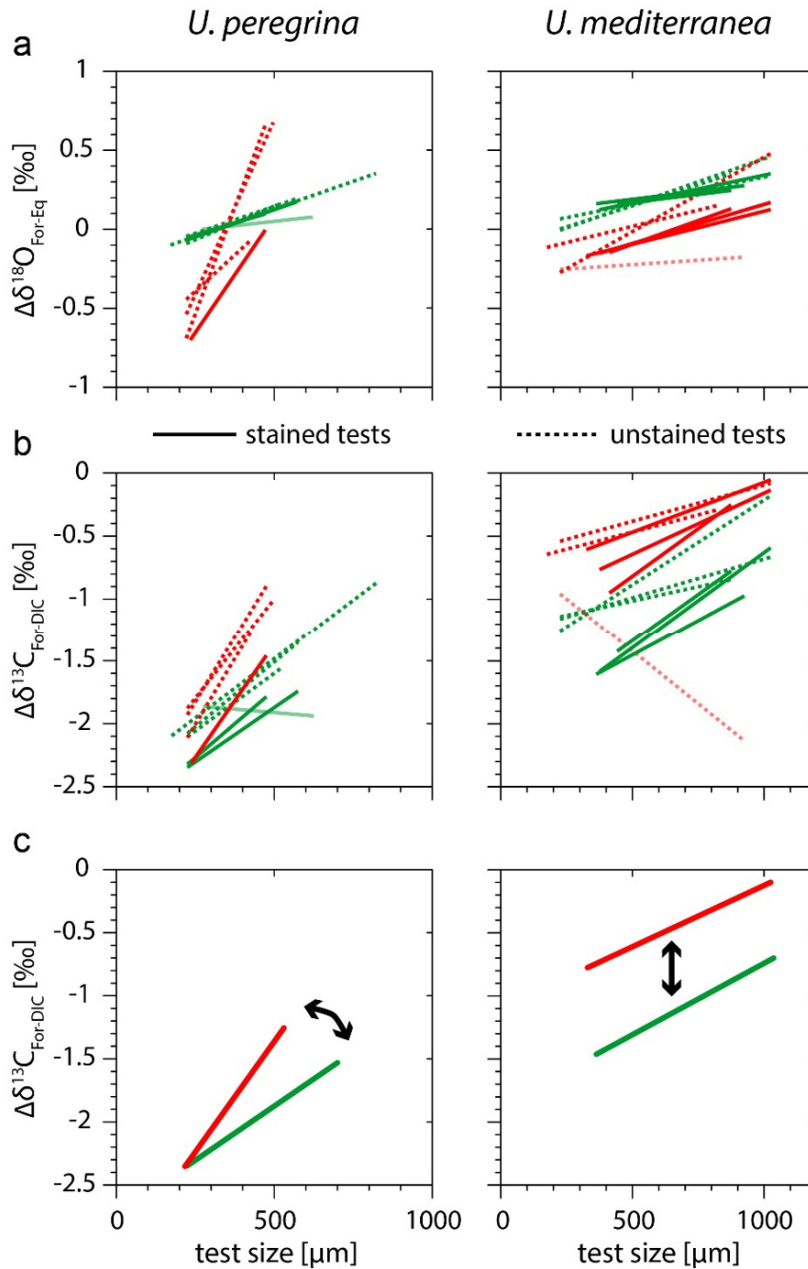


Figure 11. Ontogenetic trends of (a) $\Delta\delta^{18}\text{O}_{\text{For-EQ}}$ and (b) $\Delta\delta^{13}\text{C}_{\text{For-DIC}}$ of *Uvigerina peregrina* and *U. mediterranea* from the Alboran Sea (green) and Mallorca Channel (red). Live (Rose Bengal stained) and dead (unstained) individuals are marked by continuous and stippled lines, respectively. (c) Conceptual model showing the shift of ontogenetic trends in $\Delta\delta^{13}\text{C}_{\text{For-DIC}}$ of *U. peregrina* and *U. mediterranea* under the influence of contrasting trophic regimes, i.e. meso- to eutrophic conditions in the Alboran Sea (green) and oligo- to mesotrophic conditions in the Mallorca Channel (red). *Uvigerina peregrina* exhibits uniform $\Delta\delta^{13}\text{C}_{\text{For-DIC}}$ in small individuals but regional differences in ontogenetic slopes and average test sizes, with relatively steep slopes in the Mallorca Channel and flat slopes and larger mean test sizes in the Alboran Sea. In contrast, *U. mediterranea* shows similar ontogenetic $\Delta\delta^{13}\text{C}_{\text{For-DIC}}$ slopes in both regions but a general shift towards stronger deviations in the Alboran Sea responding to the influence of enhanced organic matter fluxes.

3.5 Discussion

The regionally different ontogenetic $\delta^{13}\text{C}_{\text{For}}$ slopes of *U. peregrina* likely mirror contrasts in growth dynamics of this species attributed to the contrasts of amount, quality and seasonality of OM fluxes in the Alboran Sea and Mallorca Channel. After reproduction in spring, reflected by the high number of unstained small tests during summer in both regions (Fig. 9), the $\delta^{13}\text{C}_{\text{For}}$ values are very low. This suggests an enhanced metabolic activity of young individuals near the sediment surface, which is corroborated by a detailed and size-dependent microhabitat study from the Gulf of Lions (Schmiedl et al., 2000). Additionally, the isotopically light fresh phytodetritus can reduce the $\delta^{13}\text{C}_{\text{DIC}}$ at the sediment water interface (Mackensen et al., 1993). Under the influence of lower seasonal contrasts and generally enhanced food availability in the Alboran Sea, *U. peregrina* can grow swiftly to test sizes as large as 850 μm . In the Mallorca Channel, *U. peregrina* responds to lower levels of fresh phytodetritus supply after the spring season by a metabolic slow-down and reduced chamber addition rates, leading to maximum test sizes of only 550 μm . Even though the relationships between calcification and stable isotope composition are not yet fully understood (Ter Kuile & Erez, 1984; de Nooijer et al., 2014), our data suggest that a reduction of chamber addition rate results in relatively heavier $\delta^{13}\text{C}_{\text{For}}$ values in larger tests. According to this observation, varying trophic conditions are mirrored by different slopes of the ontogenetic $\delta^{13}\text{C}_{\text{For}}$ gradient of *U. peregrina* (Fig. 11c). Our data demonstrate that $\delta^{13}\text{C}_{\text{For}}$ signals of *U. peregrina* and *U. mediterranea* can both be used as proxy for organic matter fluxes, taking into account their different species-specific response to changes in trophic conditions.

3.5.5 Taphonomic alteration and anthropogenic influence of the stable isotope signal

Corresponding $\delta^{18}\text{O}_{\text{For}}$ data of live (stained) and dead (unstained) individuals for each of the investigated species show comparable values at all sites. In contrast, $\delta^{13}\text{C}_{\text{For}}$ values of dead individuals were commonly higher when compared to stained tests (Figs. 9, 10). The average $\delta^{13}\text{C}_{\text{For}}$ differences are around +0.2 ‰ and occur in both study areas. A contamination of isotopically light carbon from organic matter in stained tests can be excluded since previous studies did not find any systematic differences between the $\delta^{13}\text{C}_{\text{For}}$ values of stained and unstained specimens (McCorkle et al. 1990; Mackensen et al., 1993; Mackensen et al., 2000).

Alternatively, a shift to heavier $\delta^{13}\text{C}_{\text{For}}$ values in dead individuals may be attributed to taphonomic processes including post-depositional dissolution of test surfaces. Dissolution effects have been associated with increasingly heavier stable isotope values in planktonic foraminifera (Wu & Berger, 1989; Wu et al., 1990). However, these studies revealed an even stronger dissolution effect on $\delta^{18}\text{O}_{\text{For}}$, which is not visible in our data.

Most likely, the relatively lighter $\delta^{13}\text{C}_{\text{For}}$ in live individuals represent temporal changes in bottom water $\delta^{13}\text{C}_{\text{DIC}}$ composition. The dead individuals have been selected from the 4-5 cm depth interval

3. Stable isotope composition of benthic foraminifera under contrasting trophic conditions

and thus represent an age of at least several hundreds of years, which can be estimated according to late Holocene sedimentation rates of typically between 10 and 30 cm kyr⁻¹ documented for bathyal areas of the western Mediterranean Sea (Cacho et al., 2001; Toucanne et al., 2012; Ausín et al., 2015). The residence times of intermediate and deep-water masses in the western Mediterranean basins are in the order of only a few decades (Bethoux, 1980; Bethoux et al., 1990; 1996). Therefore, the modern $\delta^{13}\text{C}_{\text{DIC}}$ signature of upper bathyal waters of this basin is likely influenced by the Suess effect, i.e. contribution of fossil fuel derived isotopically light CO₂ to the atmosphere and oceans (Keeling, 1979; Bacastow et al., 1996). In the Eastern Mediterranean Sea, the anthropogenic shift in $\delta^{13}\text{C}_{\text{DIC}}$ of -1.5 ‰ since 1750 has been documented in surface water masses (Sisma-Ventura et al., 2014), but a rapid transfer of this signal to the deeper layers can be expected in all sub-basins.

3.6 Conclusions

1) The distribution, microhabitats and stable carbon isotope composition of benthic foraminifera mirror the trophic contrasts between the meso- to eutrophic Alboran Sea and the oligo- to mesotrophic Mallorca Channel. In the Alboran Sea, faunas are characterized by relatively high standing stocks, diversity, and the development of deep infaunal niches, which are absent in the food-limited Mallorca Channel. In the Alboran Sea, the $\delta^{13}\text{C}_{\text{For}}$ values of the different epifaunal, shallow infaunal and deep infaunal taxa reveal a $\delta^{13}\text{C}_{\text{DIC}}$ pore water gradient of -1 to -1.4 ‰ cm⁻¹ which is higher when compared to reported values from oligotrophic to mesotrophic sites of the Mediterranean Sea. The $\delta^{18}\text{O}_{\text{For}}$ values of the epifaunal taxa and the infaunal *M. barleeanum* are depleted by -0.5 to -1 ‰ or even more relative to $\delta^{18}\text{O}_{\text{EQ}}$. We hypothesize that for epifaunal taxa, this depletion can be attributed to enhanced fractionation, possibly caused by the easy access to metabolic utilizable oxygen.

2) The test size distributions of *U. mediterranea* and *U. peregrina* reveal complex and often bi- or multimodal patterns suggesting the presence of more than one generation in the live population. The $\delta^{13}\text{C}_{\text{For}}$ and $\delta^{18}\text{O}_{\text{For}}$ values of the genera *Uvigerina* and *Globobulimina* increase more or less linearly during ontogenesis, suggesting a metabolic slow-down in larger individuals. The observed ontogenetic increases exhibit species-specific slopes and regional differences, and are commonly more expressed in $\delta^{13}\text{C}_{\text{For}}$ than in $\delta^{18}\text{O}_{\text{For}}$. Comparable ontogenetic fractionation seems to be absent in epifaunal taxa and *M. barleeanum*.

3) The intra-generic comparison of *U. peregrina* and *U. mediterranea* reveals a species-specific response of the $\delta^{13}\text{C}_{\text{For}}$ signal to varying OM fluxes. The highly opportunistic *U. peregrina* shows similarly low $\delta^{13}\text{C}_{\text{For}}$ values in small individuals and different ontogenetic slopes under various OM fluxes. In contrast, the less opportunistic *U. mediterranea* exhibits a more or less constant ontogenetic slope under the influence of different OM fluxes. The observed ~0.5 ‰ lower $\delta^{13}\text{C}_{\text{For}}$ values of large

3.6 Conclusions

tests of both species in the Alboran Sea can be attributed to a stronger pore water gradient in the uppermost sediment centimeter under the influence of enhanced OM fluxes.

4) In both study areas, the $\delta^{13}\text{C}_{\text{For}}$ values of live individuals are on average 0.2 ‰ lower than those of dead individuals at 4-5 cm depth, which represent an age of several hundreds of years. While taphonomic processes can be largely ruled out, we attribute this signal to the input of fossil fuel derived isotopically light CO_2 ('Suess effect') fostered by the low residence times of western Mediterranean intermediate and deep-water masses.

4. Stable carbon isotope deviations in benthic foraminifera as proxy for organic carbon fluxes in the Mediterranean Sea

Abstract

We have determined stable carbon isotope ratios of epifaunal and shallow infaunal benthic foraminifera to relate the inferred gradient of pore water $\delta^{13}\text{C}_{\text{DIC}}$ to varying trophic conditions, and to test the potential of developing a transfer function for organic matter flux rates. The data set is based on samples retrieved from a well-defined bathymetric range (400-1500 m water depth) of sub-basins in the western, central and eastern Mediterranean Sea. Regional contrasts in organic matter fluxes and associated $\delta^{13}\text{C}_{\text{DIC}}$ of pore water are recorded by the $\delta^{13}\text{C}$ difference ($\Delta\delta^{13}\text{C}_{\text{Umed-Epi}}$) between the shallow infaunal *Uvigerina mediterranea* and epifaunal species (*Planulina ariminensis*, *Cibicides pachydermus*, *Lobatula lobatula*). The $\Delta\delta^{13}\text{C}_{\text{Umed-Epi}}$ values range from -0.46 to -2.13 ‰, with generally higher offsets at more eutrophic sites. Because of ontogenetic shifts in the $\delta^{13}\text{C}$ signal of *U. mediterranea* of up to 1.04 ‰, only tests larger than 600 μm were used for the quantitative environmental evaluation. The measured $\delta^{13}\text{C}$ deviations are related to site-specific differences in microhabitat, depth of the principal redox boundary, and TOC content. The $\Delta\delta^{13}\text{C}_{\text{Umed-Epi}}$ values reveal a consistent relation to C_{org} fluxes estimated from satellite-derived surface water primary production in open-marine settings of the Alboran Sea, Mallorca Channel, Strait of Sicily and southern Aegean Sea. In contrast, $\Delta\delta^{13}\text{C}_{\text{Umed-Epi}}$ values in areas affected by intense resuspension and riverine organic matter sources of the northern to central Aegean Sea and the canyon systems of the Gulf of Lions suggest higher C_{org} fluxes compared to the values based on recent surface primary production. Considering the regional biases and uncertainties, a first $\Delta\delta^{13}\text{C}_{\text{Umed-Epi}}$ based transfer function for C_{org} fluxes could be established for the Mediterranean Sea.

This chapter is based on:

Theodor, M., Schmiedl, G., Jorissen, F., Mackensen, A., 2016. Stable carbon isotope deviations in benthic foraminifera as proxy for organic carbon fluxes in the Mediterranean Sea. Biogeosciences Discussions, doi:10.5194/bg-2016-247

4.1 Introduction

The stable isotope composition of benthic foraminifera is used in a wide range of paleoceanographic applications. The $\delta^{18}\text{O}$ signal of benthic foraminifera provides information on bottom water temperature and salinity, and has been applied for the estimation of global ice volume changes (e.g. Shackleton & Opdyke, 1973; Adkins et al., 2002; Marchitto et al., 2014). The benthic foraminiferal $\delta^{13}\text{C}$ signal ($\delta^{13}\text{C}_{\text{For}}$) is mainly used for the reconstruction of changes in deep-sea circulation, bottom water oxygen, and organic carbon fluxes to the sea floor (Curry & Lohmann, 1982; Zahn et al., 1986; McCorkle & Emerson, 1988; Mackensen & Bickert, 1999; Pahnke & Zahn, 2005). Recently, more quantitative approaches have been applied to the reconstruction of past changes in deep-water oxygenation (Stott et al., 2000; Schmiedl & Mackensen, 2006; Hoogakker et al., 2015). There have been also attempts to use multi-species $\delta^{13}\text{C}$ records for the estimation of past organic carbon fluxes (Zahn et al., 1986; Schilman et al., 2003; Kuhnt et al., 2008), however, all of these studies lack a regional calibration based on living specimens and modern environmental data.

The $\delta^{13}\text{C}$ gradient of pore water dissolved inorganic carbon (DIC) in the uppermost surface sediment is directly related to the flux and decomposition rates of organic matter (McCorkle & Emerson, 1988; McCorkle et al., 1990; Holsten et al., 2004). With increasing depth in the sediment more isotopically light organic matter (around -18 to -23 ‰, e.g. Mackensen, 2008) is remineralized by microbial activity (McCorkle et al., 1985). This process results in $\delta^{13}\text{C}_{\text{DIC}}$ pore water depletions of up to -4 ‰ relative to the bottom water signal (McCorkle & Emerson, 1988; McCorkle et al., 1990; Holsten et al., 2004). The ^{12}C release to the pore water stops when no more OM is remineralized, which mostly coincides with the total consumption of electron acceptors, of which oxygen and

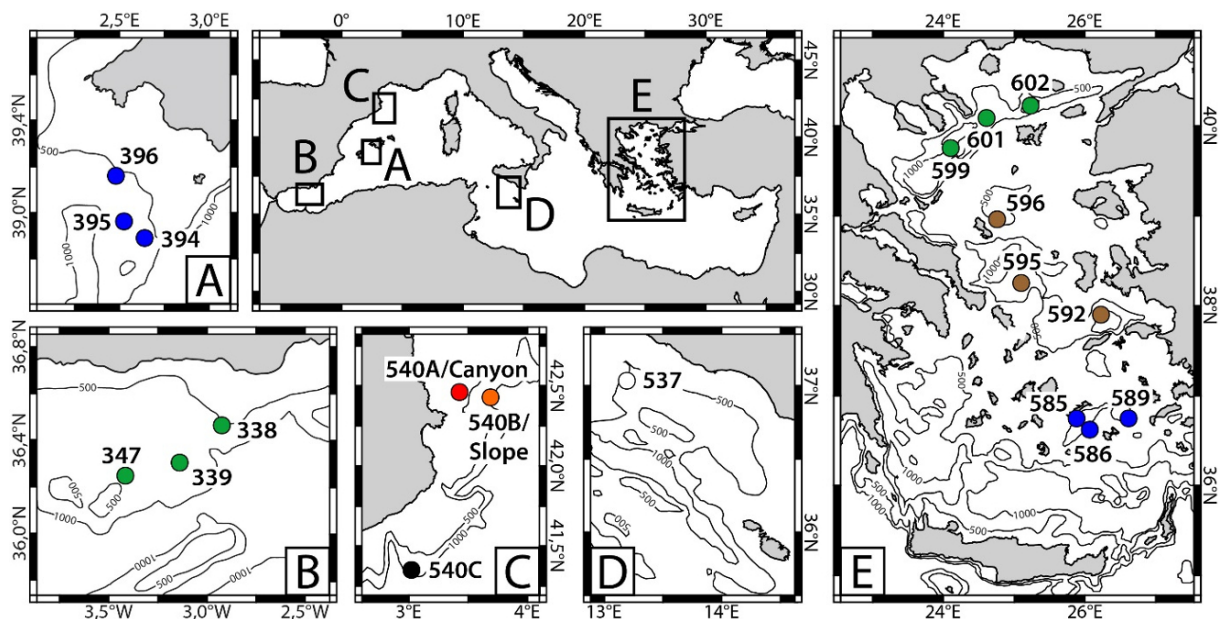


Figure 12. Location of the study areas in the Mediterranean Sea and regional bathymetric maps with locations of sample sites in the (a) Mallorca Channel, (b) Alboran Sea, (c) Gulf of Lions and Spanish Slope off Barcelona, (d) Strait of Sicily, and (e) Aegean Sea.

4. Carbon isotope deviations in foraminifera as C_{org} flux proxy

nitrate are the usually most important ones (McCorkle & Emerson, 1988; McCorkle et al., 1990; Koho & Pina-Ochoa, 2012; Hoogakker et al., 2015).

The $\delta^{13}C_{DIC}$ pore water gradient is reflected in the $\delta^{13}C$ signal of benthic foraminifera from defined microhabitats on and below the sediment–water interface (Grossman, 1984a, b; McCorkle et al., 1990, 1997; Rathburn et al., 1996; Mackensen & Licari, 2004; Schmiedl et al., 2004; Fontanier et al., 2006). Although benthic foraminifera can migrate through the sediment (Linke & Lutze, 1993; Ohga & Kitazato, 1997) and living individuals may occur across a relatively wide depth interval, the $\delta^{13}C$ signal of a certain species exhibits relatively little scattering, and all specimens tend to reflect the same calcification depth (Mackensen & Douglas, 1989; McCorkle et al., 1990, 1997; Mackensen et al., 2000; Schmiedl et al., 2004). The study of McCorkle & Emerson (1988) has shown that the difference between $\delta^{13}C_{DIC}$ of bottom water and $\delta^{13}C_{DIC}$ of pore water at the depth in the sediment where oxygen approaches zero is directly related to the oxygen content of the bottom water mass. Based on this observation, the $\delta^{13}C$ difference of epifaunal (e.g. *Cibicidoides*) and deep infaunal (*Globobulimina*) taxa was used as proxy for the quantification of past changes in deep-water oxygenation (Schmiedl & Mackensen, 2006; Hoogakker et al., 2015). Under the influence of well-oxygenated bottom waters, enhanced organic matter fluxes and associated decomposition rates result in steepening of $\delta^{13}C_{DIC}$ gradients in the uppermost sediment, which is then reflected by the $\delta^{13}C$ difference between epifaunal and shallow infaunal (e.g. *Uvigerina*) species (Zahn et al. 1986; Mackensen et al., 2000; Brückner & Mackensen, 2008). A simple relation between inferred $\delta^{13}C_{For}$ gradients and organic matter fluxes is impeded by the ability of infaunal species to shift their microhabitat in response to changing trophic conditions (Schmiedl & Mackensen, 2006; Theodor et al., 2016a). Interspecific differences in the $\delta^{13}C_{For}$ composition of benthic foraminifera are further influenced by species-specific ‘vital effects’, which can be as large as 1 ‰ (Schmiedl et al., 2004; McCorkle et al., 2008; Brückner & Mackensen, 2008) and are a reflection of metabolic processes and test calcification rates (McConnaughey, 1989a, b). Of minor impact but still traceable is the influence of carbonate ion concentration and alkalinity gradients in pore waters (Bemis et al., 1998). Finally, significant ontogenetic $\delta^{13}C_{For}$ trends have been documented for certain taxa, particularly for the genera *Uvigerina* and *Bolivina* (Schmiedl et al. 2004; Schumacher et al., 2010; Theodor et al., 2016a).

The complexity of factors influencing the stable isotope composition of deep-sea benthic foraminifera demonstrates the necessity of isotopic studies on living foraminifera in relation to their biology and microhabitat. In particular, combined ecological and biogeochemical studies on a statistically relevant number of sites and live specimens from areas with well-defined environmental gradients are required for the establishment of reference data sets and transfer functions that could then be used for a more quantitative assessment of organic matter fluxes. The Mediterranean Sea appears particularly suitable for such a study because the present deep-sea environments are characterized by systematically high oxygen contents contrasting with substantial trophic

4.1 Introduction

differences. In all basins, sub-surface water masses are highly oxygenated with O₂ concentrations of >160 μmol kg⁻¹ due to frequent replenishment of intermediate water in the Levantine Sea and deep water in the Gulf of Lions, Adriatic Sea, and Aegean Sea (Wüst, 1961; Lascaratos et al., 1999; Pinardi & Masetti, 2000; Tanhua et al., 2013, Pinardi et al., 2015). The inflow of nutrients with Atlantic surface waters causes an overall west-east gradient in primary production (PP), from values of around 225 gC m⁻² yr⁻¹ in the Alboran Sea to about 40 gC m⁻² yr⁻¹ in the extremely nutrient-depleted oligotrophic Levantine Basin (Bosc et al., 2004; Lopez-Sandoval et al., 2011; Puyo-Pay et al., 2011; Huertas et al., 2012; Tanhua et al., 2013, Gogou et al., 2014). In areas influenced by nutrient input through larger rivers and Black Sea outflow, PP can be locally enhanced, for example leading to a trend of decreasing PP values along a N-S transect in the Aegean Sea (Lykousis et al., 2002;

Table 2. Position, water depth, median living depth (MLD) of *Uvigerina mediterranea*, geochemical, primary production (PP) and C_{org} flux values of the investigated multicorer sites. Annual PP values are averages for the year previous to sampling after data from the GlobColour project. C_{org} fluxes were calculated after Betzer et al. (1984) and the MLD after Theodor et al. (2016a).

| Site | latitude | longitude | station depth | MLD _{Umed} [cm] | redox boundary depth [cm] | TOC [%] | PP [gCm ⁻² a ⁻¹] | C _{org} flux [gCm ⁻² a ⁻¹] |
|------------|-------------|-------------|---------------|--------------------------|---------------------------|---------|---|--|
| 537 | 37°02.14' N | 13°11.35' E | 472 | 0.83 | 2.75 | 0.560 | 173.06 | 12.26 |
| 540A | 42°27.69' N | 03°25.64' E | 911 | 0.43 | 2.25 | | 203.97 | 10.22 |
| 540B | 42°25.70' N | 03°41.34' E | 812 | 1.22 | 7.00 | 0.750 | 193.99 | 10.24 |
| 540C | 41°21.04' N | 03°01.36' E | 721 | 0.97 | 4.25 | 0.650 | 179.74 | 9.91 |
| 585 | 36°39.60' N | 25°55.72' E | 708 | 2.25 | 21.00 | 0.430 | 151.13 | 7.85 |
| 586 | 36°34.32' N | 25°57.91' E | 424 | 1.00 | 18.00 | 0.408 | 151.13 | 10.83 |
| 589 | 36°45.19' N | 26°35.38' E | 584 | 2.13 | 14.50 | 0.698 | 150.87 | 8.84 |
| 592 | 37°47.65' N | 26°15.72' E | 1148 | 0.38 | 16.00 | 0.630 | 151.46 | 5.81 |
| 595 | 38°15.63' N | 25°06.17' E | 662 | 0.56 | 19.00 | | 159.63 | 8.84 |
| 596 | 38°57.32' N | 24°45.20' E | 884 | 0.41 | 30.00 | 0.730 | 160.50 | 7.43 |
| 599 | 39°45.36' N | 24°05.61' E | 1084 | 0.47 | 16.50 | 0.579 | 195.88 | 8.66 |
| 601 | 40°05.22' N | 24°36.62' E | 977 | 0.27 | 6.00 | 0.750 | 206.68 | 9.97 |
| 602 | 40°13.03' N | 24°15.39' E | 1466 | 0.78 | 4.00 | 0.820 | 236.78 | 9.36 |
| 338 | 36°15.03' N | 03°24.98' W | 732 | 0.55 | 1.75 | 0.832 | 294.00 | 19.64 |
| 339 | 36°18.30' N | 03°08.39' W | 849 | 0.81 | 2.25 | 0.766 | 280.09 | 16.71 |
| 347 | 36°27.90' N | 02°55.50' W | 629 | 0.63 | 1.50 | 0.835 | 273.71 | 19.53 |
| 394 | 38°53.39' N | 02°38.40' E | 646 | 1.28 | 8.00 | | 171.05 | 9.90 |
| 395 | 38°57.70' N | 02°31.51' E | 834 | 0.81 | 7.00 | 0.463 | 170.54 | 8.40 |
| 396 | 39°09.60' N | 02°28.78' E | 562 | 0.88 | 10.00 | 0.403 | 167.82 | 10.52 |
| Canyon ø | 42°27.60' N | 03°29.80' E | 920 | 1.50 | 4.00 | 0.870 | | 19.7 |
| Canyon feb | 42°27.60' N | 03°29.80' E | 920 | 0.49 | | | | |
| Canyon aug | 42°27.60' N | 03°29.80' E | 920 | 2.50 | | | | |
| Slope ø | 42°25.60' N | 03°42.00' E | 800 | 1.81 | 11.00 | 0.720 | | 12.8 |
| Slope feb | 42°25.60' N | 03°42.00' E | 800 | 3.21 | | | | |
| Slope aug | 42°25.60' N | 03°42.00' E | 800 | 0.41 | | | | |

4. Carbon isotope deviations in foraminifera as C_{org} flux proxy

Skliris et al., 2010). In addition, resuspension and lateral transport of organic matter can lead to locally enhanced food availability in submarine canyons and isolated basins (Puig & Palanques, 1998; Danovaro et al., 1999; Heussner et al., 2006; Canals et al., 2013).

In this study we have compiled a data set on the stable carbon isotope composition of life and dead individuals of three epifaunal species (*Cibicidoides pachydermus*, *Planulina ariminensis*, *Lobatula lobatula*) and one shallow infaunal species (*Uvigerina mediterranea*) from 19 Mediterranean sites. The sites are located in a well-defined depth interval (between 400 and 1500 m) and represent a wide range of trophic conditions. Corrected for ontogenetic effects, the $\Delta\delta^{13}\text{C}_{U_{med-Epi}}$ signal was compared to the microhabitat of *U. mediterranea*, the depth of the main redox boundary, TOC content, and organic carbon flux rates calculated from satellite-derived primary production or (if available) flux measurements from sediment trap studies. Major target of this study is the development and evaluation of a transfer function for organic matter fluxes applicable to the quantification of past trophic changes in the Mediterranean Sea.

4.2 Material and methods

This study is based on a compilation of new and published isotope data of multicorer samples retrieved from various Mediterranean sub-basins covering a water depth range of 424 to 1466 m (Table 2). The study areas include the Alboran Sea and the Mallorca Channel (R.V. *Meteor* cruise M69/1 in August 2006) (Hübscher et al., 2010; data published in Theodor et al., 2016a), the Gulf of Lions, Spanish Slope off Barcelona and Strait of Sicily (M40/4 in February 1998) (Hieke et al., 1999; this study and data published in Schmiedl et al., 2004), and the Aegean Sea (M51/3 in November 2001) (Hemleben et al., 2003; this study) (Fig. 12). For each station, the sediment color change from yellowish brown to greenish gray was used as an indicator for the change in redox potential from positive to negative values, which serves as an approximation of oxygen consumption and penetration in the surface sediment (Lyle, 1983; Schmiedl et al., 2000).

The upper 10 cm of the sediment were commonly sliced into 0.5 to 1 cm intervals, in the Aegean Sea into coarser intervals below 3 cm, and all samples were subsequently preserved in Rose Bengal stained alcohol (1.5 g Rose Bengal per 1 l of 96 % ethanol) in order to stain cytoplasm of live or recently living foraminifera (Walton, 1952; Bernhard, 2000). In the laboratory, the sediment samples were wet-sieved over a 63 μm sieve and after drying at 40 °C, dry-sieved over a 150 μm (Aegean Sea samples) or 125 μm (remaining samples) mesh, respectively. From the coarse fraction of the different down-core intervals, stained individuals of selected epifaunal and shallow infaunal taxa have been counted and the Median Living Depths (MLD, equation [1]) were calculated as reference for the respective microhabitat preferences. Only tests with at least three subsequent brightly red colored chambers were considered as living. The low number of stained individuals of epifaunal taxa

4.2 Material and methods

impeded analyses, except for Site 540B, where stained tests of *C. pachydermus* were available. Likewise, stained tests of *U. mediterranea* were absent at Sites 586 and 589.

For stable isotope measurements, stained tests (and unstained tests if no stained tests were available) of three epifaunal species (*C. pachydermus*, *P. ariminensis*, *L. lobatula*) and one shallow infaunal species (*U. mediterranea*) were selected and each test was measured with a micrometer of an accuracy of 10 μm . The stable carbon and oxygen isotope measurements were performed at the Alfred Wegener Institute, Helmholtz Centre for Polar and Marine Research at Bremerhaven with two Finnigan MAT 253 stable isotope ratio mass spectrometers coupled to automatic carbonate preparation devices (Kiel IV). The mass spectrometers were calibrated via international standard NBS 19 to the PDB scale, with results given in δ -notation versus VPDB. Based on an internal laboratory standard (Solnhofen limestone) measured over a one-year period together with samples, the precision of stable isotope measurements was better than 0.06 ‰ and 0.08 ‰ for carbon and oxygen, respectively. The $\delta^{13}\text{C}$ difference between epi- and shallow infaunal taxa was calculated as a proxy for the pore water signal, i.e. the $\delta^{13}\text{C}_{\text{DIC}}$ gradient between bottom water and shallow pore water. For *U. mediterranea* this procedure was restricted to measurements from the size fraction $>600 \mu\text{m}$ in order to minimize ontogenetic effects (Schmiedl et al., 2004; Theodor et al., 2016a).

Total organic carbon (TOC) concentration in the surface sediment was measured with a Carlo Erba 1500 CNS Analyzer with a precision of 0.02 %. Before measurement, CaCO_3 was removed by adding 1 N HCl. The TOC values of Sites 596, 601 and 602 were taken from Möbius et al. (2010a, b). Bottom water oxygen concentrations are based on CTD measurements stored in the MedAtlas data set. Primary productivity values in surface waters of the year previously to sampling at each site are based on satellite data of the GlobColour project, and were calculated with the algorithms of Antoine & Morel (1996) as well as Uitz et al. (2008). If available, these estimates were compared with nearby direct primary productivity and export flux measurements. The export fluxes down to the sea floor were estimated according to the function of Betzer et al. (1984) adapted by Felix (2014).

Table 3. Average stable carbon isotope composition of selected benthic foraminifera with standard deviations. Also given are values for *Uvigerina mediterranea* tests larger than 600 μm and the difference of this species compared to the average epifaunal stable carbon isotope ratios ($\Delta\delta^{13}\text{C}_{\text{Umed-Epi}}$).

| Site | $\delta^{13}\text{C}_{Pari}$ (‰ VPDB) | st. dev. (‰) | $\delta^{13}\text{C}_{Cpac}$ (‰ VPDB) | st. dev. (‰) | $\delta^{13}\text{C}_{Clob}$ (‰ VPDB) | st. dev. (‰) | $\delta^{13}\text{C}_{Epi}$ (‰ VPDB) | st. dev. (‰) | $\delta^{13}\text{C}_{Umed}$ stained (‰ VPDB) | st. dev. (‰) | $\delta^{13}\text{C}_{Umed}$ unstained (‰ VPDB) | st. dev. (‰) | $\delta^{13}\text{C}_{Umed}$ std. (>600 μm) (‰ VPDB) | st. dev. (‰) | $\delta^{13}\text{C}_{Umed}$ unstd. (>600 μm) (‰ VPDB) | st. dev. (‰) | $\Delta\delta^{13}\text{C}_{Umed}$ <i>d-Epi</i> std. (>600 μm) (‰) | st. dev. (‰) | $\Delta\delta^{13}\text{C}_{Umed}$ <i>Epi</i> unstd. (>600 μm) (‰) | st. dev. (‰) |
|--------|---|--------------------|---|--------------------|---|--------------------|--|--------------------|--|--------------------|--|--------------------|--|--------------------|--|--------------------|---|--------------------|---|--------------------|
| 537 | | | 1.11 | ±0.32 | | | 1.11 | ±0.32 | 0.17 | ±0.38 | -0.88 | ±0.16 | 0.35 | ±0.26 | -0.82 | ±0.03 | -0.76 | ±0.58 | -1.93 | ±0.35 |
| 540A | 1.08 | ±0.14 | 0.76 | ±0.17 | | | 1.08 | ±0.14 | -0.46 | ±0.21 | | | -0.21 | ±0.09 | | | -1.29 | ±0.30 | | |
| 540B | 0.99 | | 1.01 | ±0.13 | | | 1.01 | ±0.11 | 0.13 | ±0.32 | 0.19 | ±0.35 | 0.27 | ±0.23 | 0.46 | ±0.10 | -0.74 | ±0.34 | -0.55 | ±0.21 |
| 540C | 0.76 | | 1.01 | ±0.09 | | | 1.01 | ±0.09 | -0.14 | ±0.30 | 0.06 | ±0.32 | 0.05 | ±0.26 | 0.28 | ±0.32 | -0.97 | ±0.41 | -0.74 | ±0.47 |
| 585 | 1.32 | ±0.24 | | | | | 1.32 | ±0.24 | 0.58 | ±0.22 | 0.50 | ±0.47 | 0.58 | ±0.22 | 0.50 | ±0.22 | -0.74 | ±0.46 | -0.82 | ±0.46 |
| 586 | 1.90 | ±0.15 | | | | | 1.90 | ±0.15 | | | 0.95 | ±0.46 | | | 1.11 | ±0.31 | | | -0.79 | ±0.46 |
| 589 | 1.34 | ±0.11 | | | | | 1.34 | ±0.11 | | | 0.51 | ±0.46 | | | 0.73 | ±0.39 | | | -0.61 | ±0.50 |
| 592 | 1.30 | ±0.23 | | | | | 1.30 | ±0.23 | -0.14 | ±0.02 | 0.15 | ±0.25 | -0.12 | ±0.00 | 0.24 | ±0.20 | -1.42 | ±0.23 | -1.06 | ±0.43 |
| 595 | 1.87 | ±0.15 | | | | | 1.87 | ±0.15 | 0.09 | ±0.53 | 0.67 | ±0.41 | 0.37 | ±0.31 | 0.77 | ±0.41 | -1.49 | ±0.46 | -1.09 | ±0.56 |
| 596 | 0.96 | ±0.04 | | | | | 0.96 | ±0.04 | -0.38 | ±0.38 | -0.43 | ±0.34 | -0.23 | ±0.33 | -0.27 | ±0.27 | -1.19 | ±0.37 | -1.23 | ±0.31 |
| 599 | 1.76 | ±0.12 | | | | | 1.76 | ±0.12 | 0.03 | ±0.26 | 0.25 | ±0.45 | 0.12 | ±0.20 | 0.41 | ±0.28 | -1.63 | ±0.32 | -1.35 | ±0.40 |
| 601 | | | 0.47 | ±0.06 | | | 1.02 | ±0.06 | -0.53 | ±0.27 | -0.47 | ±0.38 | -0.34 | ±0.14 | -0.37 | ±0.35 | -1.36 | ±0.20 | -1.39 | ±0.41 |
| 602 | 0.87 | | 0.31 | ±0.20 | | | 0.87 | | -1.11 | ±0.31 | -1.09 | ±0.27 | -0.98 | ±0.32 | -1.13 | ±0.26 | -1.85 | ±0.32 | -2.00 | ±0.26 |
| 338 | 1.22 | | 0.64 | ±0.21 | 0.92 | | 1.22 | | -0.05 | ±0.26 | 0.29 | ±0.37 | 0.07 | ±0.28 | 0.55 | ±0.23 | -1.15 | ±0.28 | -0.67 | ±0.23 |
| 339 | 1.22 | ±0.11 | 0.86 | | -0.12 | | 1.22 | ±0.11 | 0.02 | ±0.46 | 0.06 | ±0.20 | 0.22 | ±0.28 | 0.16 | ±0.19 | -0.99 | ±0.39 | -1.06 | ±0.30 |
| 347 | 1.16 | ±0.07 | 0.82 | ±0.06 | -0.16 | | 1.16 | ±0.07 | -0.19 | ±0.25 | 0.02 | ±0.17 | -0.13 | ±0.13 | 0.41 | ±0.00 | -1.29 | ±0.20 | -0.75 | ±0.07 |
| 394 | | | 1.52 | ±0.01 | 0.98 | | 1.28 | | 0.58 | ±0.31 | 0.61 | ±0.23 | 0.64 | ±0.26 | 0.71 | ±0.13 | -0.64 | ±0.27 | -0.58 | ±0.14 |
| 395 | | | 1.54 | | 0.80 | ±0.02 | 1.10 | ±0.02 | 0.47 | ±0.30 | 0.53 | ±0.21 | 0.53 | ±0.27 | 0.63 | ±0.13 | -0.57 | ±0.27 | -0.46 | ±0.13 |
| 396 | 1.22 | ±0.22 | 1.76 | | 0.92 | | 1.22 | ±0.22 | 0.66 | ±0.22 | -0.64 | ±0.60 | 0.72 | ±0.19 | -0.91 | ±0.42 | -0.50 | ±0.29 | -2.13 | ±0.52 |
| Canyon | | | 0.52 | ±0.04 | | | 0.80 | ±0.07 | -0.32 | ±0.29 | -0.32 | ±0.27 | -0.17 | ±0.20 | -0.21 | ±0.26 | -0.97 | ±0.27 | -1.01 | ±0.33 |
| Slope | | | 0.39 | ±0.09 | | | 1.00 | ±0.06 | 0.26 | ±0.30 | | | 0.33 | 0.26 | | | -0.67 | ±0.32 | | |

4. Carbon isotope deviations in foraminifera as C_{org} flux proxy

4.3 Results

Benthic foraminiferal $\delta^{13}\text{C}$ values cover a range of more than 3 ‰, with higher average values of epifaunal species than the shallow infaunal *U. mediterranea* (Table 3). The epifaunal species *C. pachydermus*, *L. lobatula* and *P. ariminensis* show average values between 1.90 ‰ at Site 586 (southern Aegean Sea) and -0.16 ‰ at Site 347 (Mallorca Channel) (Table 3; Fig. 13). The highest average epifaunal $\delta^{13}\text{C}_{\text{Epi}}$ values are in the southern and central Aegean Sea (Sites 586, 595), while further to the north at Site 601 (northern Aegean Sea) the average $\delta^{13}\text{C}_{\text{Epi}}$ value of 0.87 ‰ is among the lowest measured. At Site 540B in the Gulf of Lions, the average $\delta^{13}\text{C}_{\text{Epi}}$ value of 1.01 ‰ is in good agreement with 1.00 ‰ measured by Schmiiedl et al. (2004) at the same site. Size-dependent measurements did not reveal any ontogenetic trend in the $\delta^{13}\text{C}$ signal of the epifaunal taxa (Table A.4).

For *U. mediterranea* $\delta^{13}\text{C}_{\text{Umed}}$ values vary between -1.41 and 0.85 ‰ for stained tests and between -1.52 and 1.77 ‰ for unstained tests (Table A.4). The highest average values are recorded for the southern Aegean Sea, with 0.58 ‰ and 1.11 ‰ for stained and unstained tests, respectively. The lowest average values are recorded for the northern Aegean Sea, with -0.98 ‰ and -1.13 ‰ for stained and unstained tests, respectively. The variability at a single site reach 1.38 ‰ in stained (Site 537) and 2.21 ‰ in unstained tests (Site 586). The ontogenetic $\delta^{13}\text{C}_{\text{Umed}}$ trends are generally comparable for the western Mediterranean Sea and the Strait of Sicily, with $0.11 \pm 0.03 \text{‰} (100 \mu\text{m})^{-1}$ for stained and $0.07 \pm 0.03 \text{‰} (100 \mu\text{m})^{-1}$ for unstained tests, except for Site 396 that shows an anomalous negative trend (Table 4; Fig. 14). In the Aegean Sea, the ontogenetic $\delta^{13}\text{C}_{\text{Umed}}$ trends are approximately 50 % steeper with an increase of $0.16 \pm 0.04 \text{‰} (100 \mu\text{m})^{-1}$ for stained tests. Unstained tests reveal a higher variability and a less steep slope of $0.10 \pm 0.07 \text{‰} (100 \mu\text{m})^{-1}$ (Table 4, Fig. 14). In order to avoid bias due to ontogenetic effects, only $\delta^{13}\text{C}_{\text{Umed}}$ values of tests larger than 600 μm were used for comparison with $\delta^{13}\text{C}_{\text{Epi}}$ values.

The calculated $\Delta\delta^{13}\text{C}_{\text{Umed-Epi}}$ values for stained tests range from -0.64 ‰ in the Gulf of Lion (slope Site) and -0.74 ‰ (Site 585) to -1.29 ‰ in the western Mediterranean Sea (Sites 347 and 540A), to -1.85 ‰ in the northern Aegean Sea (Site 602) (Table 3). Due to the wider scattering of the $\delta^{13}\text{C}$ values of unstained tests, $\Delta\delta^{13}\text{C}_{\text{Umed-Epi}}$ values range from -0.61 ‰ (Site 589) to -2.0 ‰ (Site 602) in the Aegean Sea and from -0.55 ‰ (Site 540B) to -1.06 ‰ (Site 339) in the western Mediterranean Sea and the Strait of Sicily (Table 3). The magnitude of $\Delta\delta^{13}\text{C}_{\text{Umed-Epi}}$ values exhibits a relation with trophic conditions at each site, revealing higher differences at more eutrophic sites. Good accordance with the $\Delta\delta^{13}\text{C}_{\text{Umed-Epi}}$ show the main redox boundary depth (Fig. 15a) as well as the Median Living Depth of the shallow infaunal *U. mediterranea* (MLD_{Umed}) (Fig. 15b) and less distinctive also the TOC (Fig. 15c). However, a direct correlation with surface water productivity isn't recognizable, neither for stained nor unstained test values (Fig. 15d, e).

4. Carbon isotope deviations in foraminifera as C_{org} flux proxy

The MLD_{Umed} , which is used here to describe its microhabitat, increases at the sites with deeper main redox boundaries. The deepest MLD_{Umed} are 2.13 and 2.25 cm in the southern Aegean Sea, while the shallowest depths of 0.27 cm and 0.38 cm are recorded in the central and northern Aegean Sea, respectively (Table 1, Table A.1). In the Gulf of Lions, the MLD_{Umed} is between 0.43 and 0.49 cm in the axis of the Lacaze–Duthiers Canyon and around 1.22 cm at the open slope (Table 2, Fig. 15a). The depth of the sediment color change, which marks the shift in redox potential and thus oxygen penetration, ranges from 2.25 cm in the Gulf of Lions (Site 540A) to as much as 30 cm in the central Aegean Sea (Site 596) (Table 2, Fig. 15b). The measured TOC contents of the surface sediment range from 0.41 % (Site 586, southern Aegean Sea) and 0.58 % (Site 537, Strait of Sicily) to a maximum of 0.82 % (Site 602, northern Aegean Sea) (Table 2, Fig. 15c).

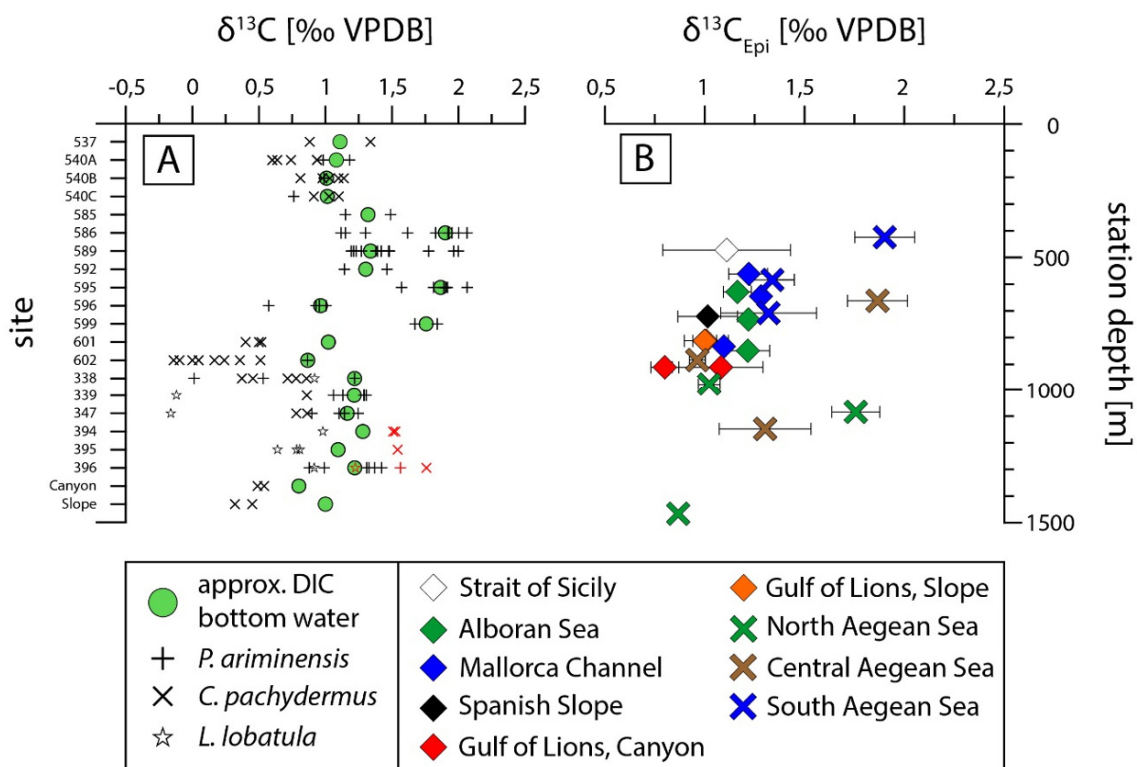


Figure 13. (a) The $\delta^{13}C$ signals of epifaunal species (*Cibicides pachydermus*, *Lobatula lobatula*, *Planulina ariminensis*) with estimated $\delta^{13}C_{Epi}$ value for each investigated site. Symbol sizes indicate different test sizes. Red symbols mark relocated fossil tests. Green circles show $\delta^{13}C_{DIC}$ value of the bottom water approximated after $\delta^{13}C_{Epi}$ values. (b) The $\delta^{13}C_{Epi}$ versus water depth shows a wider scattering for the Aegean Sea, than for the western Mediterranean Sea.

The estimated values for annual primary production range from 106 to 294 $gC\ m^{-2}\ a^{-1}$. Application of the different algorithms of Antoine & Morel (1996) and Uitz et al. (2008) resulted in an average offset of 54 $gC\ m^{-2}\ a^{-1}$, with PP values consistently higher when applying the algorithm of Antoine & Morel (1996). The highest PP values occur in the Alboran Sea (274–294 versus 192–207 $gC\ m^{-2}\ a^{-1}$ according to Uitz et al., 2008) and the northern Aegean Sea (196–237 and 139–164 $gC\ m^{-2}\ a^{-1}$, resp.), while the lowest PP values occur in the southern and central Aegean Sea (151–161 and 106–116 $gC\ m^{-2}\ a^{-1}$, resp.) (Table 2).

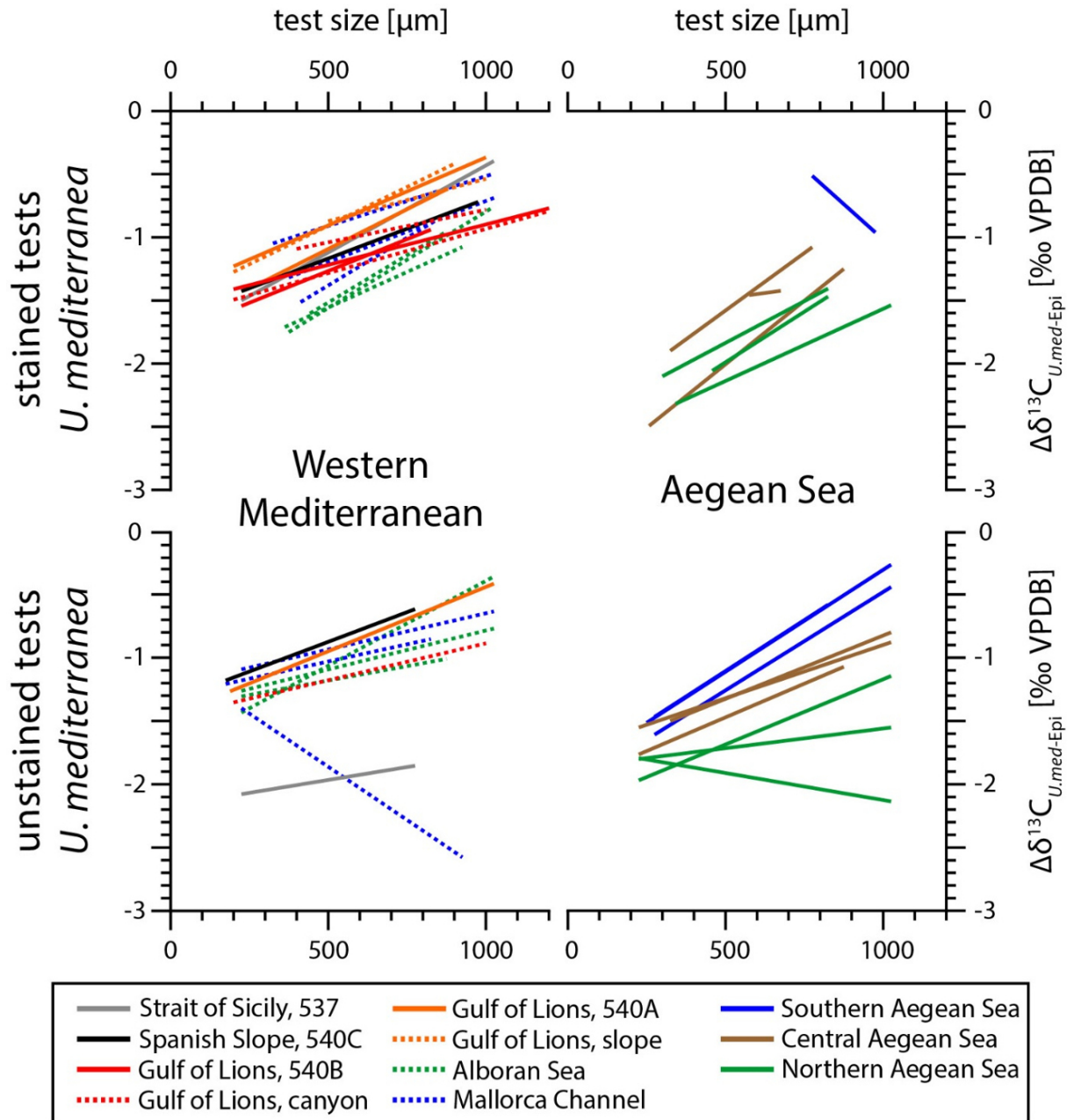


Figure 14. Ontogenetic trends in the $\delta^{13}\text{C}$ difference between *Uvigerina mediterranea* and epifaunal taxa ($\Delta\delta^{13}\text{C}_{U,\text{med-Epi}}$) based on different size classes of *U. mediterranea*. Data shown are for live (rose Bengal stained) and dead (unstained) individuals of *U. mediterranea* and for the western Mediterranean Sea (left) and Aegean Sea (right). Dashed lines represent already published data (Schmiedl et al., 2004; Theodor et al., 2016a).

4.4 Discussion

4.4.1 Stable carbon isotope signal of epifaunal foraminifera in relation to surrounding water masses

The $\delta^{13}\text{C}$ signal of *Cibicidoides pachydermus*, *Lobatula lobatula*, and *Planulina ariminensis* primarily reflects the $\delta^{13}\text{C}_{\text{DIC}}$ of the ambient bottom water since these species appear to prefer an epifaunal microhabitat (Lutze & Thiel, 1989; Kitazato, 1994; Schmiedl et al., 2000). Comparison with published water $\delta^{13}\text{C}_{\text{DIC}}$ measurements confirms $\delta^{13}\text{C}_{\text{Epi}}$ values close to equilibrium also for the Mediterranean Sea (Pierre, 1999; Schmiedl et al., 2004; Theodor et al., 2016a). Further, our new data corroborate previous observations of lacking ontogenetic effects in the $\delta^{13}\text{C}_{\text{Epi}}$ signal of these taxa (Corliss et al., 2002; Franco–Fraguas et al., 2011; Theodor et al., 2016a) (Table A.4).

In the Alboran Sea (Sites 339 and 347), we measured inter-specific $\delta^{13}\text{C}_{\text{Epi}}$ differences of up to 1.4‰ in unstained individuals. This variability is a result of implausible low $\delta^{13}\text{C}_{\text{Clob}}$ values, probably due to a relocation from shallower depths closer to the coast. Conversely, the $\delta^{13}\text{C}_{\text{Cpachy}}$ signal in the Mallorca Channel represents glacial values and is probably affected by the admixture of reworked fossil tests at the sediment surface, as indicated by $\delta^{18}\text{O}$ values of >4.0‰ (Table A.4). For all unstained tests also a shift to higher $\delta^{13}\text{C}_{\text{Epi}}$ values due to potential dissolution effects should be considered (Edgar et al., 2013). In order to minimize these effects, a large number of tests, if possible, were measured for *C. pachydermus* and *P. ariminensis*, showing commonly 0.3–0.5‰ higher $\delta^{13}\text{C}$ values for latter species (Table 3, Fig. 13a). Data of *L. lobatula* have only been used for further evaluation where no tests of other species were available for analysis (Theodor et al., 2016a) (Fig. 13a).

The $\delta^{13}\text{C}$ offset between *C. pachydermus* and *P. ariminensis* isn't constant and seems to increase on sites with deeper main redox boundaries. Suggesting a connection therefore with increasing organic matter availability, the varying offsets can be attributed to slight differences in their microhabitat (Table 3; Fig. 13a). While *P. ariminensis* is a strictly epifaunal species, living attached on surfaces on or above the sediment (Lutze & Thiel, 1989), *C. pachydermus* commonly lives at or slightly below the sediment–water interface (Rathburn & Corliss, 1994; Schmiedl et al. 2000; Licari & Mackensen, 2005). A very shallow infaunal microhabitat of *C. pachydermus* is corroborated by slightly lower $\delta^{13}\text{C}$ values relative to bottom water $\delta^{13}\text{C}_{\text{DIC}}$ suggesting pore water influence (Schmiedl et al., 2004; Fontanier et al., 2006). In order to compensate for potential pore water effects in the $\delta^{13}\text{C}$ signal of the epifaunal species, the highest $\delta^{13}\text{C}_{\text{Epi}}$ values, mostly of *P. ariminensis*, should be selected for further comparison with shallow infaunal $\delta^{13}\text{C}_{\text{Umed}}$ signals (Table 2).

The recorded $\delta^{13}\text{C}_{\text{Epi}}$ values can be related to different Mediterranean water masses (Fig. 13b). The $\delta^{13}\text{C}_{\text{Epi}}$ values of the Gulf of Lions and the Spanish Slope off Barcelona are as low as 0.8‰ suggesting a strong Levantine Intermediate Water (LIW) influence (Pierre, 1999). The $\delta^{13}\text{C}_{\text{Epi}}$ values of

4.4 Discussion

Table 4. Linear regressions of ontogenetic trends of $\delta^{13}\text{C}_{Umed}$. The measured number of stained and unstained tests as well as the significance values are added.

| <i>U. mediterranea</i> stained | | | | |
|----------------------------------|----|--------------------------------|-----------|-------------------|
| site | n | linear fit | R-squared | p-value |
| 537 | 24 | $Y = 0.001379 * X - 1.810017$ | 0.67 | $1.1065 * e^{-6}$ |
| 540A | 23 | $Y = 0.001007 * X - 1.770373$ | 0.70 | $5.746 * e^{-7}$ |
| 540B | 14 | $Y = 0.001257 * X - 1.7208851$ | 0.54 | 0.0027 |
| 540C | 46 | $Y = 0.000943 * X - 1.639236$ | 0.55 | $3.769 * e^{-6}$ |
| 585 | 3 | $Y = -0.00224 * X + 1.222667$ | 1.00 | 0.0082 |
| 592 | 2 | $Y = 0.00034 * X - 1.6535$ | 1.00 | – |
| 595 | 10 | $Y = 0.002013 * X - 3.012139$ | 0.75 | 0.0012 |
| 596 | 7 | $Y = 0.001822 * X - 2.490764$ | 0.60 | 0.0401 |
| 599 | 10 | $Y = 0.001600 * X - 2.789560$ | 0.49 | 0.0289 |
| 601 | 11 | $Y = 0.001322 * X - 2.497314$ | 0.70 | 0.0013 |
| 602 | 15 | $Y = 0.001143 * X - 2.709099$ | 0.41 | 0.0102 |
| 338 | 10 | $Y = 0.001498 * X - 2.265059$ | 0.72 | 0.0020 |
| 339 | 12 | $Y = 0.001527 * X - 2.323114$ | 0.48 | 0.0124 |
| 347 | 7 | $Y = 0.001126 * X - 2.119201$ | 0.68 | 0.0232 |
| 394 | 19 | $Y = 0.000968 * X - 1.680654$ | 0.27 | 0.0221 |
| 395 | 23 | $Y = 0.001509 * X - 2.135640$ | 0.40 | 0.0012 |
| 396 | 20 | $Y = 0.000789 * X - 1.304866$ | 0.39 | 0.0034 |
| Canyon aug | 7 | $Y = 0.000516 * X - 1.297794$ | 0.45 | 0.1015 |
| Canyon feb | 21 | $Y = 0.000701 * X - 1.634263$ | 0.43 | 0.0012 |
| Slope aug | 6 | $Y = 0.000671 * X - 1.207976$ | 0.34 | 0.2244 |
| Slope feb | 14 | $Y = 0.001223 * X - 1.518849$ | 0.48 | 0.0060 |
| <i>U. mediterranea</i> unstained | | | | |
| site | n | linear fit | R-squared | p-value |
| 537 | 7 | $Y = 0.000408 * X - 2.169793$ | 0.33 | 0.1784 |
| 540B | 16 | $Y = 0.001017 * X - 1.457536$ | 0.80 | $2.4803 * e^{-6}$ |
| 540C | 9 | $Y = 0.000938 * X - 1.343878$ | 0.53 | 0.0270 |
| 585 | 4 | $Y = 0.001610 * X - 1.910093$ | 0.85 | 0.0808 |
| 586 | 29 | $Y = 0.001555 * X - 2.035859$ | 0.48 | $2.9156 * e^{-5}$ |
| 589 | 25 | $Y = 0.001612 * X - 1.917381$ | 0.58 | $1.0482 * e^{-5}$ |
| 592 | 28 | $Y = 0.001001 * X - 1.826222$ | 0.48 | $4.5201 * e^{-5}$ |
| 595 | 36 | $Y = 0.000841 * X - 1.740275$ | 0.17 | 0.0130 |
| 596 | 37 | $Y = 0.001065 * X - 2.004262$ | 0.30 | 0.0005 |
| 599 | 12 | $Y = 0.001031 * X - 2.201211$ | 0.31 | 0.0600 |
| 601 | 21 | $Y = 0.000312 * X - 1.871316$ | 0.04 | 0.3927 |
| 602 | 14 | $Y = -0.000427 * X - 1.697763$ | 0.12 | 0.2159 |
| 338 | 10 | $Y = 0.001343 * X - 1.735480$ | 0.90 | $3.0586 * e^{-5}$ |
| 339 | 9 | $Y = 0.000456 * X - 1.408000$ | 0.31 | 0.1197 |
| 347 | 10 | $Y = 0.000615 * X - 1.400530$ | 0.71 | 0.0023 |
| 394 | 22 | $Y = 0.000573 * X - 1.221329$ | 0.32 | 0.0060 |
| 395 | 15 | $Y = 0.000544 * X - 1.301955$ | 0.33 | 0.0256 |
| 396 | 17 | $Y = -0.001682 * X - 1.020989$ | 0.50 | 0.0016 |
| Canyon aug | 36 | $Y = 0.000584 * X - 1.469912$ | 0.28 | 0.0009 |

4. Carbon isotope deviations in foraminifera as C_{org} flux proxy

the Alboran Sea, the Mallorca Channel, and the Strait of Sicily commonly vary between 1.1 and 1.2 ‰ and thus reflect the influence of deeper water masses. For the western sites an influence of the Tyrrhenian Deep Water can be assumed. This water mass originates in the Tyrrhenian Sea from a mixture of Levantine Intermediate Water (LIW) and Western Mediterranean Deep Water (WMDW) (Rhein et al., 1999; Send et al., 1999) and is characterized by a $\delta^{13}\text{C}_{\text{DIC}}$ signature between 1.0 to 1.1 ‰ (Pierre, 1999). For the Strait of Sicily the eastern position explains the influence of less mixed LIW of Eastern Mediterranean origin with a $\delta^{13}\text{C}_{\text{DIC}}$ signature of 1.15 ‰ (Pierre, 1999).

In the Aegean Sea, the broad range of recorded $\delta^{13}\text{C}_{\text{Epi}}$ values of 0.87 to 1.95 ‰ reflects the strong small-scale oceanographic differences of this region, including presence of various small isolated basins (Figs. 12, 13b). The comparatively high $\delta^{13}\text{C}_{\text{Epi}}$ values of the shallower sites indicate intensified vertical convection at sites of subsurface-water formation, which recently resumed after the stagnation phase of 1994 to 2000 (Androulidakis et al., 2012), although the main deep-water formation area is restricted to the Cretan Sea (Roether et al., 1996; Lascaratos et al., 1999). At greater depth of isolated basins, reduced replenishment of bottom waters (Zervakis et al., 2003; Velaoras & Lascaratos, 2005) is accompanied by relatively low $\delta^{13}\text{C}_{\text{DIC}}$ and accordingly low $\delta^{13}\text{C}_{\text{Epi}}$ values in these environments.

4.4.2 Biological and environmental effects on the stable carbon isotope signal of *Uvigerina mediterranea*

The size-dependent changes in the $\delta^{13}\text{C}$ signal of *Uvigerina mediterranea* can be attributed to ontogenetic effects. Small tests are depleted in ^{13}C , while larger tests are closer to $\delta^{13}\text{C}_{\text{DIC}}$ of the ambient pore water (Fig. 14). Relatively low $\delta^{13}\text{C}_{\text{Umed}}$ values of small tests suggest stronger metabolic fractionation in younger individuals (Schmiedl et al., 2004, McCorkle et al., 2008; Schumacher et al., 2010, Theodor et al., 2016a). A linear ontogenetic increase of 0.11 ‰ (100 μm)⁻¹ was observed at all sites of the western Mediterranean Sea, while a steeper slope of 0.16 ‰ (100 μm)⁻¹ was recorded in the Aegean Sea (Fig. 14). In addition, the $\delta^{13}\text{C}_{\text{Umed}}$ values of small individuals from the Aegean Sea were in the order of 1 ‰ lower compared to those from the western Mediterranean Sea.

Differences in ontogenetic $\delta^{13}\text{C}$ slopes of the related species *U. peregrina* have been attributed to its highly opportunistic response to regional contrasts in organic matter quantity and quality, and seasonality of supply (Theodor et al., 2016a). Obviously, similar effects are also operational in ontogenetic $\delta^{13}\text{C}$ trends of *U. mediterranea*. In the Aegean Sea, this species seems to respond to strong seasonal contrasts in organic matter fluxes (Siokou–Frangou et al., 2002) resulting in particularly high metabolic activity and low $\delta^{13}\text{C}_{\text{Umed}}$ values in young individuals. A steepening of the $\delta^{13}\text{C}_{\text{Umed}}$ slopes from the North to the South Aegean Sea has probably the same reasons as for *U. peregrina* in the western Mediterranean Sea. Because of the higher number of measured tests, this shift of the slope angles is more obvious in unstained than stained tests (Fig. 14). However, even with

an increased number of investigated sites compared to Theodor et al. (2016a), a similar trend in $\delta^{13}\text{C}_{U_{med}}$ is not recognizable for the western Mediterranean Sea. This might be caused by lower differences in the annual food supply between the sites or the in total higher input of organic matter compared to the Aegean Sea.

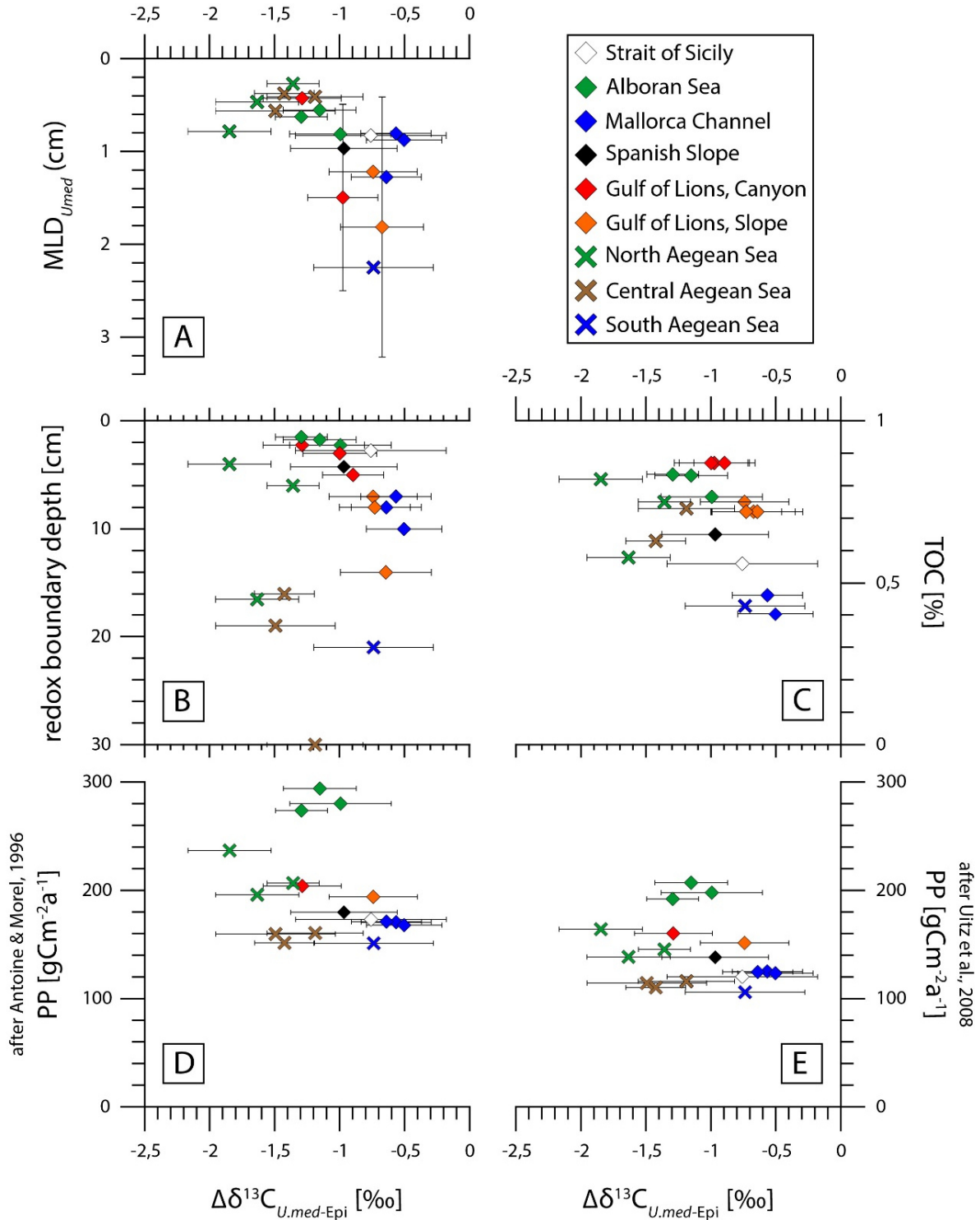


Figure 15. The $\delta^{13}\text{C}$ difference between live *Uvigerina mediterranea* and epifaunal taxa ($\Delta\delta^{13}\text{C}_{U_{med-Epi}}$) plotted against (a) Median Living Depth (MLD), (b) depth of redox boundary, (c) total organic carbon (TOC) content, (d, e) Primary production in surface waters of the year previous to sampling. The satellite derived PP was calculated with the algorithms of (d) Antoine & Morel, 1996 and (e) Uitz et al., 2008.

4. Carbon isotope deviations in foraminifera as C_{org} flux proxy

The $\delta^{13}C_{Umed}$ values of unstained individuals from 5 cm sediment depth in the western Mediterranean Sea and Strait of Sicily are on average 0.1 to 0.2 ‰ lower than those of live specimens in the topmost centimeter. This adds to previous observations (Theodor et al., 2016a) suggesting the influence of the Suess effect (Keeling, 1979; Quay et al., 1992) in live individuals while it is absent in sub-recent specimens. The Suess effect displays the reduction of $\delta^{13}C$ values in the atmosphere and oceans, due to the anthropogenic release of isotopically light CO_2 out of fossil resources, e.g. oil or coal. A similar effect could not be monitored in the Aegean Sea since live and dead individuals were selected from the same sediment depth suggesting only minor age differences (Table 3, Fig.14). The only exception is Site 595 in the central Aegean Sea, where the deviation is even higher (0.5-0.7 ‰), when compared to the western Mediterranean Sea. Since this signal is restricted to only one site it could be due to relocation of fossil tests by the effects of bioturbation or lateral sediment transport.

Under well-oxygenated conditions, the pore water $\delta^{13}C_{DIC}$ gradient depends on the organic matter fluxes and associated decomposition rates of organic matter in the surface sediment (McCorkle and Emerson, 1988; McCorkle et al., 1985, 1990, Holsten et al., 2004). Similarly, organic matter fluxes also control the depth of the oxygenated layer (Rutgers van der Loeff, 1990) and thus the microhabitat range of infaunal foraminifera (Corliss, 1985; Jorissen et al., 1995; Koho et al., 2008; Koho & Pina-Ochoa, 2012). In the Mediterranean Sea subsurface waters are well ventilated resulting in bottom water oxygen concentrations above 4.1 ml l^{-1} at all sites of our study (MedAtlas, 1997). The $\delta^{13}C$ signal of *U. mediterranea* appears particularly suitable to monitor the pore water $\delta^{13}C_{DIC}$ signal in the surface-near sediment because it seems to be less influenced by species-specific 'vital effects' (McConnaughey, 1989a, b) when compared to other shallow infaunal taxa, for example *U. peregrina* (Schmiedl et al., 2004; Theodor et al., 2016a).

In this study, the difference of $\delta^{13}C_{Umed}$ from bottom water $\delta^{13}C_{DIC}$ (reflected as higher $\Delta\delta^{13}C_{Umed-Epi}$ values) suggests logarithmic relations with the MLD of *U. mediterranea* (Fig. 15), the depth of the oxygenated layer and to the TOC content of the surface sediment. At the more oligotrophic to mesotrophic sites of the Mallorca Channel, the Gulf of Lions, the Spanish Slope off Barcelona, and the southern Aegean Sea, relatively low $\Delta\delta^{13}C_{Umed-Epi}$ values correspond to a relatively thick oxygenated layer and low TOC contents. The rather deep position of the redox boundary, exceeding 10 cm at some sites, enables *U. mediterranea* to inhabit a relatively wide microhabitat range. In contrast, at the more mesotrophic to eutrophic sites of the Alboran Sea relatively high $\Delta\delta^{13}C_{Umed-Epi}$ values coincide with relatively thin oxygenated layers and higher TOC contents. Here, the microhabitat range of *U. mediterranea* is compressed because of limited pore water oxygen (Fig. 15).

When comparing sites within the central and northern Aegean Sea, the foraminiferal stable isotope signature and the biogeochemical and ecological characteristics lack a consistent relation (Fig. 15). In these areas strongly negative $\Delta\delta^{13}C_{Umed-Epi}$ do not systematically correspond to maximum TOC contents and the shallowest redox boundary (Fig. 15). The reasons for this absence of a clear

relation between $\Delta\delta^{13}\text{C}_{U_{med-Epi}}$ and environmental parameters within this area cannot be unraveled with our available data. It may be related to the high variability in oceanographic and biogeochemical conditions of the bottom water in the isolated basins that are characterized by focusing of sedimentary material (Lykousis et al., 2002; Giresse et al., 2003; Poulos, 2009) and/or temporarily intermittent replenishment of deep-waters on seasonal to decadal time scales (Zervakis et al., 2003; Velaoras & Lascaratos, 2005; Androulidakis et al., 2012). The first possibility can increase the supply of refractory and isotopically heavy C_{org} , recorded by higher TOC contents, but with minor effects on the $\delta^{13}\text{C}_{DIC}$ pore water gradient. Latter possibility may not just reduce the $\delta^{13}\text{C}_{DIC}$ of the bottom water, but also push the pore water gradient towards stronger differences, explaining the more negative $\Delta\delta^{13}\text{C}_{U_{med-Epi}}$ values, compared to the remaining sites with similar conditions (Fig. 15).

4.4.3 Development of a stable carbon isotope based transfer function for organic carbon fluxes

Our results suggest a close relationship between the $\delta^{13}\text{C}$ gradient in the surface sediment (expressed as $\Delta\delta^{13}\text{C}_{U_{med-Epi}}$) and the organic matter (OM) fluxes to the sea floor, for open-ocean settings of the western and central Mediterranean Sea and the southern Aegean Sea (Fig. 16). Based on these observations, we tested the potential for the development of a $\delta^{13}\text{C}$ -based transfer function for OM flux rates. In open-ocean settings, the main food source of deep-sea environments is the exported OM from the surface layer, where photosynthetic primary production takes place (e.g. Boyd & Trull, 2007; Bishop, 2009). The majority of produced particulate organic carbon (POC) is recycled within the photic zone. In the open Mediterranean Sea, around 4 % of the POC is exported out of the photic zone, which is lower than for other open oceans, caused by a specific nutrient distribution in the Mediterranean Sea (Moutin & Raimbault, 2002; Gogou et al., 2014). So, the remineralization of organic matter is intensified, which leads to reduced fluxes to the sea floor.

During transfer from the surface ocean to the deep-sea, the amount of exported OM decreases exponentially reflecting microbial decay (Suess, 1980; de la Roche & Passow, 2007; Packard & Gomez, 2013). Various functions have been developed for the estimation of OM fluxes during sinking of particles through the water column integrating numerous observational data (Suess, 1980; Betzer et al., 1984; Martin et al., 1987; Antia, et al., 2001). The different functions reveal a high variability for the active surface layer, while the results for deeper parts of the water column are within a comparable range (Felix, 2014). In our study (Table 2, Fig. 16), we applied the function of Betzer et al. (1984) for calculation of the C_{org} fluxes at the different Mediterranean sites using satellite-borne PP data (Antoine & Morel, 1996; Uitz et al., 2008).

4. Carbon isotope deviations in foraminifera as C_{org} flux proxy

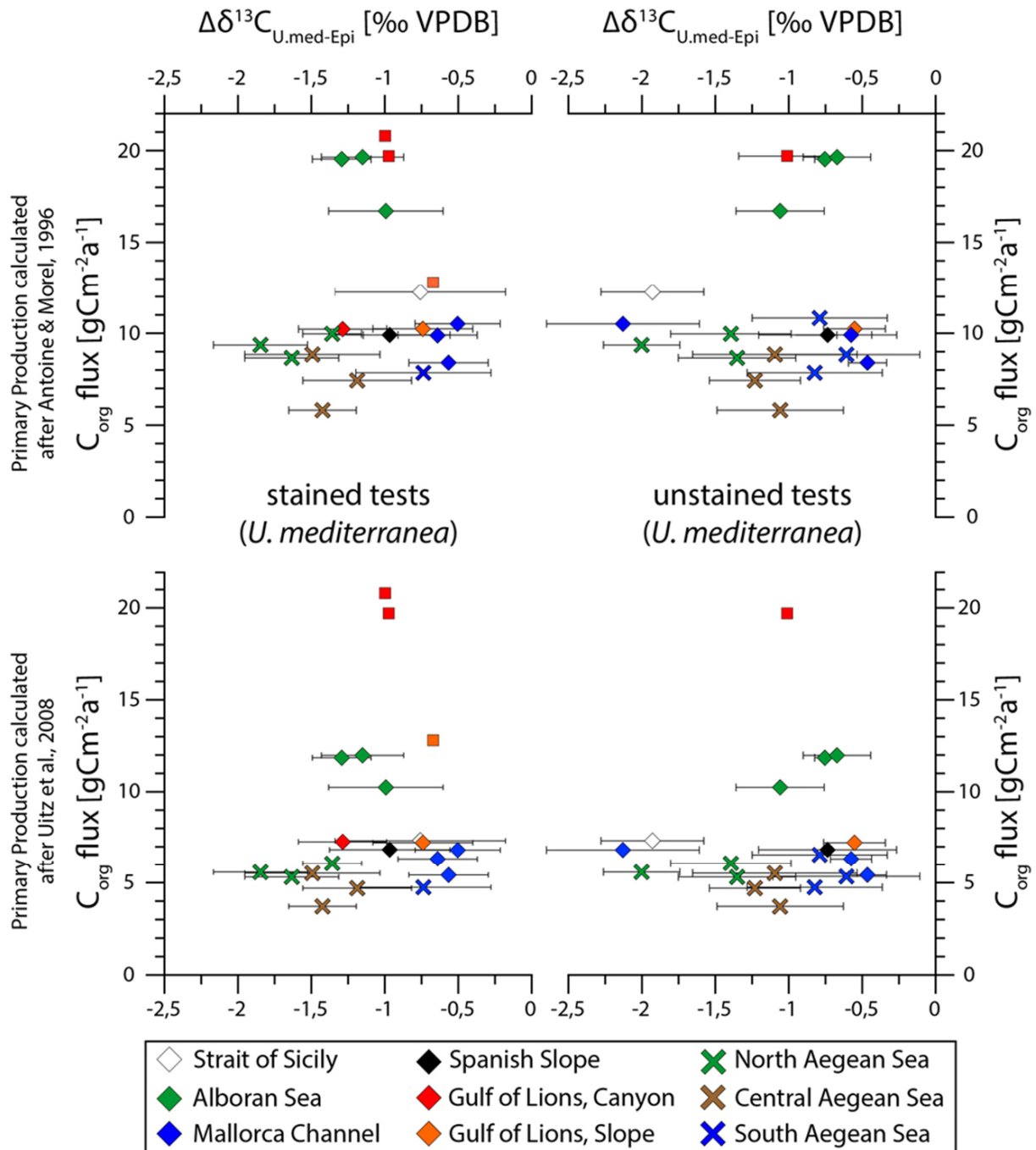


Figure 16. The $\delta^{13}C$ difference between live and dead *Uvigerina mediterranea* and epifaunal taxa ($\Delta\delta^{13}C_{Umed-Epi}$) against organic carbon flux rates (C_{org} flux) calculated from primary productivity in surface waters after Betzer et al. (1984). As in figure 15, satellite derived primary production values of Antoine & Morel (1996) (top) and Uitz et al., (2008) (bottom) were used.

A comparison with direct PP and export flux measurements of sediment trap studies revealed ambiguous results. The PP values calculated after Antoine and Morel (1996) are in a comparable range to PP measurements in the western Mediterranean (Moutin & Raimbault, 2002; Sanchez-Vidal et al., 2004, 2005; Zúñiga et al., 2007, 2008). However, the estimated export fluxes are too high in these areas compared to the direct measurements of the referred studies, probably due to the aforementioned higher remineralization rate in the Mediterranean Sea. However, the discrepancy in

4.4 Discussion

export fluxes is partly compensated by the application of the 21–30 % lower PP values calculated after Uitz et al. (2008). For the Aegean Sea, in contrast, distinctively higher measured PP values have been reported than were estimated (Siokou–Frangou et al., 2002). For the Gulf of Lions measured OM export fluxes exceed the predicted values (Heussner et al., 2006), which can be explained by the additional lateral input of organic carbon channeled within the local canyon systems (Schmiedl et al., 2000). In order to compensate these possible additional C_{org} fluxes in marginal basin areas, the application of the function of Antoine and Morel (1996) appears more useful, taking into account a potential overestimation of C_{org} fluxes in open-ocean areas.

For both approaches of PP calculation (Antoine & Morel, 1996; Uitz et al., 2008) the relation between the estimated C_{org} fluxes and the $\Delta\delta^{13}C_{Umed-Epi}$ exhibits a complex pattern and at first instance lacks a simple and statistically significant correlation (Fig. 16). Particularly, strong negative $\Delta\delta^{13}C_{Umed-Epi}$ in the central and northern Aegean Sea suggest high C_{org} fluxes, which however are not reflected in the estimated PP-based values. The eventual underestimation of C_{org} fluxes in these more marginal areas is likely caused by additional lateral OM input and the focusing of organic matter in isolated small basins. In fact, the northern and central Aegean Sea experiences high OM input from terrestrial sources through North Aegean rivers and the Black Sea outflow (Aksu et al., 1999; Tsiaras et al., 2012). In contrast, the measured main redox boundary depth and the TOC contents do not indicate a higher supply in organic matter. However, sediment trap data from the northern Aegean Sea (Lykousis et al., 2002) reveal C_{org} fluxes of 35–81 $gC\ m^{-2}\ a^{-1}$, which are 3 to 10 times higher than estimated values solely based on PP-based vertical fluxes. Although the high measured values can be partly attributed to the short sampling interval of two months in late spring and thus to elevated vertical fluxes during the spring bloom, elevated year-round lateral C_{org} fluxes can be expected, but on a clearly lower dimension. The measured ratio of primary to reworked OM in the sediment at this site is around 60–70 % (Lykousis et al., 2002; Poulos, 2009), which leaves the PP the main source of the C_{org} fluxes to the deep-sea. Similar results have been derived for canyon systems of the Gulf of Lions where OM resuspension, shelf to slope cascading and channeling results in significantly higher observed than PP-derived estimated C_{org} fluxes (Heussner et al., 2006; Pusceddu et al., 2010, Pasqual et al., 2010). Even in open slope settings, resuspended OM can significantly contribute to the total C_{org} flux (McCave et al., 2001; Tesi et al., 2010; Stabholz et al., 2013).

Despite these biases, it appears useful to develop a C_{org} flux transfer function at least for the more open marine settings of the western and central Mediterranean Sea and the southern Aegean Sea (Fig. 17). Here, vertical sinking of PP-derived OM appears to be the main source for C_{org} fluxes (Pusceddu et al., 2010) explaining the good correlation with the $\Delta\delta^{13}C_{Umed-Epi}$ values (Fig. 16). Elevated C_{org} fluxes of the upwelling affected Alboran Sea (Hernandez–Almeida et al., 2011) are reflected in rather negative $\Delta\delta^{13}C_{Umed-Epi}$ values while in the more oligotrophic regions of the Mallorca Channel, the Spanish Slope off Barcelona, the Strait of Sicily, and the southern Aegean Sea the observed $\delta^{13}C$

4. Carbon isotope deviations in foraminifera as C_{org} flux proxy

differences are lower. So, omitting the data from the northern and central Aegean Sea, and considering sediment trap data from the Gulf of Lions (Heussner et al., 2006) the derived function can be expressed as

$$C_{org} \text{ flux} = -15.99 * \Delta\delta^{13}C_{U_{med-Epi}} + 0.34 \quad [gC \text{ m}^{-2} \text{ a}^{-1}] \quad [2]$$

with a coefficient of determination (R^2) of 0.63 and a significance (p) of 0.0021 (Fig. 17). The estimated C_{org} fluxes can be used to recalculate marine PP, but should be handled carefully, due to the highly possible overestimation caused by lateral advection. Especially in more marginal areas this bias can lead to unreliable recalculated PP values. Likewise, the application of equation [2] outside of the Mediterranean Sea should be biased by differing remineralization rates, due to the specific oceanographic conditions, especially the higher temperatures, in this basin. Therefore, further refinement of this function would require interdisciplinary efforts including a larger number of direct C_{org} flux measurements in sediment trap deployments.

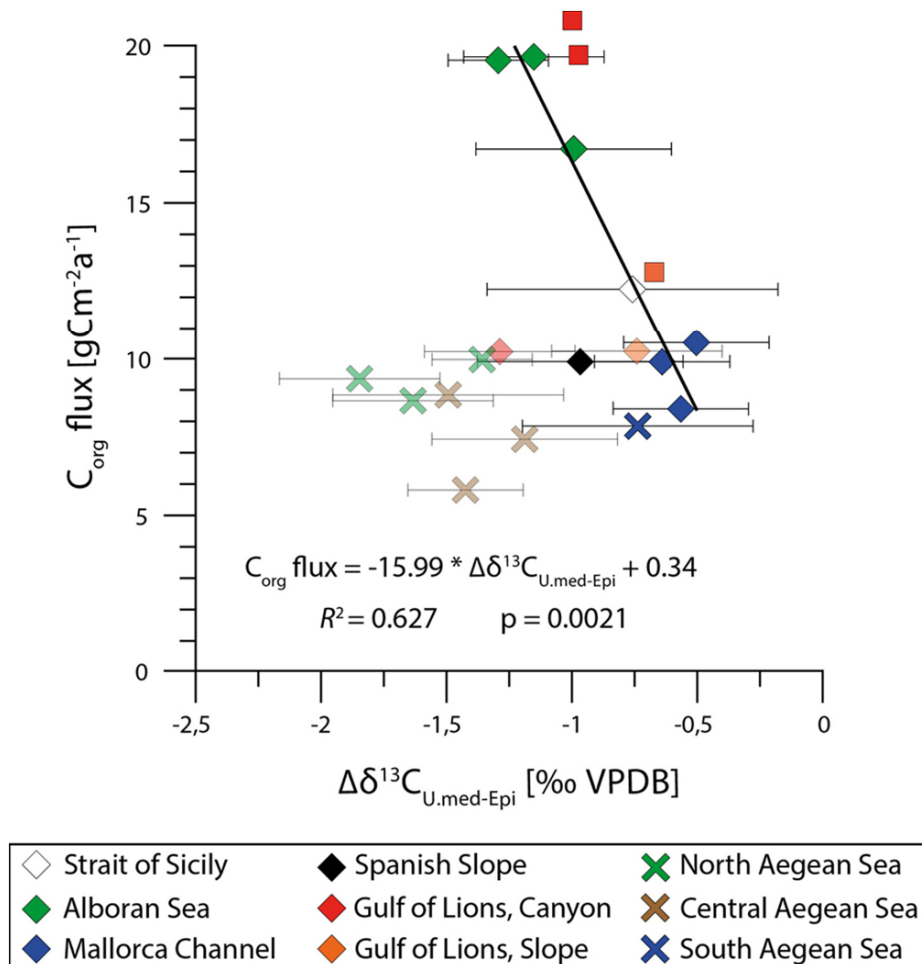


Figure 17. Correlation of the $\delta^{13}C$ difference between live *Uvigerina mediterranea* and epifaunal taxa ($\Delta\delta^{13}C_{U_{med-Epi}}$) and organic carbon flux rate (C_{org} flux) calculated according to Antoine & Morel (1996) and Betzer et al. (1984). Transparent data from the central and northern Aegean Sea and the Gulf of Lions have been removed from the function since PP-based C_{org} flux values are likely underestimated because of the additional influence of lateral organic matter fluxes on the $\delta^{13}C_{U_{med}}$ values in these areas.

4.5 Conclusions

The $\delta^{13}\text{C}$ signal of deep-sea benthic foraminifera from different areas of the western, central and eastern Mediterranean Sea reflects an integration of various environmental and biological signals. The application of epifaunal benthic foraminifera as an unbiased proxy for the $\delta^{13}\text{C}_{\text{DIC}}$ of the surrounding water mass is ambiguous, due to possible allochthonous tests, but also slight species-specific difference in the microhabitat can result in significant $\delta^{13}\text{C}_{\text{Epi}}$ shifts. The $\delta^{13}\text{C}$ signal of the strictly epifaunal *P. ariminensis* should be preferred, in contrast to the $\delta^{13}\text{C}$ signal of the very shallow infaunal *C. pachydermus*, which seems to be influenced by pore water DIC.

The $\delta^{13}\text{C}$ signal of epifaunal taxa lacks ontogenetic effects supporting results from previous studies (Dunbar & Wefer, 1984; Corliss et al, 2002; Theodor et al., 2016). Significant ontogenetic effects were recorded in the $\delta^{13}\text{C}$ signal of *U. mediterranea*. While the ontogenetic increase of $\delta^{13}\text{C}_{\text{Umed}}$ is more or less comparable ($0.11 \pm 0.03 \text{‰} (100 \mu\text{m})^{-1}$) in the western Mediterranean and the Strait of Sicily, a stronger increase and even a regional S-N trend is documented for the Aegean Sea ($0.16 \pm 0.04 \text{‰} (100 \mu\text{m})^{-1}$). In general, the $\delta^{13}\text{C}$ values of *U. mediterranea* from the Aegean Sea are more negative when compared to those from the western and central Mediterranean Sea. This regional contrast cannot be reconciled with different vital and pore water effects but instead seem to be caused by enhanced residence times of bottom waters in the partly isolated small basins within the Aegean Sea. In cases of well-oxygenated conditions the $\delta^{13}\text{C}_{\text{Umed}}$ signal, compared to bottom water, is mainly controlled by regional trophic contrasts and related remineralization rates. The $\Delta\delta^{13}\text{C}_{\text{Umed-Epi}}$ are clearly related to the median microhabitat depth, the depth of the redox boundary (indicating the extent of the oxygenated layer), and to a lower extent to the TOC of the surface sediment. Based on satellite derived primary production estimates C_{org} fluxes were calculated and related to the recorded $\Delta\delta^{13}\text{C}_{\text{Umed-Epi}}$ values. Comparison with sediment trap data reveals underestimation of C_{org} fluxes for the marginal areas of the central and northern Aegean Sea and the canyon systems of the Gulf of Lions. In these ecosystems additional lateral transport of resuspended and terrestrial OM contributes substantially to C_{org} fluxes. Considering these biases a first estimation for C_{org} fluxes in open-ocean settings of the Mediterranean Sea could be established.

5. Quantitative reconstruction of past Mediterranean organic matter fluxes and oxygen concentrations using multi-species benthic foraminiferal isotopes

Abstract

We use multi-species benthic foraminiferal stable isotope records for the reconstruction of Late Glacial and Holocene changes in productivity and bottom water oxygenation of the Mediterranean Sea. The records are based on samples from two sediment cores retrieved from bathyal environments of the Strait of Sicily and the eastern Ligurian Sea, both bathed by Levantine Intermediate Water (LIW). The $\delta^{18}\text{O}$ records reflect cool and more saline conditions during the Last Glacial Maximum (LGM) and the warming and freshening across the Termination. The observed species-specific $\delta^{18}\text{O}$ offsets can largely be attributed to vital effects. The $\delta^{13}\text{C}$ records of the strictly epifaunal species *Cibicidoides wuellerstorfi* and *Planulina ariminensis* represent suitable bottom water indicators. The species-specific $\delta^{13}\text{C}$ offsets reflect the combined influence of microhabitat and vital effects. For the Strait of Sicily, drops in oxygen to values around $200\ \mu\text{mol kg}^{-1}$ during the Bølling/Allerød interval and below $150\ \mu\text{mol kg}^{-1}$ during the early Holocene were estimated on the basis of the difference between the deep infaunal *G. affinis* and epifaunal species. The difference between the $\delta^{13}\text{C}$ signals of the shallow infaunal *Uvigerina mediterranea* and epifaunal species was used to quantify organic carbon fluxes and surface-water productivity for the well-ventilated intervals. In both study areas organic carbon fluxes increased during the Late Glacial and the Younger Dryas (values around $15\text{-}25\ \text{gC m}^{-2}\ \text{a}^{-1}$), while they were relatively lower during the Bølling/Allerød interval and the Holocene (values around $5\text{-}15\ \text{gC m}^{-2}\ \text{a}^{-1}$). The more open-marine setting of the Strait of Sicily permitted the calculation of plausible primary productivity values, while the OM fluxes in the Ligurian Sea likely include a significant terrestrial component, reflecting climate and river-runoff changes of the hinterland.

This chapter is based on:

Theodor, M., Schmiedl, G., Andersen, N., Mackensen, A., in prep. Quantitative reconstruction of past Mediterranean organic matter fluxes and oxygen concentrations using multi-species benthic foraminiferal isotopes.

5.1 Introduction

The stable carbon and oxygen isotope signatures of deep-sea benthic foraminifera provide invaluable information on physical and biogeochemical ocean processes. Accordingly, benthic foraminiferal stable isotope records have been used in a wide range of paleoceanographic studies, including the reconstruction of past changes in temperature and salinity, sea level, water mass configuration and organic carbon fluxes (Shackleton & Opdyke, 1973; Curry & Lohmann, 1982; Zahn et al., 1986; Waelbroeck et al., 2002; Lynch-Stieglitz et al., 2006; Zarriess & Mackensen, 2011). The deep-sea stable oxygen isotope signal mainly reflects global ice volume (Shackleton & Opdyke, 1973; Lisiecki & Raymo, 2005) even though it can also be used for the reconstruction of temperature and salinity changes on a regional scale (Rohling & Cooke, 1999; LeGrande & Schmidt, 2006; Herbert et al., 2010). These reconstructions are based on the assumption that the foraminifera calcify their test in equilibrium with the ambient water or with a spatially and temporally constant offset (Rohling & Cooke, 1999; Pearson, 2012). Recent studies suggest non-constant $\delta^{18}\text{O}$ 'vital effects' for which the reasons however remain largely unexplored (Schmiedl & Mackensen 2006; Theodor et al., 2016a).

The deep-sea stable carbon isotope signal documents the origin and aging of subsurface water masses but quantitative reconstructions are complicated by the influence of $\delta^{13}\text{C}_{\text{DIC}}$ gradients of bottom and pore waters (reviews in Rohling & Cooke, 1999; Mackensen, 2008). Additionally, the benthic foraminiferal $\delta^{13}\text{C}$ signal contains significant species-specific 'vital effects', which are commonly attributed to differences in metabolic and calcification rates and vary with ontogenesis in different species (McConnaughey, 1989a,b; Schmiedl et al., 2004; Theodor et al., 2016a). On the other hand, the $\delta^{13}\text{C}$ signal consistently reflects the average microhabitat depth of a certain species (McCorkle et al., 1990; 1997; Rathburn et al., 1996; Holsten et al., 2004) allowing for the reconstruction of $\delta^{13}\text{C}_{\text{DIC}}$ pore-water gradients in multi-species approaches (Schmiedl et al., 2004, Fontanier et al., 2006; Theodor et al., 2016a). The $\delta^{13}\text{C}_{\text{DIC}}$ pore-water gradient results from the bacterial remineralization of isotopically light organic matter releasing ^{12}C to the ambient water. Pore water $\delta^{13}\text{C}_{\text{DIC}}$ decreases with increasing sediment depth and the gradient is determined by the combined influences of organic matter fluxes and availability of oxygen and nitrate (McCorkle et al., 1985; Stott et al., 2000). The combined influences of biogeochemical and biological effects can lead to species-specific differences of up to 5 ‰ at a single site (McCorkle et al., 1990; 1997).

The total magnitude and shape of the pore water $\delta^{13}\text{C}_{\text{DIC}}$ gradient, as reflected by the $\delta^{13}\text{C}$ differences between different species, has been used in various paleoceanographic approaches. The $\delta^{13}\text{C}$ difference between epifaunal and *Uvigerina* species reflects the organic matter flux rate to the sea floor (McCorkle et al., 1990; Vergnaud-Grazzini & Pierre, 1991; Schmiedl et al., 2004; Grauel & Bernasconi, 2010; Theodor et al., 2016a, b). Accordingly, this proxy was successfully applied to the reconstruction of past changes in organic carbon fluxes in the North Atlantic Ocean (Zahn et al.

5. Quantitative reconstructions of past organic matter fluxes and oxygen concentrations

1986), Mediterranean Sea (Vergnaud-Grazzini & Pierre, 1991; Shilman et al., 2001; Kuhnt et al., 2008; Milker et al., 2012) and Arabian Sea (Schmiedl & Mackensen, 2006). More recently, a transfer function for organic carbon flux rate was established for the Mediterranean Sea based on the modern $\Delta\delta^{13}\text{C}$ signal of epifaunal species and the shallow infaunal *Uvigerina mediterranea* (Theodor et al., 2016b). Likewise the $\delta^{13}\text{C}$ difference between epifaunal and deep infaunal species was successfully applied to the quantitative reconstruction of past changes in bottom water oxygen concentration in the

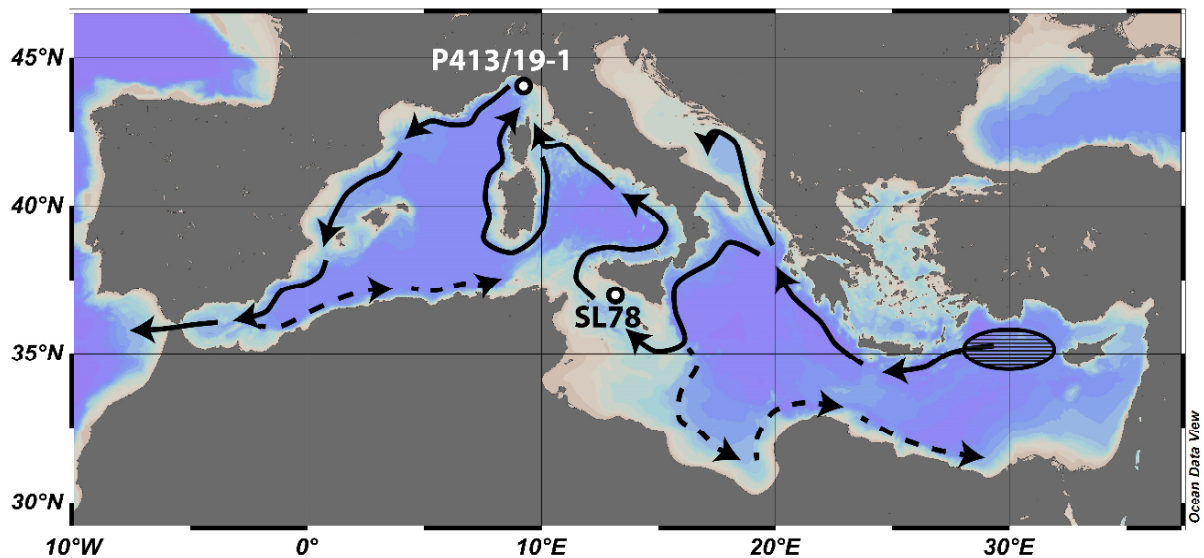


Figure 18. Bathymetric map of the Mediterranean Sea (Ocean Data View, Schlitzer, 2015). The sites of the investigated cores in the Strait of Sicily (Hieke et al., 1999) and the Ligurian Sea (Lamy et al., 2011) are marked with white dots. The recent general flow pattern of the Levantine Intermediate Water (LIW) is marked with black arrows, the region of LIW formation in the northern Levantine Sea is indicated (Millot, 1999; Millot & Taupier-Letage, 2005).

Arabian Sea and the North Atlantic Ocean (Schmiedl & Mackensen, 2006; Hoogakker et al., 2015).

Here, we examine the stable carbon and oxygen isotope signal of selected epifaunal, shallow and deep infaunal benthic foraminiferal species from two Late Glacial to Holocene sediment successions retrieved from upper bathyal sites of the Gulf of Genoa (northern Ligurian Sea) and the Strait of Sicily in the western and central Mediterranean Sea, respectively. The stable isotope records were evaluated in terms of changes in the ventilation of intermediate water masses and organic carbon fluxes during the last 22 to 30 ka. Specifically, we use the $\Delta\delta^{13}\text{C}$ signal of epifaunal species and *U. mediterranea* ($\Delta\delta^{13}\text{C}_{Umed-Epi}$) for the quantification of organic carbon fluxes, applying the recently established transfer function for the Mediterranean Sea (Theodor et al. 2016b). In addition, we apply the $\Delta\delta^{13}\text{C}$ signal of epifaunal and deep infaunal species ($\Delta\delta^{13}\text{C}_{Gaff-Epi}$) to the calculation of changes in bottom water oxygen content applying the function of Hoogakker et al (2015). The Mediterranean Sea appears particularly suitable for our study since the circulation and productivity of this marginal basin immediately reacts to climate changes on the borderlands (review in Rohling et al., 2015). In addition, extensive knowledge is available of the environmental and biological effects on the stable isotope signatures of recent deep-sea benthic foraminifera from various regions of the

5.2 Regional setting

Mediterranean Sea and adjacent areas of the North Atlantic Ocean (Schmiedl et al., 2004; Fontanier et al., 2006; Theodor et al., 2016a). This knowledge can be directly transferred to the interpretation of the new down-core data.

5.2 Regional setting

The Mediterranean Sea is a marginal sea of the Atlantic Ocean, with the Strait of Gibraltar as narrow and single connection (Fig. 18). The Sicily sill, with maximum water depths of about 360 to 430 m (Astraldi et al., 1999) divides the Mediterranean Sea into an eastern and a western basin. The Mediterranean climate is influenced by both temperate and subtropical realms (Lionello et al., 2012). The rapid water exchange with low residence times fosters immediate responses of the Mediterranean oceanography to climate changes (Béthoux et al., 1999). The North Atlantic climate influence is particularly prominent in the northern and western basin areas and also accounts for the seasonal contrast between wet and mild winters and arid and warm summers (Lionello et al., 2012). The eastern Mediterranean is additionally influenced by shifts in the Intertropical Convergence Zone as documented by the periodic formation of sapropels, which reveal a close relation to phases of intensified East African monsoon precipitation and Nile river runoff (e.g., Rossignol-Strick, 1983; Weldeab et al., 2014; Rohling et al., 2015).

The Mediterranean Sea exhibits a general anticlockwise surface circulation but its specific topography comprising numerous islands, peninsulas and narrow straits results in a more complex pattern of surface currents and gyres (Millot & Taupier-Letage, 2005; Pinardi et al., 2015). The negative water budget with high evaporation rates over the eastern basin drives an anti-estuarine circulation with inflow of relatively fresh Atlantic surface waters. The Modified Atlantic Water (MAW) comprises the upper 200 m of the water column and on its flow towards the east temperature and salinity increase (Tanhua et al., 2013; Pinardi et al., 2015). The inflow of MAW is compensated by the outflow of Levantine Intermediate Water (LIW), which is formed in the eastern basin between Crete and Cyprus due to salinity-related increase in density (Ovchinnikov, 1984) (Fig. 18). The highly saline LIW preconditions the formation of Eastern Mediterranean Deep Water (EMDW) in the Aegean and Adriatic seas, and Western Mediterranean Deep Water (WMDW) in the Gulf of Lions (Wüst, 1961; Millot, 2013; Cardin et al., 2015). While the LIW passes the Sicilian sill towards the western Mediterranean Sea, only little exchange occurs between EMDW and WMDW (Astraldi et al., 2001; Stansfield et al., 2003; Béranger et al., 2004).

The Mediterranean Sea is one of the most oligotrophic regions of the world, caused by its anti-estuarine circulation and phosphorus limitation of surface waters (Krom et al., 2010). The eastward nutrient depletion of Atlantic surface waters as main nutrient source for the whole basin results in a general west-east decrease of primary productivity, from values of about $225 \text{ gC m}^{-2} \text{ a}^{-1}$ in the

5. Quantitative reconstructions of past organic matter fluxes and oxygen concentrations

Alboran Sea to about $40 \text{ gC m}^{-2} \text{ a}^{-1}$ in the ultra-oligotrophic central Levantine Sea (Bosc et al., 2004; López-Sandoval et al., 2011; Gogou et al., 2014). Exceptions are coastal areas and smaller regions under the influence of upwelling, e.g. the Alboran Sea (Sanchez-Vidal et al., 2005), or areas receiving external nutrient supply by rivers or the Black Sea, e.g. the northern Aegean Sea (Siokou-Frangou et al., 2002). Phytoplankton blooms occur mainly during winter, due to wind-induced mixing of the upper water layers. Stratification of the water column during summer coincides with low primary productivity, with some fertilization by Sahara-derived dust input (Zuñiga et al., 2008; Stavrakakis et al., 2013; Gogou et al., 2014).

The morphological barrier of the Strait of Sicily leads to a division of the MAW south of Sardinia,

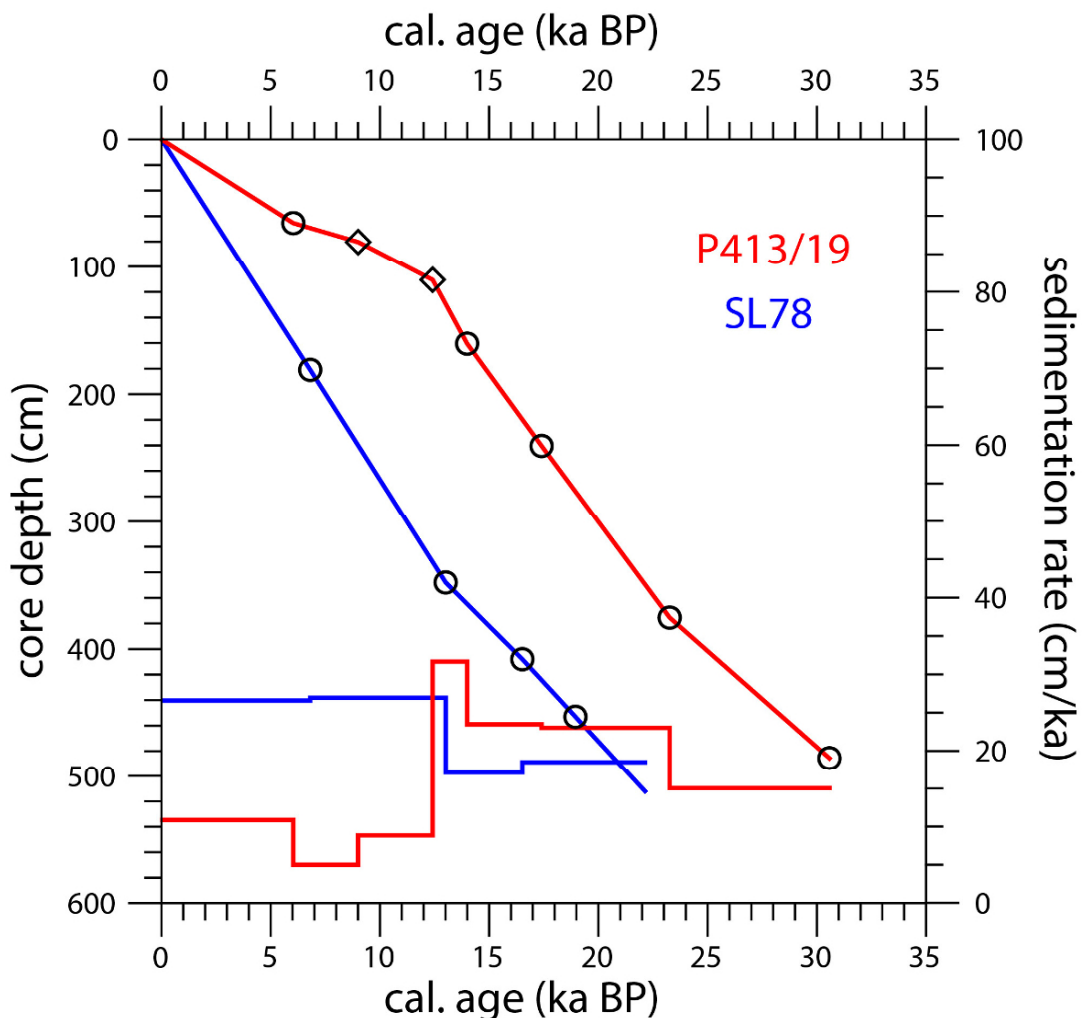


Figure 19. Age models of sediment cores SL78 (blue) and P413/19 (red) with AMS ¹⁴C ages (circles) and tie points (diamonds) for the onset and end of Termination 1b (Sierro et al., 2005; Frigola et al., 2008). The lower lines represent the corresponding sedimentation rates.

comprising an eastward flowing current into the Tyrrhenian Sea and a southeast flowing current entering the Strait of Sicily (Millot, 1999; Millot & Taupier-Letage, 2005; Pinardi et al., 2015). The southeastern branch further splits into the southern Sicily Strait Tunisian Current (SSTC) and the northern Atlantic Ionian Stream (AIS) (Robinson et al., 1999; Lermusiaux & Robinson, 2001; Béranger

5.2 Regional setting

et al., 2004). Vertical mixing along the meandering AIS provokes seasonally increased nutrient supply into the surface waters, but these features are not strong enough to break summer stratification (Robinson et al., 1999; MEDAR Group, 2002). The outflowing water from the eastern basins across the Strait of Sicily also divides in a northern and a southern branch (Stansfield et al., 2003; Beranger et al., 2004) and encompasses LIW and the upper parts of the EMDW (Lermusiaux & Robinson, 2001; Gasparini et al., 2005).

The Ligurian Sea exhibits a wind-driven cyclonic surface and intermediate water circulation (Pinardi & Masetti, 2000; Poulain et al., 2012) and is mainly influenced by the Western Corsica Current (WCC) and to a lower degree by the Eastern Corsica Current (ECC) or Middle Tyrrhenian Current (MTC) (Pinardi et al., 2015). While the WCC is more constant over the year, the ECC shows a large variability between up to 40 cm s^{-1} during winter and even reversed currents in summer (Astraldi & Gasparini, 1992; Pinardi & Masetti, 2000; Poulain et al., 2012). In the Gulf of Genoa the current turns in a western to south-western direction and forms the strong (up to 2 Sv within 33 km) and fast (up to 1 m s^{-1} at the surface) Ligurian Provençal Catalan Current (LPCC) (Poulain et al., 2012). As a result of the strong cyclonic current at the margins of the Ligurian Sea, the relatively warmer and less-dense coastal waters are separated from colder waters in the central parts. This causes a meso-scale geostrophic front leading to enhanced nutrient supply and increased surface water productivity (Boucher et al., 1987; Sournia et al., 1990). The formation of deep and intermediate water masses in the open Ligurian Sea is little constrained and of much lower relevance when compared to the main deep-water formation sites in the Gulf of Lions (MEDOC group, 1970; Sparnocchia et al., 1995; Millot, 1999).

Table 5. Age models for cores SL78 and P413/19 AMS radiocarbon and calendar ages are based on shallow-dwelling planktonic foraminifera. The ^{14}C ages were converted to calendar years using a marine reservoir effect of 400 years, additionally a regional reservoir correction of 16 ± 49 years for core P413/19 was applied (Siani et al., 2001). Tie-points are based on graphical comparison of the benthic $\delta^{18}\text{O}$ records of P413/19 and MD99-2343 east of Minorca (Sierro et al., 2005; Frigola et al., 2008). T1b = Termination 1b.

| core | core depth (cm) | conventional radiocarbon age (years BP) | calibrated age range 2σ (years BP) | calendar age, average (ka BP) | Type of age point |
|---------|-----------------|---|---|-------------------------------|---------------------|
| SL78 | 181 | | | 6.81 | AMS ^{14}C |
| | 348 | | | 13.01 | AMS ^{14}C |
| | 408 | | | 16.52 | AMS ^{14}C |
| | 453 | | | 18.95 | AMS ^{14}C |
| P413/19 | 65.5 | 5200 (± 30) | 6175 - 5895 | 6.04 | AMS ^{14}C |
| | 80.3 | | | 9.00 | end T1b |
| | 110.5 | | | 12.41 | start T1b |
| | 160.5 | 12100 (± 40) | 14125 - 13860 | 13.99 | AMS ^{14}C |
| | 240.5 | 14300 (± 60) | 17605 - 17200 | 17.40 | AMS ^{14}C |
| | 375.5 | 19320 (± 70) | 23495 - 23035 | 23.27 | AMS ^{14}C |
| | 485.5 | 26260 (± 130) | 30825 - 30330 | 30.58 | AMS ^{14}C |

5.3 Material and methods

Gravity core SL78 was retrieved during cruise M40/4 of R/V *Meteor* in February 1998 from the Strait of Sicily (37°02.20' N; 13°11.38' E) at 467 m water depth (Fig.18) (Hieke et al., 1999). The 532 cm long sediment succession consists of grayish olive nannofossil- and foraminifera-bearing mud. Gravity core P413/19 was retrieved during cruise P413 of R/V *Poseidon* in May 2011 from the Gulf of Genoa in the northern Ligurian Sea (43° 02.63' N; 9° 16.11' E) at 662 m water depth (Fig.18) (Lamy et al., 2011). The 687 cm long sediment succession consists of foraminifera-bearing mud.

The age models of the sediment cores are based on four and five accelerator mass spectrometry (AMS) ¹⁴C dates of surface-dwelling planktonic foraminifera for SL78 and P413/19, respectively (Table 5). Measurements for core SL78 were performed at the Leibniz Laboratory for Radiometric Dating and Stable Isotope Research (Kiel, Germany) and for core P413/19 at Beta Analytic Inc. (Miami, Florida, USA) (Table 5). The radiocarbon ages were converted to calendar years using the Marine13 database (Reimer et al., 2013). For the Ligurian Sea, we have additionally applied a Delta-R of -16 ± 49 years (Marine Reservoir Database, Siani et al., 2001). The age model of P413/19 was further optimized by epibenthic $\delta^{18}\text{O}$ correlation with core MD99-2343 east of Minorca (Sierro et al., 2005; Frigola et al., 2008), aided by the software AnalySeries 2.0 (Paillard et al., 1996). Mean sedimentation rates range from 17-27 cm ka⁻¹ in core SL78, and from 15-32 cm ka⁻¹ in the Late Glacial interval and 5 to 11 cm ka⁻¹ in the Holocene interval of core P413/19 (Table 5, Fig. 19).

For stable isotope analyses, core SL78 was sampled at 10 cm spacing, while the upper 487 cm of core P413/19 were sampled at 5 cm spacing. The samples were wet sieved over a 63 μm sieve, and after drying at 40 °C the residue was dry-sieved over a 125 μm sieve. Depending on the individual sizes and abundances, between 1 and 12 benthic foraminiferal tests were picked from the >125 μm size fraction for stable isotope analyses. From core SL78, the species *Planulina ariminensis*, *Cibicidoides pachydermus*, *Uvigerina mediterranea*, *Uvigerina peregrina*, *Globobulimina affinis*, and from core P413/19 the species *P. ariminensis*, *C. pachydermus*, *Cibicidoides wuellerstorfi*, *U. mediterranea*, *Angulogerina angulosa* were selected for isotope analyses. In order to account for potential ontogenetic isotope effects (Schmiedl et al., 2004; Schumacher et al., 2010; Theodor et al., 2016a), the sizes of the selected tests were measured. Due to the high abundance of *U. mediterranea* in core P413/19 exclusively tests larger than 550 μm were analyzed. The samples were measured with a Finnigan MAT 251 mass spectrometer at the Alfred-Wegener-Institute, Helmholtz Centre for Polar and Marine Research Bremerhaven (core P413/19) and at the Leibniz Laboratory for Radiometric Dating and Isotope Research Kiel (core SL78). External precision was better than 0.06 ‰ and 0.08 ‰ for stable carbon and oxygen isotopes, respectively. All values are given in delta notation against the Vienna Pee Dee Belemnite (VPDB) standard.

5.3 Material and methods

The strictly epifaunal *P. ariminensis* and *C. wuellerstorfi* (Lutze & Thiel, 1989; Kitazato, 1994) were preferably used as bottom water $\delta^{13}\text{C}_{\text{DIC}}$ proxy but owing to their intermittent occurrence the very shallow infaunal *C. pachydermus* was additionally used (Schmiedl et al., 2000; Theodor et al., 2016b). In order to account for pore water signals in $\delta^{13}\text{C}_{\text{Cpachy}}$ (Schmiedl et al., 2004), these values were corrected by adding site-specific mean deviations of 0.24 ‰ in core SL78 and 0.20 ‰ in core P413/19. The reconstruction of changes in bottom water oxygen concentration is based on the $\delta^{13}\text{C}$ difference between epifaunal taxa and the deep infaunal *G. affinis* applying the function of Hoogakker et al. (2015), that has been established for the North Atlantic Ocean.

$$[\text{O}_2] = \{(-\Delta\delta^{13}\text{C}_{\text{Gaff-Epi}}) - 0.41\} * 129.53 \quad [\mu\text{mol kg}^{-1}] \quad [3]$$

The reconstruction of changes in organic matter fluxes is based on the $\delta^{13}\text{C}$ difference between epifaunal taxa and the shallow infaunal *U. mediterranea* applying a recently established transfer function for the Mediterranean Sea (Theodor et al., 2016b).

$$\text{C}_{\text{org}} \text{ flux} = -15.99 * \Delta\delta^{13}\text{C}_{\text{Umed-Epi}} + 0.34 \quad [\text{gC m}^{-2} \text{ a}^{-1}] \quad [2]$$

Assuming marine primary productivity as the only source for the observed C_{org} fluxes, i.e. neglecting lateral organic matter fluxes, and considering sea-level changes, values for paleo-productivity can be estimated. The function of Betzer et al. (1984) was used to estimate vertical fluxes and correcting for organic matter degradation during sinking.

$$\text{PP} = [\text{C}_{\text{org}} \text{ flux} / \{0.409 * (\text{water depth}^{\wedge} - 0.628)\}]^{\wedge} 1/1.41 \quad [\text{gC m}^{-2} \text{ a}^{-1}] \quad [4]$$

The reconstructions of regional changes in paleo-water depth for the northeastern Ligurian Sea, southeast of Sicily and Lampedusa Island is based on Lambeck et al. (2011).

For better visualization of trends and to account for possible outliers, five-point running averages (5-pra) were calculated for all data series. Data points of several measurements in SL78, indicated by extreme outliers in $\delta^{18}\text{O}$ (including one for *G. affinis*, and three for *U. mediterranea* and *U. peregrina*, respectively) were omitted prior to calculation of running averages.

5.4 Results

The seven measured species of benthic foraminifera reveal a wide range of stable carbon and oxygen isotope ratios in both cores (Figs. 20, 21). Inter-specific differences are higher for $\delta^{13}\text{C}$ when compared to $\delta^{18}\text{O}$. The $\delta^{18}\text{O}$ 5-pra values at site SL78 in the Strait of Sicily vary between 4.78 ‰ (*G. affinis*) during the Last Glacial Maximum (LGM) and 1.57 ‰ (*P. ariminensis*) for the core top sample (Fig. 20). At site P413/19 in the Gulf of Genoa, the $\delta^{18}\text{O}$ 5-pra values vary between 4.96 ‰ (*U. mediterranea*) before the onset of Heinrich event 1 (H1) and 1.64 ‰ (*P. ariminensis*) for sub-recent samples. The general trends in the $\delta^{18}\text{O}$ records across Termination 1 and the Holocene are comparable for all species and at both sites. Significant inter-specific $\delta^{18}\text{O}$ variations are restricted to the intervals of the LGM, HE1 and HE2 at site P413/19 (Fig. 20).

The $\delta^{13}\text{C}$ 5-pra records reveal a more complex spatial and temporal pattern. At site SL78, the $\delta^{13}\text{C}$ values range between -1.96 ‰ (*G. affinis*) during the Early Holocene and 1.80 ‰ (*P. ariminensis*) during the LGM (Fig. 21). Interspecific $\delta^{13}\text{C}$ differences are highest during the LGM and lowest during the early Holocene when relative drops of 0.8 to 1.4 ‰ occur. At site P413/1, the $\delta^{13}\text{C}$ values range between -0.74 ‰ (*A. angulosa*) and 1.87 ‰ (*C. wuellerstorfi*) both during the LGM (Fig. 21). The epifaunal $\delta^{13}\text{C}$ records reveal a trend from higher glacial to lower interglacial values, while values remain more or less constant during the Holocene. Accordingly, interspecific $\delta^{13}\text{C}$ differences are highest during the LGM and lowest during the Late Holocene.

Within the three epifaunal species, long-term average $\Delta\delta^{18}\text{O}$ values are close to zero, with differences of -0.07 ± 0.20 ‰ (*C. pachydermus* - *P. ariminensis*, P413/19), -0.06 ± 0.23 ‰ (*P. ariminensis* - *C. wuellerstorfi*, P413/19), 0.06 ± 0.18 ‰ (*C. pachydermus* - *C. wuellerstorfi*, P413/19) and 0.10 ± 0.10 ‰ (*C. pachydermus* - *P. ariminensis*, SL78) although the records reveal significant temporal variability. The highest differences occur between *P. ariminensis* and *C. wuellerstorfi* at site P413/19 directly after the YD (-0.79 ‰ at 10.7 ka BP) and during the LGM (0.57 ‰ at 20.9 ka BP) (Fig. 22a). At site P413/19, epifaunal $\Delta\delta^{13}\text{C}$ values range between -0.30 ‰ and 0.35 ‰ for *P. ariminensis* - *C. wuellerstorfi* (long-term average of -0.03 ± 0.22 ‰) and between -0.42 ‰ and $+0.13$ ‰ for *C. pachydermus* - *C. wuellerstorfi* (long-term average of -0.17 ± 0.18 ‰) while values reveal less fluctuations for *C. pachydermus* - *P. ariminensis* (long-term average of -0.20 ± 0.12 ‰). At site SL78, a long-term average epifaunal $\Delta\delta^{13}\text{C}$ value of -0.25 ± 0.10 ‰ (*C. pachydermus* - *P. ariminensis*) is observed (Fig. 22b).

For the reconstruction of the bottom water oxygen content, most of the LGM and middle to late Holocene samples show $\Delta\delta^{13}\text{C}_{\text{Gaff-Epi}}$ values higher than the critical value of -2.23 ‰, corresponding to an oxygen concentration of $235 \mu\text{mol kg}^{-1}$ and above (Hoogakker et al., 2015). Significantly lower oxygen values of $220\text{-}235 \mu\text{mol kg}^{-1}$ are inferred for the latest glacial and earliest Holocene periods. Prior to the temporal disappearance of *G. affinis* and related data gap during sapropel S1 deposition, reconstructed oxygen concentrations drop to $162 \mu\text{mol kg}^{-1}$ at 9.5 ka BP (Fig. 23).

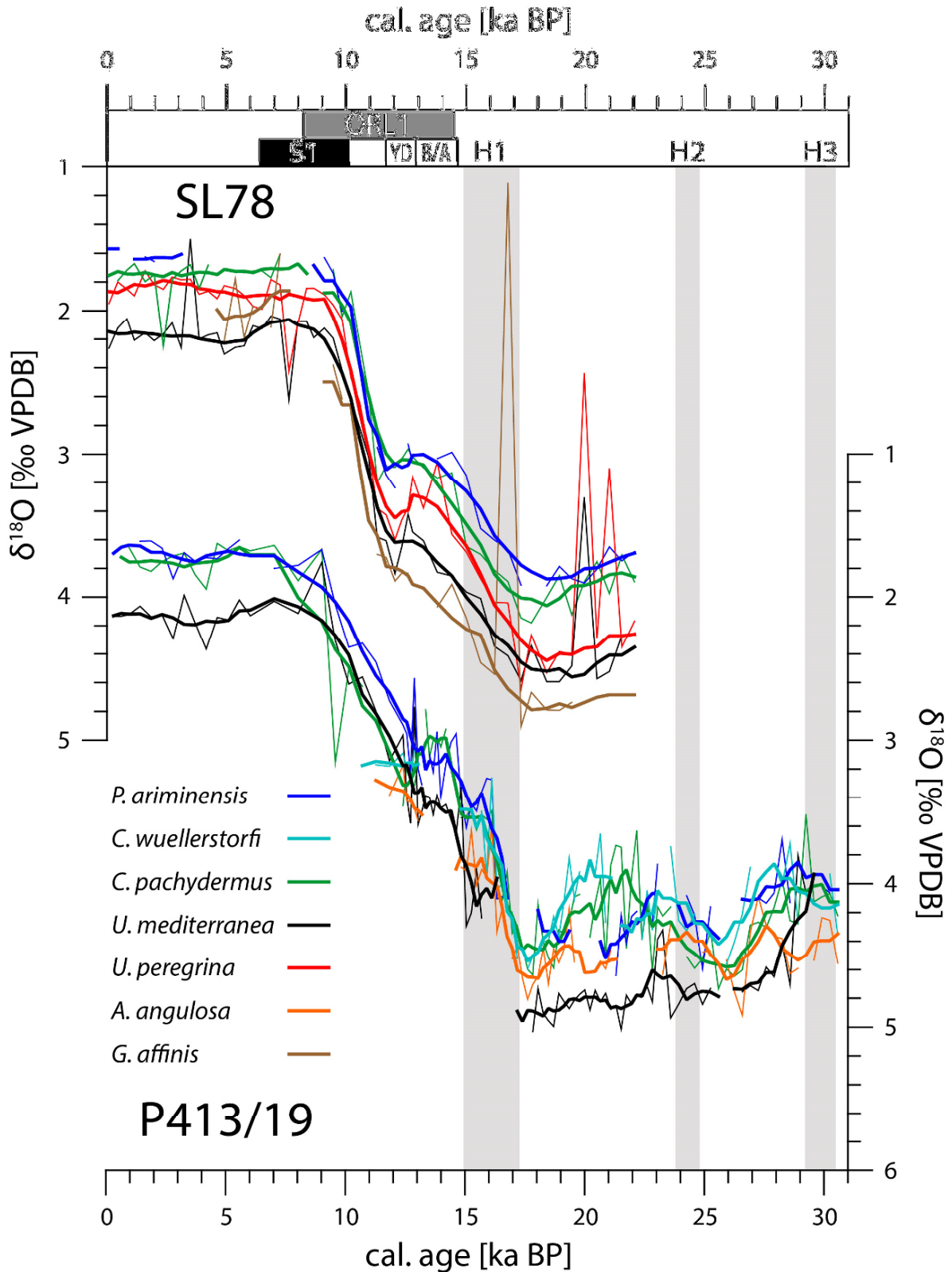


Figure 20. Stable oxygen isotope records of different benthic foraminiferal species for sediment cores SL78 (top) and P413/19 (bottom). Thick lines represent the five-point running averages (5-pra). Heinrich Events (after Siervo et al., 2005) are marked by grey vertical bars. Top bars show times of Sapropel S1 formation in the eastern Mediterranean Sea (Mercone et al., 2000), Organic Rich Layer ORL1 in the western Mediterranean Sea (Jimenez-Espejo et al., 2007), Younger Dryas (YD), and Bølling/ Allerød complex (B/A) after Cacho et al., 2001.

5. Quantitative reconstructions of past organic matter fluxes and oxygen concentrations

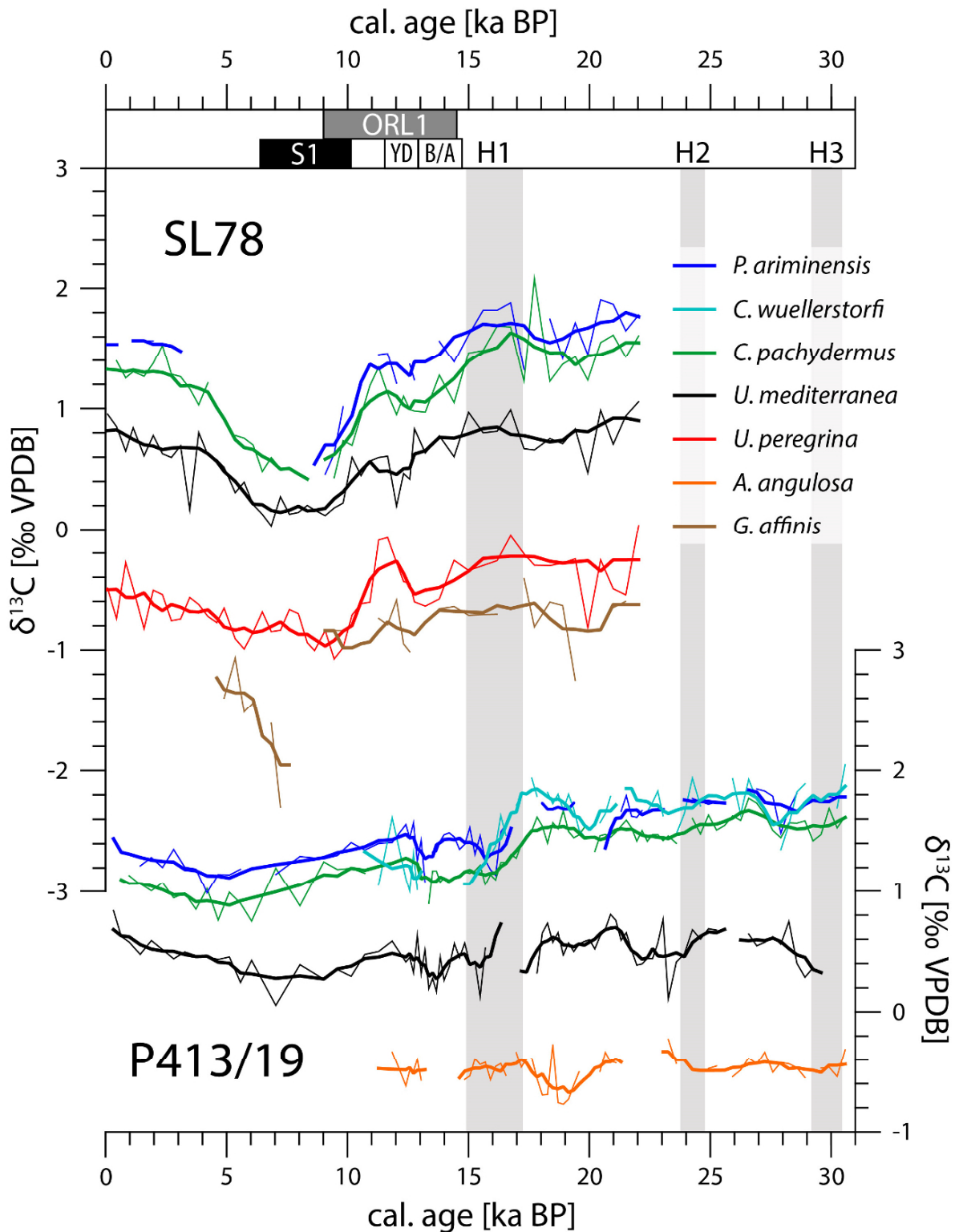


Figure 21. Stable carbon isotope data of different benthic foraminiferal species for the sediment cores SL78 (top) and P413/19 (bottom). Thick lines represent the five-point running means. Heinrich Events (after Sierrro et al., 2005) are marked by grey vertical bars. Top bars show times of Sapropel S1 formation in the eastern Mediterranean Sea (Mercone et al., 2000), Organic Rich Layer ORL1 in the western Mediterranean Sea (Jimenez-Espejo et al., 2007), Younger Dryas (YD), and Bølling/ Allerød complex (B/A) after Cacho et al., 2001.

5.5 Discussion

In the Strait of Sicily at site SL78, the $\Delta\delta^{13}\text{C}_{U_{med-Epi}}$ 5-pra values range from -0.43 ‰ at 8.3 ka BP to -1.07 ‰ at 16.8 ka BP, corresponding to estimated C_{org} fluxes of 7.24 to 17.45 $\text{gC m}^{-2} \text{a}^{-1}$ (Fig. 24). Maximum C_{org} fluxes are reconstructed for the late phase of the LGM (16.50 $\text{gC m}^{-2} \text{a}^{-1}$), the YD interval (14.73 $\text{gC m}^{-2} \text{a}^{-1}$), and the late Holocene (15.46 $\text{gC m}^{-2} \text{a}^{-1}$). After correction for changes in paleo-water depth, PP values of 194.58 $\text{gC m}^{-2} \text{a}^{-1}$ are estimated for the LGM and 202.03 $\text{gC m}^{-2} \text{a}^{-1}$ for the late Holocene (Fig. 25). Low $\Delta\delta^{13}\text{C}_{U_{med-Epi}}$ values of -0.43 ‰ during sapropel S1 deposition correspond to reconstructed C_{org} fluxes of 7.24 $\text{gC m}^{-2} \text{a}^{-1}$ and PP values of 115.60 $\text{gC m}^{-2} \text{a}^{-1}$, which are comparable to modern oligotrophic conditions of the eastern Mediterranean Sea (Fig. 24, 25).

In the Gulf of Genoa at site P413/19, the $\Delta\delta^{13}\text{C}_{U_{med-Epi}}$ 5-pra values vary between -0.65 ‰ at 16.1 ka BP and -1.45 ‰ at 30.6 ka BP, corresponding to estimated C_{org} fluxes of 10.73 to 23.53 $\text{gC m}^{-2} \text{a}^{-1}$ (Fig. 24). The estimated C_{org} fluxes exhibit an overall decrease over the past 30 ka superimposed by various millennial- to centennial-scale fluctuations. Sea-level corrected PP values vary between 170.79 and 271.19 $\text{gC m}^{-2} \text{a}^{-1}$ (Fig. 25).

5.5 Discussion

5.5.1 Stable isotope signal of different epibenthic foraminifera as bottom water proxy

The stable isotope records of the measured epifaunal species conformably reflect the glacial-interglacial transition and ventilation of intermediate waters in the Strait of Sicily and Gulf of Genoa but also reveal marked inter-specific differences (Figs. 20-22). The species *P. ariminensis* and *C. wuellerstorf* inhabit a strictly epifaunal microhabitat (Lutze & Thiel, 1989; Kitazato, 1994) and thus calcify under bottom water conditions. These species are therefore widely used in the reconstruction of intermediate and deep-water circulation changes (e.g. Duplessy et al., 1984; Bickert & Mackensen, 2003; Pahnke & Zahn, 2005; Sierro et al., 2005). The applicability of these species is further supported by the lack of ontogenetic isotope effects (Dunbar & Wefer, 1984; Corliss et al., 2002; Franco-Fraguas et al., 2011; Theodor et al., 2016a).

Little is known on the interspecific $\delta^{18}\text{O}$ and $\delta^{13}\text{C}$ variability of epifaunal taxa. In a recent study from the western Mediterranean Sea interspecific $\delta^{13}\text{C}_{Epi}$ differences exceed 1 ‰ in modern individuals from various sites, while interspecific $\delta^{18}\text{O}_{Epi}$ values either reveal little variance or lack a consistent pattern (Theodor et al. 2016a). In our present study, the long-term average $\delta^{18}\text{O}_{Epi}$ differences are close to zero in both cores although offsets of more than ± 0.5 ‰ are documented in various core intervals. The influence of environmental factors on the interspecific $\delta^{18}\text{O}_{Epi}$ differences, such as gradients in temperature, salinity and alkalinity, can be largely ruled out because of their similar microhabitat (McCorkle et al., 1990, 1997). More likely, the interspecific $\delta^{18}\text{O}_{Epi}$ differences are due to biological factors, like production of cysts during calcification with conditions out of

5. Quantitative reconstructions of past organic matter fluxes and oxygen concentrations

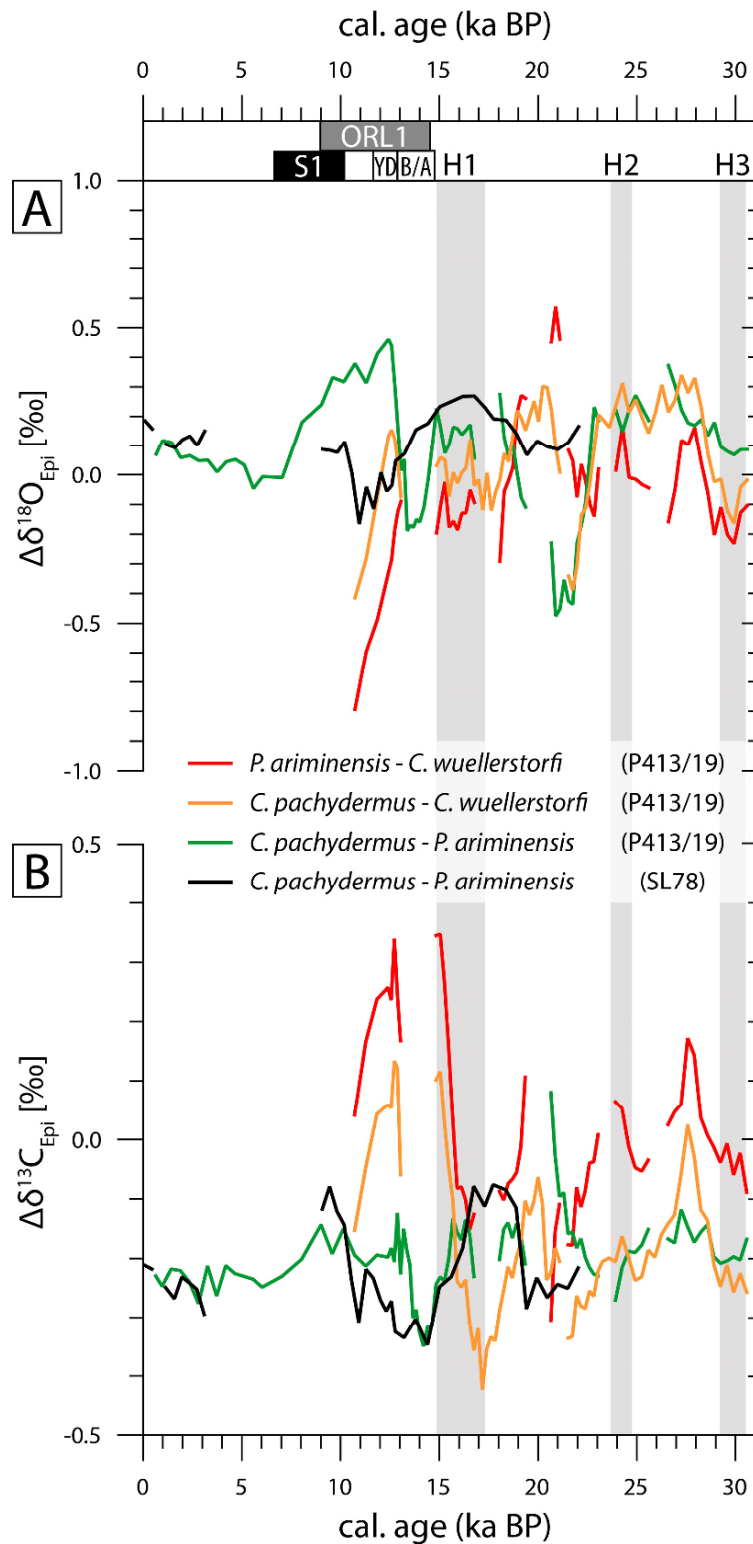


Figure 22. (a) Five-point running average (5-pra) of differences between the stable oxygen isotope records of different epifaunal benthic foraminiferal species for sediment cores SL78 and P413/19. (b) 5-pra of differences between stable carbon isotope records of epifaunal benthic foraminiferal species for sediment cores SL78 and P413/19. Top bars show times of Sapropel S1 formation in the eastern Mediterranean Sea (Mercone et al., 2000), Organic Rich Layer ORL1 in the western Mediterranean Sea (Jimenez-Espejo et al., 2007), Younger Dryas (YD), and Bølling/Allerød complex (B/A) after Cacho et al., 2001.

equilibrium (Diz et al., 2012) or utilizing oxygen directly from surrounding water or from an internal storage (de Nooijer et al., 2014). However, such effects would probably result in temporally more constant $\delta^{18}\text{O}_{\text{Epi}}$ offsets. More realistically, the observed $\delta^{18}\text{O}_{\text{Epi}}$ differences were caused by species-specific changes in metabolic fractionation (McConnaughey, 1989a, b). The observed $\Delta\delta^{18}\text{O}_{\text{Epi}}$ signals are most pronounced during the LGM and the glacial Termination, when significant changes in C_{org}

fluxes (Weldeab et al., 2003; this chapter) could have triggered species-specific changes in metabolic rates.

A comparatively stable $\delta^{13}\text{C}$ offset of 0.19-0.25 ‰ is observed between *P. ariminensis* (as bottom water indicator) and *C. pachydermus* at both sites (Fig.22b). In the modern Mediterranean Sea, the depletions of $\delta^{13}\text{C}_{C_{pachy}}$ values relative to bottom water $\delta^{13}\text{C}_{\text{DIC}}$ are in accordance with a very shallow infaunal habitat of *C. pachydermus* reflecting the influence of pore water $\delta^{13}\text{C}_{\text{DIC}}$ (Schmiedl et al., 2000, 2004; Theodor et al. 2016b). Accordingly, temporal differences in C_{org} fluxes should be reflected in variable $\Delta\delta^{13}\text{C}_{C_{pachy}\text{-DIC}}$ values with more negative values under the influence of enhanced organic carbon fluxes. Interspecific $\delta^{13}\text{C}_{\text{Epi}}$ differences between *P. ariminensis* and *C. wuellerstorfi* reveal a more inconsistent picture. While the $\delta^{13}\text{C}_{C_{wuell}}$ values are commonly similar or even heavier when compared to $\delta^{13}\text{C}_{\text{Pari}}$, the $\Delta\delta^{13}\text{C}_{C_{wuell}\text{-Pari}}$ values are more negative during the HE1-B/A interval (ca. 16-13 ka BP) (Figs. 21, 22). The observed shift in the $\Delta\delta^{13}\text{C}_{C_{wuell}\text{-Pari}}$ signal during this time interval can be best explained by the influence of seasonally enhanced phytodetritus pulses on the $\delta^{13}\text{C}_{C_{wuell}}$ signal, according to observations in the modern South Atlantic and Southern Oceans (Mackensen et al., 1993).

5.5.2 The applicability of species-specific stable carbon isotope differences as proxy for organic carbon flux and oxygen concentration

The investigated benthic foraminiferal species can be separated into strictly epifaunal (*C. wuellerstorfi*, *P. ariminensis*), epi- to very shallow infaunal (*C. pachydermus*), shallow infaunal (*Uvigerina mediterranea*, *Uvigerina peregrina*, *Angulogerina angulosa*) and deep infaunal taxa (*Globobulimina affinis*) (e.g. Corliss, 1985; Lutze & Thiel, 1989; Kitazato, 1994; Jorissen et al., 1995; de Stigter et al., 1998; Schmiedl et al., 2000). Differences in the $\delta^{13}\text{C}$ composition of epi- and infaunal species are primarily controlled by the $\delta^{13}\text{C}$ gradient of pore water DIC, resulting in decreasing foraminiferal $\delta^{13}\text{C}$ values with increasing average living depths (e.g. McCorkle et al., 1985; 1990; Schmiedl et al., 2004). Accordingly, the combination of $\delta^{13}\text{C}$ signatures of species from different microhabitats allows for the reconstruction of pore water $\delta^{13}\text{C}_{\text{DIC}}$ gradients (Schmiedl et al., 2004; Schmiedl & Mackensen, 2006; Fontanier et al., 2006; Theodor et al., 2016a, b). In this context, the $\delta^{13}\text{C}_{\text{DIC}}$ gradient in the uppermost sediment centimeter is largely controlled by the degradation of organic matter, which in turn depends on the organic matter flux rate (McCorkle & Emerson, 1988, McCorkle et al., 1990, 1997; Holsten et al., 2004). Consequently, the $\delta^{13}\text{C}$ difference between epifaunal and shallow infaunal taxa provides a measure for the local C_{org} flux (Rathburn et al., 1996; Mackensen & Licari, 2004; Schmiedl et al., 2004; Fontanier et al., 2006) and has been applied to the qualitative reconstruction of past C_{org} flux changes (Zahn et al., 1986; Vergnaud-Grazzini & Pierre, 1991; Schilman et al., 2001, 2003; Schmiedl & Mackensen, 2006; Kuhnt et al., 2008). A recently established transfer function for C_{org} fluxes in the Mediterranean Sea is based on the difference

5. Quantitative reconstructions of past organic matter fluxes and oxygen concentrations

between the $\delta^{13}\text{C}$ of epifaunal species and the shallow infaunal *U. mediterranea* (Theodor et al., 2016b). The latter species turned out as good representative of the shallow infauna since the related taxa *U. peregrina* and *A. angulosa* possess considerably stronger vital effects (i.e. metabolic and kinetic fractionation; McConnaughey, 1989a, b). These effects are likely caused by an opportunistic life style and result in average $\Delta\delta^{13}\text{C}_{Uper-Umed}$ differences of around -1.13 ‰ for SL78 and $\Delta\delta^{13}\text{C}_{Aang-Umed}$ differences of -0.93 ‰ for P413/19.

Application of the transfer function to our down-core records reveals marked C_{org} flux changes by $\sim 10 \text{ gC m}^{-2} \text{ a}^{-1}$ in the Strait of Sicily during the last 22 ka and by $\sim 13 \text{ gC m}^{-2} \text{ a}^{-1}$ during the last 30 ka in the Gulf of Genoa (Fig. 24). For the Late Glacial, the reconstructed trends are in general accordance with C_{org} flux reconstructions derived from calcareous nannoplankton assemblage changes in the Sicily Channel, which reveal relatively higher C_{org} fluxes for the LGM and the YD and lower C_{org} fluxes for the B/A interval (Di Stefano & Incarbona, 2004; Incarbona et al., 2008). In contrast, the estimated low C_{org} fluxes for the early Holocene and relatively higher C_{org} fluxes for the late Holocene around 3 ka BP at site SL78 are not corroborated by the results of other studies, which commonly report elevated C_{org} fluxes for the early Holocene interval and declining fluxes afterwards (Bárcena et al., 2001; Schilman et al., 2003; Jimenez-Espejo et al., 2007; Incarbona et al., 2008). The C_{org} fluxes for the early Holocene at site SL78 are potentially underestimated due to reduced oxygen concentrations in the intermediate water during sapropel S1 deposition as suggested by benthic foraminiferal faunal data (Tobler, 2010). Dysoxic bottom waters will lead to decreased $\delta^{13}\text{C}_{DIC}$ gradients in accordance with observations from present-day low-oxygen systems (McCorkle et al., 1985; 1990, 1997; McCorkle & Emerson, 1988; Mackensen & Licari, 2004; Holsten et al., 2004). In contrast, benthic foraminiferal faunal successions from the Ligurian Sea and Corsica Basin suggest little regional changes in oxygen concentration during the late Pleistocene and Holocene (Bartels, 2012; Angue Minto'o et al., 2015). Therefore the reconstructed C_{org} fluxes for site P413/19 are likely not biased by the influence of major drops in bottom water oxygen.

The calculation of primary productivity (PP) values based on our C_{org} flux records was facilitated by the availability of accurate regional Mediterranean sea-level reconstructions (Lambeck et al., 2011) (Fig. 25). However, while the estimated C_{org} flux values can be considered realistic for both records (except for the low-oxygen interval of S1 in the Strait of Sicily) the reconstructed PP values appear more ambiguous. In the Strait of Sicily, organic matter at the sea floor should be mainly derived from marine sources, i.e. vertical fluxes of phytodetritus produced in the surface ocean. Lateral fluxes seem to be low, due to a relatively even morphology of the sea floor and low terrestrial input of organic matter caused by the absence of major rivers at the southern border of Sicily. In contrast, the Ligurian Sea receives variable amounts of terrestrial organic matter (20-58 % at the coast, 1-30 % in the deep basin) through rivers draining the western Alps (Ivy-Ochs et al., 2009; Kaiser et al., 2014). The input of terrigenous sediment particles to site P413/19 was enhanced during the

last glacial period as reflected by approximately three-fold higher sedimentation rates relative to the Holocene. Accordingly, the estimated PP values can be regarded realistic for the Strait of Sicily, whereas PP values are likely overestimated in the Ligurian Sea at least for the glacial interval.

The presence of *G. affinis* at site SL78 facilitated the estimation of the total $\delta^{13}\text{C}$ difference in the surface sediment. Pore water studies have shown that $\delta^{13}\text{C}_{\text{DIC}}$ at sediment depth where oxygen approaches zero, i.e. in the preferred microhabitat of *G. affinis* (Jorissen et al., 1995; Fontanier et al., 2002), is determined by the overlying bottom water oxygen concentration (McCorkle and Emerson, 1988). Accordingly the $\delta^{13}\text{C}_{\text{Gaff-Epi}}$ signal can be used as bottom water oxygen proxy (McCorkle et al., 1990, 1997) and was applied to the quantification of past changes in deep-water oxygen concentrations in the Arabian Sea (Schmiedl & Mackensen, 2006) and the North Atlantic Ocean (Hoogakker et al., 2015). Applying the transfer function of Hoogakker et al. (2015) to the record of

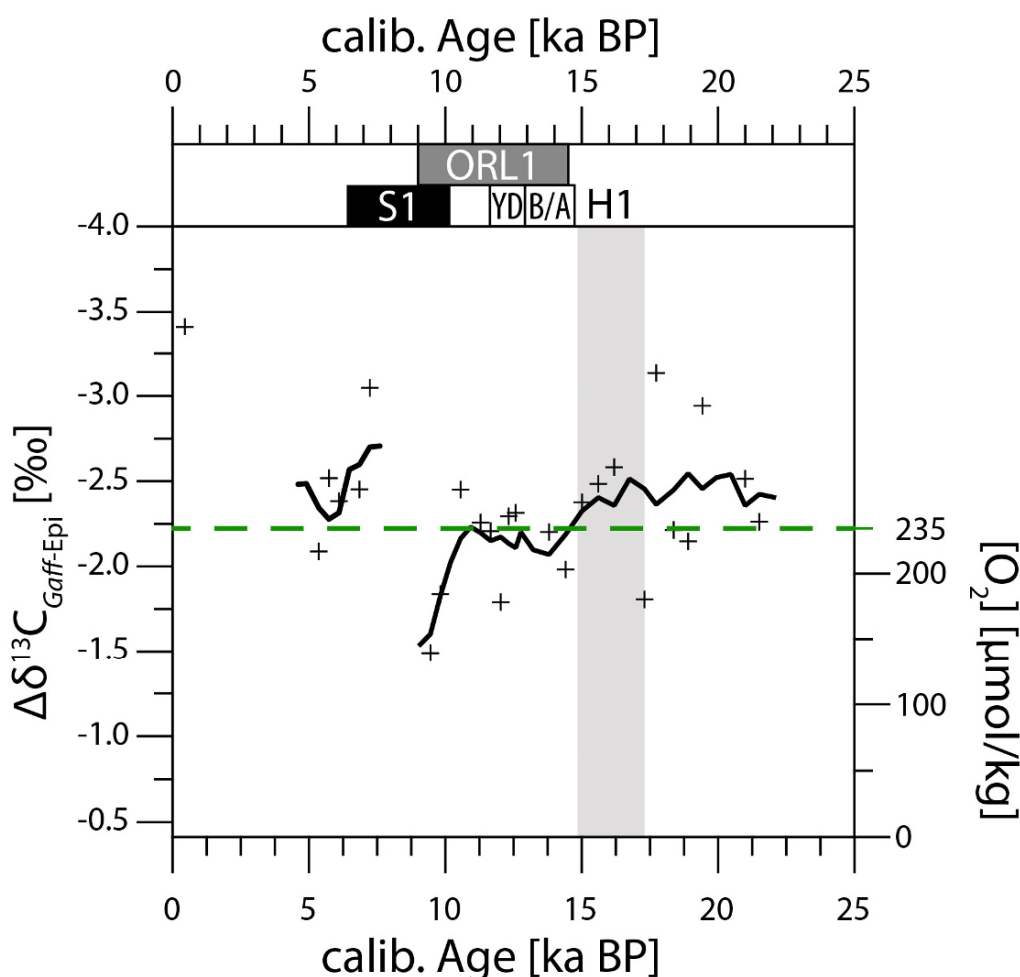


Figure 23. Stable carbon isotope differences between the deep infaunal *G. affinis* and epifaunal species of core SL78 from the Strait of Sicily, displayed as single values (crosses) and five-point running mean (thick line). The bottom water oxygen concentrations have been estimated applying the calibration of Hoogakker et al. (2015). Reconstructed oxygen concentrations are considered statistically significant below the critical threshold of $235 \mu\text{mol kg}^{-1}$ (dashed green line). Top bars show times of Sapropel S1 formation in the eastern Mediterranean Sea (Mercone et al., 2000), Organic Rich Layer ORL1 in the western Mediterranean Sea (Jimenez-Espejo et al., 2007), Younger Dryas (YD), and Bølling/ Allerød complex (B/A) after Cacho et al., 2001.

5. Quantitative reconstructions of past organic matter fluxes and oxygen concentrations

SL78, most of the reconstructed oxygen values of the past 22 ka fall above the critical threshold of $235 \mu\text{mol kg}^{-1} [\text{O}_2]$ and therefore have to be considered statistically not significant (Fig. 23). This result appears reasonable since the present-day Mediterranean Sea is well ventilated (Tanhua et al., 2013, Schneider et al., 2014) and both proxy and model studies suggest intense vertical convection also for the LGM (Schmiedl et al., 2010; Grimm et al., 2015; Rohling et al., 2015). The intermittent occurrence of *G. affinis* impeded a continuous reconstruction of oxygen values across sapropel S1 but data for the initial phase suggests that oxygen values dropped below $140 \mu\text{mol kg}^{-1} [\text{O}_2]$ during S1 at intermediate water depth of the Strait of Sicily. On the other hand, the persistence of benthic foraminifera throughout S1 demonstrates that at no time bottom waters became severely dysoxic or even anoxic at site SL78 (Tobler, 2010).

5.5.3 Changes of intermediate water circulation and oxygenation

The stable isotope records reflect differences in sources and ventilation history of intermediate water masses at 467 m water depth in the Strait of Sicily and at 662 m water depth in the Gulf of Genoa. Site SL78 is bathed by LIW and thus contains an eastern Mediterranean oceanographic signal (Béranger et al., 2004; Millot & Taupier-Letage, 2005). The $\delta^{13}\text{C}_{\text{Epi}}$ record of site SL78 resembles those from other areas in the eastern Mediterranean Sea and integrates changes in the $\delta^{13}\text{C}_{\text{DIC}}$ composition of source waters at LIW formation sites in the northern Levantine Sea and changes in LIW formation rate (Grimm et al., 2015). According to this, glacial LIW formation was similar to modern rates supporting evidence for an equivalent glacial LIW export from the eastern into the western basins (Rogerson et al., 2008). The $\delta^{13}\text{C}_{\text{Epi}}$ drop of almost 1 ‰ during the early Holocene documents a reduction of LIW formation coinciding with the time interval of sapropel S1 formation (~10.2-6.4 cal. ka BP based on ^{14}C ages of Mercone et al., 2000) in the eastern basins. The corresponding lowering of intermediate-water oxygen is first observed around 15 ka BP (Fig. 23), confirming evidence for an enhanced stratification of the water column during the Bølling/Allerød (Di Stefano & Incarbona, 2004) and for a late glacial preconditioning of Holocene eastern Mediterranean sapropel formation (Grimm et al., 2015; Cornuault et al., 2016). Although there is no information on LIW oxygen concentration across the later phase of S1 at site SL78, values as high as $140 \mu\text{mol kg}^{-1} [\text{O}_2]$ around 9.5 ka BP and the persistence of benthic foraminifera across S1 (Tobler, 2010) prove the absence of anoxia in the Strait of Sicily. This conclusion is supported by proxy and model data from the eastern Mediterranean Sea suggesting ongoing vertical convection above 1800 m water depth during S1 formation (De Lange et al., 2008; Schmiedl et al., 2010, Grimm et al., 2015; Rohling et al., 2015).

The $\delta^{13}\text{C}_{\text{Epi}}$ record of site P413/19 reveals an overall decrease of intermediate water ventilation during the past 30 ka superimposed by millennial-scale fluctuations during the late glacial (Fig. 21). Both glacial and late Holocene $\delta^{13}\text{C}_{\text{Epi}}$ values are approximately 0.2-0.3 ‰ higher than those observed in the Strait of Sicily. This difference reflects the general $\delta^{13}\text{C}_{\text{DIC}}$ gradient of Mediterranean

water masses, which is associated with the decrease of nutrients along the spread of MAW from east to the west (Pierre, 1999). Accordingly, the $\delta^{13}\text{C}_{\text{Epi}}$ record of P413/19 contains a mixture of eastern Mediterranean derived LIW and local subsurface waters formed in the northwestern Mediterranean Sea (Sparnocchia et al., 1995; Millot, 1999). The latter contribution is particularly expressed during the LGM, when $\delta^{18}\text{O}_{\text{Epi}}$ values are 0.7 to 0.9 ‰ higher than those at site SL78 (Fig. 20). Enhanced local convection in the northwestern Mediterranean Sea during the LGM can be reconciled with particularly cold sea surface temperatures reconstructed for the Gulf of Genoa based on proxy data and model results (Kuhlemann et al., 2008; Mikolajewicz, 2011). The glacial $\delta^{13}\text{C}_{\text{Epi}}$ record of P413/19 exhibits drops of 0.2 to 0.5 ‰, which are centered around 13-14, 15-16, 19-21, 23-24 and 27-29 ka BP and coincide with phases of decreased $\delta^{18}\text{O}_{\text{Epi}}$ values (Figs. 20, 21). Three of these intervals are associated with Heinrich events H3, H2 and H1 corroborating previous evidence for temporally enhanced stratification and temporarily decreased western Mediterranean deep-water formation rates during Heinrich events and DO stadials (Sierro et al., 2005; Frigola et al., 2008; Melki, 2011). The increase in surface water buoyancy during these times was triggered by the inflow of cold but fresh Atlantic surface waters linking western Mediterranean convection to the North Atlantic climate variability (Cacho et al., 2006; Sierro et al., 2009; Melki, 2011; Ausín et al., 2015). Recent stable isotope data from the Levantine Basin suggest that this process even influenced deep-water formation in the eastern Mediterranean Sea (Cornuault et al., 2016). The observed Heinrich-like event between 19-21 ka BP has no equivalent in other stable isotope records from the western Mediterranean and a potential link to the local Ligurian Sea convection and regional glaciological and climatic evolution remains unresolved.

The $\delta^{13}\text{C}_{\text{Epi}}$ drop of approximately 0.5 ‰ at site P413/19 during the Bølling/Allerød warm period coincides with the onset of formation of an organic-rich layer in the western Mediterranean Sea deep-sea at 14.5 ka BP (Jimenez-Espejo et al., 2008; Rodrigo-Gámiz et al., 2011). The inferred enhanced stratification of the water column and decreased formation of intermediate and deep-water masses during this time has been attributed to the increased inflow of fresh Atlantic surface waters with global rise of sea-level at the end of the last glacial (Siddall et al., 2003) and was further fostered by warmer and more humid conditions in the western Mediterranean region (Combourieu Nebout et al., 2009; Sicre et al., 2013).

5.5.4 Changes of organic matter fluxes and surface productivity

Application of the $\Delta\delta^{13}\text{C}_{U_{\text{med-Epi}}}$ -based transfer function of Theodor et al. (2016b) reveals generally enhanced C_{org} fluxes of $\sim 13\text{-}17\text{ gC m}^{-2}\text{ a}^{-1}$ at site SL78 and $\sim 14\text{-}23\text{ gC m}^{-2}\text{ a}^{-1}$ at site P413/19 during the last glacial maximum (Fig. 24). The C_{org} fluxes correspond to PP values of 180-195 $\text{gC m}^{-2}\text{ a}^{-1}$ and 210-270 $\text{gC m}^{-2}\text{ a}^{-1}$ in the Strait of Sicily and Ligurian Sea, respectively (Fig. 25). Evidence for increased glacial productivity in both western and eastern Mediterranean basins comes from a variety of proxy

5. Quantitative reconstructions of past organic matter fluxes and oxygen concentrations

studies (e.g., Schmiedl et al., 1998; Weldeab et al., 2003; di Stefano & Incarbona, 2004; Kuhnt et al., 2007; Abu-Zied et al., 2008; Incarbona et al., 2008; Melki et al., 2009). The glacial productivity increase is commonly attributed to enhanced wind-induced mixing (Schmiedl et al., 1998) and to nutrient pooling and shoaling of the pycnocline as a result of reduced exchange of water masses with the Atlantic Ocean (Rohling & Gieskes, 1989; Rohling, 1991). Productivity maxima occur during Heinrich events (Fig. 24) and can be associated with phases of enhanced inflow of fertilized Atlantic surface water and particularly strong wind forcing (Moreno et al., 2002; Jimenez-Espejo et al., 2008). Additional fertilization by enhanced dust fluxes from northern Africa under arid glacial conditions (Moreno et al., 2002; Bout-Roumazeilles et al., 2007; 2013; Jimenez-Espejo et al., 2008) cannot be ruled out but appear unlikely since required phosphorus is mainly derived from fluvial sources (Krom et al., 2005). In-situ experiments showed that single dust storms did not trigger a significant increase in primary production (Carbo et al., 2005) and proxy evidence from the Alboran Sea did not confirm a direct connection between dust flux and surface productivity (Rodrigo-Gámiz et al., 2011).

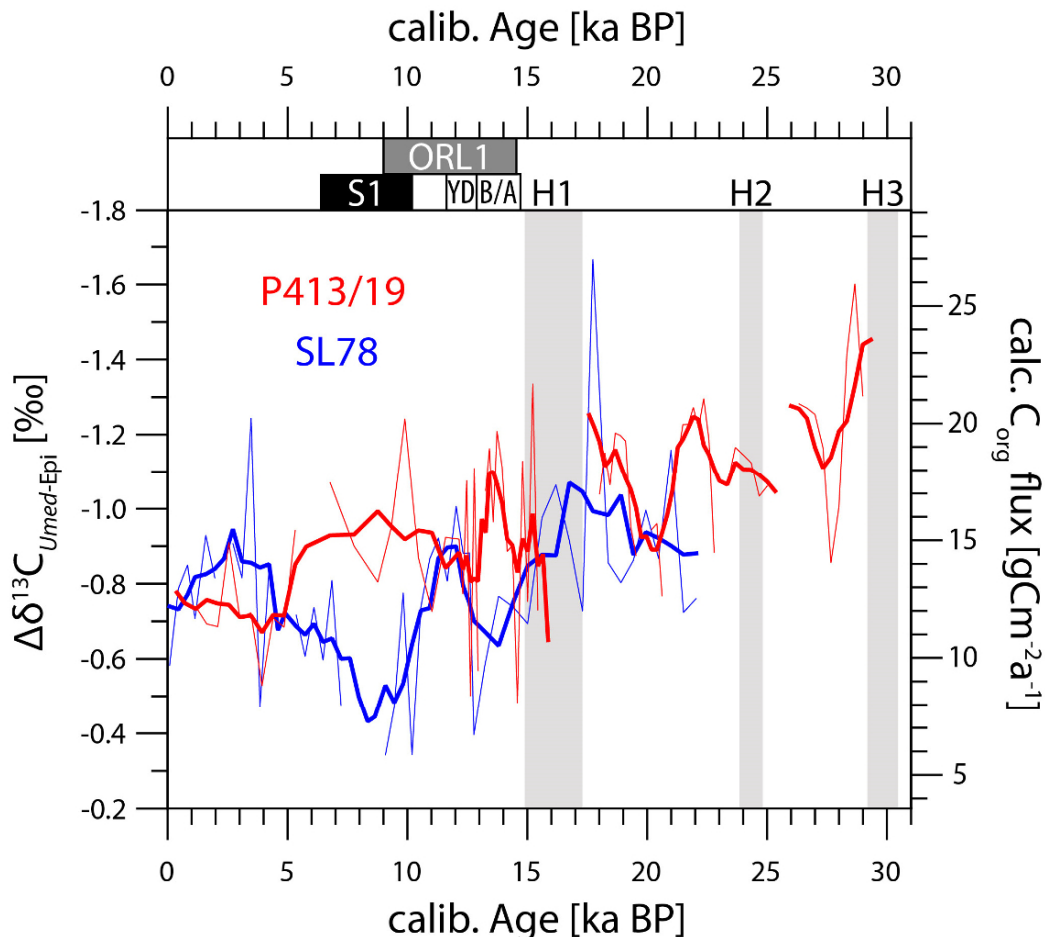


Figure 24. Stable carbon isotope differences between the shallow infaunal *U. mediterranea* and epifaunal species of sediment cores SL78 (blue) from the Strait of Sicily and P413/19 (red) from the Ligurian Sea. The organic carbon flux rates have been estimated applying the Mediterranean calibration of Theodor et al. (2016b). Thick lines represent five-point running means. Top bars show times of Sapropel S1 formation in the eastern Mediterranean Sea (Mercone et al., 2000), Organic Rich Layer ORL1 in the western Mediterranean Sea (Jimenez-Espejo et al., 2007), Younger Dryas (YD), and Bølling/ Allerød complex (B/A) after Cacho et al., 2001.

5.5 Discussion

In both studied records, C_{org} fluxes drop significantly between approximately 17 and 16 ka BP, which coincides with the onset of Termination 1 in the North Atlantic Ocean (Stern & Lisiecki, 2014) and with reduction of surface productivity in the Alboran Sea (Jimenez-Espejo et al., 2015). At site P413/19, C_{org} fluxes dropped by as much as $9\text{--}10\text{ gC m}^{-2}\text{ a}^{-1}$, which was accompanied by the short-term disappearance of *P. ariminensis* and *U. mediterranea* (Fig. 24). The strong reduction of C_{org} fluxes in the Gulf of Genoa is likely linked to initial sea-level rise at the H1-B/A transition, reflecting the combined effects of decreasing nutrients with invigoration of Mediterranean outflow (Schönfeld & Zahn, 2000; Jimenez-Espejo et al., 2015) and concurrent reduction of local lateral input of organic matter from marine and terrestrial sources. The reasons for the temporal disappearance of *P. ariminensis* and *U. mediterranea* remain elusive. Unfortunately, no local oxygen reconstruction is available for this site because of the lack of deep infaunal taxa, but the short-term significant reduction of deep-water ventilation during H1 (Sierro et al., 2005, Melki et al., 2011) may have affected the microhabitat structure and food quality at intermediate water depth in the Ligurian Sea.

The evolution of C_{org} fluxes and PP values across Termination 1 and the Holocene intervals is characterized by marked fluctuations and reveals different and partly opposing patterns in the Strait of Sicily and the Gulf of Genoa (Figs. 24, 25). The observed decrease of C_{org} fluxes at site SL78 during the B/A and subsequent increase during the YD is corroborated by nannofossil data suggesting the presence of seasonally stratified waters during the B/A and enhanced wind-induced mixing during the YD (Sprovieri et al., 2003; di Stefano & Incarbona, 2004). The formation of an organic-rich layer during the B/A and extending into the early Holocene was associated with enhanced PP in the Alboran Sea (Jiménez-Espejo et al., 2015) and Gulf of Lions (Melki et al., 2009). In the Strait of Sicily the $\delta^{13}\text{C}$ drop of *C. wuellerstorfi* indicates seasonal phytodetritus pulses. On the other hand, the enhanced accumulation of organic matter in the western Mediterranean Sea may have been facilitated by decreased ventilation of intermediate and deep-water masses as indicated by the estimated lower oxygen values for the Strait of Sicily (Fig. 23). With the onset of the YD, cold and arid conditions returned to the western Mediterranean (Combourieu Nebout et al., 2009; Abrantes et al., 2012) leading to enhanced mixing of the water column and development of a deep chlorophyll maximum layer (di Stefano & Incarbona, 2004; di Stefano et al., 2014). The associated increase in surface ocean productivity is well reflected by the $\Delta\delta^{13}\text{C}_{U.med-Epi}$ in the Strait of Sicily with peak C_{org} fluxes of almost $15\text{ gC m}^{-2}\text{ a}^{-1}$. The annual primary productivity increased to $183\text{ gC m}^{-2}\text{ a}^{-1}$, which is comparable to glacial values (Fig. 25). These results appear more realistic than previous estimates of nearly $300\text{ gC m}^{-2}\text{ a}^{-1}$, which were based on the abundance of the coccolithophore *Florisphaera profunda* (Incarbona et al., 2008). Estimated C_{org} fluxes for site P413/19 reveal a less consistent picture and the calculated values of $230\text{--}240\text{ gC m}^{-2}\text{ a}^{-1}$ may contain a mixture of vertical and lateral organic matter sedimentation.

5. Quantitative reconstructions of past organic matter fluxes and oxygen concentrations

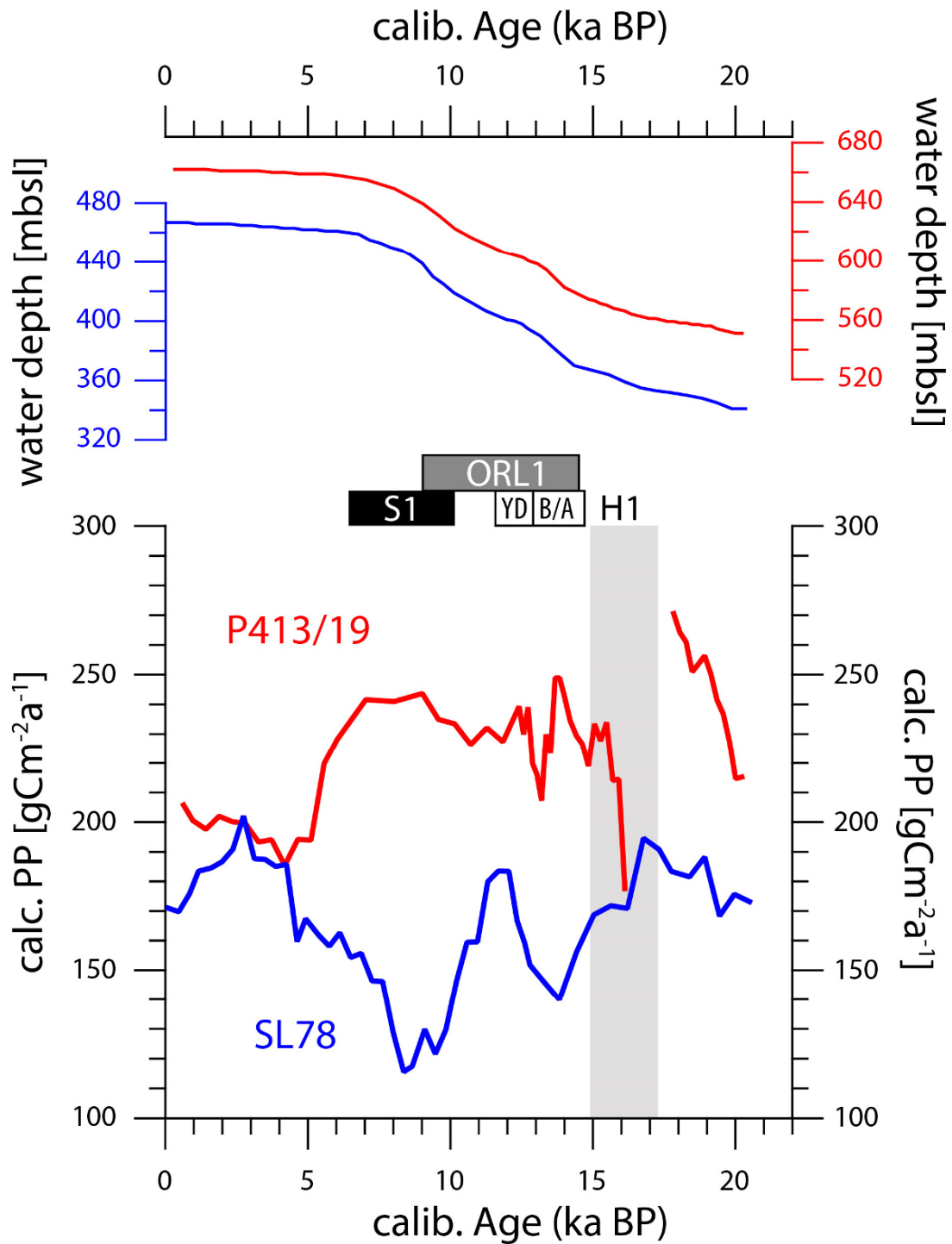


Figure 25. Five-point running means of estimated surface water primary productivity (PP) of the last 20 ka for the Strait of Sicily (SL78, blue) and the Ligurian Sea (P413/19, red). The PP values were calculated from the reconstructed organic carbon flux rates using the function of Betzer et al. (1984), and considering local sea-level evolution at each site (Lambeck et al. 2011). Bars show timing of Sapropel S1 formation in the eastern Mediterranean Sea (Mercone et al., 2000), Organic Rich Layer ORL1 in the western Mediterranean Sea (Jimenez-Espejo et al., 2007), Younger Dryas (YD), and Bølling/ Allerød complex (B/A) after Cacho et al., 2001.

5.5 Discussion

For the Holocene, the reconstructed C_{org} fluxes reveal opposing patterns in the Strait of Sicily and the Gulf of Genoa. At site SL78, C_{org} fluxes drop to oligotrophic values with onset of the Holocene accompanied by PP values as low as $\sim 115 \text{ gC m}^{-2} \text{ a}^{-1}$ during S1 formation. Although these low values likely include the bias of concurrent oxygen decrease and associated telescoping of microhabitats (see chapter 5.2), a general decrease of PP during the Holocene is documented by the establishment of epifauna-dominated benthic foraminiferal assemblages of low diversity in the eastern Mediterranean Sea (Kuhnt et al., 2007; Abu-Zied et al., 2008; Schmiedl et al., 2010). In addition, biogeochemical data and model experiments suggest that sufficient organic matter is buried in a stagnating water column under oligotrophic conditions (Möbius et al., 2010; Grimm et al., 2015; Schmiedl et al., 2015). Reduced Holocene productivity due to increased water column stratification is also derived from the distribution of coccolithophores in the Strait of Sicily (di Stefano & Incarbona, 2004; di Stefano et al., 2014). In the Gulf of Genoa, meso- to eutrophic conditions with C_{org} fluxes of $\sim 15 \text{ gC m}^{-2} \text{ a}^{-1}$ and associated PP values around $230 \text{ gC m}^{-2} \text{ a}^{-1}$ prevail during the early Holocene and are followed by more oligotrophic conditions during the late Holocene. Similar trends are also observed in the Gulf of Lions (Melki et al., 2009) and can be reconciled with enhanced early Holocene precipitation along the northern borderlands of the western and eastern Mediterranean Sea (Kotthoff et al., 2008; Dormoy et al., 2009; Fletcher et al., 2010; Perez-Obiol et al., 2011). More intense rainfall and associated riverine nutrient fluxes resulted in fertilization of near-coastal areas (Schmiedl et al., 2010; Milker et al., 2012). The humid period terminated around 5.5 ka BP (Milker et al., 2012) explaining the associated drop of C_{org} fluxes in the Gulf of Genoa. This hydrological change along the northern borderlands correlates with the abrupt termination of the African Humid Period in northwestern Africa (DeMenocal et al., 2000) suggesting a close link of hydrological changes in the southern and northern borderlands during the late Holocene.

A different late Holocene evolution of C_{org} fluxes is observed in the Strait of Sicily with a gradual but marked increase of C_{org} fluxes reaching maximum values of $\sim 14 \text{ gC m}^{-2} \text{ a}^{-1}$ and associated mesotrophic PP values of $\sim 200 \text{ gC m}^{-2} \text{ a}^{-1}$ between 2 and 3 ka BP (Figs. 24, 25). The inferred late Holocene PP increase is in contradiction to proxy data from the Strait of Sicily lacking evidence for an equivalent trend (Incarbona et al., 2008; Tobler, 2010). Enhanced influx of (nutrient-rich) dust from desiccated lakes after termination of the last African humid period (Ehrmann et al., 2013, *subm.*) would provide a reasonable mechanism. The reasons for this apparent late Holocene fertilization remain unresolved and the observed stable isotope signatures may reflect the complex sequence of ecosystem recovery and microhabitat re-organization after sapropel S1 hypoxia.

5.6 Conclusions

Multi-species benthic foraminiferal stable carbon and oxygen isotope records from two Mediterranean sediment cores reveal significant offsets between the measured species and environmental changes during the last 22-30 ka. The $\delta^{18}\text{O}$ records generally reflect the glacial-interglacial transition with a total shift of more than 2 ‰ suggesting a significant change in physical LIW properties. The freshening effects of Heinrich events H3, H2 and H1 affected the western Mediterranean Sea and are well documented in the $\delta^{18}\text{O}$ records of the Ligurian Sea. However, the reconstruction of $\delta^{18}\text{O}_{\text{EQ}}$ of bottom water is biased by non-constant species-specific offsets between the three investigated epifaunal species.

The $\delta^{13}\text{C}$ signal of the epifaunal species *P. ariminensis* and *C. wuellerstorfi* are reliable indicators for bottom water $\delta^{13}\text{C}_{\text{DIC}}$. *Cibicidoides pachydermus* exhibits an average offset between 0.20 and 0.25 ‰ relative to *P. ariminensis* underlining its very shallow infaunal microhabitat. The epifaunal $\delta^{13}\text{C}$ signals suggest well-ventilated intermediate waters in the Ligurian Sea during the past 30 ka with minor drops assigned to Heinrich events. Applying a calibration from the Atlantic Ocean (Hoogakker et al. 2015), the $\delta^{13}\text{C}$ difference between the deep infaunal *G. affinis* and epifaunal species ($\Delta\delta^{13}\text{C}_{\text{Gaff-Epi}}$) in the Strait of Sicily reveals phases of reduced bottom water oxygen, and thus LIW ventilation, for the intervals of the Bølling/Allerød (B/A) (values below 200 $\mu\text{mol kg}^{-1}$) and the sapropel S1 formation in the early Holocene (values below 150 $\mu\text{mol kg}^{-1}$).

Applying a recently established Mediterranean calibration data set (Theodor et al., 2016b), the difference between the shallow infaunal *U. mediterranea* and epifaunal species ($\Delta\delta^{13}\text{C}_{\text{Umed-Epi}}$) allowed for the estimation of past changes in organic carbon flux rates. Reconstructed C_{org} fluxes range between 15-25 $\text{gC m}^{-2} \text{a}^{-1}$ for the Last Glacial Maximum and the Younger Dryas interval while lower values between 5-15 $\text{gC m}^{-2} \text{a}^{-1}$ were estimated for the B/A interval and the Holocene. In the Strait of Sicily, reconstructed C_{org} fluxes for the time interval of sapropel S1 formation appear underestimated because low oxygen concentrations resulted in a shallower pore water $\delta^{13}\text{C}_{\text{DIC}}$ gradient and also microhabitat of *U. mediterranea*. After regional correction for the influence of sea-level-driven change in water depth it was possible to establish records of surface water primary productivity (PP). The PP reconstructions for the Strait of Sicily appear more reliable than those for the Ligurian Sea because the latter region is influenced by both vertical and lateral organic carbon fluxes, including a significant component of terrestrial origin and re-suspended organic matter from the shelf. As a consequence organic matter fluxes in the Ligurian Sea reflect changes in climate and river-runoff of the regional catchment.

6. Conclusions and Outlook

6.1 Conclusions

To conclude the important results of this thesis, it should be reasonable to return to the introducing research questions.

To which extent are the $\delta^{13}\text{C}$ and $\delta^{18}\text{O}$ differences of benthic foraminifera species-specific?
And which factors control the isotopic composition of individual species?

No matter where the tests were gathered nor if they were recent or fossil, the stable isotope ratios varied strongly between all species. The most prominent differences of more than 2 ‰ existed in the $\delta^{13}\text{C}_{\text{For}}$ values representing different microhabitats. The highest ratios appeared for the epifaunal species *Planulina ariminensis* and *Cibicidoides wuellerstorfi*, which are therefore presumably least influenced by pore water. Even between these two comparable species, with regard to their microhabitat, differences of more than 0.3 ‰ existed. The likewise epifaunal *Cibicidoides pachydermus* revealed a more constant offset against the previous species of about -0.2 ‰. This shift seems to be related to trophic conditions and, hence, a slight influence of pore water. The inconsistently lower values for *Lobatula lobatula* haven't been considered, due to low abundances and a probable relocation of the tests from shallower depths. The deep infaunal species *Globobulimina affinis*, *G. ovata*, and *G. pseudospinescens* always represented the lightest $\delta^{13}\text{C}_{\text{For}}$ values, which is in agreement with their deep microhabitat close to or below the main redox boundary.

The shallow infaunal species showed a wide range of $\delta^{13}\text{C}_{\text{For}}$ values with the highest values for *Uvigerina mediterranea*, followed by *Melonis barleeanum* and *Uvigerina peregrina*. Especially ratios of the latter species were often too low for their microhabitat, indicating a biological fractionation. Comparing the test size with the $\delta^{13}\text{C}_{\text{For}}$ higher values for larger tests are common in buliminid species, e.g. *U. peregrina*, *U. mediterranea*, *Globobulimina* spp., *Angulogerina angulosa*, indicating a decrease of biological fractionation during ontogeny. The offset of small *U. peregrina* tests was constantly more than 2 ‰ lower than the bottom water $\delta^{13}\text{C}_{\text{DIC}}$, proving that vital effects are predominating the pore water effect in small individuals of this species. Contrasting trophic conditions led to different ontogenetic increasing angles, with steeper slopes at more oligotrophic sites. Although only fossil tests of *A. angulosa* were collected from the Ligurian Sea, the relatively constant $\delta^{13}\text{C}_{\text{Aang}}$ ratio of -0.49 ‰ VPDB (± 0.12 ‰), distinctively lower than $\delta^{13}\text{C}_{\text{Umed}}$, also implies a dominance of vital effects during calcification. In contrast, for *U. mediterranea* the ontogenetic effect

6.1 Conclusions

was weaker than the environmental on the stable carbon isotope ratio. The spiral tests of *M. barleeanum* and all epifaunal species showed no connection between their size and the $\delta^{13}\text{C}_{\text{For}}$ signal.

The $\delta^{18}\text{O}$ values showed differences of more than 1 ‰ between all measured species. Infaunal species, except of *M. barleeanum*, showed higher values compared to epifaunal species, which is surprising due to their ontogenetic effect, which should shift the $\delta^{18}\text{O}$ signal towards lower values. Missing direct measurements of equilibrium bottom water stable oxygen isotope values ($\delta^{18}\text{O}_{\text{EQ}}$) hampered the possibility to decide which foraminiferal values are closer to the environmental signal. Different reasons are possible for the diverging $\delta^{18}\text{O}$ values, for example like different calcification strategies or alternative sources of the utilized oxygen. However, these biological effects can be assumed to should be constant over time, which disagrees with the observed shifts in down-core data as response to changing environmental conditions in the Strait of Sicily and the Ligurian Sea.

Which benthic foraminiferal species are less influenced by biological effects and, hence, are preferable indicator species for past environmental conditions?

The preferable indicators for bottom water $\delta^{13}\text{C}_{\text{DIC}}$ seem to be *P. ariminensis* and *C. wuellerstorfi*. The deep infaunal *Globobulimina* spp. are likewise less influenced by vital effects and are well-known proxies for pore water conditions close to or below the redox boundary depth. The shallow infaunal *U. mediterranea* seems to be less affected by vital effects, except for the ontogenetic fractionation. The extensive comparison of the $\delta^{13}\text{C}_{\text{Umed}}$ values under contrasting trophic conditions, revealed the dominance of environmental conditions over vital effects for this species.

Is it possible to correlate organic matter fluxes with epi- and infaunal benthic foraminiferal $\delta^{13}\text{C}_{\text{For}}$ ratio differences ($\Delta\delta^{13}\text{C}_{\text{For}}$), which mirror the pore water gradient?

With numerous isotopic measurements from 13 different sites of the Mediterranean Sea it was possible to establish a transfer function between calculated C_{org} fluxes and the $\delta^{13}\text{C}$ differences between *U. mediterranea* and epifaunal species. A crucial precondition for this correlation is a good bottom water oxygenation, which was applicable due to the good ventilation of the Mediterranean Sea. The calculation of C_{org} fluxes from satellite derived Primary Production values was possible, but the missing information on local lateral relocation at the investigated sites, prevented a distinct C_{org} flux estimation. This made the assumption necessary, that the correlated organic carbon origins completely from the marine primary productivity. While it worked well for distal open marine sites, while more proximal sites were influenced by sediment relocations, e.g. the marginal sites of the northern and central Aegean Sea as well as the channel system of the Gulf of Lions. Considering these biases, the following transfer function between the C_{org} fluxes and the $\Delta\delta^{13}\text{C}_{\text{Umed-Epi}}$ signal could be estimated: $\text{C}_{\text{org}} \text{ flux} = 15.99 * \Delta\delta^{13}\text{C}_{\text{Umed-Epi}} + 0.34$ ($R^2 = 0.627$; $p = 0.0021$).

6. Conclusions and Outlook

Are the stable carbon isotope ratio differences between benthic foraminiferal species applicable to reconstruct past trophic conditions of the Mediterranean Sea?

The results of the reconstructed bottom water oxygen concentrations $[O_2]$ and organic carbon fluxes at the investigated cores from the Strait of Sicily and the Ligurian Sea are mainly reliable. The reconstructed C_{org} fluxes with the previously established transfer function revealed generally higher OM fluxes of about $5 \text{ gCm}^{-2}\text{a}^{-1}$ during the Late Glacial and the YD Stadial than during the B/A Interstadial and the Holocene at both sites. The results for the Strait of Sicily seem to be less influenced by local factors, which made a recalculation of the regional PP possible, which fluctuated between 140 and $200 \text{ gCm}^{-2}\text{a}^{-1}$. An obvious bias appeared during the sapropel S1 formation with too low flux values. Due to the interaction of C_{org} fluxes and $[O_2]$ on the pore water gradient, the $\delta^{13}C_{Umed}$ shift towards isotopic heavier bottom water conditions is oxygen related. The subsequent strong increase of C_{org} fluxes until the middle Holocene, might be an aftermath of the sapropel on the stable carbon isotope signals of the epifaunal species, due to no comparable effects on other productivity proxies. In the Ligurian Sea the lack of bottom water oxygenation values hampered a clear distinguishing of biases related to low $[O_2]$. However, the resulting flux values showed a strong reaction on climatic shifts, like in humidity with subsequent variations in the riverine sediment supply. This was probably intensified by the even stronger effects on the mountainous hinterland. It can be assumed, that lateral transports play an important role in this region.

6.2 Outlook

This study tried to highlight benthic foraminifera and their specific stable isotope compositions as reactions on environmental influences. However, still some scientific questions remained or appeared during this work. The most important of them and also suggestions for future research tasks are mentioned below.

In total the stable oxygen and carbon isotope data of eleven different foraminiferal species were given. Although some of them are frequently used in paleoceanographic studies, numerous alternative species exist, even just in the Mediterranean Sea, that would be comparable or probably even better indicator species. Therefore further stable isotope research on a wider range of different benthic foraminifera is suggested. This refers to the analysis of recent sediment and fossil core samples as well as culturing experiments under controlled laboratory conditions, if possible. The latter is important, due to the always incomplete knowledge of the on-site conditions during deep-sea sampling. Still direct measurements of the surrounding bottom water during retrieving of surface samples are encouraged. In particular the $\delta^{18}O_{EQ}$ should be measured to unravel the existing insecurity, which benthic foraminifera calcify in equilibrium with the surrounding water and, hence, are a preferable proxy for water temperature and salinity.

6.2 Outlook

For the development of the transfer function between $\Delta\delta^{13}\text{C}_{\text{Umed-Epi}}$ and the organic carbon fluxes the lateral fluxes were the most important obstruction. To avoid this, benthic foraminiferal sampling should be coupled to direct flux measurements at open marine as well as coastal long term mooring sites. This would make the flux calculations unnecessary and yield the advantage of direct flux information on the specific site. Another advantage would be the possibility to gather information about seasonal changes at a specific site. Additionally, it would be interesting to quantify seasonal changes of the stable isotope deviations and the flux rates, though strongly divergent trophic conditions are known for the Mediterranean Sea throughout the year (e.g. Zuñiga et al., 2008) and likewise varying $\delta^{13}\text{C}$ values and living depths of benthic foraminifera (Kitazato et al., 2000; Corliss et al., 2002).

As a final point the further application of species-specific $\delta^{13}\text{C}_{\text{For}}$ deviations is eligible, also for sites out of the Mediterranean Sea. Either to corroborate the comprehensive possibilities or to improve the functions for differing conditions. Likewise a comparison of different biogeochemical (TOC content, Ba_{Ex}) and micropaleontological (faunal assemblages of different benthic groups) productivity and oxygen proxies within the same core would be advisable to review the stable isotope results in a more secure and extensive way.

Bibliography

- Abrantes, F., Voelker, A., Sierro, F.J., Naughton, F., Rodrigues, T., Cacho, I., Ariztegui, D., Brayshaw, D., Sicre, M.-A., Batista, L., 2012. Paleoclimate variability in the Mediterranean region. In: Lionello, P. (ed.), *The Climate of the Mediterranean Region: from the Past to the Future*. Elsevier, Amsterdam, pp. 1-86, doi:10.1016/B978-0-12-416042-2.00001-X
- Abu-Zied, R.H., Rohling, E.J., Jorissen, F.J., Fontanier, C., Casford, J.S.L., Cooke, S., 2008. Benthic foraminiferal response to changes in bottom-water oxygenation and organic carbon flux in the eastern Mediterranean during LGM to Recent times. *Marine Micropaleontology* 67, 46-68, doi:10.1016/j.marmicro.2007.08.006
- Adkins, J.F., McIntyre, K., Schrag, D.P., 2002. The Salinity, Temperature, and $\delta^{18}\text{O}$ of the Glacial Deep Ocean, *Science* 298, 1,769-1,773, doi:10.1126/science.1076252
- Aksu, A.E., Abrajano, T., Mudie, P.J., Yasar, D., 1999. Organic geochemical and palynological evidence for terrigenous origin of the organic matter in Aegean sapropel S1. *Marine Geology* 153, 303-318, doi:10.1016/S0025-3227(98)00077-2
- Altenbach, A.V., Pflaumann, U., Schiebel, R., Thies, A., Timm, S., Trauth, M., 1999. Scaling percentages and distributional patterns of benthic Foraminifera with flux rates of organic carbon. *Journal of Foraminiferal Research* 29, 173-185
- Androulidakis, Y.S., Kourafalou, V.H., Kresenitis, Y.N., and Zervakis, V., 2012. Variability of deep water mass characteristics in the North Aegean Sea: The role of lateral inputs and atmospheric conditions. *Deep-Sea Research I* 67, 55-72, doi:10.1016/j.dsr.2012.05.004
- Angue Minto'o, C.M., Bassetti, M.A., Morigi, C., Ducassou, E., Toucanne, S., Jouet, G., Mulder, T., 2014. Levantine intermediate water hydrodynamic and bottom water ventilation in the northern Tyrrhenian Sea over the past 56,000 years: New insights from benthic foraminifera and ostracods, *Quaternary International* 357, 295-313, doi:10.1016/j.quaint.2014.11.038
- Antia, A.N., Koeve, W., Fischer, G., Blanz, T., Schulz-Bull, D., Scholten, J., Neuer, S., Kremling, K., Kuss, J., Peinert, R., Hebbeln, D., Bathmann, U., Conte, M., Fehner, U., Zeitzschel, B., 2001. Basin-wide particulate carbon flux in the Atlantic Ocean: regional export patterns and potential for atmospheric CO₂ sequestration. *Global Biogeochemical Cycles* 15, 845-862, doi: 10.1029/2000GB001376
- Antoine, D., Morel, A., 1996. Oceanic primary production: 1. Adaptation of a spectral light-photosynthesis model in view of application to satellite chlorophyll observations. *Global Biogeochemical Cycles* 10, 43-55, doi:10.1029/95GB02831

Bibliography

- Astraldi, M., Gasparini, G.P., 1992. The seasonal characteristics of the circulation in the North Mediterranean Basin and their relationship with the atmospheric-climatic conditions. *Journal of Geophysical Research C* 97, 9,531-9,540, doi:10.1029/92JC00114
- Astraldi, M., Balopoulos, S., Candela, J., Font, J., Gacic, M., Gasparini, G.P., Manca, B., Theocharis, A., Tintore, J., 1999. The role of straits and channels in understanding the characteristics of Mediterranean circulation. *Progress in Oceanography* 44, 65-108, doi:10.1016/S0079-6611(99)00021-X
- Astraldi, M., Gasparini, G.P., Gervasio, L., Salusti, E., 2001. Dense water dynamics along the Strait of Sicily (Mediterranean Sea). *Journal of Physical Oceanography* 44, 3,457–3,475, DOI: 10.1175/1520-0485(2001)031<3457:DWDATS>2.0.CO;2
- Ausín, B., Flores, J.-A., Sierro, F.-J., Bárcena, M.-A., Hernández-Almeida, I., Francés, G., Gutiérrez-Arnillas, E., Martrat, B., Grimalt, J.O., Cacho, I., 2015. Coccolithophore productivity and surface water dynamics in the Alboran Sea during the last 25 kyr. *Palaeogeography Palaeoclimatology Palaeoecology* 418, 126-140, doi:10.1016/j.palaeo.2014.11.011
- Bacastow, R.B., Keeling, C.D., Lueker, T.L., Wahlen, M., Mook, W.G., 1996. The ¹³C Suess Effect in the world surface oceans and its implications for oceanic uptake of CO₂: Analysis of observations at Bermuda. *Global Biogeochemical Cycles* 10, 335-346, doi:10.1029/96GB00192
- Bárcena, M.A., Cacho, I., Abrantes, F., Sierro, F.J., Grimalt, J.O., Flores, J.A., 2001. Paleoproductivity variations related to climatic conditions in the Alboran Sea (western Mediterranean) during the last glacial-interglacial transition: the diatom record. *Palaeogeography Palaeoclimatology Palaeoecology* 167, 337-357, doi:10.1016/S0031-0182(00)00246-7
- Bárcena, M.A., Flores, J.A., Sierro, F.J., Pérez-Folgado, M., Fabres, J., Calafat, A., Canals, M., 2004. Planktonic response to main oceanographic changes in the Alboran Sea (Western Mediterranean) as documented in sediment traps and surface sediments. *Marine Micropaleontology* 53, 423-445, doi:10.1016/j.marmicro.2004.09.009
- Barras, C., Duplessy, J.-C., Geslin, E., Michel, E., Jorissen, F.J., 2010. Calibration of δ¹⁸O of cultured benthic foraminiferal calcite as a function of temperature. *Biogeosciences* 7, 1349-1356, doi:10.5194/bg-7-1349-2010
- Bartels, M., 2012. Changes in deep-water ventilation and trophic conditions in the Ligurian Sea during the Early Holocene. Unpublished Master Thesis, University Hamburg, pp. 62
- Bemis, B.E., Spero, H.J., Bijma, J., Lea, D.W., 1998. Reevaluation of the oxygen isotopic composition of planktonic foraminifera: Experimental results and revised paleotemperature equations. *Paleoceanography* 13, 150-160, doi:10.1029/98PA00070
- Béranger, K., Mortier, L., Gasparini, G.-P., Gervasio, L., Astraldi, M., Crépon, M., 2004. The dynamics of the Sicily Strait: a comprehensive study from observations and models. *Deep-Sea Research II* 51, 411-440, doi:10.1016/j.dsr2.2003.08.004

Bibliography

- Berger, W.H., Killingley, J.S., Vincent, E., 1978. Stable isotopes in deep-sea carbonates: box core ERDC-92, west equatorial Pacific. *Oceanologica Acta* 1, 203–216
- Bernhard, J.M., 2000. Distinguishing Live from Dead Foraminifera: Methods Review and Proper Applications. *Micropaleontology* 46, Supplement 1: Advances in the Biology of Foraminifera, 38-46,
- Bethoux, J.P., 1980. Mean water fluxes across sections in the Mediterranean Sea, evaluated on the basis of water and salt budgets and of observed salinities. *Oceanologica Acta* 3, 79-88
- Bethoux, J.P., Gentili, B., 1996. The Mediterranean Sea, coastal and deep-sea signatures of climatic and environmental changes. *Journal of Marine Systems* 7, 383-394, doi:10.1016/0924-7963(95)00008-9
- Bethoux, J.P., Gentili, B., Raunet, J., Tailiez, D., 1990. Warming trend in the western Mediterranean deep water. *Nature* 347, 660-662, doi:10.1038/347660a0
- Bethoux, J.P., Gentili, B., Morin, P., Nicolas, E., Pierre, C., Ruiz-Pino, D., 1999. The Mediterranean Sea: a miniature ocean for climatic and environmental studies and a key for the climatic functioning of the North Atlantic. *Progress in Oceanography* 44, 131–146, doi:10.1016/S0079-6611(99)00023-3
- Betzer, P.R., Showers, W.J., Laws, E.A., Winn, C.D., DiTullio, G.R., Kroopnick, P.M., 1984. Primary productivity and particle fluxes on a transect of the equator at 153°W in the Pacific Ocean. *Deep-Sea Research A* 31, 1-11, doi: 10.1016/0198-0149(84)90068-2
- Bickert, T., Mackensen, A., 2004. Late glacial to Holocene changes in South Atlantic deep water circulation. In: Wefer, G., Mulitza, S., Ratmeyer, V. (eds.), *The South Atlantic in the Late Quaternary: Reconstruction of Material Budgets and Current Systems*. Springer, Berlin, Heidelberg, New York, Tokyo, pp. 671–695
- Bishop, J.K.B., 2009. Autonomous observations of the ocean biological carbon pump. *Oceanography* 22, 182-193, doi:10.5670/oceanog.2009.48
- Bosc, E., Bricaud, A., Antoine, D., 2004. Seasonal and interannual variability in algal biomass and primary production in the Mediterranean Sea, as derived from 4 years of SeaWiFS observations. *Global Biogeochemical Cycles* 18, GB1005, doi:10.1029/2003GB002034
- Boucher, J., Ibanez, F., Prieur, L., 1987. Daily and seasonal variations in the spatial distribution of zooplankton populations in relation to the physical structure in the Ligurian Sea Front. *Journal of Marine Research* 45, 133-173, doi:10.1357/002224087788400891
- Bout-Roumazeilles, V., Nebout, N.C., Peyron, O., Cortijo, E., Landais, A., Masson-Delmotte, V., 2007. Connection between South Mediterranean climate and North African atmospheric circulation during the last 50,000 yr BP North Atlantic cold events, *Quaternary Science Reviews* 26, 3197-3215, doi:10.1016/j.quascirev.2007.07.015

Bibliography

- Bout-Roumazielles, V., Combourieu-Nebout, N., Desprat, S., Siani, G., Turon, J.L., Essallami, L., 2013. Tracking atmospheric and riverine terrigenous supplies variability during the last glacial and the Holocene in central Mediterranean. *Climate of the Past* 9, 1,065-1,087, doi:10.5194/cp-9-1065-2013
- Boyd, P.W., Trull, T.W., 2007. Understanding the export of biogenic particles in oceanic waters: Is there consensus?. *Progress in Oceanography* 72, 276-312, doi:10.1016/j.pocean.2006.10.007
- Brückner, S., Mackensen, A., 2008. Organic matter rain rates, oxygen availability, and vital effects from benthic foraminiferal $\delta^{13}\text{C}$ in the historic Skagerrak, North Sea. *Marine Micropaleontology* 66, 192-207, doi:10.1016/j.marmicro.2007.09.002
- Buzas, M.A., Gibson, T.G., 1969. Species diversity: Benthonic foraminifera in Western North Atlantic. *Science* 163, 72-75, doi:10.1126/science.163.3862.72
- Cacho, I., Grimalt, J.O., Sierro, F.J., Shackleton, N., Canals, M., 2000. Evidence for enhanced Mediterranean thermohaline circulation during rapid climatic coolings. *Earth and Planetary Science Letters* 183, 417-429, doi:10.1016/S0012-821X(00)00296-X
- Cacho, I., Grimalt, J.O., Canals, M., Saffi, L., Shackleton, N.J., Schönfeld, J., Zahn, R., 2001. Variability of the western Mediterranean Sea surface temperature during the last 25,000 years and its connection with the Northern Hemisphere climatic changes. *Paleoceanography* 16, 40-52, doi:10.1029/2000PA000502
- Cacho, I., Shackleton, N., Elderfield, H., Sierro, F.J., Grimalt, J.O., 2006. Glacial rapid variability in deep-water temperature and $\delta^{18}\text{O}$ from the western Mediterranean Sea, *Quaternary Science Reviews* 25, 3294-3311, doi:10.1016/j.quascirev.2006.10.004
- Calvert, S.E., 1983. Geochemistry of Pleistocene sapropels and associated sediments from the eastern Mediterranean. *Oceanologica Acta* 6, 255-267
- Calvert, S.E., Nielsen, B., Fontugne, M.R., 1992. Evidence from nitrogen isotope ratios for enhanced productivity during formation of eastern Mediterranean sapropels. *Nature* 359, 223-225. doi:10.1038/359223a0
- Canals, M., Company, J.B., Martín, D., Sánchez-Vidal, A., Ramírez-Llodrà, E., 2013. Integrated study of Mediterranean deep canyons: Novel results and future challenges. *Progress in Oceanography* 118, 1-27, doi:10.1016/j.pocean.2013.09.004
- Carbo, P., Krom, M.D., Homoky, W.B., Benning, L.G., Herut, B., 2005. Impact of atmospheric deposition on N and P geochemistry in the southeastern Levantine basin. *Deep-Sea Research II* 52, 3041-3053, doi:10.1016/j.dsr2.2005.08.014
- Cardin, V., Civitarese, G., Hainbucher, D., Bensi, M., Rubino, A., 2015. Thermohaline properties in the Eastern Mediterranean in the last three decades: is the basin returning to the pre-EMT situation?. *Ocean Sciences* 11, 53-66, doi:10.5194/os-11-53-2015

Bibliography

- Cita, M.B., Wright, R.C., Ryan, W.B.F., Longinelli, A., 1978. Messinian Palaeoenvironments. In Hsü, K.J., Montadert, L., Garrison, R.B., Fabricius, F.H., Kidd, R.B., Müller, C., Cita, M.B., Bizon, G., Wright, R.C., Erickson, A.J., Bernoulli, D., Mélières, F. (eds.). Initial Reports of the Deep Sea Drilling Project, Volume 42, Part 1: Washington, U.S. Government Printing Office, pp. 1,003-1,035, doi:10.2973/dsdp.proc.42-1.153.1978
- Combourieu Nebout, N., Fauquette, S., Quezel, P., 2000. What was the late Pliocene Mediterranean climate like; a preliminary quantification from vegetation. *Bulletin de la Societe Geologique de France* 171, 271-277, doi:10.2113/171.2.271
- Combourieu Nebout, N., Peyron, O., Dormoy, I., Desprat, S., Beaudouin, C., Kotthoff, U., Marret, F., 2009. Rapid climatic variability in the west Mediterranean during the last 25 000 years from high resolution pollen data. *Climate of the Past* 5, 503-521, doi:10.5194/cp-5-503-2009
- Corliss, B.H., 1985. Microhabitats of benthic foraminifera within deep-sea sediments. *Nature* 314, 435-438, doi:10.1038/314435a0
- Corliss, B.H., McCorkle, D.C., Higdon, D.M., 2002. A time series study of the carbon isotopic composition of deep-sea benthic foraminifera. *Paleoceanography* 17, 1036, doi:10.1029/2001PA000664
- Cornuault, M., Vidal, L., Tachikawa, K., Licari, L., Rouaud, G., Sonzogni, C., Revel, M., 2016. Deep water circulation within the eastern Mediterranean Sea over the last 95 kyr: New insights from stable isotopes and benthic foraminiferal assemblages. *Palaeogeography, Palaeoclimatology, Palaeoecology* 459, 1-14, doi:10.1016/j.palaeo.2016.06.038
- Cramp, A., O'Sullivan, G., 1999. Neogene sapropels in the Mediterranean: a review. *Marine Geology* 153, 11-28, doi:10.1016/S0025-3227(98)00092-9
- Curry, W.B., Lohmann, G.P., 1982. Carbon Isotopic Changes in Benthic Foraminifera from the Western South Atlantic: Reconstruction of Glacial Abyssal Circulation Patterns. *Quaternary Research* 18, 218-235, doi:10.1016/0033-5894(82)90071-0
- Danovaro, R., Dinet, A., Duineveld, G., Tselepides, A., 1999. Benthic response to particulate fluxes in different trophic environments: a comparison between the Gulf of Lions–Catalan Sea (western-Mediterranean) and the Cretan Sea (eastern-Mediterranean), *Progress in Oceanography* 44, 287-312, doi:10.1016/S0079-6611(99)00030-0
- De La Roche, C., Passow, U., 2007. Factors influencing the sinking of POC and the efficiency of the biological carbon pump. *Deep-Sea Research II* 54, 639-658, doi:10.1016/j.dsr2.2007.01.004
- De Lange, G.J., Thomson, J., Reitz, A., Slomp, C.P., Speranza Principato, M., Erba, E., Corselli, C., 2008. Synchronous basin-wide formation and redox-controlled preservation of a Mediterranean sapropel. *Nature Geoscience* 1, 606-610. doi:10.1038/ngeo283
- De Nooijer, L.J., Spero, H.J., Erez, J., Bijma, J., Reichert, G.J., 2014. Biomineralization in perforate foraminifera. *Earth-Science Reviews* 135, 48-58, doi:10.1016/j.earscirev.2014.03.013

Bibliography

- De Stigter, H.C., Jorissen, F.J., van der Zwaan, G.J., 1998. Bathymetric distribution and microhabitat partitioning of live (rose bengal stained) benthic foraminifera along a shelf to bathyal transect in the southern Adriatic Sea. *Journal of Foraminiferal Research* 28, 40-65
- deMenocal, P., Ortiz, J., Guilderson, T., Adkins, J., Sarnthein, M., Baker, L., Yarusinsky, M., 2000. Abrupt onset and termination of the African humid period: rapid climate responses to gradual insolation forcing. *Quaternary Science Reviews* 19, 347-361, doi:10.1016/S0277-3791(99)00081-5
- Di Stefano, E., Incarbona, A., 2004. High-resolution palaeoenvironmental reconstruction of ODP Hole 963D (Sicily Channel) during the last deglaciation based on calcareous nannofossils. *Marine Micropaleontology* 52, 241-254, doi:10.1016/j.marmicro.2004.04.009
- Di Stefano, E., Incarbona, A., Sprovieri, R., Ferraro, S., 2014. Ten Years of Paleoceanographic Studies at ODP Site 963 (Central Mediterranean Sea). *The Open Paleontology Journal* 5, 10-19, doi:10.2174/1874425701405010010
- Diz, P., Barras, C., Geslin, E., Reichart, G.-J., Metzger, E., Jorissen, F., Bijma, J., 2012. Incorporation of Mg and Sr and oxygen and carbon stable isotope fractionation in cultured *Ammonia tepida*. *Marine Micropaleontology* 92-93, 16-28, doi:10.1016/j.marmicro.2012.04.006
- Dormoy, I., Peyron, O., Combourieu Nebout, N., Goring, S., Kotthoff, U., Magny, M., Pross, J., 2009. Terrestrial climate variability and seasonality changes in the Mediterranean region between 15 000 and 4000 years BP deduced from marine pollen records. *Climate of the Past* 5, 615-632, doi:10.5194/cp-5-615-2009
- Douglas, R., Staines-Urías, F., 2007. Dimorphism, Shell Mg/Ca ratios and stable isotope content in species of *Bolivina* (Benthic Foraminifera) in the Gulf of California, Mexico. *Journal of Foraminiferal Research* 37, 189-203, doi:10.2113/gsjfr.37.3.189
- Dunbar, R.B., Wefer, G., 1984. Stable isotope fractionation in benthic Foraminifera from the Peruvian Continental Margin. *Marine Geology* 59, 215-225, doi:10.1016/0025-3227(84)90094-X
- Duplessy, J.-C., Lalou, C., Vinot, A.C., 1970. Differential Isotopic Fractionation in Benthic Foraminifera and Paleotemperatures Reassessed. *Science* 168, 250-251, doi:10.1126/science.168.3928.250
- Duplessy, J.-C., Shackleton, N.J., Matthews, R.K., Prell, W., Ruddiman, W.F., Caralp, M., Hendy, C.H., 1984. ¹³C Record of Benthic Foraminifera in the Last Interglacial Ocean: Implications for the Carbon Cycle and the Global Deep Water Circulation. *Quaternary Research* 21, 225-243, doi:10.1016/0033-5894(84)90099-1
- Duplessy, J.-C., Shackleton, N.J., Fairbanks, R.G., Labeyrie, L., Oppo, D., Kallel, N., 1988. Deepwater source variations during the last climatic cycle and their impact on the global deepwater circulation. *Paleoceanography* 3, 343-360, 10.1029/PA003i003p00343

Bibliography

- Edgar, K.M., Pälike, H., Wilson, P.A., 2013. Testing the impact of diagenesis on the $\delta^{18}\text{O}$ and $\delta^{13}\text{C}$ of benthic foraminiferal calcite from a sediment burial depth transect in the equatorial Pacific, *Paleoceanography* 28, 468-480, doi:10.1002/palo.20045
- Ehrmann, W., Seidel, M., Schmiedl, G., 2013. Dynamics of Late Quaternary North African humid periods documented in the clay mineral record of central Aegean Sea sediments. *Global and Planetary Change* 107, 186-195, doi:10.1016/j.gloplacha.2013.05.010
- Ehrmann, W., Schmiedl, G., Beuscher, S., *subm. African Humid Periods and Saharan Dust Fluxes, Climate of the Past*
- Ehrmann & Schmiedl, *in press*
- Emeis, K.-C., Camerlenghi, A., McKenzie, J.A., Rio, D., Sprovieri, R., 1991. The occurrence and significance of Pleistocene and Upper Pliocene sapropels in the Tyrrhenian Sea. *Marine Geology* 100, 155-182, doi:10.1016/0025-3227(91)90231-R
- Emeis, K.-C., Shipboard Scientific Party, 1996. Paleocyanography and Sapropel introduction. In: Emeis, K.-C., Robertson, A.H.F., Richter C., et al. (eds.), *Proceedings of the Ocean Drilling Program. Initial Reports 160*. ODP, College Station, Texas, pp. 21-28, doi:10.2973/odp.proc.ir.160.102.1996
- Emeis, K.-C., Schulz, H.M., Struck, U., Sakamoto, T., Dose, H., Erlenkeuser, H., Howell, M., Kroon, D., Paterne, M., 1998. Stable isotope and temperature records of sapropels from ODP Sites 964 and 967: constraining the physical environment of sapropel formation in the Eastern Mediterranean Sea. In: Robertson, A.H.F., Emeis, K.-C., Richter, C., Camerlenghi, A. (eds.), *Proceedings of the Ocean Drilling Program. Scientific Results 160*. ODP, College Station, Texas, pp. 309-331, doi:10.2973/odp.proc.sr.160.011.1998
- Erez, J., 1978. Vital effect on stable-isotope composition seen in foraminifera and coral skeletons. *Nature* 273, 199-202, doi:10.1038/273199a0
- Fabres, J., Calafat, A., Sanchez-Vidal, A., Canals, M., Heussner, S., 2002. Composition and spatio-temporal variability of particle fluxes in the Western Alboran Gyre, Mediterranean Sea. *Journal of Marine Systems* 33-34, 431-456, doi:10.1016/S0924-7963(02)00070-2
- Felix, M., 2014. A comparison of equations commonly used to calculate organic carbon content and marine palaeoproductivity from sediment data, *Marine Geology* 347, 1-11, doi:10.1016/j.margeo.2013.10.006
- Filipsson, H.L., Bernhard, J.M., Lincoln, S.A., McCorkle, D.C., 2010. A culture-based calibration of benthic foraminiferal paleotemperature proxies: $\delta^{18}\text{O}$ and Mg/Ca results. *Biogeosciences* 7, 1,335-1,347, doi:10.5194/bg-7-1335-2010
- Fletcher, W.J., Sanchez Goñi, M.F., Peyron, O., Dormoy, I., 2010. Abrupt climate changes of the last deglaciation detected in a Western Mediterranean forest record. *Climate of the Past* 6, 245-264, doi:10.5194/cp-6-245-2010

Bibliography

- Fontanier, C., Jorissen, F.J., Licari, L., Alexandre, A., Anschutz, P., Carbonel, P., 2002. Live benthic foraminiferal faunas from the Bay of Biscay: faunal density, composition, and microhabitats. *Deep-Sea Research I* 49, 751-785, doi:10.1016/S0967-0637(01)00078-4
- Fontanier, C., Jorissen, F.J., Chaillou, G., David, C., Anschutz, P., Lafon, V., 2003. Seasonal and interannual variability of benthic foraminiferal faunas at 550m depth in the Bay of Biscay. *Deep-Sea Research I* 50, 457-494, doi:10.1016/S0967-0637(02)00167-X
- Fontanier, C., Mackensen, A., Jorissen, F.J., Anschutz, P., Licari, L., Griveau, C., 2006. Stable oxygen and carbon isotopes of live benthic foraminifera from the Bay of Biscay: Microhabitat impact and seasonal variability. *Marine Micropaleontology* 58, 159-183, doi:10.1016/j.marmicro.2005.09.004
- Franco-Fraguas, P., Badaraco Costa, K., de Lima Toledo, F. A., 2011. Stable Isotope/Test size relationship in *Cibicides wuellerstorfi*. *Brazilian Journal of Oceanography* 59, 287-291, doi:10.1590/S1679-87592011000300010
- Frigola, J., Moreno, A., Cacho, I., Canals, M., Sierro, F.J., Flores, J.A., Grimalt, J.O., 2008. Evidence of abrupt changes in Western Mediterranean deep water circulation during the last 50 kyr: a high-resolution marine record from the Balearic Sea. *Quaternary International* 181, 88-104, doi:10.1016/j.quaint.2007.06.016
- Fuda, J.-L., Etiope, G., Millot, C., Favali, P., Calcara, M., Smriglio, G., Boschi, E., 2002. Warming, salting and origin of the Tyrrhenian Deep Water. *Geophysical Research Letters* 29, 1,898, doi:10.1029/2001GL014072
- Garcia-Castellanos, D., Estrada, F., Jiménez-Munt I., Gorini, C., Fernández, M., Vergés, J., De Vicente, R., 2009, Catastrophic flood of the Mediterranean after the Messinian salinity crisis. *Nature* 462, 778-781, doi:10.1038/nature08555
- Garcia-Gorriz, E., Carr, M.-E., 1999. The climatological annual cycle of satellite-derived phytoplankton pigments in the Alboran Sea. *Geophysical Research Letters* 26, 2,985-2,988, doi:10.1029/1999GL900529
- Garcia-Gorriz, E., Carr, M.-E., 2001. Physical control of phytoplankton distributions in the Alboran Sea: A numerical and satellite approach. *Journal of Geophysical Research* 106 C8, 16,795-16,805, doi:10.1029/1999JC000029
- Gasparini, G.P., Ortona, A., Budillon, G., Astraldi, M., Sansone, E., 2005. The effect of the Eastern Mediterranean Transient on the hydrographic characteristics in the Strait of Sicily and the Tyrrhenian Sea. *Deep-Sea Research I* 52, 915-935, doi:10.1016/j.dsr.2005.01.001
- Giresse, P., Buscail, R., Charrière, B., 2003. Late Holocene multisource material input into the Aegean Sea: depositional and post-depositional processes. *Oceanologica Acta* 26, 657-672, doi:10.1016/j.oceact.2003.09.001

Bibliography

- Gogou, A., Sanchez-Vidal, A., Durrieu de Madron, X., Stavrakakis, S., Calafat, A.M., Stabholz, M., Psarra, S., Canals, M., Heussner, S., Stavrakaki, I., Papathanassiou, E., 2014. Carbon flux to the deep in three open sites of the Southern European Seas (SES). *Journal of Marine Systems* 129, 224-233, doi:10.1016/j.jmarsys.2013.05.013
- Goldstein, S.T., 1999. Foraminifera: A Biological Overview. In: Sen Gupta, B.K. (ed.), *Modern Foraminifera*. Kluwer Academic Publishers, New York, Boston, Dordrecht, London, Moscow, pp. 37-55
- Gonfiantini, R., Stichler, W., Rozanski, K., 1995. Standards and intercomparison materials distributed by the International Atomic Energy Agency for stable isotope measurements. In: IAEA (ed.), *Reference and intercomparison materials for stable isotopes of light elements – Proceedings of a consultants meeting held in Vienna, 1-3- December 1993*, IAEA, Vienna, IAEA-TECDOC-825, pp. 13-29
- Gooday, A.J., 1988. A response by benthic Foraminifera to the deposition of phytodetritus in the deep sea. *Nature* 332, 70-73, doi:10.1038/332070a0
- Grauel, A.L., Bernasconi, S.M., 2010. Core-top calibration of $\delta^{18}\text{O}$ and $\delta^{13}\text{C}$ of *G. ruber* (white) and *U. mediterranea* along the southern Adriatic coast of Italy. *Marine Micropaleontology* 77, 175-186, doi:10.1016/j.marmicro.2010.09.003
- Grimm, R., Maier-Reimer, E., Mikolajewicz, U., Schmiedl, G., Müller-Navarra, K., Adloff, F., Grant, K.M., Ziegler, M., Lourens, L.J., Emeis, K.-C., 2015. Late glacial initiation of Holocene eastern Mediterranean sapropel formation, *Nature Communications* 6:7099, doi:10.1038/ncomms8099
- Grossman, E.L., 1984a. Carbon isotopic fractionation in live benthic foraminifera – comparison with inorganic precipitate studies. *Geochimica et Cosmochimica Acta* 48, 1,505-1,512, doi:10.1016/0016-7037(84)90406-X
- Grossman, E.L., 1984b. Stable isotope fractionation in live benthic Foraminifera from the Southern California Borderland. *Palaeogeography, Palaeoclimatology, Palaeoecology* 47, 301-327, doi:10.1016/0031-0182(84)90100-7
- Grossman, E.L., 1987. Stable isotopes in modern benthic Foraminifera: a study of vital effect. *Journal of Foraminiferal Research* 17, 48-61, doi:10.2113/gsjfr.17.1.48
- Heburn, G.W., La Violette, P.E., 1990. Variations in the Structure of the Anticyclonic Gyres Found in the Alboran Sea. *Journal of Geophysical Research* 95 C2, 1,599-1,613, doi:10.1029/JC095iC02p01599
- Hemleben, C., Becker, T., Bellas, S., Benningsen, G., Casford, J., Cagatay, N., Emeis, K.-C., Engelen, B., Ertan, T., Fontanier, C., Friedrich, O., Frydas, D., Giunta, S., Hoffelner, H., Jorissen, F., Kahl, G., Kaszemeik, K., Lykousis, V., Meier, S., Nickel, G., Overman, J., Pross, J., Reichel, T., Robert, C., Rohling, E., Ruschmeier, W., Sakinc, M., Schiebel, R., Schmiedl, G., Schubert, K., Schulz, H.,

Bibliography

- Titschak, J., Truscheit, T., 2003. Ostatlantik-Mittelmeer-Schwarzes Meer, Part 3, Cruise No.51, Leg 3, 14 November – 10 December 2001, Valetta – Istanbul. METEOR-Berichte, Universität Hamburg, 03-1, 57 pp.
- Herbert, T.D., Cleaveland Peterson, L., Lawrence, K.T., Liu, Z., 2010. Tropical ocean temperatures over the past 3.5 million years, *Science* 328, 1,530-1,534, doi:10.1126/science.1185435
- Hernández-Almeida, I., Bárcena, M.A., Flores, J.A., Sierro, F.J., Sanchez-Vidal, A., Calafat, A., 2011. Microplankton response to environmental conditions in the Alboran Sea (Western Mediterranean): One year sediment trap record. *Marine Micropaleontology* 78, 14-24 doi:10.1016/j.marmicro.2010.09.005
- Heussner, S., Durrieu de Madron, X., Calafat, A., Canals, M., Carbonne, J., Delsaut, N., Saragoni, G., 2006. Spatial and temporal variability of downward particle fluxes on a continental slope: Lessons from an 8-yr experiment in the Gulf of Lions (NW Mediterranean). *Marine Geology* 234, 63-92, doi:10.1016/j.margeo.2006.09.003
- Hieke, W., Hemleben, C., Linke, P., Türkay, M., Weikert, H., 1999. Mittelmeer 1998/99, Cruise No.40, 28 October 1997 – 10 February 1998. METEOR-Berichte, Universität Hamburg, 99-2, 286 pp.
- Hilgen, F.J., Kuiper, K.F., Krijgsman, W., Snel, E., Van der Laan, E., 2007. Astronomical tuning as the basis for high resolution chronostratigraphy: the intricate history of the Messinian Salinity Crisis. *Stratigraphy* 4, 231-238
- Holsten, J., Stott, L., Berelson, W., 2004. Reconstructing benthic carbon oxidation rates using $\delta^{13}\text{C}$ of benthic foraminifera. *Marine Micropaleontology* 53, 117-132, doi:10.1016/j.marmicro.2004.05.006
- Hoogakker, B.A.A., Elderfield, H., Oliver, K., Crowhurst, S., 2010. Benthic foraminiferal oxygen isotope offsets over the last glacial-interglacial cycle. *Paleoceanography* 25, PA4229, doi:10.1029/2009PA001870
- Hoogakker, B.A.A., Elderfield, H., Schmiedl, G., McCave, I.N., Rickaby, R.E.M., 2015. Glacial-interglacial changes in bottom-water oxygen content on the Portuguese margin. *Nature Geoscience* 8, 40-43, doi:10.1038/NGEO2317
- Hsü, K.J., Ryan, W.B.F., Cita, M.B., 1973. Late Miocene desiccation of the Mediterranean. *Nature* 242: 240-244, doi:10.1038/242240a0
- Hsü, K.J., Montadert, L., Bernoulli, D., Cita, M.B., Garrison, R.E., Kidd, R.B., Mèlières, F., Müller, C., Wright, R., 1977. History of the Mediterranean salinity crisis. *Nature* 267, 399-403, doi:10.1038/267399a0
- Hübscher, C., Betzler, C., Grevemeyer, I., 2010. Sedimentology, rift-processes and neotectonic in the western Mediterranean, Cruise No. 69, 08 August – 20 September 2006, Las Palmas (Spain) – Cartagena (Spain) – La Valletta (Malta). METEOR-Berichte, Universität Hamburg, 99-2, 86 pp.

Bibliography

- Huertas, I.E., Ríos, A.F., García-Lafuente, J., Navarro, G., Makaoui, A., Sánchez-Román, A., Rodríguez-Galvez, S., Orbi, A., Ruíz, J., Pérez, F.F., 2012. Atlantic forcing of the Mediterranean oligotrophy, *Global Biogeochemical Cycles* 26, Gb2022, doi:10.1029/2011gb004167
- Hüsing, S.K., Van Zachariasse, W.-J., Van Hinsbergen, D.J.J., Krijgsman, W., Inceöz, M., Harzhauser, M., Mandic, O., Kroh, A., 2009. Oligocene-Miocene basin evolution in SE Anatolia, Turkey: constraints on the closure of the eastern Tethys gateway. In: Van Hinsbergen, D.J.J., Edwards, M.A., Govers, R. (eds.), *Geodynamics of collision and collapse at the Africa–Arabia–Eurasia subduction zone*, Geological Society, London, Special Publications 311, 107-132, doi: 10.1144/SP311.4
- Incarbona, A., Di Stefano, E., Patti, B., Pelosi, N., Bonomo, S., Mazzola, S., Sprovieri, R., Tranchida, G., Zgozi, S., Bonanno, A., 2008. Holocene millennial-scale productivity variations in the Sicily Channel (Mediterranean Sea). *Paleoceanography* 23, 1-18, doi: 10.1029/2007PA001581
- Ivy-Ochs, S., Kerschner, H., Maisch, M., Christl, M., Kubik, P.W., Schlüchter, C., 2009. Latest Pleistocene and Holocene glacier variations in the European Alps. *Quaternary Science Reviews* 28, 2,137-2,149, doi:10.1016/j.quascirev.2009.03.009
- Jahnke, R.A., Craven, D.B., Gaillard, J.-F., 1994. The influence of organic matter diagenesis on CaCO₃ dissolution at the deep-sea floor. *Geochimica et Cosmochimica Acta* 58, 2,799-2,809, doi:10.1016/0016-7037(94)90115-5
- Jimenez-Espejo, F.J., Martinez-Ruiz, F., Sakamoto, T., Iijima, K., Gallego-Torres, D., Harada, N., 2007. Paleoenvironmental changes in the western Mediterranean since the last glacial maximum: high resolution multiproxy record from the Algero-Balearic basin. *Palaeogeography Palaeoclimatology Palaeoecology* 246, 292-306, doi:10.1016/j.palaeo.2006.10.005
- Jimenez-Espejo, F.J., Martinez-Ruiz, F., Rogerson, M., González-Donoso, J.M., Romero, O.E., Linares, D., Sakamoto, T., Gallego-Torres, D., Rueda Ruiz, J.L., Ortega-Huertas, M., Perez Claros, J.A., 2008. Detrital input, productivity fluctuations, and water mass circulation in the westernmost Mediterranean Sea since the Last Glacial Maximum. *Geochemistry Geophysics Geosystems* 9, Q11U02, doi:10.1029/2008GC002096
- Jiménez-Espejo, F.J., Pardos-Gené, M., Martínez-Ruiz, F., García-Alix, A., van de Flierdt, T., Toyofuku, T., Bahr, A., Kreissig, k., 2015. Geochemical evidence for intermediate water circulation in the westernmost Mediterranean over the last 20 kyr BP and its impact on the Mediterranean Outflow. *Global and Planetary Change* 135, 38-45, doi:10.1016/j.glopacha.2015.10.001
- Jorissen, F.J., de Stigter, H.C., Widmark, J.G.V., 1995. A conceptual model explaining benthic foraminiferal microhabitats. *Marine Micropaleontology* 26, 3-15, doi:10.1016/0377-8398(95)00047-X
- Keeling, C.D., 1979. The Suess effect: ¹³Carbon-¹⁴Carbon interrelations. *Environment International* 2, 229-300, doi:10.1016/0160-4120(79)90005-9

Bibliography

- Kim, S.-T., O'Neil, J.R., 1997. Equilibrium and nonequilibrium oxygen isotope effects in synthetic carbonates. *Geochimica et Cosmochimica Acta* 61, 3,461-3,475, doi:10.1016/S0016-7037(97)00169-5
- Kitazato, H., 1994. Foraminiferal microhabitats in four marine environments around Japan, *Marine Micropaleontology* 24, 29-41, doi:10.1016/0377-8398(94)90009-4
- Koho, K.A., García, R., de Stigter, H.C., Epping, E., Koning, E., Kouwenhoven, T.J., van der Zwaan, G.J., 2008. Sedimentary labile organic carbon and pore water redox control on species distribution of benthic foraminifera: A case study from Lisbon–Setúbal Canyon (southern Portugal). *Progress in Oceanography* 79, 55-82, doi:10.1016/j.pocean.2008.07.004
- Koho, K.A., Piña-Ochoa, E., 2012. Benthic Foraminifera: Inhabitants of low-oxygen environments. In: Altenbach, A.V., Bernhard, J.M., Seckbach, J. (eds.), *Anoxia: Evidence for Eukaryote Survival and Paleontological Strategies, Cellular Origin, Life in Extreme Habitats and Astrobiology* 21, pp. 249-285, doi:10.1007/978-94-007-1896-8_14
- Kotthoff, U., Pross, J., Müller, U.C., Peyron, O., Schmiedl, G., Schulz, H., Bordon, A., 2008a. Climate dynamics in the borderlands of the Aegean Sea during formation of sapropel S1 deduced from a marine pollen record. *Quaternary Science Reviews* 27, 832-845, doi:10.1016/j.quascirev.2007.12.001
- Krom, M.D., Emeis, K.C., Van Cappellen, P., 2010. Why is the Eastern Mediterranean phosphorus limited?. *Progress in Oceanography* 85, 236-244, doi:10.1016/j.pocean.2010.03.003
- Kuhlemann, J., Rohling, E.J., Krumrei, I., Kubik, P., Ivy-Ochs, S., Kucera, M., 2008. Regional Synthesis of Mediterranean Atmospheric Circulation during the Last Glacial Maximum. *Science* 321, 1338-11340, doi:10.1126/science.1157638
- Kuhnt, T., Schmiedl, G., Ehrmann, W., Hamann, Y., Hemleben, C., 2007. Deep-sea ecosystem variability of the Aegean Sea during the past 22 kyr as revealed by Benthic Foraminifera. *Marine Micropaleontology* 64, 141-162, doi:10.1016/j.marmicro.2007.04.003
- Kuhnt, T., Schmiedl, G., Ehrmann, W., Hamann, Y., Andersen, N., 2008. Stable isotope composition of Holocene benthic foraminifers from the Eastern Mediterranean Sea: Past changes in productivity and deep water oxygenation. *Palaeogeography Palaeoclimatology Palaeoecology* 268, 106-115, doi:10.1016/j.palaeo.2008.07.010
- Lambeck, K., Antonioli, F., Anzidei, M., Ferranti, L., Leoni, G., Silenzi, S., 2011. Sea level change along the Italian coasts during Holocene and prediction for the future. *Quaternary International* 232, 250-257, doi:10.1016/j.quascirev.2004.02.009
- Lamy, F., Arz, H., Bartels, M., Dellwig, O., Kaiser, J., Kotthoff, U., Nickel, G., Plewe, S., Ruggieri, N., Schulz, H., Weiner, A., 2011. RV Poseidon Cruise P413 - Ligurian Sea/Gulf of Genoa. Cruise Report, Bremerhaven, Alfred-Wegener-Institut, Helmholtz-Zentrum für Polar- und Meeresforschung, pp. 54

Bibliography

- Lascaratos, A., Roether, W., Nittis, K., Klein, B., 1999. Recent changes in the Eastern Mediterranean Deep Waters: a review. *Progress in Oceanography* 44, 5-36, doi:10.1016/S0079-6611(99)00019-1
- LeGrande, A.N., Schmidt, G.A., 2006. Global gridded data set of the oxygen isotopic composition in seawater. *Geophysical Research Letters* 33, L12604, doi:10.1029/2006GL026011
- Lermusiaux, P.F.J., Robinson, A.R., 2001. Features of dominant mesoscale variability, circulation patterns and dynamics in the Strait of Sicily. *Deep-Sea Res. I* 48, 1953–1997, doi:10.1016/S0967-0637(00)00114-X
- Licari, L., Mackensen, A., 2005. Benthic foraminifera off West Africa (1°N to 32°S): Do live assemblages from the topmost sediment reliably record environmental variability?. *Marine Micropaleontology* 55, 205-233, doi:10.1016/j.marmicro.2005.03.001
- Linke, P., Lutze, G.F., 1993. Microhabitat preferences of benthic foraminifera a static concept or a dynamic adaptation to optimize food acquisition?. *Marine Micropaleontology* 20, 215-234, doi:10.1016/0377-8398(93)90034-U
- Lionello, P., Galati, M.B., 2008. Links of the significant wave height distribution in the Mediterranean Sea with the north hemisphere teleconnection patterns. *Advances in Geosciences* 17, 13-18. doi:10.5194/adgeo-17-13-2008
- Lionello, P., Abrantes, F., Congedi, L., Dulac, F., Gacic, M., Gomis, D., Goodess, C., Hoff, H., Kutiel, H., Luterbacher, J., Planton, S., Reale, M., Schröder, K., Struglia, M.V., Toreti, A., Tsimplis, M.N., Ulbrich, U., Xoplaki, E., 2012. Introduction: Mediterranean Climate: Background Information. In: Lionello, P. (ed.), *The Climate of the Mediterranean Region, From the Past to the Future*, Elsevier, Amsterdam, xxxv-xc, doi:10.1016/B978-0-12-416042-2.00012-4
- Lisiecki, L.E., Raymo, M.E., 2005. A Pliocene-Pleistocene stack of 57 globally distributed benthic $\delta^{18}\text{O}$ records. *Paleoceanography* 20, PA1003, doi:10.1029/2004PA001071
- Loget, N., Van Den Driessche, J., 2006. On the origin of the Strait of Gibraltar. *Sedimentary Geology* 188-189, 341-356, doi:10.1016/j.sedgeo.2006.03.012
- López-Sandoval, D. C., Fernández, A., Marañón, E., 2011. Dissolved and particulate primary production along a longitudinal gradient in the Mediterranean Sea. *Biogeosciences* 8, 815-825, doi:10.5194/bg-8-815-2011
- Loubere, P., Meyers, P., Gary, A., 1995. Benthic foraminiferal microhabitat selection, carbon isotope values, and association with larger animals: A test with *Uvigerina peregrina*. *Journal of Foraminiferal Research* 25, 83-95, doi:10.2113/gsjfr.25.1.83
- Lutze, G.F., Thiel, H., 1989. Epibenthic foraminifera from elevated microhabitats: *Cibicidoides wuellerstorfi* and *Planulina ariminensis*, *Journal of Foraminiferal Research* 19, 153-158, doi:10.2113/gsjfr.19.2.153

Bibliography

- Lykousis, V., Chronis, G., Tselepides, A., Price, B., Theocharis, A., Siokou-Frangou, I., Van Wambeke, F., Danovaro, R., Stavrakakis, S., Duineveld, G., Georgopoulos, D., Ignatiades, L., Souvermezoglou, E., Voutsinou-Taliadouri, F., 2002. Major outputs of the recent multidisciplinary biogeochemical researches undertaken in the Aegean Sea. *Journal of Marine Systems* 33-34, 313-334, doi:10.1016/S0924-7963(02)00064-7
- Lyle, M., 1983. The brown-green color transition in marine sediments: A marker of the Fe(III)-Fe(II) redox boundary. *Limnology and Oceanography* 28, 1,026-1,033, doi:10.4319/lo.1983.28.5.1026
- Lynch-Stieglitz, J., Curry, W.B., Oppo, D.W., Ninneman, U.S., Charles, C.D., Munson, J., 2006. Meridional overturning circulation in the South Atlantic at the last glacial maximum, *Geochemistry Geophysics Geosystems* 7, Q10N03, doi:10.1029/2005GC001226
- Mackensen, A., Douglas, R.G., 1989. Down-core distribution of live and dead deep-water benthic foraminifera in box cores from the Weddell Sea and the California continental borderland. *Deep-Sea Research* 36, 879-900, doi:10.1016/0198-0149(89)90034-4
- Mackensen, A., Hubberten, H.-W., Bickert, T., Fischer, G., Fütterer, D.K., 1993. The $\delta^{13}\text{C}$ in benthic foraminiferal tests of *Fontbotia wuellerstorfi* (Schwager) relative to the $\delta^{13}\text{C}$ of dissolved inorganic carbon in southern ocean deep water: Implications for glacial ocean circulation models. *Paleoceanography*, 8, 587-610, doi: 10.1029/93PA01291
- Mackensen, A., Bickert, T., 1999. Stable carbon isotopes in benthic foraminifera: Proxies for deep and bottom water circulation and new production. In: Fischer, G., Wefer, G. (eds.), *Use of proxies in paleoceanography: Examples from the South Atlantic*. Springer, Berlin, pp. 229-254, doi:10.1007/978-3-642-58646-0_9
- Mackensen, A., Schumacher, S., Radke, J., Schmidt, D.N., 2000. Microhabitat preferences and stable carbon isotopes of endobenthic foraminifera: clue to quantitative reconstruction of oceanic new production?. *Marine Micropaleontology* 40, 233-258, doi:10.1016/S0377-8398(00)00040-2
- Mackensen, A., Licari, L., 2004. Carbon isotopes of live benthic foraminifera from the South Atlantic: Sensitivity to bottom water carbonate saturation state and organic matter rain rates. In Wefer, G., Mulitza, S., Rathmeyer, V. (eds.), *The South Atlantic in the Late Quaternary: Reconstruction of Material Budget and Current Systems*, Springer, Berlin, Heidelberg, New York, Tokyo, pp. 623-644. doi:10.1007/978-3-642-18917-3_27
- Mackensen, A., 2008. On the use of benthic foraminiferal $\delta^{13}\text{C}$ in palaeoceanography: constraints from primary proxy relationships. In: Austin, W.E.N., James, R.H. (eds.), *Biogeochemical Controls on Palaeoceanographic Environmental Proxies*. Geological Society, London, Special Publications 303, pp. 121–133, doi:10.1144/SP303.9

Bibliography

- Mackensen, A., Nam, S.-I., 2014. Taxon-specific epibenthic foraminiferal $\delta^{18}\text{O}$ in the Arctic Ocean: Relationship to water masses, deep circulation, and brine release. *Marine Micropaleontology* 113, 34-43, doi:10.1016/j.marmicro.2014.09.002
- Malanotte-Rizzoli, P., Artale, V., Borzelli-Eusebi, G.L., Brenner, S., Crise, A., Gacic, M., Kress, N., Marullo, S., Ribera d'Alcalà, M., Sofianos, S., Tanhua, T., Theocharis, A., Alvarez, M., Ashkenazy, Y., Bergamasco, A., Cardin, V., Carniel, S., Civitarese, G., D'Ortenzio, F., Font, J., Garcia-Ladona, E., Garcia-Lafuente, J.M., Gogou, A., Gregoire, M., Hainbucher, D., Kontoyannis, H., Kovacevic, V., Kraskapoulou, E., Kroskos, G., Incarbona, A., Mazzocchi, M.G., Orlic, M., Ozsoy, E., Pascual, A., Poulain, P.M., Roether, W., Rubino, A., Schroeder, K., Siokou-Frangou, J., Souvermezoglou, E., Sprovieri, M., Tintoré, J., Triantafyllou, G., 2014. Physical forcing and physical/biochemical variability of the Mediterranean Sea: a review of unresolved issues and directions for future research. *Ocean Sciences* 10, 281-322, doi:10.5194/os-10-281-2014
- Marchitto, T.M., Curry, W.B., Lynch-Stieglitz, J., Bryan, S.P., Cobb, K.M., Lund, D.C., 2014. Improved oxygen isotope temperature calibrations for cosmopolitan benthic foraminifera. *Geochimica et Cosmochimica Acta* 130, 1-11, doi:10.1016/j.gca.2013.12.034
- Martin, J.H., Knauer, G.A., Karl, D.M., Broenkow, W.W., 1987. VERTEX: carbon cycling in the northeast Pacific, *Deep-Sea Research A* 34, 267-285, doi:10.1016/0198-0149(87)90086-0
- Martin, W.R., Sayles, F.L., 1996. CaCO_3 dissolution in sediments of the Ceara Rise, western equatorial Atlantic. *Geochimica et Cosmochimica Acta* 60, 243-263, doi:10.1016/0016-7037(95)00383-5
- Masqué P., Fabres, J., Canals, M., Sanchez-Cabeza, J.A., Sanchez-Vidal, A., Cacho, I., Calafat, A.M., Bruach, J.M., 2003. Accumulation rates of major constituents of hemipelagic sediments in the deep Alboran Sea: a centennial perspective of sedimentary dynamics. *Marine Geology* 193, 207-233, doi:10.1016/S0025-3227(02)00593-5
- McCave, I.N., Hall, I.R., Antia, A.N., Chou, L., Dehairs, F., Lampitt, R.S., Thomsen, L., van Weering, T.C.E., Wollast, R., 2001. Distribution, composition and flux of particulate material over the European margin at 47°–50°N. *Deep-Sea Research II* 48, 3, 107–3,139, doi:10.1016/S0967-0645(01)00034-0
- McConnaughey, T., 1989a. ^{13}C and ^{18}O isotopic disequilibrium in biological carbonates: I. Patterns. *Geochimica et Cosmochimica Acta* 53, 151–162, doi:10.1016/0016-7037(89)90282-2
- McConnaughey, T., 1989b. ^{13}C and ^{18}O isotopic disequilibrium in biological carbonates: II. in vitro simulation of kinetic isotope effects. *Geochimica et Cosmochimica Acta* 53, 163–171, doi:10.1016/0016-7037(89)90283-4
- McCorkle, D.C., Emerson, S.R., Quay, P.D., 1985. Stable carbon isotopes in marine porewaters. *Earth and Planetary Science Letters* 74, 13-26, doi:10.1016/0012-821X(85)90162-1

Bibliography

- McCorkle, D.C., Emerson, S.R., 1988. The relationship between pore water carbon isotopic composition and bottom water oxygen concentration. *Geochimica et Cosmochimica Acta* 52, 1169-1178, doi:10.1016/0016-7037(88)90270-0
- McCorkle, D.C., Keigwin, L.D., Corliss, B.H., Emerson, S.R., 1990. The Influence of Microhabitats on the Carbon Isotopic Composition of Deep-Sea Benthic Foraminifera. *Paleoceanography* 5, 161-185, doi:10.1029/PA005i003p00295
- McCorkle, D.C., Corliss, B.H., Farnham, C.A., 1997. Vertical distributions and stable isotopic compositions of live (stained) benthic foraminifera from the North Carolina and California continental margins. *Deep-Sea Research I* 44, 983-1,024, doi:10.1016/S0967-0637(97)00004-6
- McCorkle, D.C., Bernhard, J.M., Hintz, C.J., Blanks, J.K., Chandler, G.T., Shaw, T.J., 2008. The carbon and oxygen stable isotopic composition of cultured benthic foraminifera. In: Austin, W.E.N., James, R.H. (eds.), *Biogeochemical Controls on Palaeoceanographic Environmental Proxies*. Geological Society, London, Special Publications 303, pp. 135-154, doi:10.1144/SP303.10
- MEDAR Group, 2002. *MedAtlas 2002: Mediterranean and Black Sea Database of Temperature, Salinity and Biochemical Parameters—Climatological Atlas*. IFREMER, Brest, France.
- MedAtlas, 1997. *Mediterranean Hydrographic Atlas (Mast Supporting Initiative; MAS2-CT93-0074): CD-ROM*
- MEDOC Group, 1970. Observation of formation of deep water in the Mediterranean Sea. *Nature* 277, 1037–1040, doi:10.1038/2271037a0
- Melki, T., Kallel, N., Jorissen, F.J., Guichard, F., Dennielou, B., Berné, S., Labeyrie, L., Fontugne, M., 2009. Abrupt climate change, sea surface salinity and paleoproductivity in the western Mediterranean Sea (Gulf of Lion) during the last 28 kyr. *Palaeogeography, Palaeoclimatology, Palaeoecology* 279, 96-113, doi:10.1016/j.palaeo.2009.05.005
- Melki, T., 2011. Variation of deepwater convection in the western Mediterranean Sea (Gulf of Lion) during the last 28 ka. *Quaternary International* 241, 160-168, doi:10.1016/j.quaint.2011.04.001
- Mercone, D., Thomson, J., Croudace, I.W., Siani, G., Paterne, M., Troelstra, S., 2000. Duration of S1, the most recent sapropel in the eastern Mediterranean Sea, as indicated by accelerator mass spectrometry radiocarbon and geochemical evidence. *Paleoceanography* 15, 336-347, doi:10.1029/1999PA000397
- Migon, C., Sandroni, V., Marty, J.-C., Gasser, B., Miquel, J.-C., 2002. Transfer of atmospheric matter through the euphotic layer in the northwestern Mediterranean: seasonal pattern and driving forces. *Deep-Sea Research II* 49, 2,125–2,141, doi:10.1016/S0967-0645(02)00031-0
- Mikolajewicz, U., 2011. Modeling Mediterranean Ocean climate of the Last Glacial Maximum. *Climate of the Past* 7, 161-180, doi:10.5194/cp-7-161-2011

Bibliography

- Milker, Y., Schmiedl, G., Betzler, C., Andersen, N., Theodor, M., 2012. Response of Mallorca shelf ecosystems to an early Holocene humid phase. *Marine Micropaleontology* 90-91, 1-12, doi:10.1016/j.marmicro.2012.04.001
- Millot, C., 1999. Circulation in the Western Mediterranean Sea. *Journal of Marine Systems* 20, 423-442, doi:10.1016/S0924-7963(98)00078-5
- Millot, C., Taupier-Letage, I., 2005. Circulation in the Mediterranean Sea. In: Saliot, A. (ed.), *The Handbook of Environmental Chemistry, Vol. 5: Water Pollution, Part K*, Springer, Berlin, pp. 29-66, doi:10.1007/b107143
- Millot, C., 2009. Another description of the Mediterranean Sea outflow. *Progress in Oceanography* 82, 101-124, doi:10.1016/j.pocean.2009.04.016
- Millot, C., 2013. Levantine Intermediate Water characteristics: an astounding general misunderstanding!. *Scientia Marina* 77, 217-232, doi:10.3989/scimar.03518.13A
- Möbius, J., Lahajnar, N., Emeis, K.-C., 2010. Diagenetic control of nitrogen isotope ratios in Holocene sapropels and recent sediments from the Eastern Mediterranean Sea. *Biogeosciences* 7, 3,901-3,914, doi:10.5194/bg-7-3901-2010
- Möbius, J Lahajnar, N., Emeis, K.-C., 2010. Chemical composition of surface sediment samples from the Eastern Mediterranean Sea. doi:10.1594/PANGAEA.754732
- Moran, X.A., Estrada, M., 2001. Short-term variability of photosynthetic parameters and particulate and dissolved primary production in the Alboran Sea (SW Mediterranean). *Marine Ecology Progress Series* 212, 53-67, doi:10.3354/meps212053
- Moreno, A., Cacho, I., Canals, M., Prins, M.A., Sánchez-Goñi, M.F., Grimalt, J.O., Weltje, G.J., 2002. Saharan dust transport and high latitude glacial climatic variability: the Alboran Sea record. *Quaternary Research* 58, 318-328, doi:10.1006/qres.2002.2383
- Moutin, T., Raimbault, P., 2002. Primary production, carbon export and nutrients availability in western and eastern Mediterranean Sea in early summer 1996 (MINOS cruise). *Journal of Marine Systems* 33-34, 273-288, doi: 10.1016/S0924-7963(02)00062-3
- Murat, A., 1999. Pliocene–Pleistocene occurrence of sapropels in the western Mediterranean Sea and their relation to eastern Mediterranean sapropels. In: Zahn, R., Comas, M.C., Klaus, A. (eds.), *Proceedings of the Ocean Drilling Program. Scientific Results* 161. ODP, College Station, Texas, pp. 519–527, doi:10.2973/odp.proc.sr.161.244.1999
- Ohga, T., Kitazato, H., 1997. Seasonal changes in bathyal foraminiferal populations in response to the flux of organic matter (Sagami Bay, Japan). *Terra Nova* 9, 33-37, doi:10.1046/j.1365-3121.1997.d01-6.x
- O'Neil, J.R., Clayton, R.N., Mayeda, T.K., 1969. Oxygen isotope fractionation in divalent metal carbonates. *The Journal of Chemical Physics* 51, 5.547–5.558, doi:10.1063/1.1671982

Bibliography

- Ovchinnikov I.M., 1984. The formation of intermediate water in the Mediterranean, *Oceanology*, 24, 168-173
- Packard, T.T., Gómez, M., 2013. Modeling vertical carbon flux from zooplankton respiration. *Progress in Oceanography* 110, 59-68, doi:10.1016/j.pocean.2013.01.003
- Pahnke, K., Zahn, R., 2005. Southern hemisphere water mass conversion with North Atlantic climate variability. *Science* 307, 1.741-1.746, doi:10.1126/science.1102163
- Paillard, D., Labeyrie, L., Yiou, P., 1996. Macintosh program performs time-series analysis. *Eos Transactions AGU* 77, 379, doi:10.1029/96EO00259
- Pasqual, C., Sanchez-Vidal, A., Zúñiga, D., Calafat, A., Canals, M., Durrieu de Madron, X., Puig, P., Heussner, S., Palanques, A., Delsaut, N., 2010. Flux and composition of settling particles across the continental margin of the Gulf of Lion: the role of dense shelf water cascading. *Biogeosciences* 7, 217-231, doi:10.5194/bg-7-217-2010
- Pearson, P.N., 2012. Oxygen isotopes in foraminifera: Overview and historical review. In: Ivany, L.C., Huber, T. (eds.), *Paleontological Society Short Course*, November 3, 2012. The Paleontological Society Papers, Volume 18, pp. 1-38
- Pérez-Obiol, R., Jalut, G., Julià, R., Pèlachs, A., Iriarte, M.J., Otto, T., Hernández-Beloqui, B., 2011. Mid-Holocene vegetation and climatic history of the Iberian Peninsula. *Holocene* 21, 75-93, doi:10.1177/0959683610384161
- Pierre, C., 1999. The oxygen and carbon isotope distribution in the Mediterranean water masses. *Marine Geology* 153, 41-55, doi:10.1016/S0025-3227(98)00090-5
- Pinardi, N., Masetti, E., 2000. Variability of the large scale general circulation of the Mediterranean Sea from observations and modelling: a review. *Palaeogeography, Palaeoclimatology, Palaeoecology* 158, 153-174, doi:10.1016/S0031-0182(00)00048-1
- Pinardi, N., Zavatarelli, M., Adani, M., Coppini, G., Fratianni, C., Oddo, P., Simoncelli, S., Tonani, M., Lyubartsev, V., Dobricic, S., Bonaduce, A., 2015. Mediterranean Sea large-scale low-frequency ocean variability and water mass formation rates from 1987 to 2007: A retrospective analysis. *Progress in Oceanography* 132, 318-332, doi:10.1016/j.pocean.2013.11.003
- Pinot, J.-M., López-Jurado, J.L., Riera, M., 2002. The CANALES experiment (1996-1998). Interannual, seasonal, and mesoscale variability of the circulation in the Balearic Channels. *Progress in Oceanography* 55, 335-370, doi:10.1016/S0079-6611(02)00139-8
- POEM Group, 1992. General circulation of the eastern Mediterranean Sea. *Earth Science Reviews* 32, 285-309, doi:10.1016/0012-8252(92)90002-B
- Popescu, S.-M., Biltekin, D., Winter, H., Suc, J.-P., Melinte-Dobrinescu, M.C., Klotz, S., Rabineau, M., Combourieu-Nebout, N., Clauzon, G., Deaconu, F., 2010. Pliocene and Lower Pleistocene vegetation and climate changes at the European scale: Long pollen records and climatostratigraphy. *Quaternary International* 219, 152-167, doi:10.1016/j.quaint.2010.03.013

Bibliography

- Poulain, P.-M., Gerin, R., Rixen, M., Zanasca, P., Teixeira, J., Griffa, A., Molcard, A., De Marte, M., Pinardi, N., 2012. Aspects of the surface circulation in the Liguro-Provençal basin and Gulf of Lion as observed by satellite-tracked drifters (2007-2009). *Bollettino di Geofisica Teorica ed Applicata* 53, 261-279, doi:10.4430/bgta0052
- Poulain, P.-M., Bussani, A., Gerin, R., Jungwirth, R., Mauri, E., Menna, M., Notarstefano, G., 2013. Mediterranean surface currents measured with drifters: From basin to subinertial scales. *Oceanography* 26, 38-47, doi: 10.5670/oceanog.2013.03
- Poulos, S.E., 2009. Origin and distribution of the terrigenous component of the unconsolidated surface sediment of the Aegean floor: A synthesis. *Continental Shelf Research* 29, 2045-2060, doi:10.1016/j.csr.2008.11.010
- Psarra, S., Tselepidis, A., Ignatiades, L., 2000. Primary productivity in the oligotrophic Cretan Sea (NE Mediterranean): seasonal and interannual variability. *Progress in Oceanography* 46, 187-204, doi:10.1016/S0079-6611(00)00018-5
- Puig, P., Palanques, A., 1998. Temporal variability and composition of settling particle fluxes on the Barcelona continental margin (Northwestern Mediterranean). *Journal of Marine Research* 56, 639-654, doi:10.1357/002224098765213612
- Pujo-Pay, M., Conan, P., Oriol, L., Cornet-Barthaux, V., Falco, C., Ghiglione, J.-F., Goyet, C., Moutin, T., Prieur, L., 2011. Integrated survey of elemental stoichiometry (C, N, P) from the western to eastern Mediterranean Sea. *Biogeosciences* 8, 883-899, doi:10.5194/bg-8-883-2011
- Pusceddu, A., Bianchelli, S., Canals, M., Sanchez-Vidal, A., Durrieu de Madron, X., Heussner, S., Lykousis, V., de Stigter, H., Trincardi, F., Danovaro, R., 2010. Organic matter in sediments of canyons and open slopes of the Portuguese, Catalan, Southern Adriatic and Cretan Sea margins. *Deep-Sea Research I* 57, 441-457, doi:10.1016/j.dsr.2009.11.008
- Quay, P.D., Tilbrook, B., Wong, C.S., 1992. Oceanic Uptake of Fossil Fuel CO₂: Carbon-13 Evidence. *Science* 256, 74-79, doi: 10.1126/science.256.5053.74
- Rathburn, A.E., Corliss, B.H., 1994. The ecology of living (stained) deep-sea benthic foraminifera from the Sulu Sea. *Paleoceanography* 9, 87-150, doi: 10.1029/93PA02327
- Rathburn, A.E., Corliss, B.H., Tappa, K.D., Lohmann, K.C., 1996. Comparisons of the ecology and stable isotopic compositions of living (stained) benthic foraminifera from the Sulu and South China Seas. *Deep-Sea Research I* 43, 1.617-1.646, doi:10.1016/S0967-0637(96)00071-4
- Rathburn, A.E., Levin, L.A., Held, Z., Lohmann, K.C., 2000. Benthic foraminifera associated with cold methane seeps on the northern California margin: Ecology and stable isotopic composition. *Marine Micropaleontology* 38, 247-266, doi:10.1016/S0377-8398(00)00005-0
- Ravelo, A.C., Fairbanks, R.G., 1995. Carbon isotopic fractionation in multiple species of planktonic foraminifera from core-tops in the tropical Atlantic. *Journal of Foraminiferal Research* 25, 53-74, doi:10.2113/gsjfr.25.1.53

Bibliography

- Ravelo, A.C., Hillaire-Marcel, C., 2007. The use of oxygen and carbon isotopes of foraminifera in paleoceanography. In: Hillaire-Marcel, C., De Vernal, A. (eds.), *Proxies in Late Cenozoic paleoceanography*, Elsevier, Amsterdam, pp. 735-764, doi:10.1016/S1572-5480(07)01023-8
- Reimer, P. J., Bard, E., Bayliss, A., Beck, J. W., Blackwell, P. G., Bronk Ramsey, C., Buck, C. E., Cheng, H., Edwards, R. L., Friedrich, M., Grootes, P. M., Guilderson, T. P., Hafliðason, H., Hajdas, I., Hatté, C., Heaton, T. J., Hoffmann, D. L., Hogg, A.G., Hughen, K. A., Kaiser, K. F., Kromer, B., Manning, S. W., Niu, M., Reimer, R. W., Richards, D. A., Scott, E. M., Southon, J. R., Staff, R. A., Turney, C. S. M., van der Plicht, J., 2013. IntCal13 and Marine13 radiocarbon age calibration curves 0–50 000 years cal BP. *Radiocarbon* 55, 1869-1887, doi:10.2458/azu_js_rc.55.16947
- Rhein, M., Send, U., Klein, B., Krahnemann, G., 1999. Interbasin deep water exchange in the western Mediterranean. *Journal of Geophysical Research* 104 C10, 23.495-23.508, doi:10.1029/1999JC900162
- Robinson, A.R., Sellschopp, J., Warn-Varnas, A., Leslie, W.G., Lozano, C.J., Haley Jr., P.J., Anderson, L.A., Lermusiaux, P.F.J., 1999. The Atlantic Ionian Stream. *Journal of Marine Systems* 20, 129-156, doi:10.1016/S0924-7963(98)00079-7
- Rodrigo-Gámiz, M., Martínez-Ruiz, F., Jiménez-Espejo, F.J., Gallego-Torres, D., Nieto-Moreno, V., Romero, O., Ariztegui, D., 2011. Impact of climate variability in the western Mediterranean during the last 20,000 years: oceanic and atmospheric responses. *Quaternary Science Reviews* 30, 2018-2034, doi:10.1016/j.quascirev.2011.05.011
- Roether, W., Manca, B.B., Klein, B., Bregant, D., Georgopoulos, D., Beitzel, V., Kovacevic, V., Luchetta, A., 1996. Recent changes in eastern Mediterranean deep waters. *Science* 271, 333-335, doi:10.1126/science.271.5247.333
- Roether, W., Klein, B., Hainbucher, D., 2014. The Eastern Mediterranean Transient. In: Borzelli, G.L.E., Gačić, M., Lionello, P., and Malanotte-Rizzoli, P., (eds.), *The Mediterranean Sea: Temporal Variability and Spatial Patterns*, John Wiley & Sons, Oxford. pp. 75-83, doi: 10.1002/9781118847572.ch6
- Rogerson, M., Cacho, I., Jimenez-Espejo, F., Reguera, M.I., Sierro, F.J., Martinez-Ruiz, F., Frigola, J., Canals, M., 2008. A dynamic explanation for the origin of the western Mediterranean organic rich layers. *Geochemistry Geophysics Geosystems* 9, Q07U01, doi:10.1029/2007GC001936
- Rögl, F., 1999. Short note Mediterranean and Paratethys. Facts and hypotheses of an Oligocene to Miocene Paleogeography (Short overview). *Geologica Carpathica* 50, 339-349
- Rohling, E.J., Gieskes, W.W.C., 1989. Late Quaternary changes in Mediterranean Intermediate Water density and formation rate. *Paleoceanography* 4, 531-545, doi:10.1029/PA004i005p00531
- Rohling, E.J., 1991. A simple two-layered model for shoaling of the eastern Mediterranean pycnocline due to glacio-eustatic sea-level lowering. *Paleoceanography* 6, 537-541, doi:10.1029/91PA01328

Bibliography

- Rohling, E.J., Hilgen, F.J., 1991. The eastern Mediterranean climate at times of sapropel formation: a review. *Geologie en Mijnbouw* 70, 253–264
- Rohling, E.J., 1994. Review and new aspects concerning the formation of Mediterranean sapropels. *Marine Geology* 122, 1–28, doi:10.1016/0025-3227(94)90202-X
- Rohling, E.J., Cooke, S., 1999. Stable oxygen and carbon isotopes in foraminiferal carbonate shells. In: Sen Gupta, B.K. (ed.), *Modern Foraminifera*, Kluwer Academic Publishing, New York, Boston, Dordrecht, London, Moscow, pp. 239–258
- Rohling, E.J., Marino, G., Grant, K.M., 2015. Mediterranean climate and oceanography, and the periodic development of anoxic events (sapropels). *Earth-Science Reviews* 143, 62–97, doi:10.1016/j.earscirev.2015.01.008
- Rosignol-Strick, M., Nesteroff, W., Olive, P., Vergnaud-Grazzini, C., 1982. After the deluge: Mediterranean stagnation and sapropel formation, *Nature* 295, 105–110, doi:10.1038/295105a0
- Rosignol-Strick, M., 1983. African monsoons, an immediate climate response to orbital insolation. *Nature* 304, 46–49. doi:10.1038/304046a0
- Rutgers van der Loeff, M.M., 1990. Oxygen in pore waters of deep-sea sediments. *Philosophical Transactions of the Royal Society London A* 331, 69–84, doi: 10.1098/rsta.1990.0057
- Sanchez-Vidal, A., Calafat, A., Canals, M., Fabres, J., 2004. Particle fluxes in the Almeria-Oran Front: control by coastal upwelling and sea surface circulation. *Journal of Marine Systems* 52, 89–106, doi:10.1016/j.jmarsys.2004.01.010
- Sanchez-Vidal, A., Calafat, A., Canals, M., Frigola, J., Fabres, J., 2005. Particle fluxes and organic carbon balance across the Eastern Alboran Sea (SW Mediterranean Sea). *Continental Shelf Research* 25, 609–628, doi:10.1016/j.csr.2004.11.004
- Schilman, B., Almogi-Laban, A., Bar-Matthews, M., Labeyrie, L., Paterne, M., Luz, B., 2001. Long- and short-term carbon fluctuations in the Eastern Mediterranean during the late Holocene. *Geology* 29, 1099–1102, doi:10.1130/0091-7613(2001)029<1099:LASTCF>2.0.CO;2
- Schilman, B., Almogi-Labin, A., Bar-Matthews, M., Luz, B., 2003. Late Holocene productivity and hydrographic variability in the eastern Mediterranean inferred from benthic foraminiferal stable isotopes. *Paleoceanography* 18, 1064, doi:10.1029/2002PA000813
- Schlitzer, R., 2015. Ocean Data View, <http://odv.awi.de>
- Schmiedl, G., Hemleben, C., Keller, J., Segl, M., 1998. Impact of climatic changes on the benthic foraminiferal fauna in the Ionian Sea during the last 330,000 years. *Paleoceanography* 13, 447–458, doi:10.1029/98PA01864
- Schmiedl, G., de Bovée, F., Buscail, R., Charrière, B., Hemleben, C., Medernach, L., Picon, P., 2000. Trophic control of benthic foraminiferal abundance and microhabitat in the bathyal Gulf of

Bibliography

- Lions, western Mediterranean Sea. *Marine Micropaleontology* 40, 167–188, doi:10.1016/S0377-8398(00)00038-4
- Schmiedl, G., Pfeilsticker, M., Hemleben, C., Mackensen, A., 2004. Environmental and biological effects on the stable isotope composition of recent deep-sea benthic foraminifera from the western Mediterranean Sea. *Marine Micropaleontology* 51, 129–152, doi:10.1016/j.marmicro.2003.10.001
- Schmiedl, G., Mackensen, M., 2006. Multispecies stable isotopes of benthic foraminifers reveal past changes of organic matter decomposition and deepwater oxygenation in the Arabian Sea. *Paleoceanography* 21, PA4213, doi:10.1029/2006PA001284
- Schmiedl, G., Kuhnt, T., Ehrmann, W., Emeis, K.-C., Hamann, Y., Kotthoff, U., Dulski, P., Pross, J., 2010. Climatic forcing of eastern Mediterranean deep-water formation and benthic ecosystems during the past 22 000 years. *Quaternary Science Reviews* 29, 3006-3020, doi: 10.1016/j.quascirev.2010.07.002
- Schneider, A., Tanhua, T., Roether, W., Steinfeldt, R., 2014. Changes in ventilation of the Mediterranean Sea during the past 25 year, *Ocean Sciences* 10, 1-16, doi:10.5194/os-10-1-2014
- Schönfeld, J., Zahn, R., 2000. Late Glacial to Holocene history of the Mediterranean Outflow. Evidence from benthic foraminiferal assemblages and stable isotopes at the Portuguese margin. *Palaeogeography, Palaeoclimatology, Palaeoecology* 159, 85-111, doi:10.1016/S0031-0182(00)00035-3
- Schönfeld, J., 2006. Taxonomy and distribution of the *Uvigerina peregrina* Plexus in the tropical to northeastern Atlantic. *Journal of Foraminiferal Research* 36, 355–367, doi:10.2113/gsjfr.36.4.355
- Schulz, H.M., Bechtel, A., Sachsenhofer R.F., 2005. The birth of the Paratethys during the Early Oligocene: From Tethys to an ancient Black Sea analogue?. *Global and Planetary Change* 49, 163-176, doi:10.1016/j.gloplacha.2005.07.001
- Schumacher, S., Jorissen, F.J., Mackensen, A., Gooday, A.J., Pays, O., 2010. Ontogenetic effects on stable carbon and oxygen isotopes in tests of live (Rose Bengal stained) benthic foraminifera from the Pakistan continental margin. *Marine Micropaleontology* 76, 92–103, doi:10.1016/j.marmicro.2010.06.002
- Schweizer, M., 2006. Evolution and molecular phylogeny of *Cibicides* and *Uvigerina* (Rotaliida, Foraminifera), PhD thesis. *Geologica Ultraiectina* 261, University Utrecht, pp.167
- Send, U., Font, J., Krahnemann, G., Millot, C., Rhein, M., Tintore, J., 1999. Recent advances in observing the physical oceanography of the western Mediterranean Sea. *Progress in Oceanography* 44, 37-64, doi:10.1016/S0079-6611(99)00020-8

Bibliography

- Sen Gupta, B.K., 1999. Introduction to modern Foraminifera. In: Sen Gupta, B.K. (ed.), *Modern Foraminifera*, Kluwer Academic Publishing, New York, Boston, Dordrecht, London, Moscow, pp. 3–6
- Shackleton, N.J., Opdyke, N.D., 1973. Oxygen Isotope and Palaeomagnetic Stratigraphy of Equatorial Pacific Core V28-238: Oxygen Isotope Temperatures and Ice Volumes on a 10⁵ Year and 10⁶ Year Scale. *Quaternary Research* 3, 39-55, doi:10.1016/0033-5894(73)90052-5
- Shackleton, N.J., Wiseman, J.D.H., Buckley, H.A., 1973. Non-equilibrium Isotopic Fractionation between Seawater and Planktonic Foraminiferal Tests. *Nature* 242, 177-179, doi:10.1038/242177a0
- Shackleton, N.J., 1974. Attainment of isotopic equilibrium between ocean water and the benthonic foraminifera genus *Uvigerina*: Isotopic changes in the ocean during the last glacial. *Colloques Internationaux du C.N.R.S.* 219, 203- 209
- Siani, G., Paterne, M., Michel, E., Sulpizio, R., Sbrana, A., Arnold, A., Haddad G., 2001. Mediterranean Sea Surface Radiocarbon Reservoir Age Changes since the Last Glacial Maximum. *Science* 294, 1917-1920, doi:10.1126/science.1063649
- Sicre, M.-A., Siani, G., Genty, D., Kallel, N., Essallami, L., 2013. Seemingly divergent sea surface temperature proxy records in the central Mediterranean during the last deglaciation. *Climate of the Past* 9, 1375-1383, doi:10.5194/cp-9-1375-2013
- Siddall, M., Rohling, E.J., Almogi-Labin, A., Hemleben, Ch., Meischner, D., Schmeltzer, I., Smeed, D.A., 2003. Sea-level fluctuations during the last glacial cycle. *Nature* 423, 853–858, doi:10.1038/nature01690
- Sierro, F.J., Hodell, D.A., Curtis, J.H., Flores, J.-A., Reguera, I., Colmenero-Hidalgo, E., Bárcena, M.A., Grimalt, J.O., Cacho, I., Frigola, J., Canals, M., 2005. Impact of iceberg melting on Mediterranean thermohaline circulation during Heinrich Events. *Paleoceanography* 20, PA2019, doi:10.1029/2004PA001051
- Sierro F.J., Ledesma S. Flores J.A., 2008. Astrobiochronology of Late Neogene deposits near the Strait of Gibraltar (SW Spain). Implications for the tectonic control of the Messinian Salinity Crisis. In: Briand, F. (ed.), *CISEM 2008. The Messinian Salinity Crisis from mega-deposits to microbiology- A consensus report. CIESM Workshop Monographs* 33, 73-82
- Sierro, F.J., Andersen, N., Bassetti, M.A., Berné, S., Canals, M., Curtis, J.H., Dennielou, B., Flores, J.A., Frigola, J., Gonzalez-Mora, B., Grimalt, J.O., Hodell, D.A., Jouet, G., Pérez-Folgado, M., Schneider, R., 2009. Phase relationship between sea level and abrupt climate change. *Quaternary Science reviews* 28, 2867-2881, doi:10.1016/j.quascirev.2009.07.019
- Siokou-Frangou, I., Bianchi, M., Christaki, U., Christou, E. D., Giannakourou, A., Gotsis, O., Ignatiades, L., Pagou, K., Pitta, P., Psarra, S., Souvermezoglou, E., Van Wambeke, F., Zervakis, V., 2002. Carbon flow in the planktonic food web along a gradient of oligotrophy in the Aegean Sea

Bibliography

- (Mediterranean Sea). *Journal of Marine Systems* 33-34, 335-353, doi:10.1016/S0924-7963(02)00065-9
- Sisma-Ventura, G., Yam, R., Shemesh, A., 2014. Recent unprecedented warming and oligotrophy of the eastern Mediterranean Sea within the last millennium. *Geophysical Research Letters* 41, 5158-5166, doi:10.1002/2014GL060393.
- Skirris, N., Mantziafou, A., Sofianos, S., Gkanaos, A., 2010. Satellite-derived variability of the Aegean Sea ecohydrodynamics. *Continental Shelf Research* 30, 403-418, doi:10.1016/j.csr.2009.12.012
- Smith, R.O., Bryden, H.L., Stansfield, K., 2008. Observations of new western Mediterranean deep water formation using Argo floats 2004–2006. *Ocean Sciences* 4, 133–149, doi:10.5194/os-4-133-2008
- Sournia, A., Brylinski, J.-M., Dallot, S., Le Corre, P., Leveau, M., Prieur, L., Froget, C., 1990. Fronts hydrologiques au large des côtes françaises : Les sites-ateliers du programme Frontal. *Oceanologica Acta* 13, 413-438
- Sparnocchia, S., Picco, P., Manzella, G.M.R., Ribotti, A., Copello, S., Brasey, P., 1995. Intermediate water formation in the Ligurian Sea. *Oceanologica Acta* 18, 151-162
- Spero, H.J., Lea, D.W., 1996. Experimental determination of stable isotope variability in *Globigerina bulloides*: implications for paleoceanographic reconstructions. *Marine Micropaleontology* 28, 231-246, doi:10.1016/0377-8398(96)00003-5
- Spero, H.J., Bijma, J., Lea, D.W., Bemis, B.E., 1997. Effect of seawater carbonate concentration on foraminiferal carbon and oxygen isotopes. *Nature* 390, 497-500, doi:10.1038/37333
- Sprovieri, R., Di Stefano, E., Incarbona, A., Gargano, M.E., 2003. A high-resolution record of the last deglaciation in the Sicily Channel based on foraminifera and calcareous nannofossil quantitative distribution. *Palaeogeography Palaeoclimatology Palaeoecology* 202, 119–142, doi:10.1016/S0031-0182(03)00632-1
- Stabholz, M., Durrieu de Madron, X., Canals, M., Khripounoff, A., Taupier-Letage, I., Testor, P., Heussner, S., Kerhervé, P., Delsaut, N., Houpert, L., Lastras, G., Dennielou, B., 2013. Impact of open-ocean convection on particle fluxes and sediment dynamics in the deep margin of the Gulf of Lions. *Biogeosciences* 10, 1097-1116, doi:10.5194/bg-10-1097-2013
- Staines-Urías, F., Douglas, R.G., 2009. Environmental and intraspecific dimorphism effects on the stable isotope composition of deep-sea benthic foraminifera from the Southern Gulf of California, Mexico. *Marine Micropaleontology* 71, 80–95, doi:10.1016/j.marmicro.2009.01.007
- Stansfield, K., Gasparini, G.P., Smeed, D.A., 2003. High-resolution observations of the path of the overflow from the Sicily Strait. *Deep-Sea Research I* 50, 1129–1149, doi:10.1016/S0967-0637(03)00099-2
- Stavarakakis, S., Gogou, A., Krasakopoulou, E., Karageorgis, A.P., Kontoyiannis, H., Rousakis, G., Velaoras, D., Perivoliotis, L., Kambouri, G., Stavrakaki, I., Lykousis, V., 2013. Downward fluxes of

Bibliography

- sinking particulate matter in the deep Ionian Sea (NESTOR site), eastern Mediterranean: seasonal and interannual variability. *Biogeosciences* 10, 7235-7254, doi:10.5194/bg-10-7235-2013
- Stern, J.V., Lisiecki, L.E., 2014. Termination 1 timing in radiocarbon-dated regional benthic $\delta^{18}\text{O}$ stacks. *Paleoceanography* 29, 1127-1142, doi:10.1002/2014PA002700
- Stott, L.D., Berelson, W., Douglas, R., Gorsline, D., 2000. Increased dissolved oxygen in Pacific intermediate waters due to lower rates of carbon oxidation in sediments. *Nature* 407, 367-370, doi:10.1038/35030084
- Suess, E., 1980. Particulate organic carbon flux in the oceans - surface productivity and oxygen utilization. *Nature* 288, 260-263, doi:10.1038/288260a0
- Tanhua, T., Hainbucher, D., Schroeder, K., Cardin, V., Álvarez, M., Civitarese, G., 2013. The Mediterranean Sea system: a review and an introduction to the special issue. *Ocean Science* 9, 789-803, doi:10.5194/os-9-789-2013
- Ter Kuile, B., Erez, J., 1984. In situ growth rate experiments on the symbiont-bearing foraminifera *Amphistegina lobifera* and *Amphisorus hemprichii*. *Journal of Foraminiferal Research* 14, 262-276, doi: 10.2113/gsjfr.14.4.262
- Tesi, T., Puig, P., Palanques, A., Goñi, M.A., 2010. Lateral advection of organic matter in cascading-dominated submarine canyons. *Progress in Oceanography* 84, 185-203, doi:10.1016/j.pocean.2009.10.004
- Theodor, M., Schmiedl, G., Mackensen, A., 2016. Stable isotope composition of deep-sea benthic foraminifera under contrasting trophic conditions in the western Mediterranean Sea. *Marine Micropaleontology* 124, 16-28, doi:10.1016/j.marmicro.2016.02.001
- Theodor, M., Schmiedl, G., Jorissen, F., Mackensen, A., (2016). Stable carbon isotope deviations in benthic foraminifera as proxy for organic carbon fluxes in the Mediterranean Sea. *Biogeosciences Discussions*, doi:10.5194/bg-2016-247
- Tobler, S., 2010. Benthische Foraminiferen als Umweltanzeiger in der Straße von Sizilien während der vergangenen 22 ka. Unpublished diploma thesis, University Hamburg, pp. 84
- Toucanne, S., Jouet, G., Ducassou, E., Bassetti, M.-A., Dennielou, B., Minto'o, C.M.A., Lahmi, A., Touyet, N., Charlier, K., Lericolais, G., Mulder, T., 2012. A 130,000-year record of Levantine Intermediate Water flow variability in the Corsica Trough, western Mediterranean Sea. *Quaternary Science Reviews* 33, 55-73, doi:10.1016/j.quascirev.2011.11.020
- Traub, M., Fischer, H., de Reus, M., Kormann, R., Heland, J., Ziereis, H., Schlager, H., Holzinger, R., Williams, J., Warneke, C., de Gouw, J., Lelieveld, J., 2003. Chemical characteristics assigned to trajectory clusters during the MINOS campaign. *Atmospheric Chemistry and Physics* 3, 459-468, doi:10.5194/acp-3-459-2003

Bibliography

- Trigo, R., Xoplaki, E., Zorita, E., Luterbacher, J., Krichak, S.O., Alpert, P., Jacobeit, J., Sáenz, J., Fernández, J., González-Rouco, F., Garcia-Herrera, R., Rodo, X., Brunetti, M., Nanni, T., Maugeri, M., Türkeş, M., Gimeno, L., Ribera, P., Brunet, M., Trigo, I.F., Crepon, M., Mariotti, A., 2006. Relations between variability in the Mediterranean region and mid-latitude variability. *Developments in Earth and Environmental Sciences* 4, 179-226, doi:10.1016/S1571-9197(06)80006-6
- Tsiaras, K.P., Kourafalou, V.H., Raitsos, D.E., Triantafyllou, G., Petihakis, G., Korres, G., 2012. Inter-annual productivity variability in the North Aegean Sea: Influence of thermohaline circulation during the Eastern Mediterranean Transient. *Journal of Marine Systems*, 96-97, 72-81, doi:10.1016/j.jmarsys.2012.02.003
- Tsimplis, M.N., Bryden, H.L., 2000. Estimation of the transports through the Strait of Gibraltar. *Deep-Sea Research I* 47, 2219-2242, doi:10.1016/S0967-0637(00)00024-8
- Tsimplis, M.N., Zervakis, V., Josey, S.A., Peneva, E.L., Struglia, M.V., Stanev, E. V., Theocharis, A., Lionello, P., Malanotte-Rizzoli, P., Artale, V., Tragou, E., Oguz, T., 2006. Changes in the Oceanography of the Mediterranean Sea and their Link to Climate Variability. In: Lionello, P., Malanotte-Rizzoli, P., Boscolo, R. (ed.), *Mediterranean Climate Variability*, Elsevier, Amsterdam, 227-282, doi:10.1016/S1571-9197(06)80007-8
- Uitz, J., Huot, Y., Bruyant, F., Babin, M., Claustre, H., 2008. Relating phytoplankton photophysiological properties to community structure on large scales. *Limnology and Oceanography* 53, 614-630, doi:10.4319/lo.2008.53.2.0614
- Vazquez, A., Zamarreño, I., 1993. Late Quaternary hemipelagic carbonate oozes on the southwestern Balearic slope (western Mediterranean). *Marine Geology*, 112, 71-87, doi:10.1016/0025-3227(93)90162-O
- Velaoras, D., Lascaratos, A., 2005. Deep water mass characteristics and interannual variability in the North and Central Aegean Sea. *Journal of Marine Systems*, 53, 59-85, doi:10.1016/j.jmarsys.2004.05.027
- Vergnaud Grazzini, C., Pierre, C., 1991. High fertility in the Alboran Sea since the last glacial maximum. *Paleoceanography* 6, 519-536, doi:10.1029/91PA00501
- Waelbroeck, C., Labeyrie, L., Michel, E., Duplessy, J.C., McManus, J.F., Lambeck, K., Balbon, E., Labracherie, M., 2002. Sea-level and deep water temperature changes derived from benthic foraminifera isotopic records. *Quaternary Science Reviews* 21, 295-305, doi:10.1016/S0277-3791(01)00101-9
- Walton, W.R., 1952. Techniques for recognition of living foraminifera. *Contributions from the Cushman Foundation for Foraminiferal Research* 3, 56-60
- Wefer, G., Berger, W.H., 1991. Isotope paleontology: growth and composition of extant calcareous species. *Marine Geology* 100, 207-248, doi:10.1016/0025-3227(91)90234-U

Bibliography

- Weldeab, S., Siebel, W., Wehausen, R., Emeis, K.-C., Schmiedl, G., Hemleben, C., 2003. Late Pleistocene sedimentation in the Western Mediterranean Sea: implications for productivity changes and climatic conditions in the catchment areas. *Palaeogeography, Palaeoclimatology, Palaeoecology* 190, 121-137, doi:10.1016/S0031-0182(02)00602-8
- Weldeab, S., Menke, V., Schmiedl, G., 2014. The pace of East African monsoon evolution during the Holocene, *Geophysical Research Letters*, 41, 1724-1732, doi:10.1002/2014GL059361
- Wu, G., Berger, W.H., 1989. Planktonic Foraminifera: Differential dissolution and the quaternary stable isotope record in the West Equatorial Pacific. *Paleoceanography* 4, 181-198, doi:10.1029/PA004i002p00181
- Wu, G., Herguera, J.C., Berger, W.H., 1990. Differential Dissolution: Modification of Late Pleistocene oxygen isotope records in the Western Equatorial Pacific. *Paleoceanography* 5, 581-594, doi:10.1029/PA005i004p00581
- Wüst, G., 1961. On the vertical circulation of the Mediterranean Sea. *Journal of Geophysical Research* 66, 3261-3271, doi:10.1029/JZ066i010p03261
- Zachos, J., Pagani, M., Sloan, L., Thomas, E., Billups, K., 2001. Trends, Rhythms, and Aberrations in Global Climate 65 Ma to Present. *Science* 292, 686-692, doi:10.1126/science.1059412
- Zahn, R., Winn, K., Sarnthein, M., 1986. Benthic Foraminiferal $\delta^{13}\text{C}$ and accumulation rates of organic Carbon: *Uvigerina peregrina* group and *Cibicidoides wuellerstorfi*. *Paleoceanography* 1, 27-42, doi:10.1029/PA001i001p00027
- Zarriess, M., Mackensen, A., 2011. Testing the impact of seasonal phytodetritus deposition on $\delta^{13}\text{C}$ of epibenthic foraminifer *Cibicidoides wuellerstorfi*: A 31,000 year high-resolution record from the northwest African continental slope. *Paleoceanography* 26, PA2202, doi:10.1029/2010PA001944
- Zeebe, R.E., Bijma, J., Hönisch, B., Sanyal, A., Spero, H.J., Wolf-Gladrow, D.A., 2008. Vital effects and beyond: a modelling perspective on developing palaeoceanographical proxy relationships in foraminifera. In: Austin, W.E.N., James, R.H. (eds.), *Biogeochemical Controls on Palaeoceanographic Environmental Proxies*. Geological Society, London, Special Publications 303, pp. 45-58, doi:10.1144/SP303.4
- Zervakis, V., Krasakopoulou, E., Georgopoulos, D., and Souvermezoglou, E., 2003. Vertical diffusion and oxygen consumption during stagnation periods in the deep North Aegean. *Deep-Sea Research I* 50, 53-71, doi:10.1016/S0967-0637(02)00144-9
- Zúñiga, D., Calafat, A., Sanchez-Vidal, A., Canals, M., Price, B., Heussner, S., Miserocchi, S., 2007. Particulate organic carbon budget in the open Algero-Balearic Basin (Western Mediterranean): Assessment from a one-year sediment trap experiment. *Deep-Sea Research I* 54, 1530-1548, doi:10.1016/j.dsr.2007.06.001

Bibliography

Zúñiga, D., Calafat, A., Heussner, S., Miserocchi, S., Sanchez-Vidal, A., Garcia-Orellana, J., Canals, M., Sánchez-Cabeza, J.A., Carbonne, J., Delsaut, N., Saragoni, G., 2008. Compositional and temporal evolution of particle fluxes in the open Algero-Balearic basin (Western Mediterranean). *Journal of Marine Systems* 70, 196-214, doi:10.1016/j.jmarsys.2007.05.007

Appendix

Appendix I

Taxonomy of benthic foraminifera investigated in this thesis

Class: Globothalamea Pawlowski, Holzmann, Tyszka, 2013

Order: Rotaliida Delage & Hérouard, 1896

Suborder: Rotaliina Delage & Hérouard, 1896

Superfamily: Buliminoidea Jones, 1875

Family: Buliminidae Jones, 1875

Genus: *Globobulimina* Cushman, 1927

Globobulimina affinis (d'Orbigny) = *Bulimina affinis* d'Orbigny 1839, p. 105, pl. 2, figs. 25-26.

(PLATE 1, FIG. 1)

Globobulimina pseudospinescens (Emiliani) = *Bulimina pyrula* d'Orbigny var. *pseudospinescens*

Emiliani 1949, p. 9, pl. 2, figs. 24-25.

(PLATE 1, FIG. 2)

Globobulimina ovata (d'Orbigny) = *Bulimina ovata* d'Orbigny 1846, p. 185, pl. 11, figs. 13-14.

(PLATE 1, FIG. 3)

Family: Uvigerinidae Haeckel, 1894

Subfamily: Uvigerininae Haeckel, 1894

Genus: *Uvigerina* d'Orbigny, 1826

Uvigerina mediterranea Hofker = *Uvigerina mediterranea* Hofker 1932, p. 118-121, fig. 32.

(PLATE 1, FIGS. 4-6)

Uvigerina peregrina Cushman = *Uvigerina peregrina* Cushman 1923, p. 166, pl. 42, figs. 7-10.

(PLATE 1, FIGS. 7-9)

Subfamily: Angulogerininae Galloway, 1933

Genus: *Angulogerina* Cushman, 1927

Angulogerina angulosa (Williamson) = *Uvigerina angulosa* Williamson, 1858, p. 67, pl. 5, fig. 140.

(PLATE 1, FIGS. 10-12)

Superfamily: Chilostomelloidea Brady, 1881

Family: Anomalinidae Cushman, 1927

Genus: *Cibicidoides* Thalmann, 1939

Cibicidoides pachydermus (Rzehak) = *Truncatulina pachyderma* Rzehak 1886, p. 87, pl. 1, fig. 5.

Appendix I

(PLATE 2, FIGS. 1-3)

Cibicoides wuellerstorfi (Schwager) = *Anomalina wuellerstorfi* Schwager, 1866, p. 258-259, pl. 7, figs. 105, 107.

(PLATE 2, FIGS. 4-6)

Superfamily: Planorbuloidea Schwager, 1877

Family: Planulinidae Bermúdez, 1952

Genus: *Planulina* d'Orbigny, 1826

Planulina ariminensis d'Orbigny = *Planulina ariminensis* d'Orbigny 1826, p. 280, pl. 14, figs. 1-3.

(PLATE 2, FIGS. 7-9)

Family: Cibicididae Cushman, 1927

Subfamily: Cibicidinae Cushman, 1928

Genus: *Lobatula* Fleming, 1828

Lobatula lobatula (Walker & Jakob) = *Nautilus lobatulus* Walker & Jacob 1798, p. 642, pl. 14, fig. 36.

(PLATE 2, FIGS. 10, 11)

Superfamily: Nonionoidea Schultze, 1854

Family: Nonionidae Schultze, 1854

Subfamily: Pulleniinae Schwager, 1877

Genus: *Melonis* de Montfort, 1808

Melonis barleanum (Williamson) = *Nonionina barleeanum* Williamson 1858, p. 32, pl. 3, figs. 68-69.

(PLATE 2, FIGS. 12, 13)

Appendix II

Counted benthic foraminifera

Table A.1. Counted numbers of living (stained) calcareous benthic foraminifera from surface samples of the western Mediterranean Sea and the Aegean Sea. Additionally depth intervals and partitions of the investigated samples are given.

Table A.2. Counted numbers and percentage of dead (unstained) benthic foraminifera from surface samples of the western Mediterranean Sea. The samples were constantly taken from 4-5 cm depth.

Appendix III

Test size distribution

Table A.3. Test size distributions of shallow infaunal *Uvigerina mediterranea* for all investigated sites, for the likewise shallow infaunal *Uvigerina peregrina* and *Melonis barleeanum* from all western Mediterranean sites and for three deep infaunal benthic foraminifera (*Globobulimina pseudospinescens*, *Globobulimina ovata*, *Globobulimina affinis*) from the Alboran Sea sites. Measurements were performed on stained and unstained tests.

Appendix IV

Stable isotope data

Table A.4. Stable carbon and oxygen isotope measurements of stained and unstained benthic foraminifera from surface samples of the western Mediterranean Sea and the Aegean Sea. Values are given against foraminiferal test size and sediment depth.

Table A.5. Stable carbon and oxygen isotope measurements of various benthic foraminifera from core SL78 (Strait of Sicily). Values are given against cal. age and sediment depth.

Table A.6. Stable carbon and oxygen isotope measurements of various benthic foraminifera from core 19-1 (Ligurian Sea). Values are given against cal. age and sediment depth.

Tables A.1 to A.6 are available on the attached enclosure

Plate 1

All scale bars equal 100 μ m

| | | | |
|----|---------------------------------------|-----------------------|----------------|
| 1 | <i>Globobulimina affinis</i> | site 339, 1.0-2.0 cm | side view |
| 2 | <i>Globobulimina pseudospinescens</i> | site 347, 1.0-2.0 cm | side view |
| 3 | <i>Globobulimina ovata</i> | site 339, 1.0-2.0 cm | side view |
| 4 | <i>Uvigerina mediterranea</i> | core 19-1, 485-486 cm | side view |
| 5 | <i>Uvigerina mediterranea</i> | site 540A, 1.0-1.5 cm | side view |
| 6 | <i>Uvigerina mediterranea</i> | site 540A, 3.5-4.0 cm | side view |
| 7 | <i>Uvigerina peregrina</i> | core 19-1, 270-270 cm | side view |
| 8 | <i>Uvigerina peregrina</i> | site 540C, 0.0-0.5 cm | side view |
| 9 | <i>Uvigerina peregrina</i> | site 338, 0.5-1.0 cm | side view |
| 10 | <i>Angulogerina angulosa</i> | core 19-1, 270-271 cm | side view |
| 11 | <i>Angulogerina angulosa</i> | core 19-1, 485-486 cm | side view |
| 12 | <i>Angulogerina angulosa</i> | core 19-1, 270-271 cm | apertural view |

Plate 1

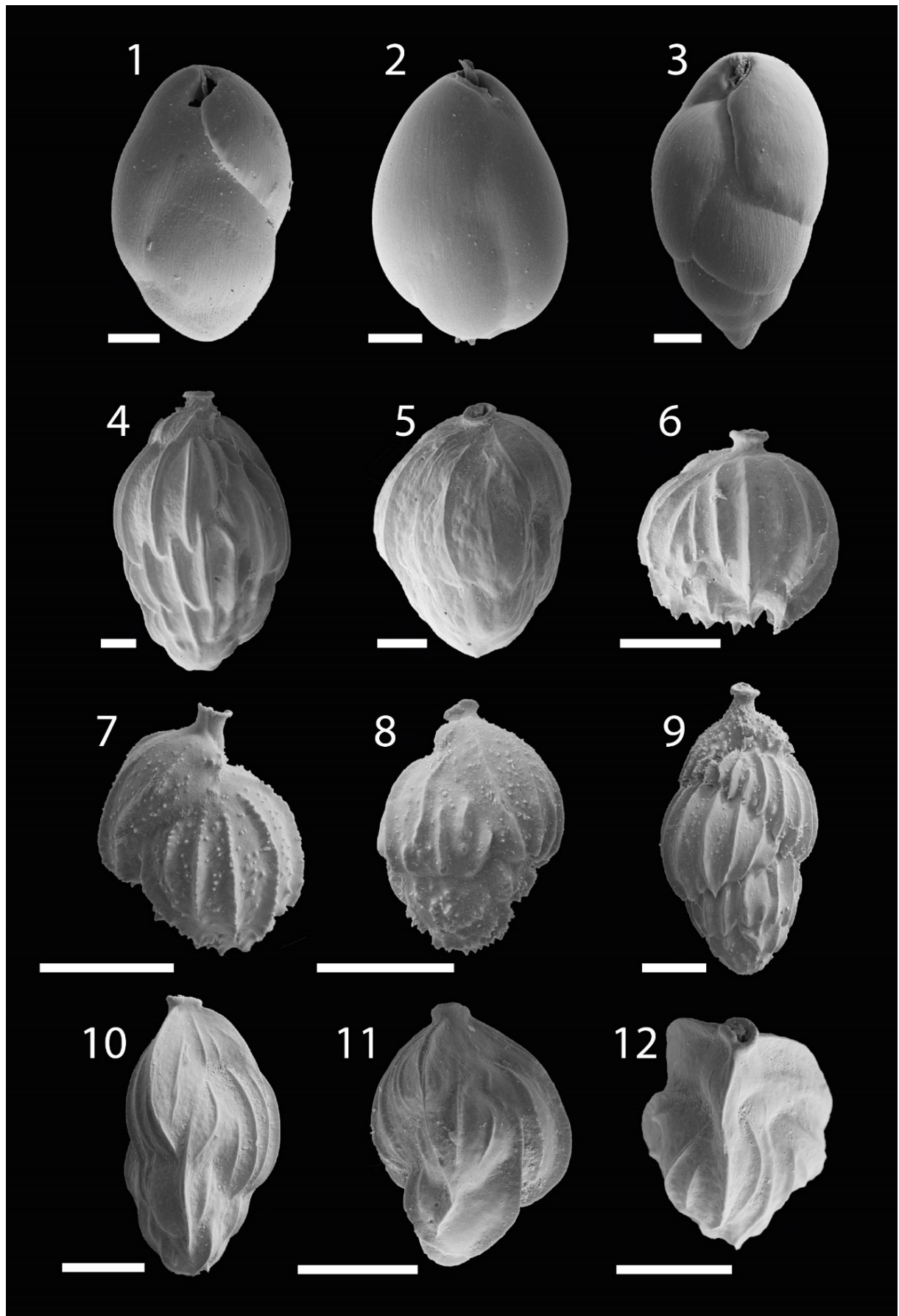
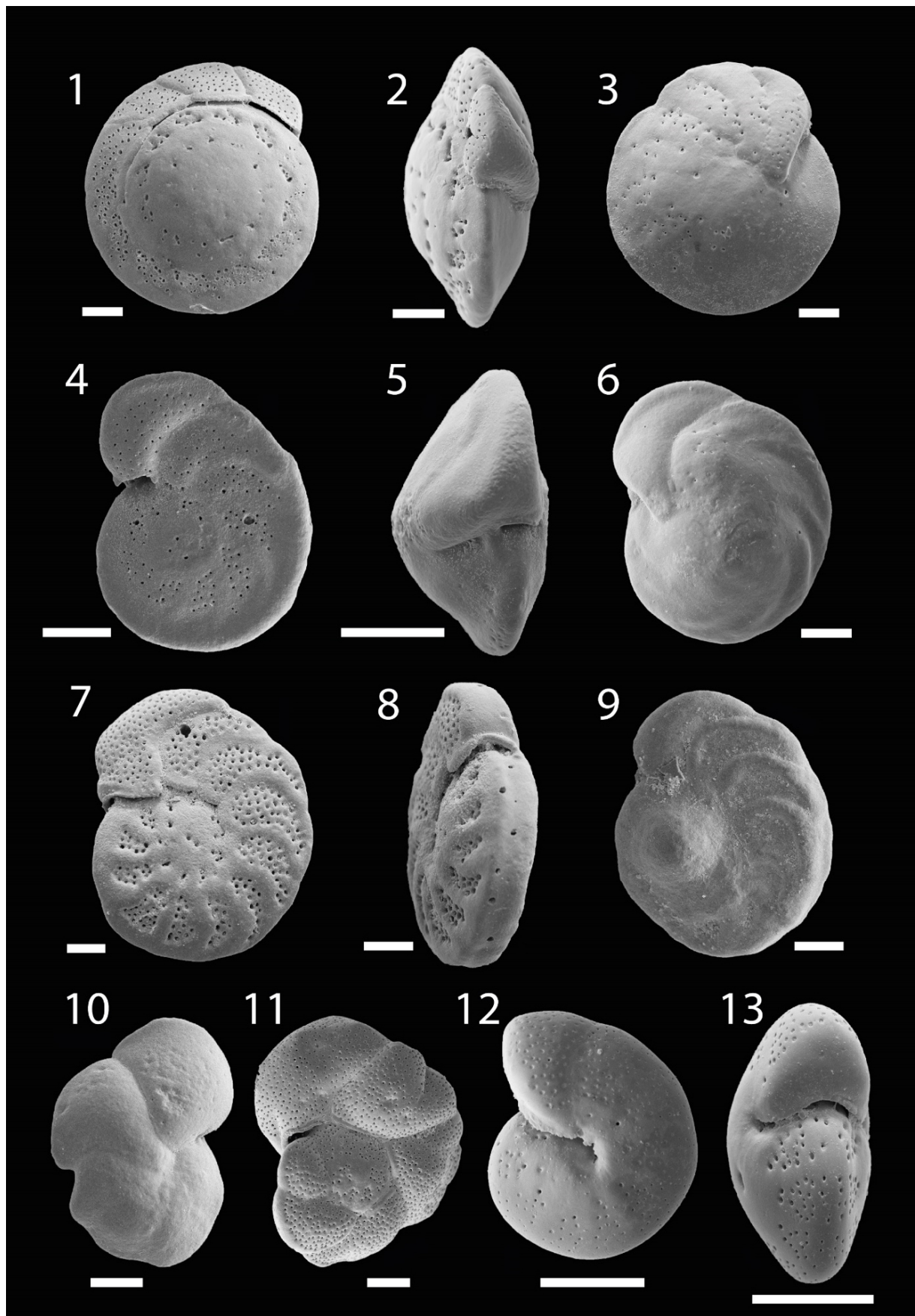


Plate 2

All scale bars equal 100 μ m

| | | | |
|----|-----------------------------------|-----------------------|----------------|
| 1 | <i>Cibicidoides pachydermus</i> | site 602, 0.0-2.0 cm | umbilical view |
| 2 | <i>Cibicidoides pachydermus</i> | site 602, 0.0-2.0 cm | apertural view |
| 3 | <i>Cibicidoides pachydermus</i> | site 602, 0.0-2.0 cm | spiral view |
| 4 | <i>Cibicidoides wuellerstorfi</i> | core 19-1, 455-456 cm | umbilical view |
| 5 | <i>Cibicidoides wuellerstorfi</i> | core 19-1, 455-456 cm | apertural view |
| 6 | <i>Cibicidoides wuellerstorfi</i> | core 19-1, 440-441 cm | spiral view |
| 7 | <i>Planulina ariminensis</i> | site 595, 0.0-1.0 cm | umbilical view |
| 8 | <i>Planulina ariminensis</i> | site 396, 0.0-0.5 cm | apertural view |
| 9 | <i>Planulina ariminensis</i> | site 589, 0.0-2.0 cm | spiral view |
| 10 | <i>Lobatula lobatula</i> | core 19-1, 455-456 cm | spiral view |
| 11 | <i>Lobatula lobatula</i> | site 347, 1.0-2.0 cm | umbilical view |
| 12 | <i>Melonis barleanum</i> | site 596, 0.5-1.0 cm | side view |
| 13 | <i>Melonis barleanum</i> | site 540A, 1.0-2.0 cm | apertural view |

Plate 2



Danksagung

Da mich im Laufe der Zeit viele Menschen beim Erstellen dieser Dissertation unterstützt haben, wäre ohne diese Hilfe die vorliegende Arbeit in ihrer jetzigen Form nie zustande gekommen. Daher möchte ich hiermit allen Beteiligten meinen tiefsten Dank aussprechen.

Voran steht selbstverständlich mein Doktorvater Prof. Dr. Gerhard Schmiedl. Schon allein für die Vergabe dieser Arbeit und die stets hilfreiche Beratung bei widersprüchlichen Ergebnissen gebührt ihm mein Dank. Insbesondere aber für die ausgezeichnete Betreuung, bei der er mir selbst in den stressigsten Zeiten das wertvollste Gut der Wissenschaft zukommen ließ: Zeit. Ebenso gebührt mein Dank Prof. Dr. Andreas Mackensen für seine wichtigen Hinweise und Erklärungen als auch kritische Nachfragen, was ich im Nachhinein viel zu selten in Anspruch genommen habe.

Für seine kritischen Anmerkungen und sinnvollen Verbesserungsvorschläge sei Prof. Dr. Frans Jorissen sehr gedankt. Großer Dank gebührt Frau Lisa Schönborn und Herrn Günther Meyer vom Alfred-Wegener-Institut in Bremerhaven für die Durchführung und Unterstützung bei den zahlreichen Isotopenmessungen. Dr. Jürgen Möbius danke ich sehr für die schnelle und unkomplizierte Hilfe, wenn z.B. noch in kürzester Zeit geochemische Messungen durchgeführt werden mussten. Ich danke Prof. Dr. Helge Arz und Dr. Jérôme Kaiser für ihre Unterstützung beim Beprobieren des Kerns P413/19, sowie Prof. Dr. David Antione für seine Beratung bei satellitengestützten Produktivitätsdaten. Frau Dipl. Geol. Steffi Tobler sei gedankt für die Bereitstellung ihrer Diplomarbeit zu Foraminiferenverteilungen im Kern SL78. Für die diversen unterstützenden Arbeiten, explizit aber nicht nur dafür, möchte ich besonders Mareike Paul, Nina Nikolic, Valerie Menke und Helge Winkelbauer meinen Dank aussprechen.

Ein besonderes Verdienst gebührt Frau Dr. Yvonne Milker für eine sehr lehrreiche Zeit bereits lange vor dem Start dieser Dissertation. Die Fälle sind gar nicht zu zählen, in denen sie mir stets eine wichtige Ratgeberin in fachlichen und auch persönlichen Fragen war und ist. Gleichsam danke ich Paul Kowalski für viele Liter besten Tees, noch mehr wertvolle Gespräche, das er meine Hilfestellungen ausgehalten hat und ganz einfach die gute Arbeitsatmosphäre. Für ihre Freundschaft danke ich ganz besonders Yasmin van Yperen und Gregor Otto, explizit vor allem für die unzähligen und schönen gemeinsamen Mittagspausen. Eine wichtige indirekte Hilfe waren auch die zahlreichen Gesprächen und Diskussionen mit all den Wegbegleitern, und war es auch nur für kurze Zeit, auf diesem langen Weg: Martin Bartels, Swaantje Brzelinski, Doro Bunzel, Caro Clotten, Mathias Feldtmann, Amelie Hagen, Natalie Iwanczuk, Ulrich Kotthoff, Steffi Langer, Valerie Menke, Jürgen Möbius, Katharina Müller-Navarra, Lena Narman, Nina Nikolic, Matthias Ottmar, Mareike Paul, José Pérez, Sabine Prader, Jesús Reolid, Amineh Sadr, Imke Schäfer, Velda Schultz, Kristoff Svensson, Coca Tornier, Truong Tran, Ole Valk, Gerard Versteegh, Helge Winkelbauer, Karin Zonneveld.

Zu guter Letzt möchte ich mich ganz herzlich bei meiner Familie, die sich in der Zwischenzeit ja verdoppelt hat, für die fabelhafte moralische Unterstützung bedanken. Meiner Frau Alexandra möchte ich abschließend für die bedeutendste Unterstützung in diesen schönen gemeinsamen Jahren danken. Sowohl für ihr Verständnis, wenn ich wiederholt in der Welt unterwegs war (z.B. im Winter aufs Mittelmeer), ihren Beistand auch in den schwereren Phasen, ihr Verständnis, wenn ich mal wieder etwas vergaß, und ganz besonders dafür, dass sie mit ihrer Planung und Umtriebigkeit mir ein steter Antrieb war und ist.